Proceedings of the ICEFA : 3rd international conference on electrical fuses and their applications, Eindhoven (Veldhoven), the Netherlands, May 11-13, 1987

Proceedings of the

Third International Conference on Electrical Fuses and their Applications

Eindhoven (Veldhoven), the Netherlands
May 11-13, 1987

Editors:

V.K.I. Kalasek
W.M.C. van den Heuvel

Eindhoven University of Technology
P.O. Box 513
5600 MB Eindoven
the Netherlands

More copies order from:
Electric Energy Systems
High Current and Transmission Group
Department of Electrical Engineering
Eindhoven University of Technology
P.O.Box 513
5600 MB Eindhoven
The Netherlands

The aim of the Third International Conference on Electrical Fuses and their Applications is to bring together researcher, manufacturers and users of electrical fuses, in order to discuss the various problems and solutions, to investigate new designs, applications, standards and tests for fuses and to provide guidelines for future research.

CIP-gegevens Koninklijke Bibliotheek, Den Haag
Proceedings
Proceedings of the third international conference on electrical fuses and their applications: Eindhoven (Veldhoven), the Netherlands: May 11-13, 1987
ed. by V.K.I. Kalasek and W.M.C. van den Heuvel.
Eindhoven: University of Technology. - Fig., tab.
Met lit. opg., reg.
ISBN 90-6144-966-0
SISO 661.56 UDC 621.316.923 NUGI 832
Trefw.: smeltveiligheden.

CONTENT

Session VII: Miniature Fuses 2

Session VIII: Application Aspects

Session IX: Testing and Standardisation

Closing Address

Opening Session

RECENT ADVANCES IN FUSE TECHNOLOGY

By C Turner

INTRODUCTION

The subject of fuses remains a lively one in the technical world, and it is interesting to consider developments and changes since our last meeting in 1984. These changes and developments may be due to a shift in emphasis, because of the developments in other areas, in particular the growth in automation and electronic control of processes in industry and the enormous expansion of home electronics and computers, or they may be related to the greater importance given to safety and reliability of electrical supplies and circuits, as witnessed by the developments and improvements in Standards and Regulations.

In the last meeting the papers were classified into sessions dealing with:

Pre-arcing and temperature rise
Disruption and arcing phenomena
Protection and co-ordination problems
Applications and developments
Tests and Standards
Models of fuse behaviour
Ageing and deterioration.

The shift in emphasis during the three years can be seen from the subjects for the different sessions in the present Conference, in particular the separate session on miniature fuses, related to the expanding field of electronics and low voltage circuits. During the past three years there have been at least 1400 papers worthy of note in the field of protective devices (1), and so it has been necessary to make some selection for this presentation.

It seemed most useful to me therefore, to relate the information published during the last three years to the subjects covered in the sessions of the present meeting. These published papers include the nine papers in the Lodz Conference, which is the only other Conference specifically concerned with fuse operation.

PRE-ARCING PHENOMENA

A number of papers have been published in this period dealing with pre-arcing phenomena of various designs and types of fuses, for instance the low watts-losses required of 500 V supply fuses, to obtain the necessary low temperature rise in consumer units (2); or measurements of the heat loss mechanism of fine wire fuses in vacuum or in air (3), showing that operating power has to be derated considerably for a vacuum fuse compared to a wire fuse sealed in air in a small tube.

Cyclic loading of fuses, which may cause premature operation, has been investigated (4) and related to the shape of the tape elements. The importance of heat dissipation and uniform current distribution in preventing tensile rupture forces is stressed, for elements which have bent shapes in air. When elements are embedded in sand, cycling stability is greatly improved, because of improved heat dissipation, uniform current distribution between elements and prevention of direct tensile rupture forces. There is no corresponding improvement in stability when straight elements are used.

A new controversial theory of current density distribution in a wire during electrical explosion is proposed (5), calculated from the effect of a single dc pulse. It is suggested that the current increases more rapidly in the non-inductive axial area of the wire, so that initially current density is greater in the centre than on the surface, but as the current also decreases more rapidly in the centre, the current density during current fall is smaller in the axis than on the surface. This 'skin effect' is an instantaneous process governed by fluctuations in the circuit current.

Temperature measurements for thin-film fuses of single layers of silver on silica or alumina substrates are reported (6) using a special transient thermography method to study the behaviour under ac and pulsed conditions. This study is a continuation of the work discussed in Trondheim. Important differences for the two substrates are shown up, in particular a much lower temperature rise for alumina substrate in pre-arcing conditions.

The papers in the present conference show that the above problems continue to occupy a place in fuse investigations, in particular with regard to the possibility of more accurate calculations and modelling methods.

ARCING AND DISRUPTING PHENOMENA

The operation of fuse-links under various environmental and circuit conditions remains one of the main topics of investigation, as this is directly related to their co-ordination with other protective and control devices, their ability to protect various circuits and equipment and the safety of personnel. It is therefore not surprising that a substantial number of publications on this subject has been produced both during the period between this meeting and the Trondheim meeting, and at the present meeting itself.

I will give a short resume of the most interesting papers produced in the last three years.

The exploding foil (7,8) is probably not directly relevant to this conference, but the methods employed in modelling of the phenomena prior to and during vaporisation would equally apply to the operation of more conventional fuses under high short circuit conditions. Two models are used, one based upon observation of the fractional increase in resistance of the foil on vaporisation, which is determined by the energy per unit mass supplied to the foil by ohmic heating; the other model using tables of specific energy, pressure and resistivity to compute the ohmic heating, translation and expansion of the exploding foil. The effects of filler material are included in the model.

The phenomena in the corona of an exploded wire have been investigated (9) with time-resolved X-rays, showing that the development of constrictions in the corona is preceded by the appearance of superheated ring-shaped structures.

Exploding wires remain a subject of some interest. Several papers have been published on this subject, for instance in the Gas Discharge Conference in October 1985 (10,11).

Optical and electrical investigations of a wire with a single neck (10), subjected to a slow energy input show up a series of voltage peaks due to partial explosions causing microscopic arcs. If the initial energy is increased, the number of partial explosions is increased correspondingly. The spherical shock waves from these partial explosions produce a cylindrical shock wave. The generation of a heavy current arc depends upon the way the partial explosions occur. In the vaporisation stage, a cylindrical phase of heated air appears, which assists in the promotion of a shock wave consisting of cylindrical wavelets.

The literature on the pressures produced by heavy current interruption in an hrc fuse is reviewed (11). Two phases of the generated pressure are considered: The explosion of the element producing a sudden pressure elevation, followed by subsequent burn-back producing a slow pressure rise.

For more conventional fuses, a model hrc fuse has been used (12) with a copper wire element and sand filler, to investigate the pressure on the wall and its movement through the sand filler and the change with time after element interruption. The shock waves in air, due to the disruption of a copper wire have been investigated (13), where partial disintegration due to a slow energy input rate produces microscopic arcs, and spherical shock waves which have a cylindrical envelope. The process is analysed theoretically using Taylor's flow equations. The radial distribution of the pressure and particle velocities behind the shock waves are related to specific heat and gas temperature.

A theoretical, computational and experimental study of the factors which govern the arcing I^2t integral of current-limiting fuses has been made (14). These include the effect of closing angle and the influence of test voltage. It is shown how the values obtained at one voltage should be corrected for application at different test voltages. The electrical and dimensional parameters of hrc fuses have been correlated with the arc energy at short-circuit interruption (15). Model tests are used to measure and analyse the internal pressure due to arcing and vaporisation of the element. It is shown that the pressure is related to the element material, size and shape of the fuse, rather than the arc energy.

The arc voltage for interruption of a uniform copper element in sand has been related to the resistivity of the element material, its length and cross section (16) using a method of calculation in which the average voltage for a single interruption is determined by division of the total voltage by the number of arcs in series. This number is determined from the striations observed in the fulgurite. The disintegration modulus is defined as the distance between consecutive striations, and is proportional to the cross sectional area to a power 0.3. The theoretical results differ by about 20% from the experimental data.

Copper elements with necks in sand have been subjected to short circuits (17) to obtain experimental relations between arcing I^2t and number of necks. It is shown that for a number larger than 7 the dependence is a weak one.

The effect of element material on the arcing process in sand-filled fuses has been investigated (18) using copper, aluminium and silver elements with a single neck. It was found that arc quenching deteriorates with increase in thickness, arc energy increases, length of element consumed increases and the maximum pressure on the fuse body increases. For less than 0.15 mm thickness, it is shown that arc extinction is better for copper than for silver, while aluminium is better than both. An increase in width increases arc time, arc energy and arc integral, but not length of element consumed. Cut-off potential decreases with increased width. Expressions are obtained to relate energy liberated in the arc to thickness, width and length consumed.

DEVELOPMENT AND DESIGN ASPECTS

The great advances made in computers and the fact that computer modelling is now much more widely available have been reflected in the developments in fuse design. It is now feasible to investigate fundamental changes in parameters and their likely effects on fuse operation without the need for extensive and costly manufacturing and testing, although eventual likely designs obviously still require to be made and tested.

A number of new developments have appeared, some of which were already mentioned in Trondheim, but have been developed further into higher ratings, like the Fullran fuse (19).

A fast-acting high capacity current limiting fuse has been developed by using direct forced cooling of the fusible tubular element (20). Several coolants were investigated but water was found to be the most effective. The design can be incorporated into both ac and dc high voltage current limiters for the protection of thyristors in ac/dc substations. Other high voltage fuse developments include the cadmium element high voltage fuse-link (21) which can be constructed with concentric elements for high ratings, as the elements do not require support, as opposed to silver elements which need a core.

A general analysis of the design of fuses on the basis of optimisation and identification theories has been given (22), in which the principle of maximum and non-linear programming methods is developed. Step-by-step approximations are sometimes necessary to approach the optimum design.

A special design for interruption of dc high voltage current has been developed (23) using a composite resistance commutator system with three parallel circuits: an electrode, normally passing current; a high voltage generating fusing element; and an energy dissipating non-linear resistance. High voltage interruption is obtained by using a multi-stage fusing element. High current is interrupted by having an additional gap in series with the fuse.

A special electromigration fuse is used for protection at the other end of the spectrum (24) for electronic components, utilising the heat generated in the component when it enters a runaway condition to increase electromigration in a constriction to create high resistance or open circuit.

A high interrupting capacity, low deterioration, small dimension high voltage vacuum fuse has been developed (25). These properties are achieved by application of an axial magnetic field during arcing, and structural arrangements to provide power dissipation when carrying current. The element is copper, with copper arcing electrodes in a ceramic barrel, together with a magnetic field generating coil. The fuse can have general purpose or motor protection characteristics.

Further developments in the self-restoring fuse field include experiments on various dielectric inserts and different liquid metals (26). These include quartz glass, corundum, steatite, cordierite and beryllium oxide in conjunction with the eutectic of indium, gallium and lead, a potassium-sodium alloy and pure sodium.

A further development of the two-part fuse already described in Trondheim has a long arcing element in sand in parallel with a short main element in air (27). The period of switch-over of the current from the main element to the arcing element is of particular importance, and this can be related to the time current characteristics of the two parts. Special problems still exist for the application of the principle to high voltage fuses, but for low voltage fuses it is now feasible and has a number of advantages.

New devices for interruption of high-voltage faults are being developed, for instance the 'electronic fuse' (28) consisting of an electronic control module providing a large selection of time-current characteristics and the energy to initiate interruption, and an interrupting module which carries the current normally and interrupts when a fault occurs. The control module is re-usable. The interrupting module consists of a main current carrying section and a current-limiting section in parallel. Both elements are copper in sand.

Improvements in element design, shape and materials, as well as improvements in filler have been made (29). These include the use of aluminium elements, and improvements in thermal conductivity of the filler by means of binding agents. Gas-evolving materials on the core or on the elements provide arc control.

New developments in thermal fuses (30) include new alloys which can be used for intermediate currents between the organic chemical compounds used for large currents and the low melting point alloys used for low currents.

AGEING AND M-EFFECT

The problems of ageing of fuses, and in particular the influence of M-effect materials continues to be of interest. A number of papers have been published, dealing with this subject, and with tests to determine the physical processes involved. A general survey of these processes has been published (31), in which diffusion, temperature and the effect of shape and material of the M-effect pill on the time-current characteristic are dealt with as well as the shape and material of the element, and the position of the pill in relation to necks.

Ageing of copper elements with or without M-effect for elements with or without constrictions, when subject to current cycling has been investigated (32), using a model fuse element in air, with Sn or Sn/Pb 60/40 as the M-effect material. A number of regions of cyclic loading are considered: For relatively low currents and long periods of current carrying, the diffusion of the solder into the element has the most effect, but for higher currents and shorter periods the melting point of the solder becomes more important. Without M-effect, the ageing is due to oxidation and grain growth at the constrictions. This is

a relatively slow process. For elements with both M-effect and constrictions both mechanisms take place, dependent upon current and duration of cycle. At high currents and short durations the neck-ageing mechanism is prominent, but at low currents and long cycles the diffusion process predominates.

Long-time behaviour of Al and Cu fuse-links with various M-effect materials has been investigated (33) with the aim of producing fuses with low loss and low temperature rise, by making the shape and size of the element such that the reaction temperature needed for operation lies only slightly above the melting point of the M-effect material.

Ageing of fuse contacts has also been considered (34). Investigations into the resistance of fuse-links with silver-plated, nickel-plated and tinned contacts at high environmental temperatures on no load, show that silver-plated contacts retain a low contact resistance even after long periods of slow temperature cycling, while the resistance of nickel-plated or tinned contacts tends to rise.

MINIATURE FUSES

The main developments in miniature fuse design have been concerned with thin film or thick film fuses for use in electronic circuits. High-speed thick-film fuses have been developed (35) compatible with modern assembly procedures in electronic systems at low voltage and low current. Three-layer co-fired thick-film fuses are capable of very high speed protection. They can be incorporated in a total circuit, or made as surface-mounted chip components. Semiconductor protection can be closely controlled by using a metal film (36) applied to an insulating backing.

The number of publications in this field has been very limited, and there is scope for further development.

STANDARDISATION

In standardisation of low voltage fuses 1986 marked a major advance in the issue of a world standard, containing a single band of characteristics for all general purpose fuse-links, offering discrimination world-wide on a ratio of rated currents of 1:1.6. This standard, IEC Publications 269-1 and 269-2, is a major advance on all previous standards. This advance ensures a uniformity of performance throughout the world, which has the practical advantage that any item of electrical equipment designed to be protected by a given fuse rating in the country of manufacture will now be equally well protected by the local product if it complies with IEC Publication 269.

In the North American Continent it is difficult to exploit this satisfactory situation because of the independent line of reasoning followed by those who establish the testing requirements of the Underwriters Laboratories, which are completely out of line with those of the rest of the world in certain fundamental aspects. Not least of these is the basis of rating, which results in an IEC rating approximately 80% of the UL rating for identical fuse-links.

In the case of miniature fuse-links, a concerted attempt was made to resolve this ridiculous situation and agreement was achieved on the technical plane with a universally accepted compromise solution. Unfortunately, this technical agreement could not be translated into practice, because of administrative and political obstacles.

A completely new type of miniature fuse-link called the 'Universal Modular Fuse' (UMF) is being developed and a framework of standards is being created to accommodate it. This new concept is designed for use in conjunction with the new technology associated with solid state circuits, which have now largely replaced the electronic circuits for which the original miniature fuse-links were designed. The UMF takes into account the lower voltages at which such circuits normally operate and seeks to accommodate the requirements of automatic insertion of fuse-links into PCB's. These developments have the potential to completely revolutionise the field of miniature fuse technology.

In the standardisation of high voltage fuses, the third edition of Publication 282-1 was issued, representing an advance over previous editions and incorporating Amendments introduced since the 1974 2nd edition. The on-going problem of the definition of a general-purpose/full-range fuse, as opposed to a back-up/high-minimum-breaking-current fuse is again seeking resolution, stimulated by recent developments in the technology of fuse design in this field. There are proposals for reducing the energy required in testing to Test Duty 3 by the use of a 'two power factor' method. There are also new proposals on waterproof testing, energy delivered by strikers, switching voltages of fuse-links of small current rating and simplification of the homogeneous series rules.

APPLICATION ASPECTS

One of the most widely considered fields of study for fuses is still their application, as the range of applications changes towards the protection of more and more complicated electronic circuits and towards ever closer protection of devices and circuit components.

In the field of semi-conductor protection, very fast-acting current limiting fuses are necessary, and various solutions have been investigated (37), for instance flat pack fuses with water cooling, which can carry high currents, and which have low let-through I^2t for protection of large medium voltage semiconductors. Conditions and circuits are very varied, and a useful guide for selection of fuses for typical circuits has been provided (38).

Transformer protection has been improved in various ways. One solution to the problem of surges from fuse operation causing damage to the transformer (39), is to use expulsion fuses and metal oxide arresters. A special device for transformer protection (40) uses a disposable single-phase fault thrower mounted within the high voltage cable entry of the transformer, operated by a chemical actuator fed by a resistor circuit, using time-limit fuses for time grading. Another possible solution is to use an expulsion fuse backed by a current-limiting fuse in one envelope. Expulsion fuses have been improved by using replaceable elements and increasing their breaking capacity (41).

Protection of motors and co-ordination with other protective devices has been improved by the design of special fuses for motor circuits (42), and by using permanent power fuses in cascade protection of mccb's (43). The necessity for derating fuses for use in SF6-gas insulated tanks (44) has been shown.

Computer programs can now be used to calculate co-ordination of operating and tripping characteristics of breakers and fuses in series (45), and for determining the optimum economic selection of cable sizes and fusing (46).

Special internal fuses have been designed for internal protection of capacitors (47).

The above selection of publications is by no means exhaustive, but is merely an indication of the wide variety of fuse applications, and the particular problems associated with them.

FUTURE DEVELOPMENTS

After this short survey of the main publications on fuses during the last three years, the questions of future developments remains. It seems to me that the task of the present conference is to show the way to further improvements and developments in the fuse field. The particular directions to be followed should be formulated at the end of the conference, when it will hopefully have become clear in which directions our efforts should be concentrated to ensure the continued improvement in fuse protection and application.

REFERENCES

1 Digests of Information on Protective Devices, ERA 2979, 1984-1986.

2 Rex, H G: ETZ, 105, 21, 1984, pp.1138-9.

3 Loh, E: IEE Trans. Comp. Hybrids Manuf. Techn., CHMT-7,3, 1984, pp.264-7.

4 Namitokov, K K: Isv. Vuz. Elektromekh, 10, 1984, pp.78-85.

5 Nasilowski, J: Switching Arc Phenomena, Lodz, 1985, pp.352-7.

6 de Cogan, D et al: IEE Proc, 132, Pt.I, 3, 1985, pp.143-6.

7 Lindemuth, I R et al: IEEE Int. Conf. Plasma Sci, St Louis, 1984, p.103.

8 Lindemuth, I R et al: J. Appl. Phys., 57, 9, 1985, pp.4447-60.

9 Aivazov, I K et al: J E P T Lett., 41, 3, 1985, pp.135-9.

10 Yukimura, et al: Gas Discharges and their Applications, Oxford, 1985, pp.83-6.

11 Lipski, T: Gas Discharges and their Applications, Oxford, 1985, pp.87-90.

12 Gul, A; Lipski, T: Switching Arc Phenomena, Lodz, 1985, pp.326-30.

13 Yuimura, K; Urabe, J: Switching Arc Phenomena, Lodz, 1985, pp.331-5.

14 Wafer, R V; Wilkins, R: Switching Arc Phenomena, Lodz, 1985, pp.358-62.

15 Barbu, I: Switching Arc Phenomena, Lodz, 1985, pp.363-7.

16 Hibner, J: Switching Arc Phenomena, Lodz, 1985, 368-71.

17 Krapek, K; Paukert, J: Tekh. Elektr. Pristr. a Rozvadecu, 2/3, 1984, pp.94-104.

18 Namitokov, K K, Frenkel, Z M: Sov Electr. Eng. 55, 9, 1984, pp.113-7.

19 van der Scheer, D: Elektrotechniek, 62, 5, 1984, pp.461-4.

20 Inaba, T: IEEE Trans. Power Appl. Syst., PAS-103, 7, 1984, pp.1888-94.

21 van der Zwaag, H: Elektrotechniek, 162, 7, 1984, pp.621-3.

22 Namikotov, K K: Izv. Vuz. Elektromekj, 4, 1984, pp.56-62.

23 Inaba, T: IEEE Trans. Power App. Syst., PAS-103, 7, 1984, pp.1903-8.

24 Horstmann, R E; Pratt, J D: Tech. Disclosure Bull, 27, 4A, 1984, pp.1884-5.

25 Tanaka T et al: IEEE Trans. Power Appl. Syst., PAS-104, 9, 1985, pp.2472-80.

26 Andreeev, V A et al: Izv. Vuz. Elektromekh., 11, 1984, pp.84-9.

27 Krasuski, B et al: Switching Arc Phenomena, Lodz, 1985, pp.336-40.

28 Glenn, D J; Cook, C J: IEEE Trans. Ind. Appl., IA-21, 5, 1985, pp.1324-32.

29 Ranjan, R: IEEE Conf. Ind. and Comm. Power Syst., 1985, pp.64-70.

30 Tsutsui, K et al: NEC Tech. J., 38, 8, 1985, pp.112-17.

31 Klepp, G: ETZ, 105, 16, 1984, pp.846-7.

32 Hofmann, M; Lindmayer, M: Switching Arc Phenomena, Lodz, 1985, pp.346-51.

33 Grundmann, P et al: ETZ, 107, 10, 1986, pp.438-44.

34 Klepp, G: ETZ, 107, 4, 1986, pp.164-6.

35 Marriage, A J; McIntosh, B: Hybrid Circuits, 9, 1986, 15-17.

36 Marsh, D: El. Rev., 216, 6, 1985, pp.29-30.

37 Benouar, M: Ind. and Comm. Power Syst. Tech. Conf., Atlanta, 1984, pp.86-96.

38 Howe, A F et al: Conf. Rec. Ind. Appl. Soc. IEEE-IAS Ann. Meeting, 1985, pp.916-22.

39 Moylan, W J: Ind. and Comm. Power Syst. Tech. Conf., Atlanta, 1984, pp.112-15.

40 Oakes, M: El. Rev., 281, 14, 1986, pp.14-15.

41 S Gruziecki, et al: Energetyka, 39, 1, 1985, pp.14-17.

42 Tambe, P S: Conf. Pulp and Paper Ind., Toronto, 1984, pp.188-95.

43 Jones, S: El. Rev., 216, 6, 1985, pp.30-31.

44 Schaffer, J S; Patel, J R: IEEE, Trans. Power App. Syst., PAS-103, 12, 1984, pp.3573-7.

45 Sachs, U, et al: Siemens Power Eng. and Autom., 7, 2, 1985, pp.72-6.

46 Rudolph, W: ETZ, 106, 6, 1985, pp.264-8.

47 Danemar, A; Eriksson, E: ASEA J., 57, 3, 1984, pp.14-19.

Session I

PRE-ARCING PHENOMENA 1

Chairman: Prof. Dr. M. Lindmayer

ANALOG SIMULATIONS OF THE HEAT FLOW IN A HIGH VOLTAGE FUSE.

J.C.J. Sloot
Department of Electrical Engineering
Eindhoven University of Technology.

Abstract.
The heat flow in a high voltage fuse has been simulated by an electrical analog model. The design and analysis was performed interactively on the screen of a personal computer.
The model has been used to determine the melting time curve of a full range type commercial fuse.

1. Introduction.

Within high voltage fuses heat is generated by Joule-losses. In fact the functioning of the fuse depends on heat flow processes. For short circuit currents the fuse is activated when narrow parts of a silver strip reach their melting temperature.
In the overcurrent range the heating of less narrow parts often becomes dominant (for instance with the M-spot effect).
This article discusses the calculation of such thermal processes in a commercial fuse by using an electric analog model.
The method first was developed using real electric components, like resistors and capacitors, but today it is more attractive to use the the method with personal computers when graphic interaction on the screen is possible.

2. The dimensions of the fuse.

Fig 1 shows the exploded view of a commercial fuse (40 A, 12 kV) of the full range type.

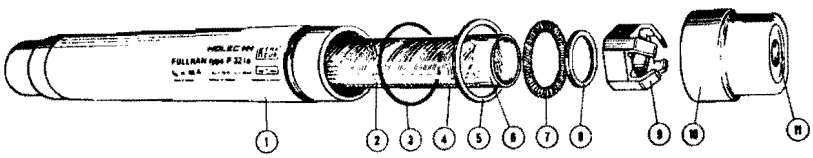

fig. 1 Exploded view of the fuse.

Within a porcellan housing, a number of parallel fuse strips (N) with thickness Δ are wounded helically with an angle β around a quartz cylinder.
The fuse strips are provided with notches (length L_{not}, heigth H_{not}) between less narrow bandparts (L_{ban}, H_{ban}).
The inner and outer space of the quartz cylinder is filled with sand.

Fig. 2 shows a part of the longitudinal cross section of a fuse slice.

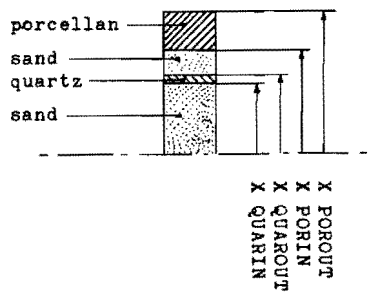

Fig. 2 Longitudinal section of the fuse.

Because of symmetry reasons, only an angular part of a slice needs to be considered (see fig. 3).

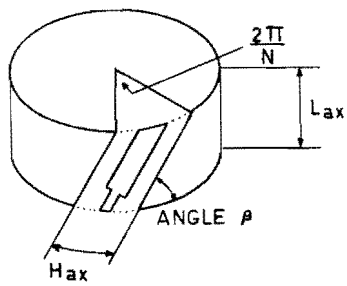

Fig. 3 Angular part of slice.

The angular part represents a fraction 1/N of the slice and corresponds with half a notch and half a band. The part has an axial length
$L_{ax} = 0.5\ (L_{not} + L_{ban})\ \sin\beta$.
(This means that the silver strip element corresponds with an outside quartz surface $L_{ax}H_{ax}$ with $H_{ax} = 2\pi X quarout/N$).

The angular part is now further divided into pieces according to fig. 4.

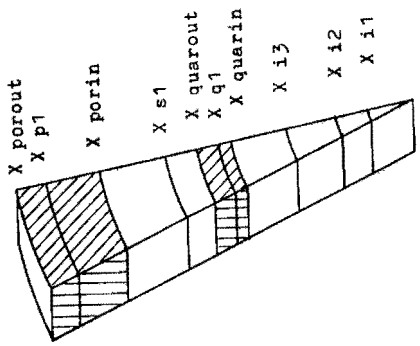

Fig. 4 Angular division of the fuse-slice.

3. The thermal model.

Joule heat is generated in the notch and the bandpart on the outside quartz surface.
Because of its higher resistance the notch will heat the band.
On a longer time scale both will heat the quartz and the sand. The fuse is relatively long compared to the diameter, therefore it is assumed that the heatflow in the middle of the fuse is directed radially. The outside of the porcellan is cooled by convection and radiation. The governing heat equations are the following:

a. Heat sources.

The Joule heat of the band and the notch represent heat sources P_{ban} and P_{not} with:

$$P_{ban} = (I/N)^2 R_{ban}$$
$$R_{ban} = Rb_o(1 + \alpha (T - T_o))$$
$$Rb_o = \rho_o \, 0.5 \, L_{ban}/(H_{ban}\Delta)$$
$$\rho_o = \rho (T_o) \text{ with ambient temperature } T_o$$
$$P_{not} = (I/N)^2 R_{not}$$
$$R_{not} = Rn_o (1 + \alpha (T - T_o))$$
$$Rn_o = \rho_o \, 0.5 \, L_{not}/(H_{not}\Delta)$$

The coefficient α can be considered as a constant for the temperature range 295K - 1234K, as illustrated in fig. 5.

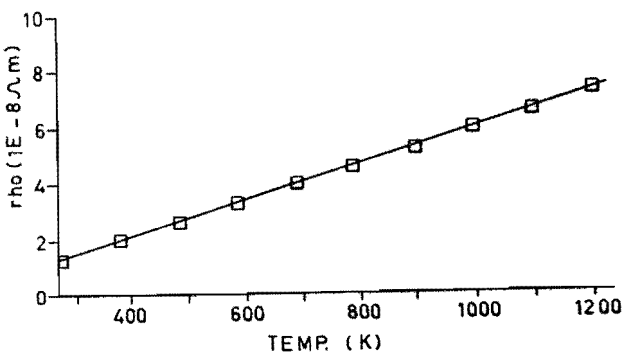

Fig. 5 Specific electrical resistivity of silver.
*: exp values [1]
curve: linear regression
$\rho = \rho_o (1 + \alpha (T - T_o))$
with T_o = 295 [K]
ρ_o = 1.51 E-8 [Ωm]
α = 0.0045 [1/K]

b. Storage of heat energy.

The Joule heat of the fuse strip results in an increase of the temperature T of the subsequent cylindrical layers with length L_{ax} between radius r_1 and r_2.
This power P_{store} can be represented by:

$$P_{store} = \gamma S \pi (r_2^2 - r_1^2) L_{ax} \frac{dT}{dt}/N \quad \ldots\ldots\ldots (1)$$

with γ for the specific density and S for the specific heat.

c. Radial conduction.

The radial heatflux density can be represented by:

$$q = -\lambda \frac{dT}{dr} \quad \ldots\ldots\ldots\ldots\ldots\ldots\ldots (2)$$

For the heat flow through a cylindrical surface it follows

$$P_{cond} = -\lambda 2\pi r L_{ax} \frac{dT}{dr}/N \quad \ldots\ldots\ldots\ldots (3)$$

From this equation the temperature-difference between two radial positions can be calculated:

$$T_1 - T_2 = \frac{P_{con} N}{\lambda 2\pi L_{ax}} \ln\left(\frac{r_2}{r_1}\right) \quad \ldots\ldots\ldots (4)$$

d. Convection and radiation.

The convection-losses of the porcellan surface with temperature T_w, to the surrounding at temperature T_o can be presented by Newton's law of cooling:

$$q = h(T_w - T_o) \quad \ldots\ldots\ldots\ldots\ldots\ldots (5)$$

The heat-transfercoefficient h for horizontally positioned cylinders with a radius r less than 10 cm can be described [2] by:

$$h = 1.3 \left[\frac{T_w - T_o}{2r}\right]^{0.25} \quad \ldots\ldots\ldots\ldots (6)$$

This gives an equation for the convective cooling:

$$P_{conv}=2\pi r L_{ax} 1.3\ (2r)^{-0.25}(T_w - T_o)^{1.25}/N \quad ..(7)$$

The radiation heatflux of the outside porcellan surface is given by the formula:

$$q = \sigma\ \epsilon_p\ (T_w^4 - T_o^4) \quad .....(8)$$

with universal radiation constant:
σ = 5.67 E-8 [W/m2K4]
emission coefficient of porcellan: ϵ_p = 0.93
surrounding temperature : T_o=295 [K]

This means a powerflow due to radiation from the surface of:

$$P_{rad} = 2\pi r L_{ax}\ \sigma\ \epsilon_p\ T_o^4[(T_w/T_o)^4 - 1]/N \quad .....(9)$$

The total cooling power flow through the outside porcellan surface part is:
$P_{conrad} = P_{conv} + P_{rad}$.

Fig. 6 presents the calculated relation between P_{conrad} and T_w-T_o for a porcellan radius r = 27.4 mm, N = 15, L_{ax} = 3.6 mm and T_o = 295 K.
The upper curve represents the quadratic regression:

$$P = A + B\ (T_w - T_o) + D\ (T_w - T_o)^2$$

with A = -3.54-4, B = 4.62E-4 and D = 2.63E-6.

The validity of this equation was confirmed by some experiments, where the quartz tube was replaced by a tungsten core. The results are presented in fig. 6 by the +marks.

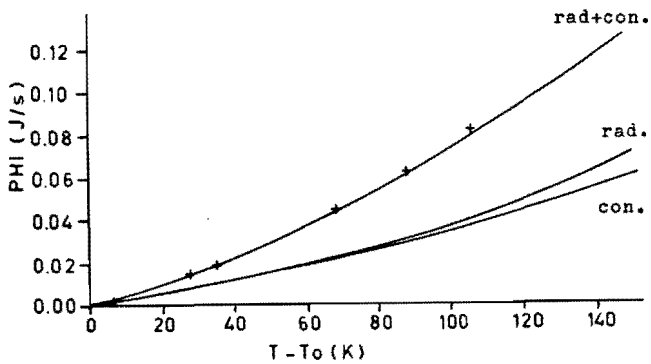

Fig. 6 The cooling power P_{conrad} of an elementary surface as a function of the temperature difference $T_w - T_o$.

The surface cooling relationship corresponds with a temperature dependent resistance, which has been plotted in Fig. 7.

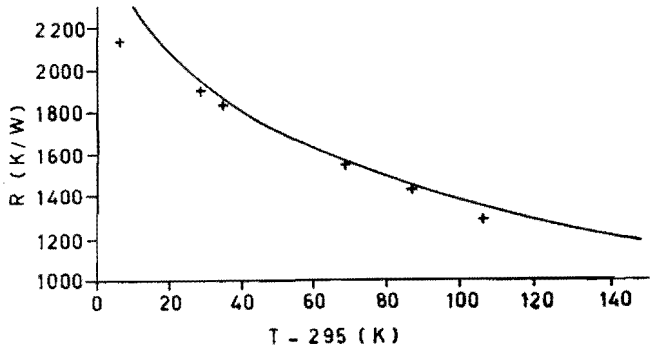

Fig. 7 The elementary surface transition resistance R_{conrad} as a function of the temperature difference with the surrounding (+ for the experimental values).

4. Analogy between thermal and electrical equations.

It is generally known that there exists a great analogy between the equations describing thermal or electrical problems.
Table 1 shows the equivalent equations and quantities:

Thermal	Electrical
storage: $P=\gamma S\pi(r_2^2 - r_1^2)\ L_{ax}(\frac{dT}{dt})/N$	$I = C\ \frac{dU}{dt}$
conduction: $P=\frac{\lambda 2\pi L_{ax}}{N\ \ln(r2/r1)}\ (T_1 - T_2)$	$I = \frac{U_1 - U_2}{R(1,2)}$
radiation + convection: $P=(T_w - T_o)/R_{conrad}$ with $R_{conrad}=f(T_w-T_o)$	$I = \frac{U_w - U_o}{R_{conrad}}$
heat flux: P	current: I
temperature: T	voltage: U
thermal capacitance: $\gamma S\pi(r_2 - r_1)L_{ax}/N$	capacitance: C(1,2)
thermal resistance: $\frac{N\ \ln(r_2/r_1)}{2\pi L_{ax}\lambda}$	electrical resistance: R(1,2)
surfaceresistance: $f(T_w - T_o)$	surface resistance: R_{conrad}

Table 1. Equivalent thermal and electrical expressions.

With the formulas of table 1 it was possible to calculate the equivalent circuit components for the elementary part of Fig 4.
The resulted values are listed in table 2.

Capacitances	Resistances
Ci1 = 2.6E-2	Ri12 = 1664
Ci2 = 6.0E-2	Ri23 = 741
Ci3 = 1.0E-1	Riq = 300
Cq1 = 1.1E-1	Rq1n = 429
Cqn = 2.7E-3	Rqnn = 425
Cnot = 1.4E-5	Rsnn = 1550
Csn = 2.1E-3	Rsn1 = 1700
Cs1 = 1.4E-1	Rsp = 190
Cp1 = 3.9E-1	Rpw = 72
Cw = 2.2E-1	Rq1b = 38
Cqb = 3.4E-2	Rqbb = 34
Cban = 4.9E-4	Rnb = 333
Csb = 2.6E-2	Rsbb = 123
	Rsb1 = 273
	Rqs = 103

Table 2. Equivalent component for the element in fig. 4.

5. Electrical analogon of the thermal model.

The equivalence of thermal and electrical quantities can be used to construct an electrical analogon for the discussed thermal model (see fig. 8).

An interactive computer program was developed, to calculate the values of all circuit components, after it was supplied with the fuse dimensions, the material properties and the fault current.

Voltage dependent current sources P_{not} and P_{band} have to be used for the representation of the powerflow from the notch and the band.

The convection/radiation is represented by a voltage dependent resistor CONRAD. Their description was already discussed in paragraph 3. The other component values are listed in table 2.

6. Simulation of the nominal current-situation.

The analog model was first applied to simulate the warming-up of the fuse with the nominal current (40 A) flowing.

Fig. 9 shows the calculated temperature rise of the porcellan surface, and the silver strip.

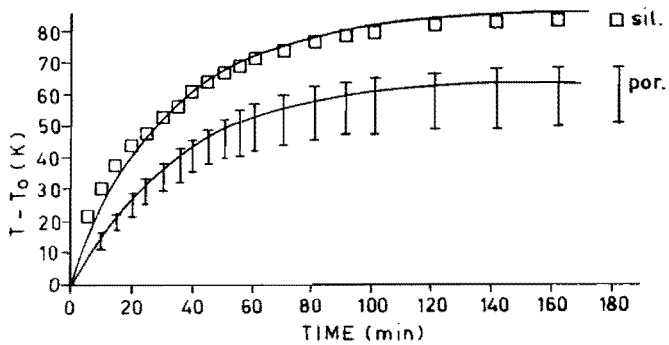

Fig. 9 Comparison of computer predictions and experimental results of temperature rises in a fuse, at a current I = 40 A
(□ = exp silver, I = exp porcellan).

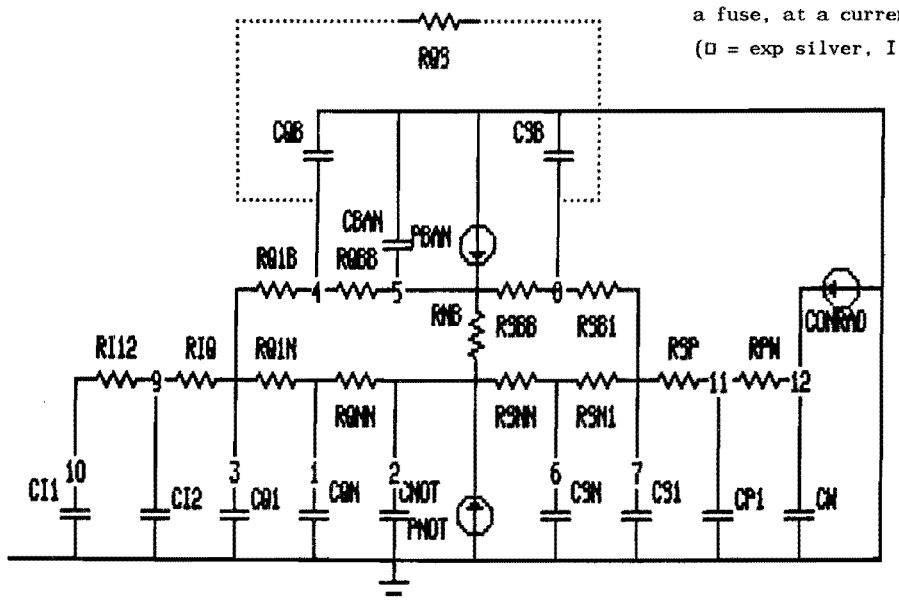

Fig. 8 Electrical analogon for a thermal elementary part.

As a verification of the validity of the model, the actual temperature-rise of the porcellan surface was also measured.
The fuse was positioned horizontally in a set-up according to the requirements of IEC 282-1.
The nominal values of the model and the experiment are reasonably in accordance with each other; this is an indication that the choice of the fractional radial losses and the value of the resistances is acceptable.
From the similarity of the dynamic curves it can be concluded that also the choice of the capacitances is acceptable.

As a raw verification of the silver curve, the experimental strip-temperature was estimated from the voltage measurements during the heating up process, by substituting these values in the resistance-relationship:

$$R(T) = R_o [1 + \alpha(T - T_o)] \quad \ldots\ldots (10)$$

with $R = U/I$

it follows $T(t) = T_o + (1 - \frac{U(t)}{IRO})/\alpha \quad \ldots\ldots (11)$

7. The prediction of the fuse characteristic.

Encouraged by the accordance of the dynamic situation, a prediction was made for the melting curve.
The moments were determined when either the temperature of the silver band reached 500 K, being the critical value of the M_{spot}, or the notch temperature reached its melting temperature 1234 K.
The results are presented in fig. 10 and compared with the specifications of the manufacturer.

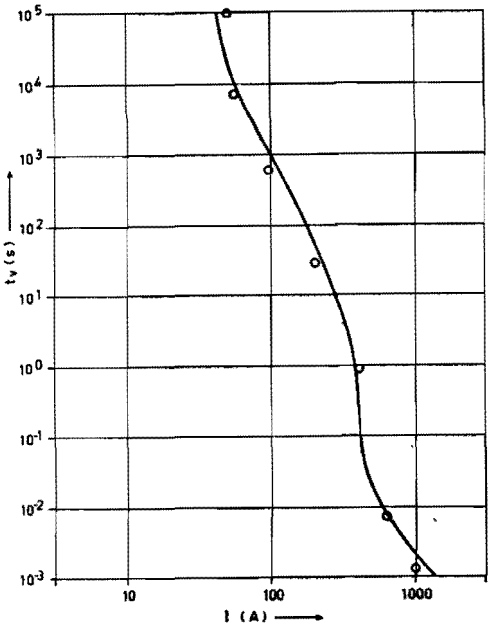

Fig. 10 The melting curve for In = 40 A.
——: specification of the manufacturer.
o : results of the analog model.

Similar agreement like fig. 10 shows for In = 40 A, was obtained for 25 A and 16 A.

Conclusions.

Obviously this analog model offers a valid method for the simulation of the thermal behaviour of fuses over an extended current range. With the analog model a quick impression can be got of the melting curve and this forms a powerful tool for the development engineer.
The individual influence of the silver strip dimensions, the sand, quartz and porcellan parts can be characterized separately; the effect from changes in the fuse design on the I - t characteristic can be concluded directly.
A similar calculation programm is under development for designing more classical constructions.

References.

[1] Tslaf, A.: Combined Properties of Conductors.
Elsevier, Amsterdam (1981).

[2] Perry, R.H. and Chilton C.H.: Chemical Engineer's Handbook, Fifth ed., Sec 10, McGraw-Hill, New York (1973).

TLM MODELLING OF THIN FILM FUSES ON SILICA AND ALUMINA

D. de Cogan and M. Henini
Department of Electrical and Electronic Engineering
University Park
Nottingham NG7 2RD, (UK).

ABSTRACT

Thin film electric fuses comprising of a metal layer bonded to an electrically insulating substrate such as silica or alumina have distinct advantages over conventional types. The element is in intimate contact with its support which provides an efficient sink for heat dissipated during quiescent operation. However the temperature dependence of the thermal time constants of alumina and silica are radically different; the former increases with increasing temperature while the latter decreases. This gives rise to a thermal feedback effect which is perhaps the most significant factor in determining pre-arcing performance in this type of device.

In this paper a novel numerical technique, three dimensional transmission line matrix (TLM), is used to predict the pre-arcing behaviour of thin film electric fuses on silica and alumina substrates. The results indicate that there is a complex interaction between the temperature dependence of the conductor resistance and the substrate thermal parameters (specific heat and thermal conductivity) which has important consequences for fast power semiconductor protection fuses.

INTRODUCTION

The development of new types of very fast power semiconductors has created considerable problems in terms of protection. Many of these devices can fail in times which are short compared to the pre-arcing time of conventional sand filled electric fuses. An alternative and potentially faster fuse can be constructed by depositing a very thin film of conducting metal on an electrically insulating substrate. In addition to providing mechanical support for the conductor, the substrate also acts as a heat sinking component during quiescent operation. The thermal behaviour of thin film fuses on insulating substrates has been examined experimentally and the results were reported at a previous ICEFA Conference[1]. It has been shown[2] that the properties of thin film fuses are dominated by the thermal properties of the substrate.

The effort involved in performance optimisation can be significantly reduced by means of device modelling. The time and space variation of parameters such as temperature can be described by means of a suitable differential equation. However for a given set of boundary conditions an analytic solution is not always possible and this is particularly true if one attempts to include the temperature dependence of parameters such as substrate specific heat and thermal conductivity or conductor resistivity.

The advent of digital computers has stimulated the use of numerical methods of solution. The numerical solution of equations which are functions of space and time generally involves two discretisation steps i.e. one for each variable. The discretisation of space into nodes is simple enough but the subsequent time discretisation can, as in the case of the heat flow equation, lead to instabilities unless special precautions are taken.[3] In this paper a relatively novel technique, the transmission line matrix (TLM) method, is used to solve the three dimensional non-linear thermal diffusion equation for a thin film fuse.

THE TLM METHOD

The use of electrical analogies for the solution of differential equations is well accepted and the transmission line matrix (TLM) technique represents a new development in this area. It arises from the fact that any transmission line has capacitance (C_d), inductance (L_d) and resistance (R_d) distributed along its length. It can be shown that[4] Maxwell's equations for propagation along a lossy transmission line can be expressed in one dimension as:

$$\frac{\partial^2 T}{\partial x^2} + \frac{\partial^2 T}{\partial y^2} + \frac{\partial^2 T}{\partial z^2} = L_d C_d \frac{\partial^2 T}{\partial t^2} + R_d C_d \frac{\partial T}{\partial t} \qquad \ldots (1)$$

This describes the propagation of a wave which becomes attenuated. The first term represents lossless wave motion. A spike impulse launched into a transmission line will take a definite time to travel along the line. Thus if a physical problem can be modelled by an electrical network consisting of a matrix of transmission lines, then a solution of the network will provide a solution to the problem without the necessity of a separate time discretisation step. The TLM technique involves a discretisation of the problem space. Each spatial node is replaced by transmission line components in an analogous electrical network. Current or voltage impulses are injected into the network. During their progress through the network they obey Maxwell's equations. Thus the population of impulses as a function of time and position provides a solution to equation 1.

Under circumstances where a lossy transmission line fulfills the condition that $R_d C_d \ll (\text{impulse velocity})^{-2}$ then equation 1 reduces to an analogue of the heat flow equation. This forms the basis of the TLM method of thermal modelling. Figure 1 shows a three dimensional node together with a one dimensional lumped equivalent circuit. Any physical problem is modelled using a matrix of these nodes. Heat is input as impulse analogues at appropriate parts of the matrix. An iteration commences with a scattering of impulses. They travel along the lines and experience reflections if the impedances of adjacent nodes are unequal. At the end of a period Δt all impulses arrive at their new positions. The temperature rise at a particular node is then the sum of all incident impulses at that location. The process ends with an adjustment of the thermal capacitance, line impedance and thermal resistance (all functions of temperature) at each node in preparation for the next step.

Boundaries can be treated in the following ways:

(i) The terminating impedance is infinite (an electrical open circuit). In this case any impulse encountering the termination will be reflected back along the line with its phase unaltered.

(ii) The terminating impedance is zero (an electrical short circuit). In this case any impulse encountering the termination will be reflected with the opposite phase.

(iii) The terminating impedance is identical to the impedance of the line (matched load condition). In this case no heat is reflected at the termination and it provides a good approximation of a semi-infinite sample.

TLM MODEL OF A THIN FILM FUSE

Dimensions and boundaries

The fuse structure that was considered is shown in Figure 2. The symmetry permits one to simplify the treatment by considering one quarter of the entire problem. Figure 2 also shows the physical dimensions and the boundary analogues. [O C] implies that the boundary is equivalent to an electrical open circuit, which is a good approximation since radiative losses are very small compared with thermal conduction. The matched load boundary (designated [M L]) has been used to simulate a structure whose horizontal dimension is very large compared to the region of maximum thermal dissipation. The matched load at the under surface of the substrate implies that it is likewise much larger than the geometry of the hottest region. For the timescales involved in the pre-arcing process this simplification is found to be valid.

The conductor

Silver was used as the electrical conductor in all simulations. In order to provide a comparison with experimental data[1] a conductor thickness of 2.2μ was used for simulations on silica. 1μ was the value used with alumina. The values of electrical resistance and its variation with temperature were derived from the American Institute of Physics Handbook[6]. Within the routine the resistivity for each discretised volume of conductor was adjusted at the end of every timestep. The adjusted value of resistance was determined by the temperature of the substrate node immediately below it.

Since the values of conductor thickness were very much less than the minimum dimension of any substrate node, the thermal contributions were initially ignored and the conductor treated only as a heat source.

Substrate

Values of specific heat and thermal conductivity were abstracted from Touloukian[7,8]. The thermal resistance, capacitance and hence line impedance were calculated for each node at the end of a time step.

RESULTS

Comparison with thermal imaging results

The three dimensional TLM routine was tested for a thin film silver element (2.2μ thick) carrying 1A DC on silica. When the calculated results were compared with experiment it was found that agreement was good only at locations remote from the region of maximum dissipation. One source of discrepancy was obviously the silver conductor itself. In the initial formulation it was ignored on the basis thatit was very thin compared with the thickness of the nearest silica node. If all node sizes were reduced to accommodate the conductor thickness the computational efficiency would have been reduced drastically. Nevertheless it can be seen that even for very thin layers, the thermal parameters of silver can make a significant contribution. If one considers the relative dimensions of a silver element and its adjacent substrate node, one can see that the silver makes a small contribution to the thermal capacitance. In the vertical direction the silica and silver thermal resistances add in series. As the thermal resistance of silver in this direction is negligible compared to the silica thermal resistance its contribution can be ignored. In the horizontal directions the two resistances sum in parallel and total resistance will therefore be dominated by that of the silver.

This suggests that the thermal effects of the conductor can be included without any loss of computational efficiency if one uses a composite surface node like that shown as an inset in Figure 3. When this was taken into account there was a considerable improvement in the extent of agreement between theory and experiment and the results for a latitudinal (x-direction) temperature profile are shown in Figure 3. Residual differences can be attributed to resolution errors. The 10 x lens used in the original measurement had a minimum resolution of 150μ. Experiments with a 40 x lens (resolution 38μ) confirms that there is a small underestimate of temperature when a 10 x lens is used on this type of structure.

The effects of thermal feedback

The influence of the insulating substrate was investigated for the pre-arcing period. For simulation purposes this was assumed to be the time necessary for the conductor to reach its melting point. TLM was used to model the case of a thin film silver fuse (of the lateral dimensions shown in Figure 2). Currents were chosen so that the 2.2μ thick conductor on silica would reach melting at about the same time as a 1μ thick element on alumina. The effect of thermal feedback for both substrates can be seen in Figure 4. The rate of temperature rise increases in the case of the element on alumina. For silica the rate of temperature decreases with time. The influence of the positive thermal feedback effect in alumina can be seen over a range of currents in Figure 5. The results suggest that a thin film fuse on alumina should be more sensitive to overloads. At 7.5A the element is in a steady state condition. There is a transition somewhere above 8A. Melting is reached within 105ms at 8.5A and within 30ms at 9A. These effects become even more

significant at higher current levels. Figure 6 shows the variation of maximum temperature with time when 29A is passed through a 1μ thick silver conductor on alumina during 10ns. It is quite clear that this does not display an I^2t dependence. Tests of the model have confirmed that the behaviour is largely due to the interactions between the temperature dependence of substrate thermal parameters and conductor resistivity. A rise in temperature leads to a rise in electrical resistance and under conditions of constant current increases the dissipation rate until the melting point of silver is reached.

The effects of negative thermal feedback on a silica substrate are remarkably different. Figure 7 shows the time variation of maximum temperature when 24A is passed through a 2μ thick silver conductor. There is an initial fast rise in temperature which then settled down to an I^2t relationship. The inset provides some details about the initial thermal transient for a number of different currents.

CONCLUSION

Transmission line modelling is a fast, efficient and unconditionally stable technique for solving non-linear physical problems. Once it is mastered the user has at all times a reassuring sense of the physical nature of the problem which is being modelled; something that is not often possible with the more conventional finite difference and finite element methods.

TLM has been used to simulate the thermal behaviour of thin film fuses on silica and alumina substrates. The negative thermal feedback effect and the resulting I^2t behaviour suggests that silica is indeed a most inappropriate substrate material. Thin film fuses on alumina should represent a considerable saving in terms of the conductor required for a particular current rating. The temperature-time dependence at high current levels indicates that fuse structures based on alumina should be capable of providing protection for fast power semiconductors.

ACKNOWLEDGEMENT

The continuing encouragement of Brush Fusegear and their support in presenting this paper is gratefully acknowledged.

REFERENCES

1. D. de Cogan, A.F. Howe, P.W. Webb and N.O. Nurse
International Conference on Electric Fuses and their Applications
Trondheim, June 1984, pp. 12-23.

2. D. de Cogan, A.F. Howe and P.W. Webb
IEE Proceedings Vol. 132, P.tI (1983), 143-146.

3. G. Kiebmann
British Journal of Applied Physics 6, (1955), 129.

4. P.B. Johns and R.L. Beurle
Proc. IEE 118(9), (1971), 1203 - 1208.

5. D. de Cogan and M. Henini
Transactions of the Faraday Society (to be published)

6. American Institute of Physics Handbook 3rd Edition
Ed. Dwight E. Gray

7. Thermophysical Properties of Matter (Vol. 5, Specific Heat)
Ed. Y.S. Touloukian. p. 26 (Alumina), p. 207 (Silica)

8. Thermophysical Properties of Matter (Vol. 2, Thermal Conductivity)
Ed. Y.S. Touloukian. p.98 (Alumina), p.183 (Silica)

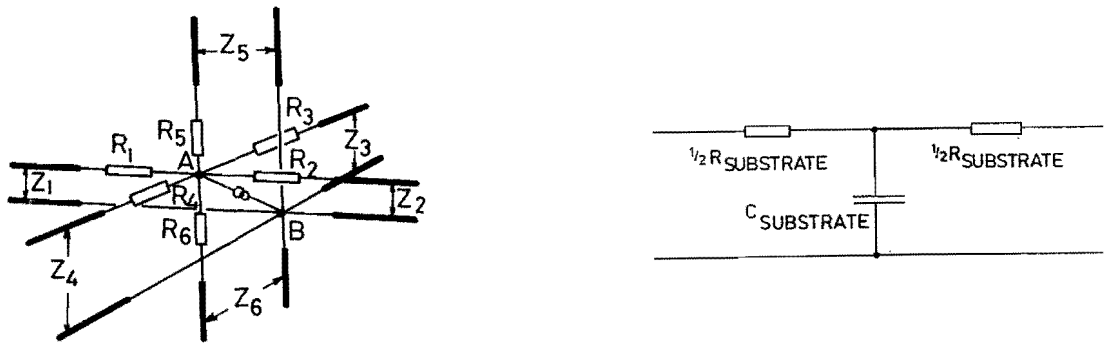

Figure 1. A three-dimensional transmission line node and a one-dimensional lumped equivalent circuit

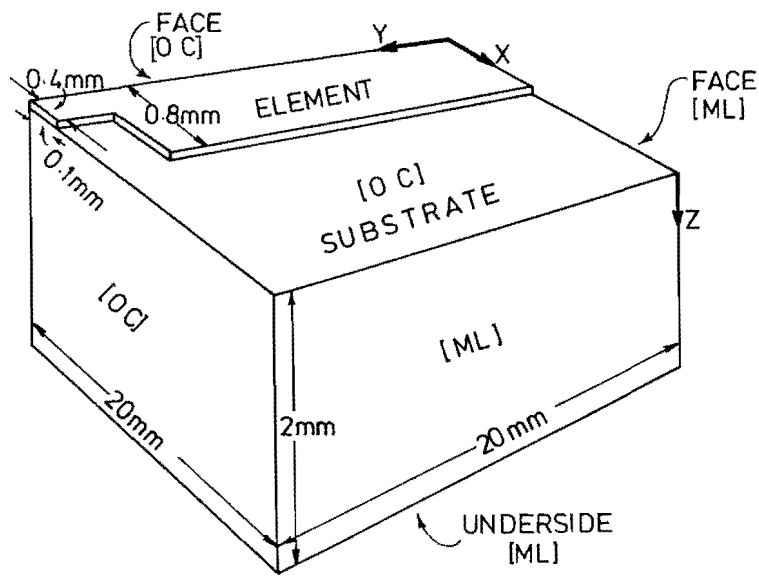

Figure 2. Fuse element and substrate used in TLM model

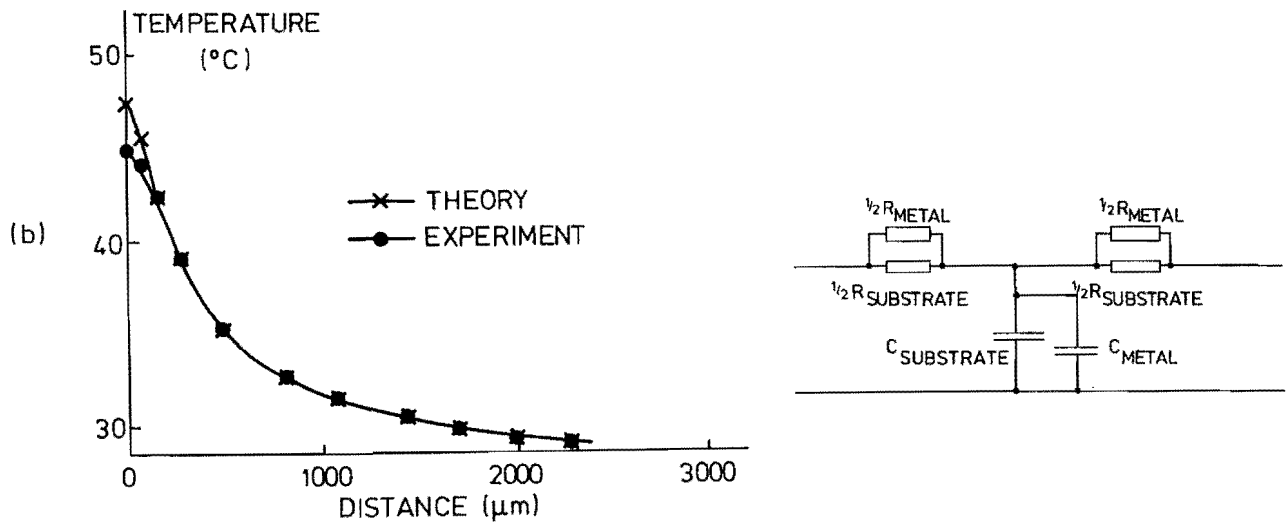

Figure 3. Comparison between theory and experiment: X-direction temperature profiles for a 2.2μ silver conductor on silica with a current of 1A. The composite surface node is shown as an inset.

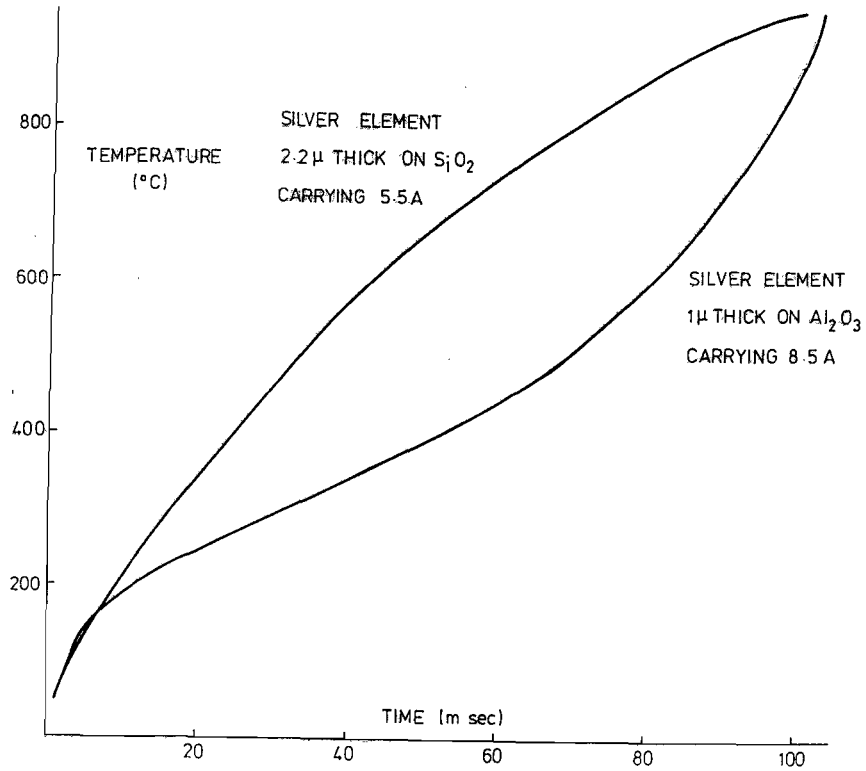

Figure 4. Plot of maximum temperature versus time for silver elements on silica and alumina substrates

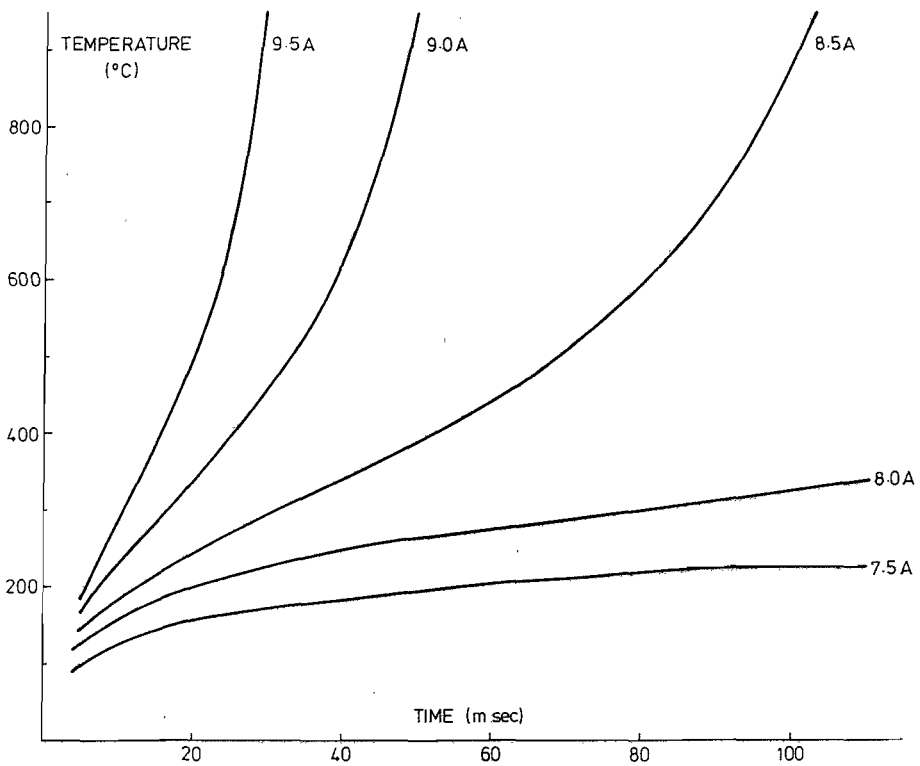

Figure 5. The influence of conductor current for silver element on alumina, plotted as maximum temperature versus time.

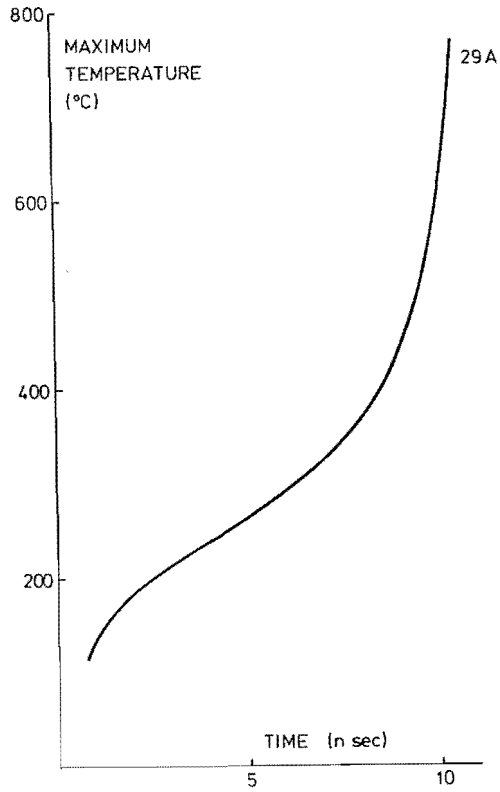

Figure 6. The variation of maximum temperature as a function of time for a 1μ silver element on alumina with a current of 29A.

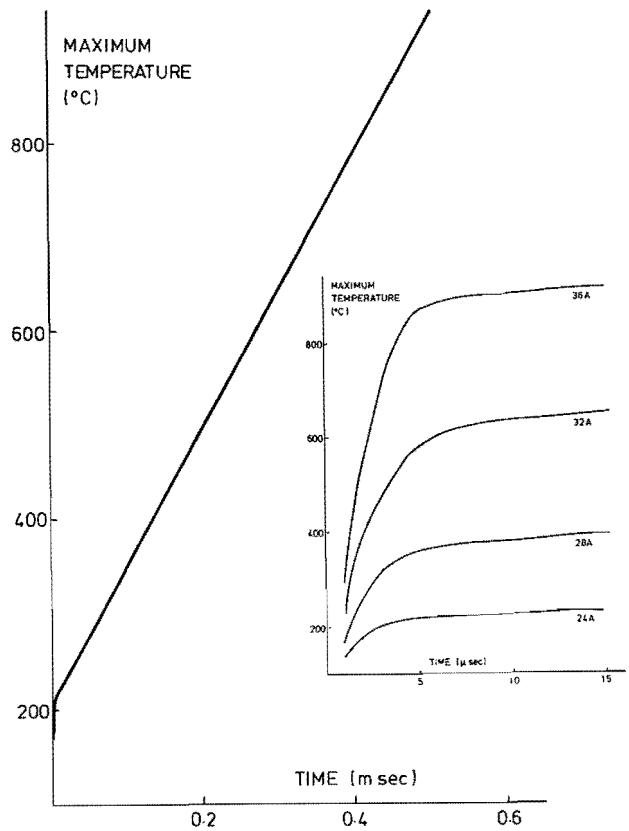

Figure 7. The variation of maximum temperature as a function of time for a 2.2μ silver element on silica with a current of 24A. The effect of current on the initial transient is shown as an inset.

Calculations of models for non-adiabatic processes

Hans-Günter Rex EFEN Elektrotechnische Fabrik GmbH , D-6228 Eltville

A melting element very often is sheet metal containing parts of reduced cross-section which represent weak areas when current is flowing through. Undoubtedly a melting element therefore is a two-dimensional structure. But yet it is possible to have the process of heating-up the melting element by a short circuit current described very neatly by a simple one-dimensional model. The advantages of such a method are simpler relations, less supporting points for the calculation of the temperature along the melting element and therefore less time for the calculation of the temperature distribution.
The processes of heating-up and melting both combined with heat transport along the metal are demonstrated by simple differential equations. These equations are solved by approximation by means of a small computer and the results are compared with experimental values.

Material constants:

abbreviations , definitions , dimensions , numerical values		Ag	Cu
Ao = resistivity of the conductor at 20 degr. cent.	$\Omega*mm^2/mm$	.000016	.0000175
A1 = first order temp. coeff. of resistivity	1/K	.00377	.0039
A2 = second order temp. coeff. of resistivity	$1/K^2$	5.7 E-7	6.7 E-7
A3 = thermal conductivity k at 20 degr. cent.	W/(mm*K)	.428	.385
A4 = first order temp. coeff. of thermal conductivity	1/K	- .00018	- .0002
A5 = thermal capacity c at 20 degr. cent.	W*s/(g*K)	.237	.377
A6 = first order temp. coeff. of thermal capacity	1/K	.00020	.00024
A7 = coeff. of linear thermal expansion	1/K	.000024	.000020
A8 = density d of solid conductor at 20 degr. cent.	g/mm^3	.0105	.00895
A9 = resistivity of liquid conductor at melt. temp.	$\Omega/mm^2/mm$	.00016	.00022
Bo = melting temp. Ts of the material, degr. cent.	K	960	1083
B1 = latent heat of the conductor material	W*s/g	105	214
W9 = resistivity of solid conductor at melt. temp.	$\Omega*mm^2/mm$	.0000808	.000103

B4 = density of the liquid conductor and B8 = density of solid conductor at melt. temp.

1.1. Current heat and heat loss along the melting element

The behaviour of a melting element at very short current pulses can be described by a model for adiabatic heating. When the current pulses become longer there will be heat loss during the time the current flows. The heating up will be delayed and the melting time will grow up. If the melting element is a wire of constant cross section maximum melting time and current for adiabatic heating can be determined according to (4). A lower current heat and a delayed melting time mean heat loss by heat conduction along the wire.
These melting times may reach 50 ms for respective wires.
In this essay we will only look at the heat loss by conduction along the melting element. Longer current pulses which lead to additional heat loss into the sand are forbidden.
A lot of melting elements consist of homogenous sheet metal with rows of accurately punched restrictions in it. This results in parts of smaller cross section on the melting element. A current flowing through a small cross section means large heating but little heat conduction. A large cross section at the same current means little heating but remarkable heat conduction and therefore great influence on the melting time.
The instantaneous value of the current can determine whether the current heat exceeds the heat loss by conduction and heats up the melting element or whether the heat loss at small values of the current prevents the temperature rise.
In the following model calculation we limit the melting time to 50 ms. In this period only heat loss along the metal exists. Heat loss to surrounding sand is not yet important.
We construct for the calculation a model that contains simple differential equations and that enables us to solve the formulas by means of a small computer. We only want the solution to be as correct as the result found by the experiment. The calculation will be made stepwise by approximation. At the beginning of the experiment or the calculation we define a temperature portrait of the melting element and we calculate the temperature values changed after a fixed time interval dt.

1.2. Construction of the model of the calculation

1.2.1. The melting element as a one-dimensional model

A high current flowing along a broad melting element will be driven by its dynamic forces to the lateral edge of the element. We will neglect this effect and assume homogenous current density. We imagine the melting element is cut lengthwise in small parallel strips. A current pulse along such a strip will warm up the restrictions on the strip. The material between the restrictions stays at its temperature. Because of the good thermal conductivity of the metal we have constant temperature transverse to the strip, but not constant along the strip. The temperature on that part of the strip without restrictions is constant in all directions.
As a first approximation we obtain a one-dimensional temperature portrait along each parallel strip of the broad melting element. The constant current density across the whole melting element causes the temperature to have the same value transverse to all parallel strips.
By this method we can calculate the temperature portrait on a broad melting element with a one-dimensional model. The formulas are much simpler. We need less supporting points for the temperature. This means less memory capacity and calculating time and results in the applicability of a small personal computer.

1.2.2. The restrictions on a strip

In many cases a melting element contains several rows of restrictions normally symmetrical in respect to the midst of the restriction. This limitation does not alter the method of calculation. Current heat will produce the highest value of the temperature in the midst M1 of the restriction. In the midst M2 of two rows of restrictions current heat will be minimal. The heat flows from the midst M1 to the midst M2 between two rows of restrictions. The effect of heat conduction is symmetrical in respect to the midst M1 of the restriction. Therefore it is sufficient to select for the model a region M1-M2 on one small strip of the melting element. The calculating model enables us to calculate the temperature values on the region M1-M2 as a function of the instantaneous time.
Production of the heat by the current and heat conduction along the strip are simultaneous. Because we want to have a very simple model we assume heat production and heat conduction to be two effects at two different moments following close to each other.
Then we can calculate both effects separatedly and simply add the results. The heating-up can be treated as adiabatic heating and it is possible to calculate with known simple formulas.

1.2.3. The model of the chain of pearls

For the calculation of the heating-up of the melting element the current density and the time after the commencement of the current must be known. The heat conduction will be calculated with the values of the cross section and the distance of the transportation of the heat, the temperature difference at the ends of the distance and the fixed time interval. Because the shape of the resctrictions shall not be significant for the solution of the differential equations we must find a solution independent of the shape of the restrictions.
This will be gained by deviding the region M1-M2 of the melting element into several small intercepts m. Each intercept is described by its real length, by a mean value of the cross section for the calculation of the current heat and by a realistic cross section for the heat conduction.
We assume furthermore the mass to be heated up will be concentrated in one point in the midst of each intercept. With the above mentioned model the temperature deviation and the temperature of each mass point will be calculated.
Normally the cross section varies in each intercept. As to the heat conduction we must define two different values for the cross section at both ends of the intercept. The distance for the heat to flow to within the time interval dt is described by the distance x of the mass points and by an active cross section between the two mass points.
This delivers us a model like a chain of pearls. It shows us a stepped temperature curve.
We divide one restriction from its midst M1 to its end M3 into several intercepts of different length and we have the intercept from M3 to the end M2 as the last intercept with only one temperature value in each midst point. The number of intercepts depends on the shape of the restrictions. When the cross section changes very much with the distance of the midst M1 of the restriction it is helpful to have ten intercepts. When the cross section is nearly constant six intercepts will result in a sufficient correct value. A greater number of intercepts does not deliver very much better results but will need more time for calculation. Because a higher temperature of the material delivers a higher current heat it is suggested to have the length of the intercepts adapted to its cross section.

1.3. Current heat in the solid material

The following calculation is valid for each intercept m of the region M1-M2. R(T,m) is the resistance of the intercept at the beginning of the time interval, dt the length of the time interval for the calculation of the current heat dQa and i(t) the instantaneous value of the current in the middle of the time interval dt. When we refer the literature (4) we find a maximum time tm without remarkable heat conduction for each length x.

1.3.1. Ag : $tm = 0.5*x^2$ Cu : $tm = 0.8*x^2$ (tm in ms ; x in mm)

In general a current i(t) produces current heat dQa within the time interval dt

1.3.2. $dQa = R(T)*i^2(t)*dt$

We obtain the resistance R(T,m) of the selected intercept m when we know the length x of the intercept, an average cross section q and the resistivity Ro. These three values depend on the temperature and on the measures of the intercept m. The resistance is

1.3.3. $R(T,m) = Ro*x/q = Ro(T) * x(T) / q(T)$

As shown before in (4) we express each value as a product of a material constant independant on the temperature and of the beginning of a power series of the temperature T. We collect all values depending on the temperature T to a temperature function f4(T).

1.3.4. $f4(T) = (1 - A1*To + (A1-2*A2*To)*T + A2*T^2) / (1+A7*T)$

After a short time the function f4(T) reaches a different value for each intercept in the same moment. Therefore the resistance depending on the temperature of the intercept m will be

1.3.5. $R(T,m) = (Ao*xo/qo) * f4(T)$

Ao , xo , qo are the values of the intercept m at a temperature of 20 degrees centigrade.
We write the current i(t) as a product of a constant value D and a time function f(t).
After n time intervals dt we take the value of the current i(t) in the moment t = (n-1/2)*dt and the temperature values at the beginning of the time interval dt and obtain the current heat dQa(m) of the intercept m produced in the time interval dt.

1.3.6. $dQa(m) = (Ao*xo*/qo) * f4(T,m) * D^2 * f^2(t) * dt$

Because we divide the restriction M1-M3 of the segment M1-M2 into several intercepts we will have for each intercept a differential equation ananlogous to equ. 1.3.6.
In general this cross section is not identical to the cross section for the heat conductivity from one intercept to the next one. The last intercept M2-M3 of the section M1-M2 has got a constant scross section.
Because the current through all intercepts of a section M1-M2 has the same value but the cross section and the energy necessary for the melting of the intercept normally not we calculate with the value of the current i(t).
At the beginning of the current all intercepts shall have the same temperature value To.
In the first time interval dt the current i(t) produces an amount of heat dQa(m) in the intercept m.

1.3.7. $dQa(m) = (Ao*xo/qo) * f4(To,m) * D^2 * f^2(dt-dt/2) * dt$

After a period of n time intervals dt the intercept m has gained the temperature Tm(m).
The current i(t) produces an amount of heat dQa(m) in the intercept m in the next interval dt.

1.3.8. $dQa(m) = (Ao*xo/qo) * f4(Tm,m) * D^2 * f^2(n*dt-dt/2) * dt$

1.4. The heat conducted away in the solid material

We begin with a simple equation for the heat conduction. The heat dQk(m) which flows from one mass point m of the chain of pearls to the next one is given by the distance x of the two mass points, by an active cross section qk, by the thermal conductivity k of the material of the melting element, by the temperature difference dT of the two mass points and by the length of the fixed time interval dt.

1.4.1. $dQk(m) = k * qk * dT * dt / x$

Because we want the time interval dt to be respectively small according to chapter 1.3. the temperature values of the two mass points alter only a little. Therefore we can assume the temperature difference dT in equ. 1.4.1. as a constant value for each single step.
Because we know that we calculate especially time intervals dt with current heat the model will work. We calculate the amount of heat dQk(m) that flows from one mass point m to the next one. The material values k, qk and x depend on the temperature. The values qk and x depend on the shape of the restriction too. That means they depend on the intercept m.
Once more we write the material constants at the temperature T as a product of values at 20 degrees centigrade and a function of the temperature T(m) of the intercept m .
Hence we obtain the heat dQk(m) which flows from the mass point m to the mass point m+1 within the time interval dt.

1.4.2. $dQk(m) = (A3*qo/xo) * (1+(A4+A7)*T(m)) * dt * (T(m) - T(m+1))$

The active cross section qo is a real value between the two mass points m and m+1 and depends on the shape of each intercept.
At the commencement of the current all intercepts have the same temperature. The heat conducted away therefore is zero. When the current gains a measurable value temperature differences are produced and heat conduction will occur.

1.5. The current heat produced during the transition solid/liquid

When a material is heated up to the melting temperature Ts the temperature rests constant while the current still produces current heat. The resistivity changes during the transition from the value W9 for the solid state to the value A9 for the liquid material. Is the heat necessary to make the material fluid produced by the current then the dynamic forces of the current can interrupt the melting element. The process of the melting is finished. We obtain the the amount of heat Pm necessary for the transition in each intercept when we multiply the latent heat Bl with the mass of the intercept m which depends not on the temperature.

1.5.1. $Pm = Bl * A8 * qo * xo$

A simple relation between the resistivity Ro and the amount of heat Q(m) left in the mass of the intercept m is a linear function. Thus we write the resistivity of the intercept m as a product of a function fl(Q) and the resistivity W9 of the solid material.
The amount of heat added up in the intercept m depends on the current heat produced at the melting temperature Ts and on the heat loss that means on the dimensions of the intercept. The function fl(Q,m) yields different values for each intercept in the same moment.

1.5.2. $fl(Q,m) = (Pm + Q(m)*(A9-W9)/W9) / (Pm + Q(m)*(1-B4/B8)/3)$

fl(Q,m) is of no dimension. In (4) the function fl(Q) is explained in details.
When the intercept m gains the melting temperature Ts the length shall be x(Ts) and the cross section q(Ts). At this moment the value of Q(m) is zero.
The resistance R(Ts,m) of the intercept during the transition solid/liquid then is given by

1.5.3. $R(Ts,m) = W9 * fl(Q,m) * x(Ts) / q(Ts)$

After n time intervals dt we take the value of the current i(t) in the moment t=(n-1/2)*dt and the value of the added-up heat Q(m) at the beginning of the time interval dt and obtain the current heat dQa(m) of the intercept m produced within the time interval dt.

1.5.4. $dQa(m) = W9 * fl(Q,m) * (xo/qo/(1+(Ts-To)*A7)) * D^2 * f^2(t) * dt$

1.6. The heat conducted away during the transition solid/liquid

The calculation of the model for adiabatic heating showed that about 90 % of the value of the melting integral were needed to heat the material up to the melting temperature Ts. The remaining 10 % could do the transition from solid to liquid.
An error of 50 % at the calculation of the transition integral because of an inaccurate model then yields an error of 5 % at the melting integral of the melting element.
The heat conduction during the transition solid/liquid results in a higher value of the heat produced by the current at the melting temperature Ts. The portion of the transition energy may increase up to 50 % of the melting integral. An error in the model for the calculation of non adiabatic heating will influence very much the melting integral of the melting element at longer melting times.
During the transition solid/liquid of the material the temperature of the material remains at the melting temperature Ts. Are the temperature values of two intercepts equal to the value Ts then the temperature difference between these two intercepts is zero. The use of formula 1.4.1. results in no heat conduction.
Arrive these two intercepts at the melting temperature at different moments then the transition solid/liquid normally is not in the same state. The added-up heat of transition in the two intercepts is different and we will have heat conduction between the intercepts. It is necessary to find a method to calculate heat conduction during the transition from solid to liquid. As a first approximation we assume the active force of heat conduction will be the difference of the added-up energy Q in both intercepts.
Hence we yield the heat dQk(m) conducted away from the intercept m within the time interval dt analogous to equ. 1.4.1.

1.6.1. $dQk(m) = k * q(Ts) * (Q(m)-Q(m+1)) * dt / x(Ts)$

The conductivity k of the material changes during the transition solid to liquid. It is difficult to find numerical values in the literature. Hence we assume the conductivity k to be constant during the transition solid to liquid. Comparing of calculated and measured values will show the applicability of this simplification.
When a heat dQ is added to a mass m with the thermal capacity c then the temperature T(m) will change by a value dT according to the relation

1.6.2. $dQ = m * c * dT$

Is the material heated up to the melting temperature Ts before no additional temperature rise will occur. Yet we are not forbidden to define a virtuel inner temperature T(m) for the material. Equ. 1.6.2. gives us the value dT of the change of this inner temperature. At the beginning of a time interval dt an amount Q(m) of heat of transition is stored in the intercept m and therefore a value of its inner temperature exists. When we add a virtuel temperature difference dT then we obtain a changed virtuel temperature T(m) of the intercept m. This is valid for each intercept.

1.6.3. $T(m) = Q(m) / (m*c) + Ts$

When in equ. 1.4.2. the real temperature difference is replaced by the difference of the virtuel temperatures and the temperature value T(m) by the value Ts then we can calculate the heat dQk(m) which is conducted away from the intercept m to the next one m+1 .

1.6.4. $dQk(m) = (A3*qo/xo) * (1+(A4+A7)*Ts) * (T(m)-T(m+1)) * dt$

The amount of heat conducted away from intercept m is conducted to and added to the next intercept m+1.
Is intercept m already heated up to the melting temperature Ts but not yet intercept m+1 then it is possible too to calculate the heat conducted away from the intercept m by means of equ. 1.6.4. Then the value T(m) means the virtuel temperature of the intercept m and the value T(m+1) means the real temperature of the intercept m+1 .

1.7. Calculation of the temperature values

Current heat and heat conduction in the melting element define the amounts of energy dQ(m) left in each intercept within the time interval dt. For temperature values below the melting temperature Ts exist other formulas than for temperature values at the melting temperature. When we add the current heat dQa(m), the heat dQk(m-1) conducted to and the heat dQk(m) conducted away from the intercept m we obtain the energy dQ(m) stored in the intercept m within the time interval dt.

1.7.1. $dQ(m) = dQa(m) + dQk(m-1) - dQk(m)$

When the energy dQ(m) is added to a mass m of the thermal capacity c the temperature of the mass changes by the value dT(m). We obtain

1.7.2. $dT(m) = dQ(m) / (m*c) / (1+A6*T)$

The thermal capacity c depends on the temperature T, the mass m does not.
Is the intercept m heated up to the temperature T1(m) then after a time interval dt the temperature of the intercept m has changed to

1.7.3. $T2(m) = T1(m) + dT(m)$

The first calculation round yields the temperature values of all intercepts after the first time interval dt by means of the above mentioned formulas. The same formulas used with the calculated temperature values yield the second series of temperature values of all intercepts. When we go on this way we obtain in every moment the temperature portrait of the chain of pearls which represents the melting element.

1.8. Some details of the programm

The program is written in basic and was developped to run on a cbm 4032 basic computer of 32 KB RAM and 8-bit cpu 6502. Later on the program was tested on a cbm 610 basic computer of 128 KB RAM, 8-bit cpu and 80 columns screen.
This program is made for rising currents only. With little additional software it is possible to calculate temperature values too when the current decreases. Then the run time of the programm will encrease by about 30 %.
When the current passes a maximum before the intercept melts then the heat loss will exceed the current heat and the error of the result increases by using this simple model.
The run time is valid for a program that calculates one type of restrictions only. When there are two or more restrictions of different shape on the melting element all different restrictions had to be calculated under the very same conditions. The restriction which needs the least current heat starts to interrupt the melting element. The total run time of the program is the sum of all single run times of each restriction.
The computer displays all temperature values, the instantaneous time and the instantaneous run time. Temperature values above the melting temperature Ts are displayed as Ts-values. This makes the program comfortable but slow.When we divide the section M1-M3 of a restriction into ten parts of equal length the run time is about 34 minutes for a real melting time of 6 ms. To make the program faster it needs to eliminate the basic lines for the display of the instantaneous values. The run time then decreases to 30 minutes.

1.9. Discussion of the results

It is most important to have accurate numerical values of the material of the melting element. Then we can ask the program for the instantaneous values of time and temperature and for the i^2t-values in every moment.
We find the fact that the values of the melting integral by experiment are lower than the calculated values. The lowest limits are delivered by calculation of adiabatic heating. The difference between the results of calculation and experiment may be caused by incorrect numerical values of the material, by inhomogenous current density in the melting element and by the fact that until now the tolerances of the values in the experiment were not measured as accurate as it would be necessary today. For silver material only a few values existed. For copper material we had a lot of values and we found a result by calculation as accurate as by experiment.

Table 1.9.1.

material	silver	copper		
melt.integr. at	132.5	168.7	A^2s	experiment
virt.time 4 ms	162.7	179.3	A^2s	calculation

Table 1.9.2. shows the result of a calculation of a melting element of copper material. The restrictions are round holes of 1.5 mm in diameter and a distance of 1.8 mm from centre to centre in the line. The distance of the lines is 3 mm minimum. The cross section of all restrictions in a line is 1.00 mm^2 .

table 1.9.2.: (power factor 0.3 ; making angle 0 degrees)

current	4000	5000	6000	6500	7000	11000	21000	A
time until Ts	8.42	7.04	6.25	5.95	5.70	4.47	3.27	ms
integral value	191.7	172.6	162.6	159.1	156.2	142.8	129.9	*1000 A^2s
melting time	8.86	7.31	6.46	6.15	5.89	4.61	3.36	ms
melt. integral	219.4	196.0	184.5	180.7	177.3	162.1	147.9	*1000 A^2s
virt.melt.time	13.7	7.84	5.12	4.27	3.61	1.33	0.33	ms
run time	41.13	36.28	33.10	31.90	30.83	26.16	22.23	minutes

We did not take care to the influence of the resistance of the melting element to the current. When the test voltage is high enough then we may neglect this influence.

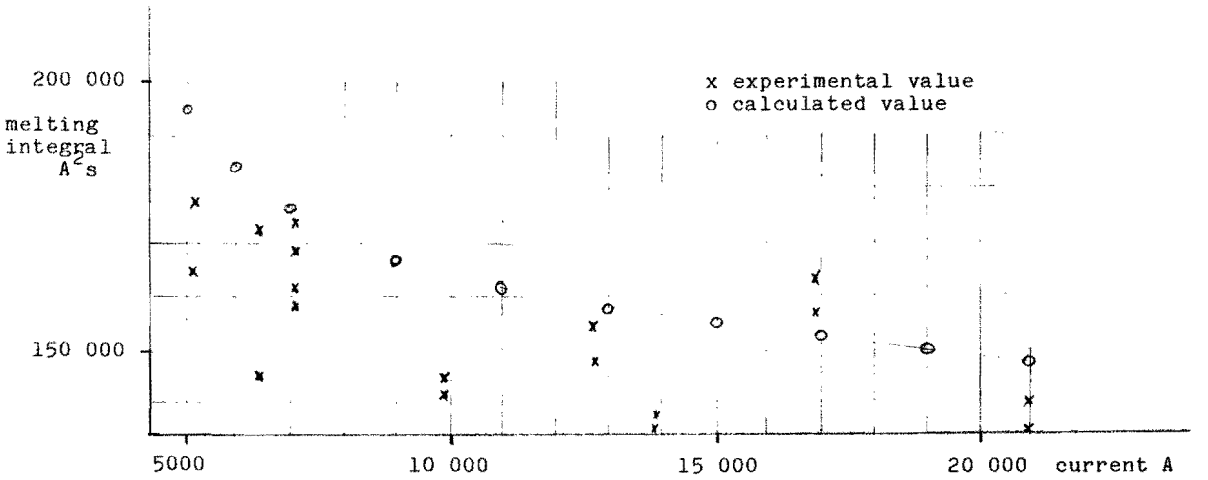

Literature:

1 D'Ans Lax: Taschenbuch für Chemiker u. Physiker , Springer 1967
2 Ulich-Jost: Physikalische Chemie
3 Robert M. Eisberg: mathem. Physik für Benutzer programm.Taschenrechner , Oldenbourg 1978

Conference papers , Trondheim 1984:
4 H.G.Rex: calculations of adiabatic models

Conference papers , Liverpool 1976:
5 P.H.McEwan and L.Warren: survey of num. methods for solving time varying fuse equations
6 M.M.McEwan and R.Wilkins: a decoupled method for predicting time-current charact.of fuses
7 A.Hirose: mathematical analysis of breaking performance of current limiting fuses

Session II

PRE-ARCING PHENOMENA 2

Chairman: Dr. L. Wilkins

THE SIMULATION OF PREARCING CHARACTERISTICS OF FUSE ELEMENTS IN THE FINITE ELEMENT METHOD

Meng Xian-zhong Wang Ji-mei

Xi'an Jiaotong University
The People's Republic of China

Abstract

The authors use the finite element method to calculate the prearcing characteristics, theoretically explain the calculation results, compare the virtual t-I characteristic and the theoretical t-I characteristic consider the deviation very small and the method can be used in the fuse-element design.

1. INTRODUCTION

A lot of different methods have been developed for the simulation of prearcing characteristics of notched fuse elements with heavy short circuit currents, as is well known, the simulation is very sucessful, for example, the finite difference method (1). If the distributions of temperature and electric potential are taken into acount for different shapes of notched fuse-elements, the finite element method would be more convenient because of its process of boundary conditions, fuse-element geometry and the positive stiffness matrix, that is why the f.e.m. (finite element method) is used here. After the distributions are carried out, all the parameters required can be obtained to simulate the prearcing phenomena.

2. THEORETICAL ANALYSIS

2.1 General discription

As far as two dimensional electric current flow fields and temperature fields, general equations are:

$$\frac{\partial}{\partial x}(K_x\frac{\partial \phi}{\partial x}) + \frac{\partial}{\partial y}(K_y\frac{\partial \phi}{\partial y}) = f(x,y) + K_t\cdot\dot{\phi}_t \qquad (1)$$

$$\forall\ (x,y) \in \Omega$$

where K_x, K_y, K ——conduction coefficient, K_t——damped coefficient, ϕ——potential function, $\dot{\phi}$ ——derivative of potential function, Ω ——calculation region.

boundary conditions:

$$\phi = \phi(x,y,t) \qquad t > 0, \quad \text{on} \quad \Gamma_1$$

$$K_x\frac{\partial \phi}{\partial x}n_x + K_y\frac{\partial \phi}{\partial y}n_y + q(x,y,t) = 0 \qquad t > 0, \quad \text{on} \quad \Gamma_2$$

$$\Gamma = \Gamma_1 \cup \Gamma_2 \qquad (2)$$

initial conditions:

$$\phi = \phi_0(x,y) \quad t = 0, \quad \forall(x,y)\in\Omega \quad \dot{\phi} = \xi_0(x,y) \quad t = 0, \quad \forall(x,y)\in\Omega \qquad (3)$$

By using the f.e.m. (2), the following equations can stem from (1),(2),(3).

$$[K_t]^{(e)}\{\dot{\phi}\}^{(e)} + [K]^{(e)}\{\phi\}^{(e)} + \{R_1(t)\}^{(e)} = \{0\}^{(e)}$$

Where

$$K_{tij} = \int_{\Omega^{(e)}} K_t\cdot N_i\cdot N_j \, d\Omega^{(e)}; \quad K_{ij} = \int_{\Omega^{(e)}} (K_x\cdot\frac{\partial N_i}{\partial x}\cdot\frac{\partial N_j}{\partial y} + K_y\frac{\partial N_i}{\partial y}\cdot\frac{\partial N_j}{\partial y})\cdot d\Omega^{(e)}$$

$$R_{1i} = \int_{\Omega^{(e)}} f\cdot N_i\cdot d\Omega^{(e)} + \int_{\Gamma_2^{(e)}} q_i\cdot d\Gamma_2^{(e)}$$

The resultant equation is

$$[C]\cdot\{\dot{\phi}\} + [K]\cdot\{\phi\} = \{R(t)\} \qquad (4)$$

Where [C] —— Thermal capacity matrix (or damped matrix);
[K] —— Stiffness matrix; [R(t)] —— Right hand vector.

Supposing that $t_\theta = t_n + \theta\cdot\Delta t$, $\{\dot{\phi}\}_\theta = (\{\phi\}_{n+1} - \{\phi\}_n)/\Delta t$;

$$\{R(t_\theta)\} = (1-\theta)\{R(t)\}_n + \theta\{R(t)\}_{n+1} \ ; \quad \{\phi\}_\theta = (1-\theta)\{\phi\}_n + \theta\{\phi\}_{n+1}$$

According to (4) we get

$$[C]\cdot\{\dot{\phi}\}_\theta + [K]\{\phi\}_\theta = \{R(t_\theta)\} \ (5) \text{ and } \quad [\bar{K}]\{\phi\}_{n+1} = [\bar{R}]_{n+1} \qquad (6)$$

Where $[\bar{K}] = \theta[K] + 1/\Delta t \cdot [C]$; $[\bar{R}]_{n+1} = \{-(1-\theta)[K] + 1/\Delta t \cdot [C]\} \cdot \{\phi\}_n + (1-\theta) \cdot \{R\}_n + \theta\{R\}_{n+1}$.

$\{\phi\}_{n+1}$ is unknown array and other parameters are known , so the equation (6) is solvable.

2.2 The electric current flow field

When electric currents flow through the fuse-element, the electric potential equation is stated as follows:

$$\frac{\partial}{\partial x}(\gamma\frac{\partial \phi}{\partial x}) + \frac{\partial}{\partial y}(\gamma\frac{\partial \phi}{\partial y}) = 0$$

Because of the symmetry of the fuse-element as shown in Fig. 1 (A), the calculation region may be greatly simplified into Fig. 1 (B) and the current direction is taken as that of X-axis.

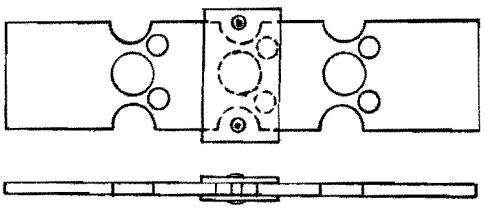

Fig. 1 (A) Fuse-element

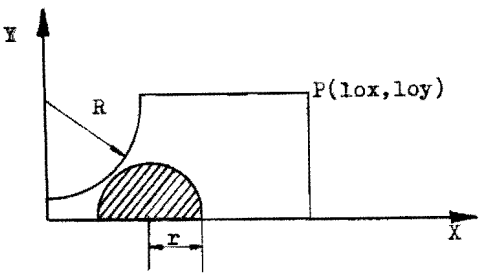

Fig. 1 (B) Calculation region

Considering the geometry of the fuse-element, Lox > R, Lox > r, in order to decrease the calculation time, supposing

$$\phi\big|_{x=0} = 0, \quad \gamma\frac{\partial \phi}{\partial x}\Big|_{x=lox} = J_0$$

where J_0 is a constant determined by the transient current through the fuse-element.

$\gamma\frac{\partial \phi}{\partial n} = 0$ on the other boundaries therefore the electric potential distribution satisfies the following equation:

$$\frac{\partial}{\partial x}(\gamma\frac{\partial \phi}{\partial x}) + \frac{\partial}{\partial y}(r\frac{\partial \phi}{\partial y}) = 0, \qquad \phi\big|_{x=0} = 0, \qquad \gamma\frac{\partial \phi}{\partial x}\Big|_{x=lox} = J_0 \tag{7}$$

It is the special form of (1),(2),(3), after solving $\{\phi\}$, the electric strenth and the current density distribution can be gotten from $E_x = -\partial\phi/\partial x$, $E_y = -\partial\phi/\partial y$, $J_x = \gamma E_x$, $J_y = \gamma E_y$. For the simplicity, is taken as only a function of the position or the local temperature, during the melting of the fuse-element, the resistance coefficient is greatly changable, it is therefore not suitable that γ is considered not to vary with the time variable, at least, it would lead to a large model error. The heat energy produced by the current heating effect in dv at any point p(x,y) in the unit time and volume is

$$q(IE) = \gamma E_x^2 + \gamma E_y^2 \tag{8}$$

2.3 The temperature field of the fuse-element

The heat conduction equation (2), (3) is

$$\rho C\frac{\partial T}{\partial t} = \frac{\partial}{\partial x}(K_x\frac{\partial T}{\partial x}) + \frac{\partial}{\partial y}(K_y\frac{\partial T}{\partial y}) + \frac{\partial}{\partial Z}(K_z\frac{\partial T}{\partial z}) + q'(x,y,z,t) \tag{9}$$

it is difficult to precisely and directly calculate the temperature distribution of the fuse-element and its temperature field in the media (fillers), because the caps, tags and fillers surrounding the fuse-element and the surrounding temperature in the media influence on thermal fields, especially the precise thermal data of fuse fillers are lack.

In addition, there are some more problems in the calculation of long time transient fields which need to be solved, for example, the stability of solution, the velocity of convergence and the cost of calculation (cpu time), what is more, the coupled two dimensional problems with the electric field.

We start with the penetration depth to discuss how to simplify equation (9). The penetration depth of thermal fields:

$$\delta(t) = \sqrt{12\alpha_0 t}, \qquad \alpha_0 = K/\rho C \tag{10}$$

where t is time variable for copper, silver, quartz and PTFE, we can get the following results:

$$\alpha_{o\,Cu}/\alpha_{oq} = 419.036, \quad \delta_{Cu}/\delta_q = 20.47 ; \quad \alpha_{o\,Ag}/\alpha_{oq} = 625.62, \quad \delta_{Ag}/\delta_q = 25.012$$

$$\alpha_{oF}/\alpha_{oq} = 2.38365 - 0.76778 ; \qquad \delta_q/\delta_F = 2.6055 - 1.30245$$

A. It is obvious that for small time or short circuit current, comparing δ_{cu}, δ_{Ag} with δ_q neglecting δ_q can't cause large error, the range of time depends on the fuse geometry and the calculation accuracy required. In other words, within this range, three dimensional heat conduction equation can be deduce to two dimensional heat conduction equation.

B. For medium and long time overload, we take the surfacial dissipated coefficient into acount which can be obtained from the experimental results, this item is apt to take part in the f.e.m. equations.

Another method for long time overload is to use semi-experienced formula which is based on the f.e.m. and the heat conduction theory.
In case B, we must describe the item $-\int_{\Omega^{(e)}} \mu \cdot N_i d\Omega^{(e)}$ and put it into R_{1i}. Up to now, we can get the following equations;

$$\rho C\frac{\partial T}{\partial t} = \frac{\partial}{\partial x}(K_x\frac{\partial T}{\partial x}) + \frac{\partial}{\partial Y}(K_y\frac{\partial T}{\partial y}) + q'(x.y.t)$$

$$K\frac{\partial T}{\partial n}(x,y,t) = q_B \ ; \qquad T(x,y,0) = C_0 \tag{11}$$

The general calculation region is shown in Fig. 1 (B). We don't consider the conduction among the symetric sections of fuse elements. With short circuit current, $q_B = 0$, that means the heat conduction doesn't exist in the element symetric lines and on the contact surfaces between fillers and the fuse-element or covered materials, if any, and the fuse element. In general, q_B depends on the surfacial state of heat discipation and $q_B \neq 0$ (related to μ), C_0 indicates the initial temperature distribution and takes a constant. We also give K_x, K_y, ρ, C constant values respectively before the fuse-element melts.

3. PHASE CHANGE ALGORITHMS

When electric currents flow through the fuse-element, the element and the media around are heated due to Joule effect, and the temperature rises, if the energy put into the element is more than that discipated, the element temperature will go high, while the temperature is up to or above the melting point of the fuse-element, the solid-liquid phase change occurs, if it continues, maybe the liquid-gas phase change will take place.
As a basic element, the triangle element is used here, the average temperature of the local element or division element:

$$T_{ave.} = 1/3\sum_{i=1}^{3} T_i, \qquad \Delta T_m = H_m/C_{ps} \tag{12}$$

for each triangle element, when T_{ave} exceeds T_m, it should be changed to T_m, and write down $(T-T_m)$ or (T_i-T_m). If $(T-T_m) \geqslant \Delta T_m$, the temperature of local element is admitted to increase in normal way, for each node, it is similar. Further more, the similar algorithm is suitable for the vaporization and M-spots.
It is hard to say shen notched elements begin to arc, because the initial arc is related to the electric current density, the fuse-element geometry, the properties of materials and so on. We suppose that arc occurs when the temperature of local element begins to rise after the melting of the local region, therefore the temperature lies in the range of T_m to T_a or more high.
The prearcing virtual time $t_v = \int i^2dt \ / \ I_p^2$ (13)
The calculation results prove that it is true.

4. PROGRAM DESIGN

The diagram (see Fig. 2) shows us how to finish the simulation work in f.e.m. Fig.2(B) gives the block for CURRENT DISTRIBUTION AND TEMPERATURE DISTRIBUTION. All the programs are written in FORTRAN 77 running well in Dps 8/52 in COMPUTER CENTER of Xi'an Jiaotong University, China.

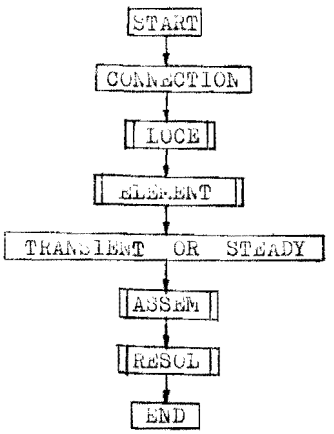

FIG. 2 (B) BLOCK DIAGRAM

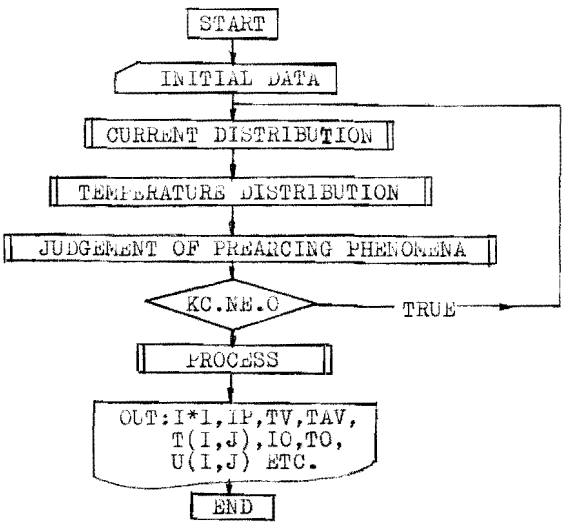

FIG. 2 (A) BLOCK DIAGRAM

5. THE FORMULA FOR LOW OVERLOAD

we recommand a simi-experienced formula which is suitable for the fuse-element with M-spots and covered materials throughlow overload currents.
The virtual time $t_v = t_m + t_r$, where t_r depends on the following equations:

$$\vartheta = \frac{I_p^2}{I_c^2}\cdot T_w(1-e^{-t_r/\tau}); \quad \tau = \rho C T_w / C_e.I_c^2\cdot\rho_0(1-\eta) \ ; \quad T_w = K_0(T_{sold} + H_m/C_{pl}) \tag{14}$$

where C is specific heat, C_e is f.e.m. division coefficient, η is heat discipated coefficient from the specified elements and τ is time constant, $0 \leqslant K_0 \leqslant 1$.

The M-effect time $t_m = Z^2/N_p \cdot D$ (15)

where N_p is the distribution coefficient, Z is the element thickness and D is the diffusion coefficient. If $\upsilon = (T_{sold} + H_m/C_{pl})$, it is said that the melted M-spots will flow along the element to the neck and cause the rupture of the fuse element due to M-effect.

6. APPLICATIONS

The programs in f.e.m. and the formula (14), (15) have been used to simulate the prearcing phenomena of a type of full range fuses and got some sucessful results given in figures (from Fig. 3 to Fig. 10), the element of which is shown in Fig. 1 (A). The fuse rated current and voltage are respectively 63A and 500V. For different shapes of elements, the parameters needed to be changed are the f.e.m. division grid and physical data of the fuse-element, so it is very convinient for users and designers to use this method to simulate.

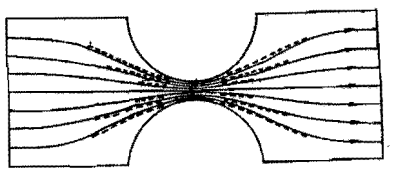

Fig. 3 Current flow distribution

——— Distribution in cold state

----- Distribution in hot state

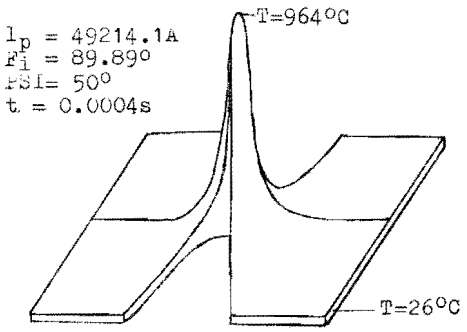

Fig. 4 Temperature field with short circuit current

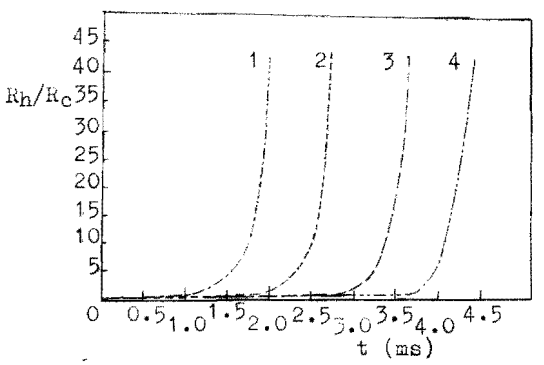

Fig. 5 Hot state R_h/Cold state R_c VS time

Curve 1 I_p = 5001.33A, ϕ = 88.78°, ψ = 67°

Curve 2 I_p = 3889.69A, ϕ = 88.79°, ψ = 60°

Curve 3 I_p = 2500,67A, ϕ = 88.96°, ψ = 47°

Curve 4 I_p = 1750.57A, ϕ = 89.16°, ψ = 47°

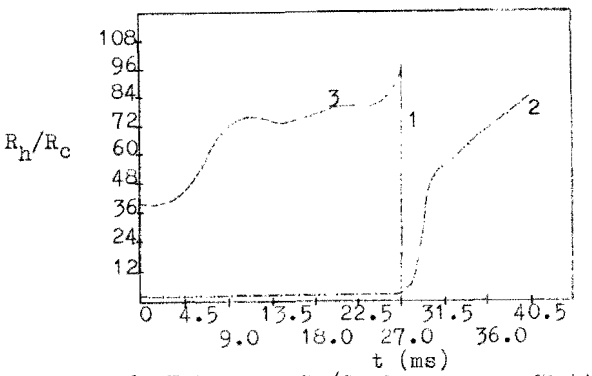

Fig. 6 Hot state R_h/Cold state R_c VS time

I_p = 580.32A, φ = 83.94°, ψ = 56°

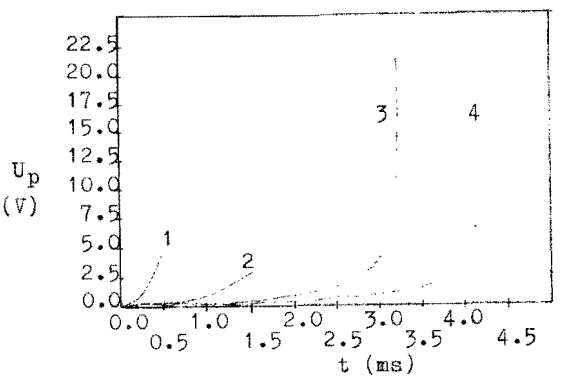

Fig. 7 Prearcing voltage VS time

Curve 1 I_p = 50021.5A, φ =89.89°, ψ = 67°

Curve 2 I_p = 8753.50A, φ =89.91°, ψ = 60°

Curve 3 I_p = 3070.92A, φ =88.82°, ψ = 40°

Curve 4 I_p = 1750.57A, φ =89.16°, ψ = 47°

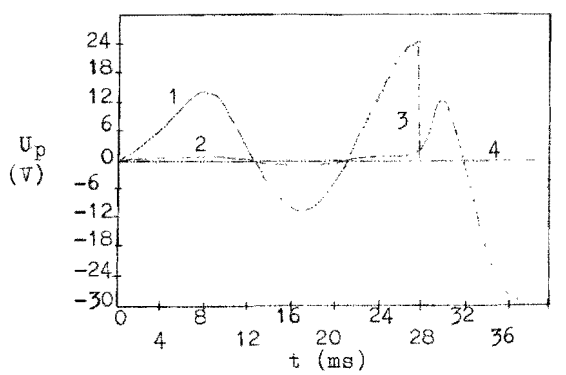

Fig. 8 Prearcing voltage VS Time

I_p = 580.32A, φ = 83.94°, ψ = 56°

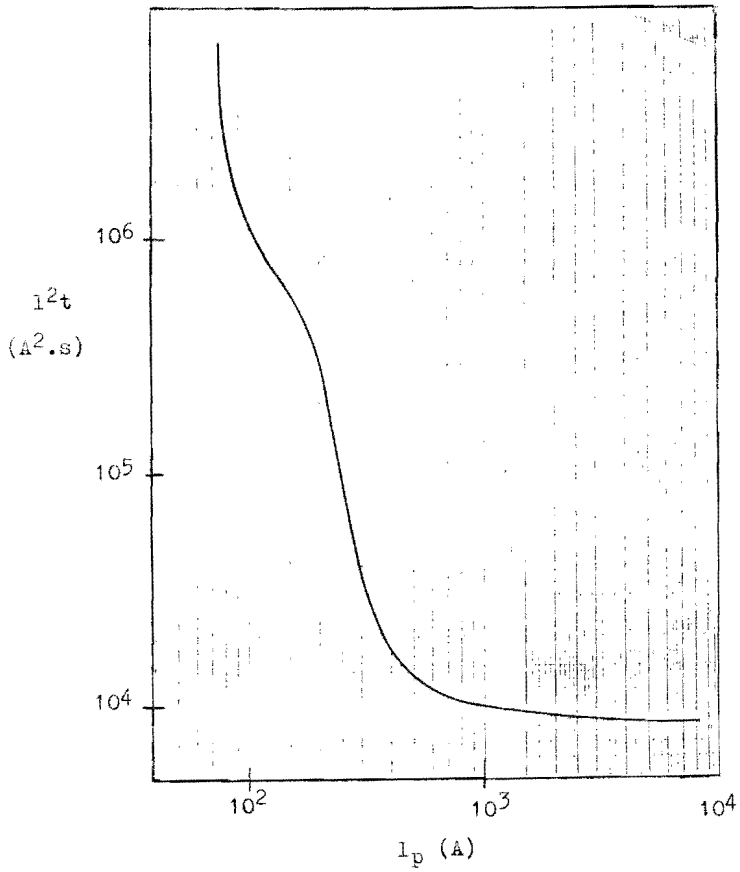

Fig. 9 I^2t - I_p characteristic

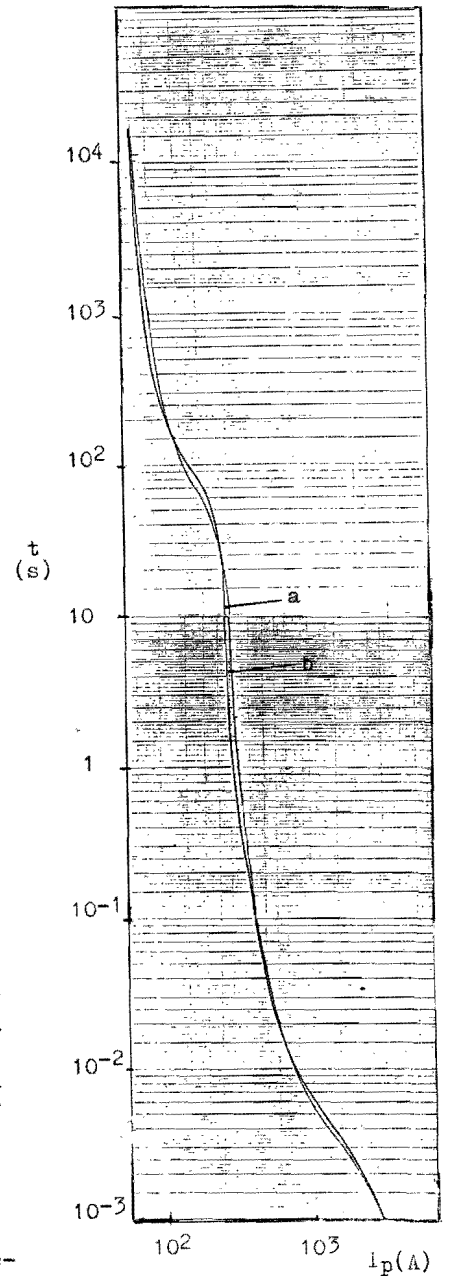

a. theoretical curve
b. test results

Fig.10 t—I characteristic

7. DISCUSSION

Fig. 2 is suitable for current fields and temperature fields of the fuse-element on principle, in oder to reduce the CPU time, small time steps Δt are taken to solve the two set of equations respectively for compensation.

It will be seen from Fig. 3 that the current flowing through element is concentrated towards the edge with time, especially in the constrictions. The reason for which is that the temperature in this region is lower than that in the middle of the element, so the resistantivity in the middle is greater.

Fig. 5 and Fig. 6 prove that the larger the prospective current, the smaller the time when the ratio of the heat resistance to the cold resistance begins to increase extremely. In other words, the prearcing time is smaller for a larger prospective current. The similar cases exist in the variation of the pre-arcing voltage shown in Fig. 7 and Fig.8. In the breaking tests of low overload currents several changes of pre-arcing voltage are observed by the indicator, before elements melt. There are three times of the voltage increase, this is a indirect evidence of the calculation results. I^2t-I_p characteristic of the single element is given in Fig. 9. While $I_p > 3000A$, the value of I^2t is kept constant, nearly having nothing to do with I_p, when $I_p < 1000A$, the value of I^2t increases rapidly as the prospective current I_p decreases, at the neighbour of 180A, as I_p decreases the value increases slowly, as I_p approaches $1.25I_n$, the value increases rapidly too. It is considered that M-effect has great influence in the range of $1.25I_n$ to 180A, when $I_p$has the lowest value, which is near the MFC, therefore I^2t has a large value, the heat conduction of element is in action from 200A to 2000A, however, for the large prospective current ($I_p > 3000A$), the adiabatic process is under control.

The comparasion has been made in Fig. 10 between the theoretical curve and tested results. It proves that the deviation between the two is small and the calculation results are helpful for future test.

8. CONCLUSION

The method above may be used to simulate the pre-arcing phenomena of the fuse-element and the acceptable accuracy is achieved in calculation and good correlation is obtained between calculated and measured values of cold resistances and t-I characteristics. Therefore the method could be used in CAD of fuses.

LIST OF PRINCIPAL SYMBOLS

K_x, K_y, K conduction coefficient;
K_t damped coefficient;
ϕ potential function;
$\dot{\phi}$ derivative of potential function;
Ω calculation region;
N_i shape function;
γ electric conductivity;
E electric field strength;
J current density;
IE division number;
ρ mass density, resistantivity;
C thermal capacity, specific heat;
μ surfacial heat discipated coefficient;
C_e f.e.m. division coefficient;
η heat discipated coefficient from the specified elements to tags and end caps.

APPENDIX

PHYSICAL DATA FOR COPPER

ρ_0 resistantivity at the room temperature 1.6961×10^{-6} Ω.cm;
ρ_{01} resistantivity in liquid phase at melting point 21.3×10^{-6} Ω.cm;
α resistance temperature coefficient 0.0045 $^{o}C^{-1}$;
T_m melting point 1084.5 ^{o}C;
H_m melting latent heat 211.4 $J.g^{-1}$;
T_a vaporization temperature 2543 ^{o}C
H_A vaporization latent heat 4752.16 $J.g^{-1}$
K thermal conductivity 4.01 $w.cm^{-1}.^{o}C^{-1}$;
ρ density 8.93 $g.cm^{-3}$;
C_{ps} specific heat in solid state 0.385 $w.s.g^{-1}.^{o}C^{-1}$.

PHYSICAL DATA FOR M-SPOTS

T_{sold} melting point 227-231.9 ^{o}C ;
H_s melting latent heat 60.66 $J.g^{-1}$.

OTHER DATA

$K_o = 0.9$, $\tau = 1089$, $I_c = 73A$, $D = 10^{-4}$-10^{-6} $cm^2.s^{-1}$.

REFERENCES

(1) J. G. Leach, P. G. Newbery and A. Wright: "Analysis of high-rupturing-capa bility fuse-link pre-arcing phenomena by a finite-difference method". Proc. IEE, pp987, 1973
(2) Dhatt Canada, Touzot France: "The finite element method displayed". /a book/, 1984
(3) Meng Xianzhong: "Research on low voltage full-range fuse and its pre-arcing characteristics". Master-thesis, Xi'an Jiaotong University, 1986.

Pre-calculation of time/current characteristics of "M"-effect fuse elements

M. Hofmann and M. Lindmayer

Abstract

A finite element method is used for a fuse element model and for the calculation of the time/current characteristic. The basic data which are needed for the calculation consist of material data (electrical conductivity, thermal conductivity, heat capacity, convection and radiation coefficients) and data which describe the dissolution processes related to the "M"-effect. The data concerning the dissolution behaviour between solder and fuse element metal were gained from micrographs of heat treated fuse elements. These fuse elements were exposed to different temperatures and times in a furnace in order to measure the dissolution depth. These dissolution process data were integrated into the program at each calculation time step.

The results of the calculation carried out for a Cu fuse element with tin solder show good agreement in a melting time range between 12 s and 200 min at overload currents.

1. Introduction

In "M"-effect fuses the dissolution of the base metal (Cu, Ag) by a deposit of soft solder is utilized to adjust the time/current characteristics in the overload range. The current heating of the fuse element causes melting of the solder spot and a dissolution process starts. This dissolution leads to a reduced cross section of the base metal. The dissolution behaviour is dependent of the load current because the effective remaining cross section, the resistance, the temperature and the dissolution velocity mutually influence and enhance each other. The fusing time lies in a range between some seconds and several hours.

Up to now no attempts to calculate the time/current characteristic in this time range are known.

Good solutions exist for the calculation of the time/current characteristics of fuse elements without "M"-effect for fusing times up to 100 seconds. Especially McEwan and Wilkins /1-3/ have done a lot of work in this field by using a finite difference method.

Earlier investigations /4/ with Cu fuse elements with Sn-solder spot showed that it is possible to calculate the dissolution depth when the fuse element is annealed at constant temperatures (without current load). Fig. 1 shows an example, the dissolution depth $\bar{x}$ starts at $t = 0$ with a steep increase and reaches a saturation value after some time. This saturation value can be derived from the saturation concentration for Cu in liquid Sn according to the liquidus line in the Cu-Sn phase diagram.

Other tests /5/ were performed with cyclic current load of Cu fuse elements with Sn solder. It was found that in each load cycle the dissolution only proceeds during the time span in which the maximum temperature of the preceding cycle is exceeded. This and the results of /4/ showed that the fuse element temperature is the ruling factor of the fusing behaviour caused by the "M"-effect.

Dipl.-Ing. M. Hofmann and Prof. Dr.-Ing. M. Lindmayer
Institut für Elektrische Energieanlagen
Technische Universität Braunschweig
D-3300 Braunschweig, Germany

The calculations of the time/current characteristic were carried out using the finite element program ADINAT /6/*.

The calculation is based on the heat flow equation:

$$\operatorname{div}(\lambda \cdot \operatorname{grad} T) = -q_G + c\,\frac{\partial T}{\partial t} \tag{1}$$

The solution of this problem with the finite element method (FEM) leads to the variation-integral, which is solved by ADINAT:

$$\Pi = \int_V \frac{1}{2} \cdot \lambda \cdot \left[\left(\frac{\partial T}{\partial x}\right)^2 + \left(\frac{\partial T}{\partial y}\right)^2 + \left(\frac{\partial T}{\partial z}\right)^2 \right] \cdot dV - \int_V T \cdot \left(q_G - c \cdot \frac{\partial T}{\partial t}\right) \cdot dV + \int_A T \cdot q_{ks} \cdot dA \tag{2}$$

with:
- Π variation integral
- λ heat conductivity
- T temperature
- x,y,z coordinate axes
- V volume
- q_G internal generated heat per unit volume (ohmic heating of the fuse element)
- c heat capacity per unit volume
- t time
- A surface
- q_{ks} heat flow at surface A

q_G can be described by

$$q_G = j^2 \cdot \rho\,(T) \tag{3}$$

where j is the current density and $\rho(T)$ the temperature dependent specific resistance.

q_{ks} can contain a convection term q_k and/or a radiation term q_s.
q_k is defined by equation (4):

$$q_k = h \cdot (T_U - T) \tag{4}$$

and q_s is analogous to equation (4):

$$q_s = \kappa \cdot (T_R - T) \tag{5}$$

with:
- h convection coefficient
- κ radiation coefficient
- T_U surrounding temperature
- T_R temperature of external radiation sink
- T element/node temperature

κ is defined by the following equation:

$$\kappa = \sigma \cdot \varepsilon \cdot f \cdot (T_R^2 - T^2)\,(T_R + T) \tag{6}$$

---

* ADINAT (A Finite Element Program for Automatic Dynamic Incremental Non Linear Analysis of Temperatures) for the linear and nonlinear, steady state and transient finite element analysis of heat transfer - and temperature field problems in dependence of linear and nonlinear material properties.

with: σ Stefan-Boltzmann constant
ε emission factor
f form factor

2. Solution with the FEM-program ADINAT

ADINAT calculates the temperature distribution and the temperature/time curve respectively. The calculation is stopped when one of the following criteria is fulfilled:

a) The maximum fuse element temperature becomes greater than the melting temperature of the base metal.

b) The base metal beneath the solder is fully dissolved in the liquid solder at one place.

Fig. 2 shows a schematic diagram of the calculation.

The input block starts with the input of the control data (no. of nodes, element groups, time increment, starting time) and calculation data (convergence criterion, time integration method, etc.). Then the number of time increments, the nodal data, the starting conditions and the heat flow input data (esp. the time functions) are defined. The time functions describe the generated ohmic heat per volume $j^2 \cdot \rho(T)$ for every single element at all times and temperatures. The input block is terminated with the assignment of the material property data to the elements. The material property data (specific resistance, heat conductivity, heat capacity) were chosen according to fig. 3. The convection coefficient h (equation (4)) was chosen $h_o = 1{,}2 \cdot 10^{-6}\,W/mm^2 \cdot K$ for the upper and side surfaces of the fuse element and $h_u = 6{,}5 \cdot 10^{-9}\,W/mm^2 \cdot K$ for the underside. Considering the Cu oxidation the emission factor was set to rise from $\varepsilon = 0{,}1$ to $\varepsilon = 0{,}6$ in a temperature range from 20 °C to 600 °C and $\varepsilon = 0{,}6$ at $T \geq 600$ °C. The form factor f (equation (6)) is set to 1 because all radiation is absorbed by the environment. At the fuse element terminals the temperature random condition is T = const = 20 °C.

The analyzing program integrates an additional iterative loop into ADINAT. This loop computes the correction of the time functions. The time functions, i.e. the generated power at each element, are not known at the start, because they are a function of the specific resistance ρ and hence of the temperature. The calculation therefore starts with estimated time functions. Each run of ADINAT yields the temporal and local dependence of the temperature. After each run the time functions are corrected according to the calculated temperatures in a loop outside ADINAT until a given temperature difference between two iterations is not exceeded. After this iteration the diffusion process at the solder is taken into account in a second loop outside ADINAT, as shown later.

3. Example: Cu fuse element without constriction/with Sn-solder surrounded by air

Fig. 4a shows the dimension of the simple straight fuse element, the test arrangement is described in /4/.

The FEM-model (fig. 4b) represents geometrically a quarter of the real fuse element. The asymmetric position of the solder is neglected, that means it is assumed that the solder is about 8 mm long. All elements range over the whole fuse element thickness.

The thickness dimensions of the solder area are relatively small, so it could be assumed that a fast heat balance within the solder and the base metal thickness occurs. Therefore in the solder area the electrically and thermally conducting path as well as the ohmic heat

generation can be replaced by a body of a constant thickness equal to the base metal thickness, but with material data adjusted to the decreasing base metal and increasing solder cross section. In detail this is achieved as follows:

Estimations show that the current and heat flow within the original solder of thickness d_{Sn} can be neglected. Within the total base metal thickness (0.2 mm) there are two parallel paths consisting of the remaining copper of thickness $d_{Cu} - x$ and the dissolution depth x.

The equivalent electric resistivity then reads

$$\rho = \frac{\rho_x \cdot \rho_{Cu} \cdot d_{Cu}}{\rho_x \cdot (d_{Cu} - x) + \rho_{Cu} \cdot x} \tag{7}$$

The heat conductivity and heat capacity are treated analogously.

Fig. 1 shows that the beginning of dissolution at a fixed temperature can be described by a nearly constant dissolution velocity. Assuming that no saturation occurs because of the steady increase of the resistance and the temperature the dissolution can be approximated by that value $v = dx/dt$ at $t = 0$. In fig. 5 this dissolution velocity is plotted as a function of temperature. Intermediate values are interpolated linearly between the measured values.

In the beginning the temporal and local temperature dependence is calculated without considering the dissolution. When the solder melting point is exceeded, an increase Δx in dissolution depth is calculated for each time step according to

$$\Delta x = v\ (T_{Solder}) \cdot \Delta t \tag{8}$$

In the following time steps corrections of the materials properties and the watt losses in the solder area are made according to equation (7).

Fig. 6 is an example for such a calculation. In this case the initial transient heating which is short in comparison with the total fusing time was neglected. The temperature distribution at the beginning was assumed to have reached already equilibrium, hence the steady-state version of ADINAT could be used.

After switching on current the measured temperature at the solder increases within 1 minute to T = 335 °C, the melting point of Sn (232 °C) is reached already after t = 25 s. In a time range 1 min to 15 min the temperature increases only slightly from 335 °C to 400 °C. In this range the dissolution depth of the fuse element is relatively small (60 µm according to micrographs). At greater dissolution depth the changes in resistance become more important, so that the temperature, the resistance and the dissolution velocity enhance each other. Therefore a steep increase of the temperature occurs above 400 °C until the total copper thickness is dissolved. The measured temperature at this point is 740 °C, the melting point of Cu (1083 °C) is not reached. The measured fusing time is 20,6 min.

The result of the steady-state calculation at the beginning is a solder temperature of 330 °C, the further increase is a result of the stepwise dissolution calculation.

The total dissolution is reached after 21,6 min at T = 770 °C. The comparison shows a rather good agreement between measurement and calculation for the temperature-time dependence as well as for the fusing time.

Similar calculations were carried out for other currents. A result is the time/current characteristic (fig. 7). At I = 150 A, 160 A the fusing time becomes relatively small. Therefore the effect of the heat capacity was included in the calculation, which then takes into account the transient temperature rise. The agreement is generally good, except for 120 A. The deviation in terms of current is about 10 % in this area and below 3 % in the area around 100 A (fusing times around 1 to 3 hours).

Conclusions

The results show that it is possible to estimate the time/current characteristic of fuse elements with a solder spot by using a finite element method for the temperature field. The dissolution of the base metal into liquid solder is modelled by temperature-dependent dissolution velocity. The changing thickness of the base metal and solder respectively is replaced by appropriate material properties at the solder spot.

References

/1/ McEwan, P.M.: Numerical prediction of the pre-arcing performance of H.R.C. fuses
Thesis, Liverpool Polytechnic, 1975

/2/ Wilkins, R., McEwan, P.M.: A.C. short-circuit performance of notched fuse elements.
Proc. IEE 122 (1975), No. 3, p. 289-292

/3/ McEwan, P.M., Wilkins, R.: A decoupled method for predicting time-current characteristics of H.R.C. fuses
Int. Conf. on Electric Fuses and Their Applications, Liverpool, 1976

/4/ Hofmann, M., Lindmayer, M.: Fusing and ageing behaviour of fuse elements with "M"-effect at medium- and long-time overload
Int. Conf. on Electric Fuses and Their Applications, Trondheim, 1984

/5/ Hofmann, M., Lindmayer, M.: Alterungs-Verhalten von Sicherungsschmelzleitern bei zyklischen Überstrombelastungen
Int. Symp. on Switching Arc Phenomena, Lodz, 1985

/6/ - ADINAT - A Finite Element Program for Automatic Dynamic Nonlinear Analysis of Temperatures
Report AE 81-2 (1981)
ADINA Engineering AB, Västeras, Sweden

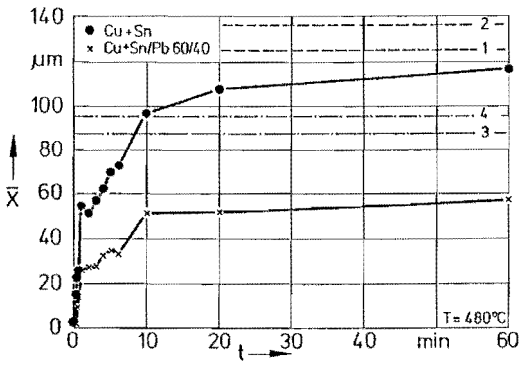

Fig. 1: Dissolution depth x as function of time t for different fuse elements

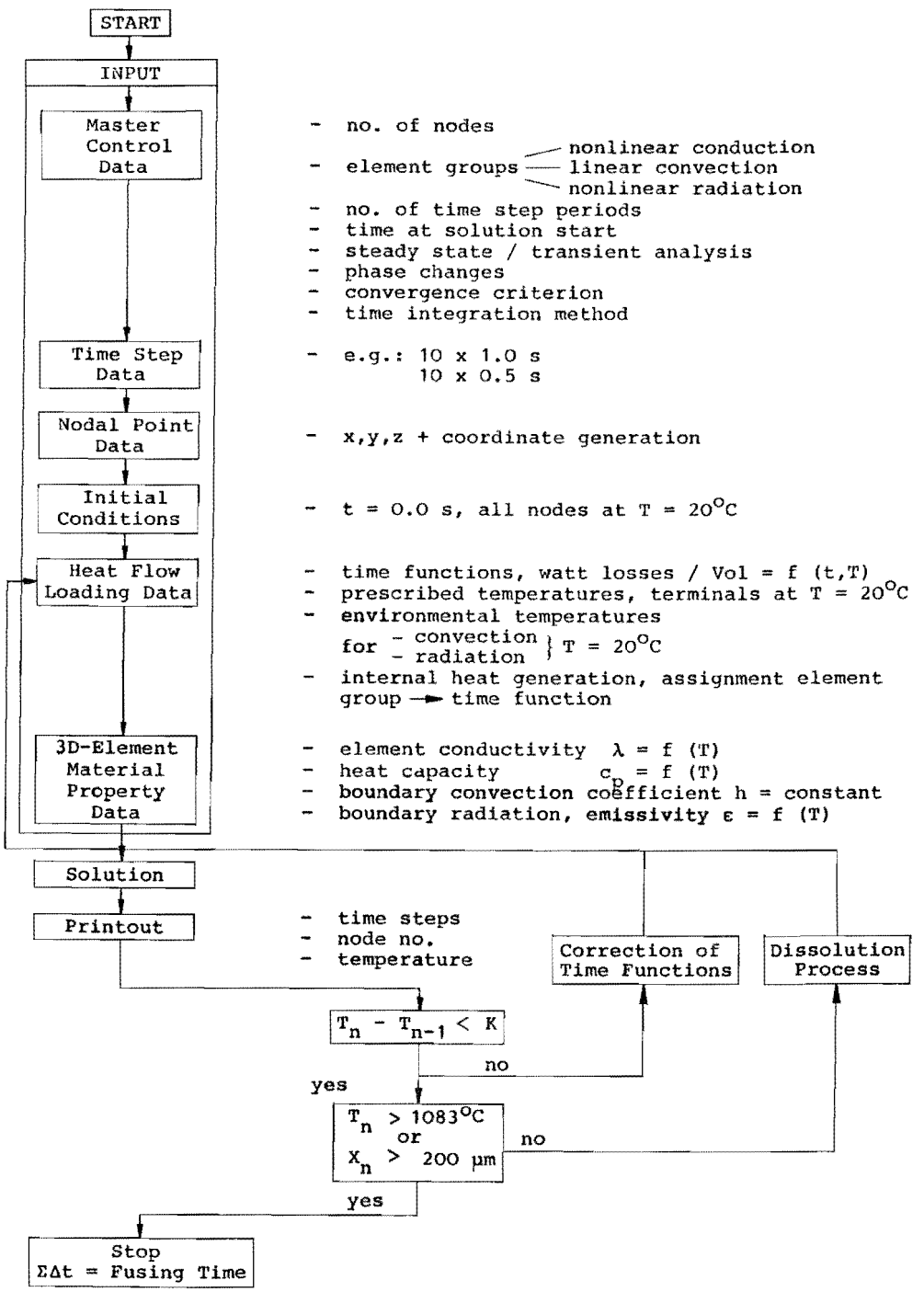

Fig. 2: Schematic diagram of the calculation

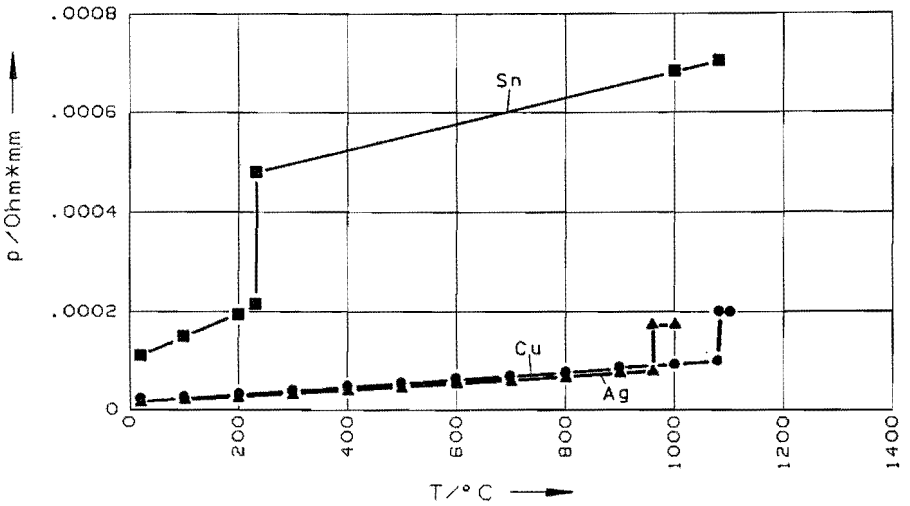

a) Specific resistance ρ as function of the temperature T

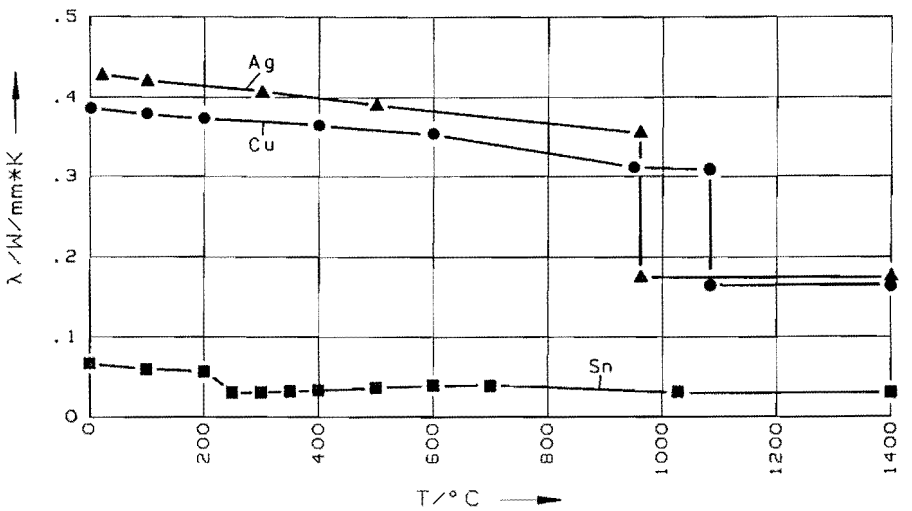

b) Heat conductivity λ as function of the temperature T

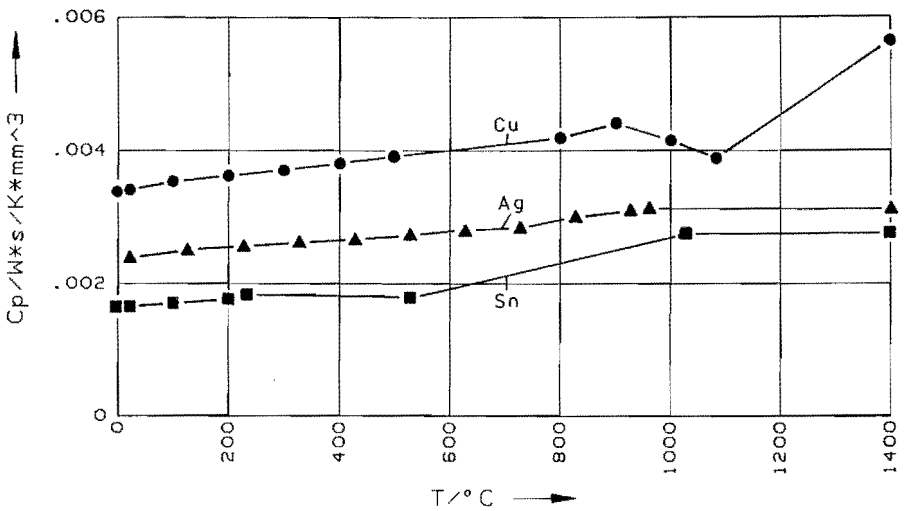

c) Heat capacity C_p as function of the temperature T

Fig. 3: Material property data of some important metals

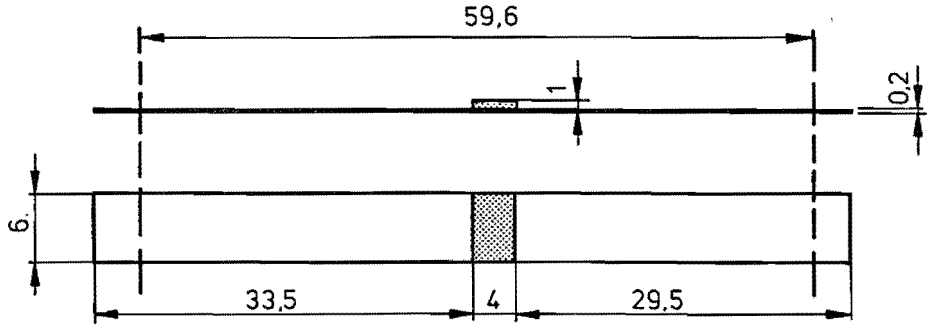

Fig. 4a: Dimensions of the straight fuse element with "M" - effect

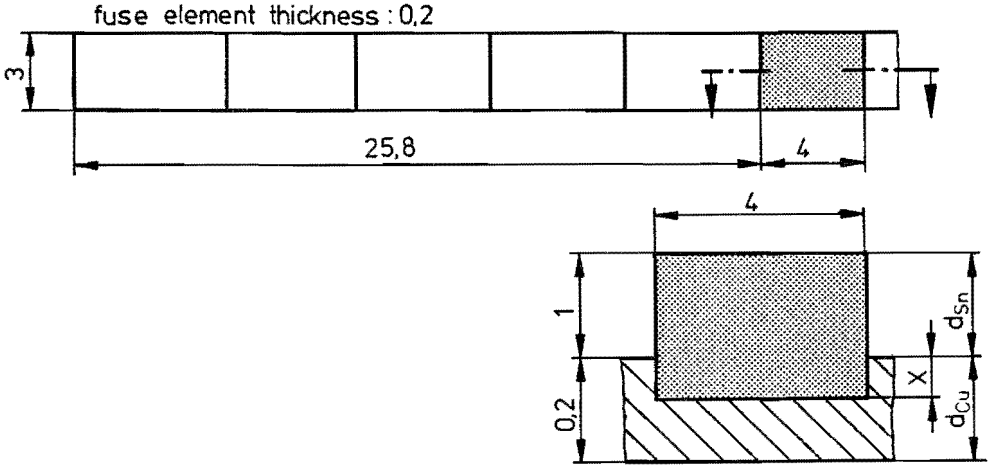

Fig. 4b: FEM - model of a straight fuse element with "M" - effect

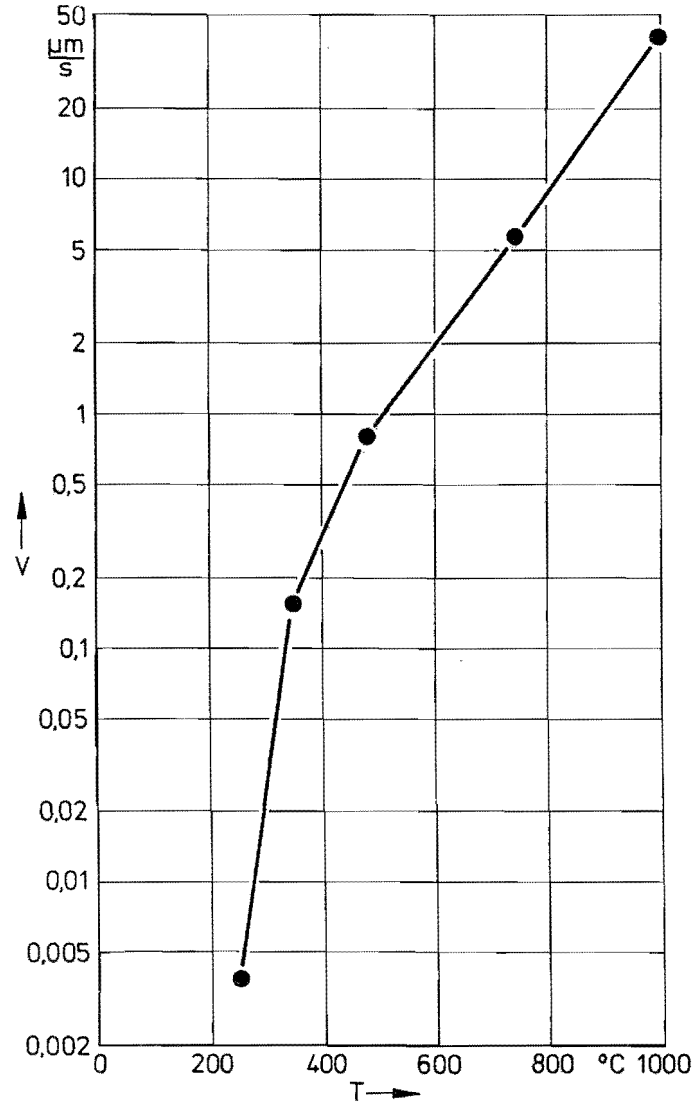

Fig. 5: Dissolution velocity v = dx/dt as function of the temperature T for Cu fuse elements with Sn solder spot

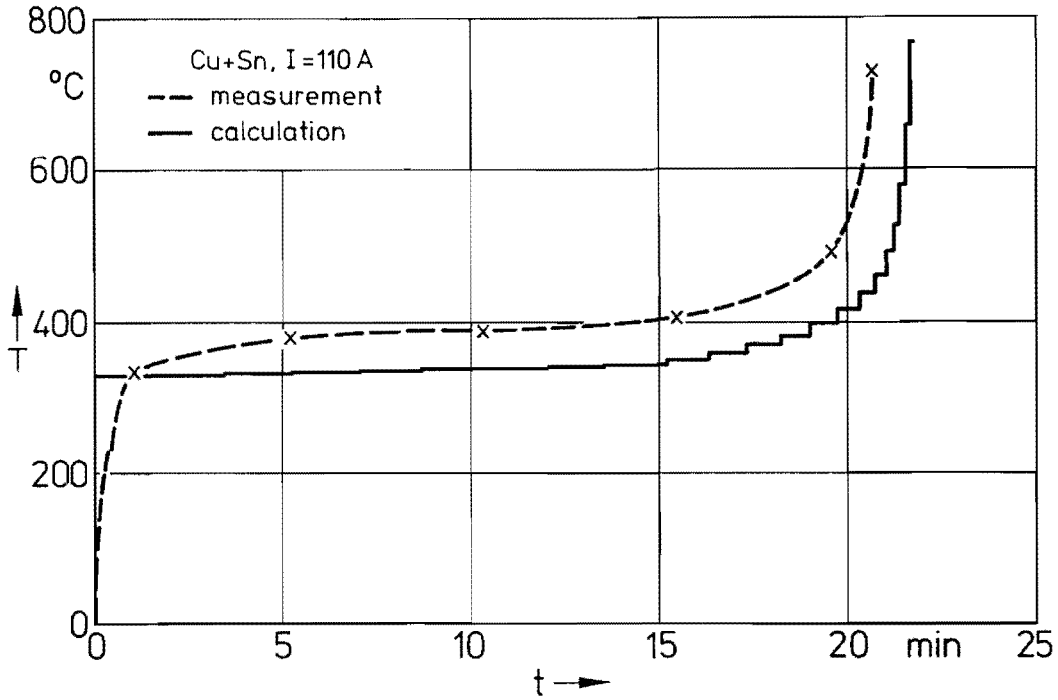

Fig. 6: Comparison of the calculated and measured temporal increase of the temperature T for Cu fuse elements with Sn solder spot at a load current I = 110 A

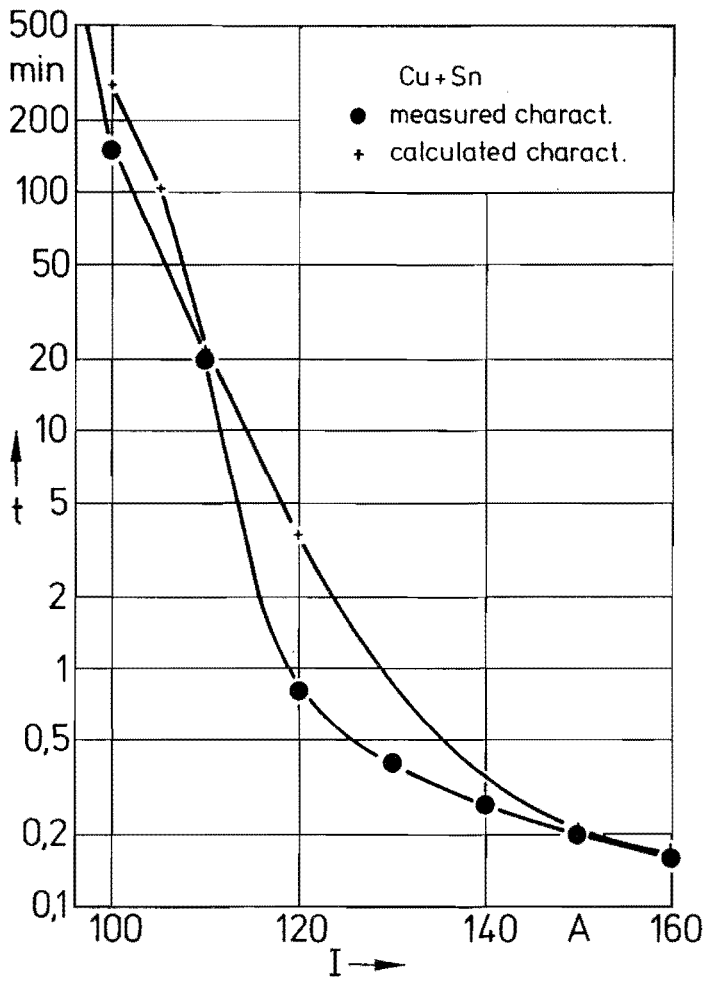

Fig. 7: Comparison of the calculated and measured time/current characteristics for the Cu fuse element with Sn solder spot

FUSE-ELEMENT - AGEING AND MODELING

Michel LAURENT - Laboratoire de Physique Industrielle
Bat.502 - Institut National des Sciences Appliquées F-69621 VILLEURBANNE

Pierre SCHADITZKI - Laboratoire de Recherches B.T. A.M.Ampère
SOCOMEC BP10 F-67230 BENFELD

Abstract :

As motor fault current protection the "gI" or "aM" fuses come sometime to prematurely melting, not in accordance with standards.

A better knowledge of the ageing mechanisms should permit to design new types of fuse element.
The cycle loading investigations on a 100A gI fuse (size 1 of IEC 269 Standard) were performed on a high power testing station.
Metallographie observations were made as a function of the fuse element ageing. The solder migration around the copper dissolutions explain the phenomena.
Then, to redure the ageing two possibilities appear :

- to prevent the solder migration
- to delay the dissolution time

All these possibilities require to know the temperature along the fuse element, therefore the heat transfers were modeled.

The temperature evolutions were calculated in the fuse element and in the sand.
The model validity was checked by comparing the calculated and experimental fuse time/current fonction.

FUSE-ELEMENT - AGEING AND MODELING

It often occurs that in the production units the fuses melt prematurely after several overloadings which, in accordance with the standards did not and should not lead to melting.
In order to study the fuses ageing, we have submitted them to overload cycles, and we first measured the variation of the electric withstand, according to the number of cycles. Then, we performed some metallographic observations at various stages of ageing. At least, we carried out the modeling of thermal transfers in order to know the distribution of temperatures within the fuse.

1. EXPERIMENTAL STUDY

The studied fuse is represented on figure 1. Its main characteristics are :

- fuse HPC according to standard IEC 269 gI 100A
- fuse element of copper + tin
- application voltage : 500V AC

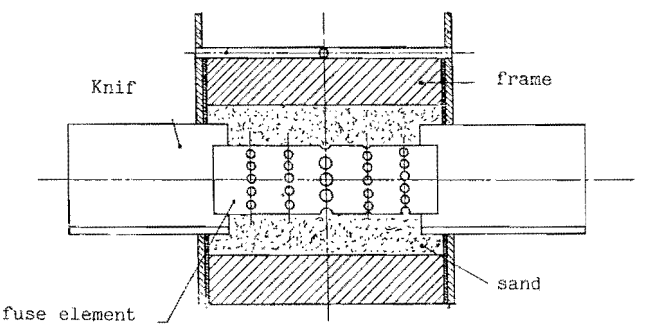

Figure 1

The fuses have been first submitted to repeated ageing cycles made of a load of 3xI = 300A during 1,82 s followed by a period of rest of 12 s. The time of 1,82 s corresponds to 0,9 times the average melting time for 12 fuses submitted to a load of 300 A. These cycles have been performed to a serie of fuses and the melting process occured for an average number of cycles N = 1614.

Then the resistance of 22 fuses submitted to these same cycles have been measured for $\frac{N}{2}$, $\frac{3N}{4}$, $\frac{7N}{8}$, cycles

First, we can notice that all fuses do not age in the same way, some melted prematurely. We nevertheless can note that according to the ageing, the resistance increases, then decreases and increases again before the melting process.
A metallographic study has been carried out in order to explain this behaviour.
For fuses with little developed ageing, the tin has melted, is oxydised and presents marks of sand grains and has barely migrated. On the surface, the copper is oxidised, especially in the areas between the holes. On the metallographics (figure 2) we can see that the copper presents the same volume as the copper of a new fuse. There are some toothlike imperfections in tin.
For fuses with more developed ageing, the tin is oxidised, it migrated and went to the other side through the central holes. Besides them, we can see toothlike imperfections near the copper (figure 3) together with a slight reduction of the fuse section. The remaining copper has not been modified.
For fuses with extremely developed ageing, the tin has completely limited the copper parts between the holes and it is oxidised. On the metallographics we can see that the copper is completely dissolved in the areas between the holes and has been replaced by tin with a great amount of toothlike imperfection (figure 4). These toothlike imperfection corresponds to the dilution of copper within tin. Regarding the volume, the remaining copper has not been modified.

The ageing is originated by the tin migration at the copper surface towards the areas between the holes and by the diffusion of tin within copper there seams not to be a grain sweling.
In a first step, the oxydation increases the withstand, then when the tin migrates into the inter-holes area, the copper is partly short-circuited, which decreases the resistance, then the copper dissolves which increases the resistance until the melting process.

Other tests have been carried out, at low constant overload (1,6xIn) for increasing durations and at high overload (10xIn) during 0,08 s followed by rests of 600 s, these cycles have been repeated until melting of one fuse of the range.
For these tests, the ageing processes occur the same way as those previously described.
In order to limit the ageing, it is possible :

- to treat the copper surface which makes it less wetable and which bothers the tin migration.
- to place a deposit at the copper surface wich acts as a diffusion barrier and which makes the copper dissolves slowlier.

These various possibilities require to know the distribution of the temperatures and therefore, we carried out a modeling of heat transfers in the fuse and sand which surrounds it.

Figure 2

metallographic little ageing copper-tin

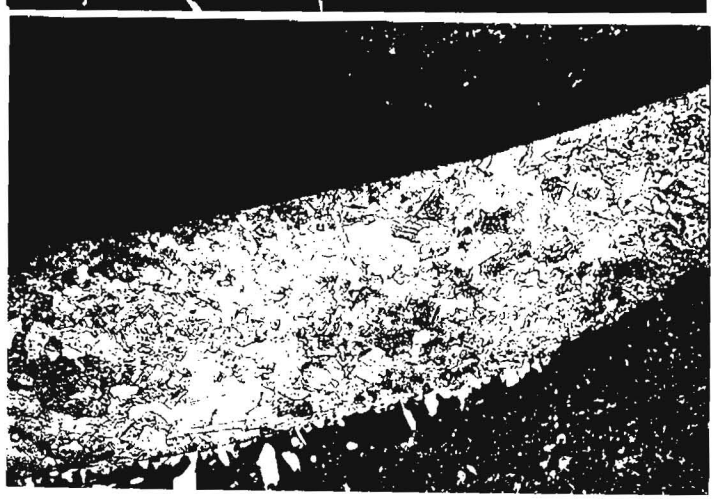

Figure 3

metallographic more developed ageing copper-tin

Figure 4

metallographic extremely developed ageing copper dissolved in tin

2. MODELING OF THE HEAT TRANSFERS

The power by length unit of the fuse is represented on figure 5. (For symmetrical reasons, the calculation has been made on a quarter of the fuse).
Each part of the curve P (Y) has the following shape : $P(y) = I^2 \left(A_{o+3i}\, y^2 + A_{1+3i}\, y + A_{2+3i} \right)$ $i = 0,1,2,3,4,5$

The parts at the holes levels are parabolic so that the maximum correspond to the powers extracted at the abscissa of the holes centers and so that the surfaces under the parabola are equal to the powers extracted at the holes level. The uniform parts represent the heat emission between the holes.

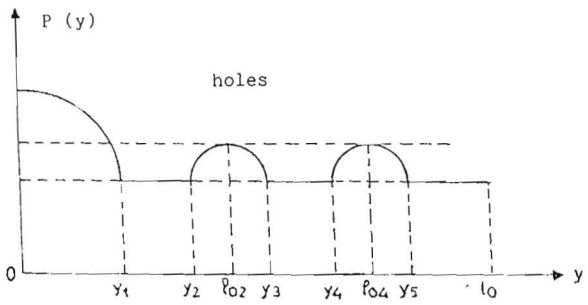

Figure 5 Power dissipated along the fuse element

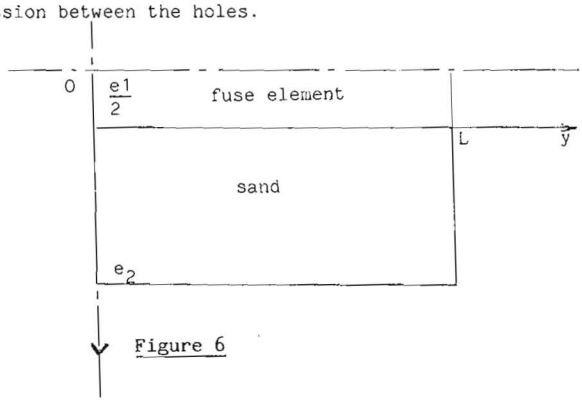

Figure 6

For a current I passing through the fuse during a time DT, the temperature range can be obtained from the following pattern (see figure 6)

$$\frac{\partial^2 T_1}{\partial y^2} = \frac{1}{\alpha_1} \frac{\partial T_1}{\partial t} \qquad \frac{\partial T_1}{\partial y} = 0 \text{ for } y = 0 \qquad k_1 \frac{\partial T_1}{\partial u} = -h_1 T_1 \text{ for } y = L$$

$$T = \frac{dt}{e_1 \ell \rho_1 c_1} \left[I^2 \left(A_{o+3i}\, y^2 + A_{1+3i}\, y + A_{2+3i} \right) - \varphi \right] \text{ at } t = 0$$

The term in square brackets represents the heat emission by joule effect in the fuse and φ the thermal leaks towards the sand.
For the sand :

$$\frac{\partial^2 T_2}{\partial x^2} = \frac{1}{\alpha_2} \frac{\partial T_2}{\partial T} \qquad \frac{\partial T_2}{\partial x} = 0 \text{ at } x = 0 \qquad k_2 \frac{\partial T}{\partial x} - h_2 T \text{ for } x = e_2$$

$$T = \frac{dt}{\varepsilon \ell \rho_2 c_2} \varphi \text{ for } t = 0 \qquad 0 < x < \varepsilon$$

The solution of this pattern is (1) :

$$T_1 = \frac{dt}{e_1 \ell \rho_1 c_1} \left[\Sigma_n \frac{1}{N_{1n}} \left(I^2 \left(\Sigma_{j=0}^{17} A_j F_{nj} \right) - \varphi F_n \right) \cdot \cos \left(\gamma_{1n} y \right) \exp \left(-\alpha_1 \gamma_{1n}^2 t \right) \right]$$

$$N_{1n} = \frac{1}{2} \left[L + \frac{h_1 \lambda_1}{(\gamma_{1n} \lambda_1)^2 + h_1^2} \right]$$

(Each therm marked by J corresponds to a term A)

$$F_{nj} = \int_{y_i}^{y_{i+1}} \left(A_{o+3i}\, y^2 + A_{1+3i}\, y + A_{2+3i} \right) \cos \left(\gamma_{1n} y \right) dy$$

$$F_n = \int_0^L \varphi \cos \left(\gamma_{1n} y \right) dy \; ; \; \gamma_{1n} \text{ solution of } \operatorname{cotg} \gamma_{1n} L = \gamma_{1n} \lambda / h_1$$

$$T_2 = \frac{\varphi\, dt}{\ell \rho_2 c_2} \Sigma_m \frac{1}{N_{2m}} \cos \varphi \left(\gamma_{2m} . x \right) \exp \left(-\alpha_2 \gamma_{2m}^2 t \right) \; ; \; N_{2n} = \frac{1}{2} \left[e_2 + \frac{h_2 \lambda_2}{(\gamma_{2m} \lambda_2)^2 + h_2^2} \right]$$

γ_{2n} solution of $\operatorname{cotg} \gamma_{2n} e_2 = \gamma_{2m} \lambda_2 / h_2$

This auxiliary result permits one to calculate the temperature range for a current I according to factor time.

We are describing here the method for a constant current I from t = 0. by applying DUHAMEL theroem (2), the solution is :

$$T_1 = \int_0^t \frac{1}{c_1 \rho_1 c_1} \left[\Sigma_n \frac{1}{N_{1n}} \left[I^2 \left(\sum_{j=0}^{17} A_j F_{nj} \right) - \varphi(t) F_n \right] . \cos\left(\gamma_{1n} y\right) \exp\left(-x_1 \gamma_{1n}^2 \left(t - Z\right)\right) \right] dZ$$

$$T_2 = \int_0^t \frac{\varphi(t)}{\ell \rho_2 c_2} \Sigma_m \frac{1}{N_{2m}} \left[\cos\left(\gamma_{2m} x\right) \exp\left(-x_2 \gamma_{2m}^2 \left(t - Z\right)\right) \right] dZ$$

By taking the LAPLACE transformation of these expressions :

$$\overline{T_1} = \Sigma_n \frac{\cos \gamma_{1n} y}{e_1 \ell \rho_1 c_1 N_{1n} \left(P + \alpha_1 \gamma_{1n}^2 \right)} \left[I^2 \left(\sum_{j=0}^{17} A_j F_{nj} \right) \frac{1}{P} - \overline{\varphi}_{(P)} F_n \right]$$

$$\overline{T_2} = \Sigma_m \frac{\cos(\gamma_{2m} x)}{\ell \rho_2 c_2 N_{2m}} \left[\frac{\overline{\varphi}(P)}{P + \alpha_2 \gamma_{2m}^2} \right]$$

$\overline{\varphi}_P$ is determined by using a coupling condition between the middles 1 and 2 : $\frac{1}{L} \int_0^L \overline{T_1} \, dy = \left(\overline{T_2}\right) \; x = 0$

which shows that the average temperature of the middle 1 is equal to the temperature in x = 0 of the middle 2.

The expression of $\overline{\varphi}$ (P) is transfered to $\overline{T1}$ and $\overline{T2}$
The temperature of the middles 1 and 2 is calculated by using a numerical method of LAPLACE inversed transformation (3).

NOMENCLATURE :

1. - Indication for the fuse element
2. - Indication for the sand
-. - LAPLACE transformation
T. - Temperature
t. - Time

y and x - Coordinates

L. - Length of the fuse
l. - Width of the fuse
e. - Depth
K. - Conductivity
ρ - Volumic mass
c. - Massic heat
h. - Exchange coefficient with the outer environment
α - Diffusivity
I. - Intensity
φ - Flow exchanged between the fuse element and the sand
P. - Variable in LAPLACE transformation
ϵ - Infinitely little

The validity of the hypothesis accepted in this pattern have been checked out by comparing the curves of experimental meltings and the melting curves calculated for various fuses (exemple figure 7).

For this very fuse, the temperature evolution arround the hole is shown on figure 8 as regards to the nominal intensity. We can see that in these conditions, the tin has melted.

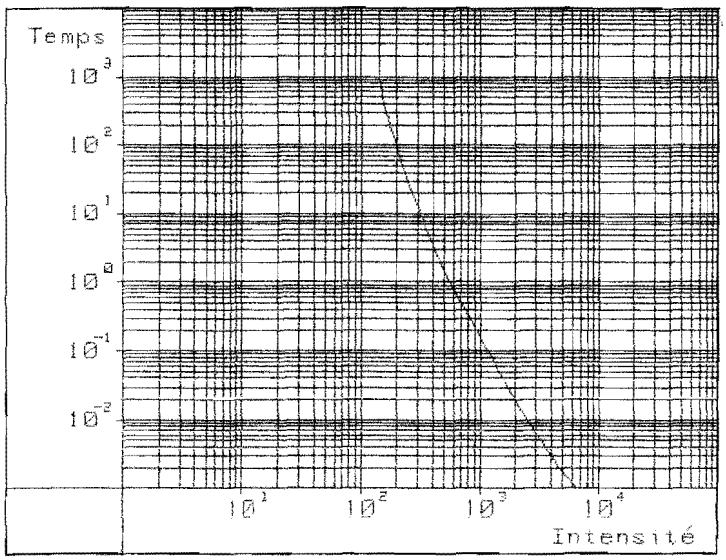

Figure 7

Calculated melting curve
(time-current)

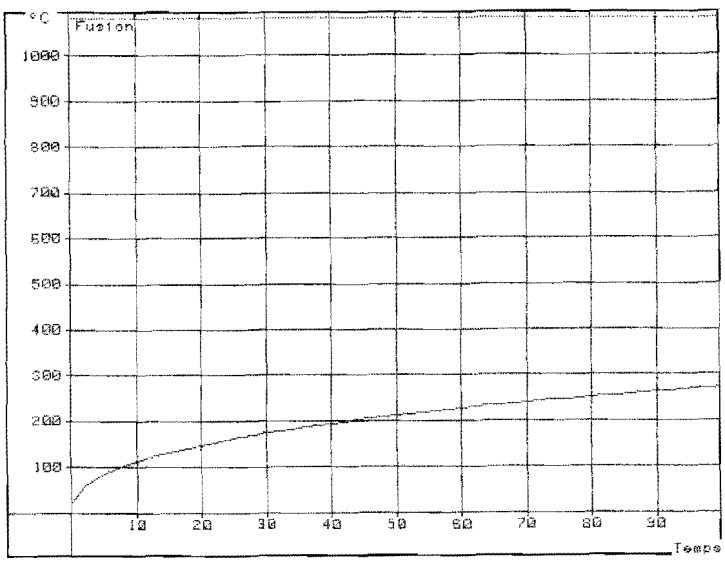

Figure 8

Temperature evolution at one
aera of fuse element

CONCLUSION :

Modeling of the heat transfer has been performed on a HP calculator with graphic printing. It enables to totally simulate the fuse operating in prearc period.

Although this pattern is suited to a given technology of fuse blade, it can easily be modified according to other conceptions.
Finally, the experimental checking of the curves time/current confirmed the validity of the pattern together with its significance regarding the optimation of the fuse element, either according to the relevant standard or according to economical matters.

REFERENCES :

(1) N.ÖZISIK Heat conduction J.Wiley and Sons page 25 to 38

(2) N.ÖZISIK " " J.Wiley and Sons page 246 to 265

(3) B.LASSAGNE These Nantes 11-1985

Session III

ARCING AND DISRUPTION PHENOMENA 1

Chairman: Dr. L. Vermij

Search for new extinguishing media for LV fuses

Josef PAUKERT

There are described the results of a search for new extinguishing media for LV fuses, especially focused to lowering the Joule integral I^2 . dt.

1. Introduction

The aim of the research was the discovering of new extinguishing media for LV fuses, which would be minimally equivalent with a quartz sand, but preferably with a lower value of Joule integral I^2 . dt.

The possibility of exploiting some waste materials was taken in account at choice of tested extinguishing media, but first of all, this chice was directed to verify the following hypotheses for improved behaviour of fuses:

a/ the presence of an electronegative compound

b/ the pressure rise inside of the fuse-link caused by chemical decomposition or by loss of crystal water

c/ the pressure rise in the immediate vicinity of the melting-element
   ca/ by forming an unpenetrable layer on the surface of the melting element
   cb/ by reinforcement of extinguisher /in form of a porous filler/.

According to Bron [1] , the pressure rise causes the lowering of ionisation rate and the rise of thermal conductivity, too. The result is in both cases the rise of arc-voltage gradient and thus the increase of arc instability.

52 kinds of extinguishing media were investigated, see tab. 1 and 2.

2. Test method

Individual extinguishing media were tested in a fuse, all other parts of which were taken from a factory made fuse. The reason was not only the easy availability of these parts but especially the use of a al ready proved construction, verified by a complete type test. In the beginning of our work we used high-breaking capacity fuses type PH 0, 100 A, gF characteristics, with a copper fuse-element. Later was the work directed to semiconductor fuses, type PC, 100 A, with a silver fuse-element.

The breaking-test were made in accordance with IEC 269-1, /first edition 1968/ and IEC 269-4 /first edition 1974/ at test current I_2, thus with the maximum arc energy. Because some of tested extinguishing media were of organic nature, the recovery voltage was maintained for 5 minutes at all samples tested.

In the first line, the acceptability of test results was evaluated in accordance with IEC Publication 269, namely

- nonpermissible overvoltage

- no externam effects /permanent arcing, flashover or daugerous ejection of flames/
- no desintegration or deformation of replaceable fuse link, which vould prevent its taking off in one piece
- allready mentioned effects shall not occur even in the period of recovery voltage
- insulation resistance shall not be lower thau 100 k

Furthermore, for every extinguishing medium the lowering of Joule integral $J = \int i^2 \, dt$ in comparison to standard extinguisher - quartz sand was evaluated.

Because for our tests no meter for $\int i^2 dt$ was available, it was necessary to evaluate this quantity graphicaly from oscillograms by hand, this has been very laborions and time consuming. However, the meter for quantity $E = \int i \, . \, u \, . \, dt$ was at disposal. As can be seen from fig. 1, the correlation betwen J and E exists

$$J = \int i^2 dt = k \, . \, E \qquad /1/$$

Therefore, for evaluation of let-through energy the quantity E was usad and thegraphical control of J was made for that extinguishing mediums only, which had the value of E lower than quartz sand.

5 samples were made with each extinguishing medium. The actual number n of tested samples is given in tab. 1 and 2.

Individual extinguishing media were applied with following methods:

- as filling /F/
- as coat /C/ on the melting-element, formed by technology of painting, vacuum evaporation or fluid-bed deposition
- as a pressed-on body on the melting-element /P/
  /prism 4 x 14 mm at PC type or 8 x 16 mm at PH type along all active lenght of melting element/.

When using methods C or P, the prepared melting element was placed in a filling of quartz sand of the same grain size /0,3 to 0,4 mm/ as in manufactured fuses.

Characteristics of fuse types used are as follows:

	Type PH	Type PC
active lenght of melting-element 50 mm	50 mm	47 mm
dimensions of melting-element	10 x 0,2 mm	10 x 0,17 mm
number of notches	4	7
cross-section reduction in a notch	12 %	8 %
melting element of	Cu	Ag
volume of fuse-link	21,95 cm^3	19,10 cm^3
cavity dimensions of fuse-link	24 x 15,5 x 59 mm	∅ 23...46 mm

3. Results

The results of the search for new extinguishing media are sumarized in table 1 /experiments on high breaking-capacity fuses PH/ and in table 2 /semiconductor fuses PC/. Besides information on composition of individual extinguishing media, about number of tested samples n and about tested hypothesis the tables contain also informations on the

method of application of extinguishing medium and about the acceptability of breaking test results according to individual criteria /+ complied with, - not complied/. Effects during tests are characterised by abbreviations: E explosion, D deformation of lids, C cracks in the body of fuse-link, F flames ejection. Unacceptable overvoltage was not observed. Particulars about tests are given in headings of tables.

From tables 1 and 2 can be seen, that a number of extinguishing media is equivalent to quartz sand as regards the breaking capacity at the I_2 current according to IEC 269, the insulation withstand for 5 min after switching and the insulation resistance greater than 100 kΩ . They are either extinguishing media in form of a coat or fillings, which contain at least 80 % of quartz sand. With regard to the fact, that even the melting elements with extinguishing medium in form of a coat were placed in a filling of quartz, good breaking capacity of these media can be attributed from the theoretical point of view to the quartz sand, because the relatively thin coat of extinguisher is rapidly destructed by the arc. This result is in a good agreement also with older, hitherto unpublished experiments, which followed the influence of impurities in quartz sand /in form of metal oxides, especially of ferric and ferrous oxides/ up to concentrations of about 10 %. The influence of impurities on breaking capacity of fuses was not found at that time.

The lowering of quantity E and of Joule integral J as well was found at three sorts of special ceramics NE2,NE3, NE7 only. Their base was quartz sand with the same grain size as in manufactured fuses /0,3 to 0,4 mm/ with organic binder of silicate nature. After thermal treatment the organic component volatilizes and the remaining porous body is of anorganic nature. As however the systematic research of influence of compositin and manufacturing technology of extinguishing media of this type on value of Joule integral J was not made, the boundary value of lowering J in comparison to current fuses with quartz sand is not known.

4. Conclusion

Extinguishing media, which are equivalent to quartz sand, are mixtures with minimal content of quartz sand of 80 %, or coats on melting elements placed in filling of quartz sand. From the economical point of view they are therefore disadvantageous in comparison with pure sand. Extinguishing medium of another chemical composition than SiO_2 was not found.

The lowering of let-through energy /Joule integral can be realited only by use of reinforced porous extinguishing medium on the base of SiO_2 with a binder, which remains after thermal treatment anorganic silicate /"artifical sandstone"/. Boundary value of lowering the Joule integral cannot be determined from existing experiments, but the reached results suggests the way of future work.

From the working hypotheses those of influence of electronegative compounds, of pressure rise by decomposition of chemical compounds or by loss of crystal water and of pressure rise in immediate vicinity of the melting element by means of a layer on it are to be rejected. The influence on lowering the value of Joule integral has the reinforcement of extinguishing medium only /hypothesis ca/.

The mention worth is the failure of Al_2O_3 as extinguisher, not only in calcinated but in crystalic form, too, even when a priori on account of chemical composition and of physical properties at least the equivalence with SiO_2 was expected.

5. References

[1] Bron O.B.: Arc in switchgear. /in russian/. Gosenergoizdat, Moskva - Lemingrad 1954.

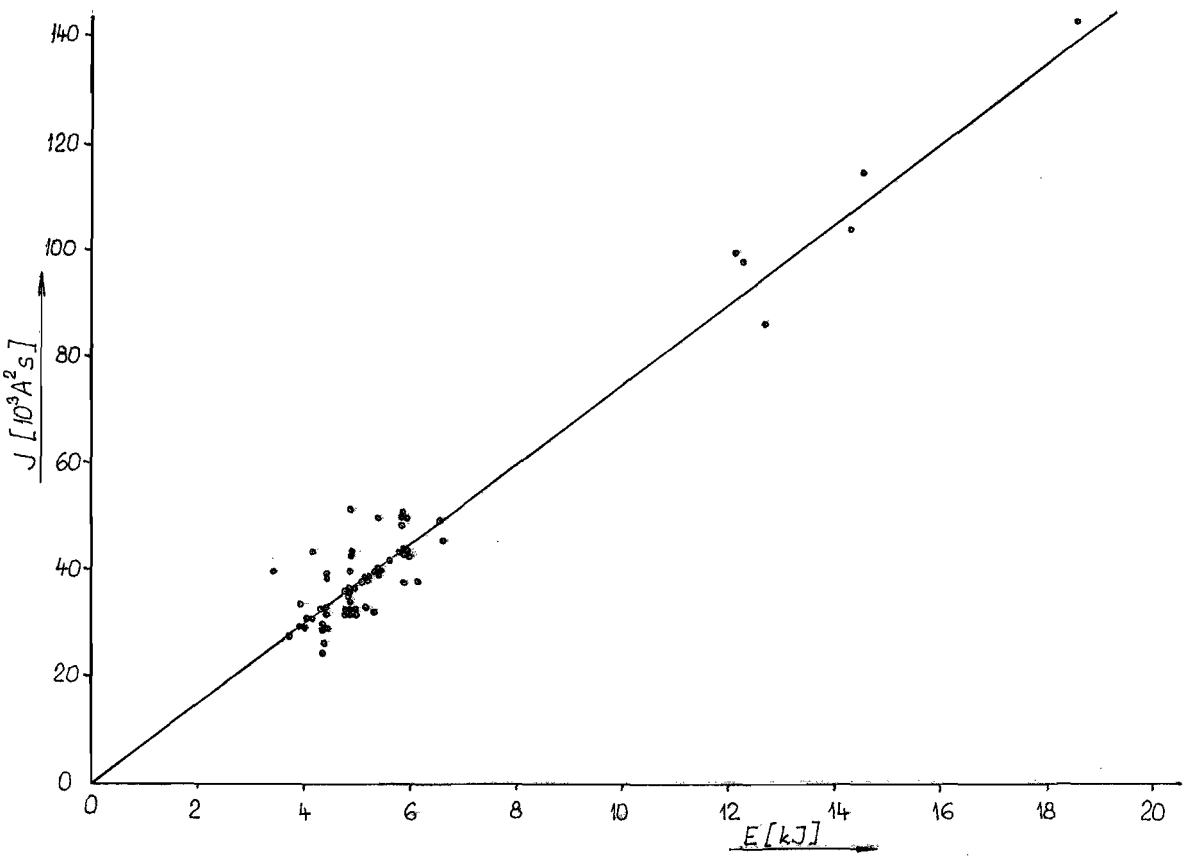

Fig. 1

Tab. 1 Experiments with extinguishing media in high-breaking capacity fuses, type PH 0, 100 A, characteristics gF. No 1 to 11: I_2 = 2700 A, cos phi=0,25. No.12 to 25: I_2 = 2800 A, cos phi = 0,2. All tests at 550 V, 50 Hz. Binder LH 20 on epoxy base

No.	Composition	Hypothesis	Application	Number of samples	Evaluation			
					breaking capac.	insul. ability	insul. resistance	lowering of $I^2.t$
1	MoS_2, binder PMMA	ca	C	5	-CF	+	+	-
2	PMMA	ca	C	4	+F	+	+	-
3	ground mica 0,25 mm	b	F	5	-F	+	+	-
4	ground mica 0,75 mm	b	F	5	-F	+	+	-
5	carborundum /SiC/ grain 0,5mm		F	5	-E	+	+	-
6	white corund /Al_2O_3/,grain 0,4		F	5	-CD	+	+	-
7	brown corund /Al_2O_3/,grain 0,32		F	5	-E	+	+	-
8	$Al_2O_3.3H_2O$, grain 0,1 mm	b	F	5	-F	+	+	-
9	PTFE, powder	a	F	5	-F	+	+	-
10	MoS_2, binder water glass	ca	C	5	+	+	+	-
11	water glass	ca	C	4	+	+	+	-
12	evaporated PTFE,layer 5 µm	ca	C	5	+	+	+	-
13	evaporated PTFE,layer 10 µm	ca	C	5	+	+	+	-
14	PTFE fluid bed deposited	ca	C	4	+C	+	-	-
15	10% PTFE,10% binder LH 20, 80% SiO_2	a	F	5	+	-E	-	-
16	80% PTFE, 20% binder LH 20	a	F	5	+	-E	-	-
17	10% PTFE, 15% binder LH 20, 75% $Al_2O_3.3H_2O$ /grain 0,1/	a	F	5	+	+	+	-
18	ground mica 0,75 mm	b	F	5	-F	+	+	-
19	$Al_2O_3.3H_2O$ grain 0,1 mm	b	F	5	+	+	-	-
20	20% $Al_2O_3.3H_2O$, grain 0,2 mm, 80% SiO_2	b	F	5	+	+	-	-
21	40% $Al_2O_3.3H_2O$, dtto 60% SiO_2	b	F	5	+	+	-	-
22	60% $Al_2O_3.3H_2O$, dtto 40% SiO_2	b	F	4	+	+	-	-
23	80% $Al_2O_3.3H_2O$, dtto 20% SiO_2	b	F	4	+	+	-	-
24	100% $Al_2O_3.3H_2O$ dtto	b	F	5	+	+	-	-

Tab. 2 Experiments with extinguishing media in semiconductor fuses PC, 100 A. I_2 = 1800 A, 550 V, 50 Hz, cos phi = 0,2.

No	Composition	Hypothesis	Application	Number of samples	Evaluation			
					breaking capac.	insul. ability	insul. resistance	lowering of $I^2 \cdot t$
25	10% MoS_2, 90% SiO_2	a	F	5	+	+	+	-
26	20% MoS_2, 80% SiO_2	a	F	5	-F	+	+	-
27	5% PTFE, 10% $Al_2O_3.3H_2O$,85%SiO_2	a+b	F	4	+	+	+	-
28	10%PTFE,20%$Al_2O_3.3H_2O$,70% SiO_2	a+b	F	5	-D	+	+	-
29	10%PTFE,60%$Al_2O_3.3H_2O$,30% SiO_2	a+b	F	5	+	+	-	-
30	10% mica 0,75, 90% SiO_2	b	F	5	-E	+	+	-
31	20% Ca SO_4 powder, 80% SiO_2	b	F	5	+	+	+	-
32	50% Ca SO_4 powder, 50% SiO_2	b	F	5	-F	+	+	-
33	80% Ca SO_4 powder, 20% SiO_2	b	F	5	-F	+	+	-
34	10% $Na_2B_4O_7$. 10 H_2O,90% SiO_2	b	F	5	+	+	+	-
35	20% $Na_2B_4O_7$. 10 H_2O,80% SiO_2	b	F	5	+	+	-	-
36	50% $Na_2B_4O_7$. 10 H_2O,50% SiO_2	b	F	4	+	+	-	-
37	5 % H_3BO_3, 95% SiO_2	b	F	5	+	+	+	-
38	10% H_3BO_3, 90% SiO_2	b	F	5	+	+	+	-
39	20% H_3BO_3, 80% SiO_2	b	F	5	+	+	+	-
40	10%PTFE, 8% binder LH20,82%SiO_2	ca	P	5	+	-E	-	-
41	17%PTFE, 8% binder LH20, 75 % Al_2O_3 . $3H_2O$	ca	P	5	+	-E		
42	20% binder LH20, 80% SiO_2	ca	P	5	-D	+	-	-
43	10% binder LH20, 10% mica 0,75 80% SiO_2	ca	P	5	+	-E	-	-
44	10% binder LH20, 10%$Al_2O_3.3H_2O$, 80% SiO_2	ca	P	5	+	-C	-	-
45	special ceramics NE1	cb	P	3	+	+	+	-
46	dtto NE2	cb	P	3	+	+	+	+
47	dtto NE3	cb	P	3	+	+	+	+
48	dtto NE7	cb	P	5	+	+	+	+
49	water glass, coat 1 mm thick	ca	C	5	+	+	+	-
50	PMMA, 0,1 mm thick	ca	C	5	+	+	+	-
51	20% mica, 80% water glass, 0,1 mm thick	ca	C	5	+	+	+	-
52	10% H_3BO_3, 90% PMMA, 0,2 mm thick	ca	C	5	+	+	+	-

SWITCHING PERFORMANCE OF HIGH-VOLTAGE FUSE-ELEMENTS IN DIFFERENT SOLID AND GASEOUS FILLING MEDIA

D. König, J. Trott, H.J. Müller, B. Müller

ABSTRACT

HV-fuses that are back-up fuses do not interrupt overload currents below a minimum braking current I_{mbc} because of thermal overheating caused by the overload current arcing. The rupturing capacity of the switching device High Voltage Fuse is essentially determined by the arrangement of the fuse-elements and the used filling media. Quartz sand has not proved to be the most proper medium for arc extinction during current zero in the small overload current range. However, quartz sand has proved to be the proper medium for current limiting arc extinction in the heavy fault, short-circuit current range.

The burn-back performance of fuse elements was tested with different filling media. It appears that the burn-back rate of a fuse element surrounded by electronegative gases is much higher than when surrounded by quartz sand. The significant increased arc length assists the arc extinction. In addition, the dielectric strength of electronegative gases during current zero of an overload current arc is much higher. Both features lead to a significant increase of the rupturing capacity of fuse-elements surrounded by electronegative gases, thus enabling overcurrent protection. Fuse-elements that are surrounded by electronegative gases represent in principle a current zero switching device. To obtain additionally current limitation, preference should be given to a combination of fuse-elements in electronegative gases with conventional current limiting switching device consisting of fuse-elements in quartz sand, e.g. a conventional back-up fuse.

INTRODUCTION

High Voltage fuses are in large majority so called back-up fuses. Back-up fuses provide satisfactory clearance of all currents below their maximum breaking capacity down to their minimum breaking current I_{mbc}. Currents below the minimum breaking current I_{mbc} that cause melting of the fuse element may produce the destruction of the fuse body. The low overload current arc cannot be extinguished by the filling medium due to the fact that the power loss of the arc

$$W_a = \int_0^{t_a} u_a(t) \cdot i(t)\, dt \qquad (1)$$

W_a ≙ power loss of the arc
t_a ≙ arcing time
u_a ≙ arc voltage
i ≙ arc current

leads during a significant long arcing time t_a to thermal overheating of the fuse body and thus to the mechanical destruction of the ceramic body /1/. Therefore, for safe interruption of low overload currents an early extinction of the established low overload current arc is important.

General purpose fuses according to IEC.282-1 /2/ must break currents leading to a melting time of t_m = 1 h. The value of 1 h-melting currents normally is below the value of minimum breaking currents I_{mbc} of back-up fuses with the same rated current. Quartz sand, due to its thermal and dielectric features, cannot give sufficient assistance to the arc extinction in the low overload current range. This applies particularly to fuses with high voltage- and high current ratings. The present report tries to point out the reasons for failure of common back-up fuses in the range below I_{mbc} and discusses an approach to solve the overload current problem. The performed investigations deal exclusively with the effects that different filling media have on arc extinction in HV fuses. Modifications of the fuse elements have not been investigated.

1 TEST ARRANGEMENT

To reproduce the breaking performance of HV fuses a test arrangement was used complying in its construction with HV fuses (Fig. 1). The fuse-element (6) is wound around a ceramic supporting core (5). The fuse body is an epoxy resin tube (1) where at both sides metal end caps (2) are glued on. Via O-rings (3) the test body can be closed gas-tight by means of additional metal flanges (4). As the investigations are restricted to the low overload current range the use of a fuse-element arrangement with notches could be omitted. Fine grained silver fuse wire of d = 0,15 mm to 0,4 mm diameter were used. In order to avoid current commutation processes between different fuse elements only one fuse wire was wound on the core. The test body (Fig. 1) was alternatively filled with quartz sand in grain size proportions of d_g = 0,3 - 0,35 mm (d_g = grain diameter) or with the gases air, nitrogen and sulphurhexafluoride. Prior to be filled with gas the body was evacuated to a residual pressure of p = 6 kPa.

Prof. Dr.-Ing. D. König
Dipl.-Ing. J. Trott
Institut für Hochspannungs- und Meßtechnik, TH Darmstadt
D-6100 Darmstadt, Germany

Dipl.-Ing. H. J. Müller
Dr.-Ing. B. Müller
Jean Müller GmbH
Elektrotechnische Spezialfabrik
D-6228 Eltville 1, Germany

2 TEST CIRCUIT

The breaking capacity tests in the low overload current range of HV fuses were performed singlepole in a three-phase network system with a recovery voltage of U_r = 20 kV. The current setting was made by reactance regulators. A simplified equivalent circuit diagram of the test circuit is illustrated in Fig. 2. The investigated test currents are within the low overload current range of HF fuses with a rated current of I_r = 10 A. The power factor of the test circuit is cos φ = 0,125. The slope of the transient recovery voltage is du_c/dt = 220 V/µs. Thus, the test conditions are much more severe that it is required for the minimum breaking current test (test duty 3 according to IEC /2/) and cover at the same time the test specifications for the critical current (test duty 2 according to IEC /2/). The permissible tolerances for the performance of overload current breaking capacity tests are not utilized.

3 BURN-BACK PERFORMANCE OF FUSE ELEMENTS IN DIFFERENT FILLING MEDIA

During the melting period the ohmic loss on the fuse-element

$$W_m = \int_0^{t_m} R_m(t) \cdot i(t)\, dt \qquad (2)$$

W_m ≙ power dissipation of the fuse link R_m ≙ ohmic restistance

t_m ≙ melting time

results in heating the complete fuse body /3/. Under low overload current conditions the fuse-element reaches its melting temperature right in the middle of the fuse wire and one arc is established. This arc is lenghtened along the axis of the fuse wire. As long as the low overload current keeps running, the established arc burns back. The burn-back rate of the fuse-element is depending on the fuse-element material, its geometric dimensions, the filling medium and the current rating.
Since in the performed tests fuse wires of only one type of fine grained silver were used it is possible to determine the burn-back rate in relation of the filling medium and to the current density within the fuse-element. The rupturing process was controlled in such a way that the current continued to run some few current cycles after the arc has been established until it was interrupted by the safety-switch E (see Fig. 2). By measuring the length of the partly burnt-off fuse-element (burn-back lenght ℓ) or of the fulgurite in the quartz sand and by determination of the arcing time the burn-back rate v can be calculated with

$$v = \frac{\ell}{t_a} \,. \qquad (3)$$

The test results for the filling media quartz sand, air, SF_6 are illustrated in Fig. 3. The burn-back rate is directly proportional to the current density in the fuse-element /4,5/. Hereby it is to be taken into account that the burn-back rate is determined by the distance growth of the opposite arcing foot points in both directions of the fuse-element axis starting from the melting point.

From the proportional relations given in Fig. 3 the specific burn-back volume c can be calculated in the dimension mm³/As. In Table 1 the calculated specific burn-back volumes for silver wires and the mentioned filling media are registered.

filling media	specific burn-back volume c	burn-back length ℓ t_a = 10 ms	heat conductivity λ_w	specific. heat capacity c_{vw}
quartz sand	1,4 mm³/As	11 mm	0,35 W/mK	840 J/kgK
air	8,5 mm³/As	67 mm	0,0257 W/mK	715,9 J/kgK
SF_6 (p=0,3MPa)	11,5 mm³/As	91 mm	-	608,6 J/kgK
SF_6 (p=0,1MPa)	14,5 mm³/As	115 mm	0,01778 W/mK	625,7 J/kgK

Table 1: Filling media, specific burn-back volumes and burn-back lengths at a current density of J = 792 A/mm² with fuse-elements of fine grained silver. Heat characteristic values λ_w and c_{vw} taken from /6,7/

The specific burn-back volume depends on the heat transport features of the filling medium figured in Table 1 by the thermal conductivity and the volume rated specific heat capacity of the filling medium. Media with good heat conduction (e.g. quartz sand) reduce the burn-back rate because of its cooling effect. Media with bad heat conduction (gases) on the other hand, enable quick lengthening of the arc.

The arcing development in the low overload current range of HV fuses can therefore be influenced by the choice of the filling medium. Quartz sand leads at small current densities to little burn-back lengths ℓ, For this reason the arc extinction below the minimum breaking current I_{mbc} is aggravated. Only if the current density is increased to such an extend that the fuse-element melts simultaneously at several points, a significant arc extension may be obtained. When gases are used as filling medium (e.g. SF_6) considerable arc lengths can already be achieved with significant smaller current densities within the time of half a current cycle.

4 INVESTIGATION OF THE DIELECTRIC STRENGTH AFTER OVERLOAD CURRENT ZERO

According to the tests described in Chaper 3 the arc length during low overload current arcs in quartz sand is only some mm in length at the first current zero after arc ignition. Since the fuse body is heated up according to Equation (1) by the power loss of the arc an early rupturing of the low overload current is important. The aim is to obtain arc extinction at the first zero of the arc current.

4.1 Current and voltage development after current zero

The low overload current arcs in HV fuses are exclusively extinguished during current zero. As arc current and arc voltage are in phase during the arcing time and the power factor of the test circuit is cos $\varphi < 1$ the arc gap is heavily stressed by the steep transient recovery voltage as soon as the current remains zero. During test performance the transient recovery voltage amounted to $d_{uc}/dt = 220$ V/µs.
Current and voltage development of the restriking of a low overload current arc in quartz sand and SF_6 are plotted in Fig. 4 and Fig. 5. The plots demonstrate restriking arcs directly after the first current zero. While the arc current in quartz sand is running linear through the natural zero of current, in SF_6, however, a distinct zero phase of current can be realized. The ignition voltage U_Z which is characteristic for the extinction ability of an arcing arrangement with equal arc length and equal current rating, is significantly higher in SF_6 than in quartz sand. The higher U_Z the better is the cooling of the rupturing arc /8,9/.

4.2 Dielectric strength of an arc gap caused of an overload current arc

At a current density of J = 792 A/mm² and for an arc length (burn-back length ℓ of the silver element) of ℓ = 10 mm (see Table 1) the cumulative frequency distribution of the measured ignition voltages in quartz sand was statistically calculated and is illustrated in Fig. 6. According to this 70 % of the measured ignition voltages are smaller than U_Z = 2 kV. Due to different burn-back rates v a comparison with gaseous filling media, however, is possible only on condition that the arc length is constant. This can be achieved by reducing the fuse wire length in such a way that the burn-back length per half current cycle is of the same order as in quartz sand. For measuring the ignition voltage in gaseous media the arc length is reduced to l = 10 mm by the arrangement of Fig. 7 in the fuse body. From the measured ignition voltages and accurately adjusted burn-back lengths the external ignition field strength E_Z of the arcing arrangement can be determined:

$$E_Z = \frac{U_Z}{l} . \qquad (4)$$

The arithmetic mean values of the ignition field strength $\bar{E}_Z$ are given in Table 2 for the tested filling media.

filling media	field strength $\bar{E}_Z$
quartz sand	1,5 ± 0,5 kV/cm
O_2 (p=0,1 MPa)	0,075 ± 0,025 kV/cm
N_2 (p=0,1 MPa)	0,075 ± 0,025 kV/cm
SF_6 (p=0,1 MPa)	3,5 ± 0,5 kV/cm
SF_6 (p=0,3 MPa)	16,0 ± 0,5 kV/cm

Table 2: Ignition field strength $\bar{E}_Z$ in dependence of the filling media at a current density of J = 792 A/mm².

According to Table 2 the dielectric strength of the same arc gap is in SF_6 higher than in quartz sand. According to Table 1 the arc in a fuse filled with SF_6 may obtain a burn-back length ℓ that is sufficient to extinguish the arc already after half a current cycle. In quartz sand, however, the burn-back rate and the ignition field strength is so small that a quick arc extinction is not possible. Only if the fuse-element melt up at increased current density at various different locations forming multiple partial arcs the burn-back performance causes the necessary length for arc extinction.

5 MINIMUM BURN-BACK LENGTH OF THE FUSE WIRE FOR ARC EXTINGUISHING IN SULPHURHEXAFLUORIDE

By lengthening of the wire in Fig. 7 the ignition voltage increases. In dependence of the pressure and of the field strength $\bar{E}_Z$ of the filling media SF_6 (see Table 2) the arc is extinguished at a definite minimum burn-back length of the wire. The drawn line in Fig. 8 shows the minimum arc length of overload currents in static SF_6. Experiments with successfull arc extinction have been done with a larger arc length. Experiments without arc extinction were performed with smaller arc length. In the media SF_6 it is possible to extinguish an overload current arc during the first current zero after arc ignition by a arc length of only some cm.

SUMMARY

The low burn-back rate of low overload current arcs in quartz sand and the small dielectric strength of the achieved arc gap at current zero may lead to malfunction of HV fuses filled with quartz sand below a minimum breaking current I_{mbc}. Because if its high dielectric strength during current zero and of the high burn-back rate for low current densities, SF_6 offers the possibility to rupture low overload currents with long melting times before the fuse body failes due to thermal overheating.

REFERENCES

/1/ Stenzel, H.-D.: Auswirkungen der Verlustleistungen in Hochspannungs-Hochleistungssicherungen auf den Sicherungskörper bei Betrieb mit kleinem Überlaststrom. Diss. TU Hannover 1972.

/2/ VDE 0670 Teil 4/...79 Entwurf: Wechselstromschaltgeräte für Spannungen über 1 kV - Strombegrenzende Sicherungen. VDE-Verlag GmbH: Berlin 1979.

/3/ Weißgerber, W.: Untersuchungen über die Temperaturfelder von Hochspannungs-Hochleistungs-Sicherungen. Diss. TU Hannover 1971.

/4/ Daalder, J. E.; Hartings, R. M.: The Burn Back Rate of High Voltage Fuses. Fourth International Symposium on Swichting Arc Phenomena Lodz/Poland 1981. Part II: Postconference Materials, S. 158 - 164.

/5/ Kroemer, H.: Der Lichtbogen an Schmelzleitern in Sand. Archiv für Elektrotechnik 36 (1942), Heft 8, S. 455 - 470.

/6/ Mosch, W.; Hauschild, W.: Hochspannungsisolierungen mit Schwefelhexafluorid. Hüting Verlag: Heidelberg, Basel 1978.

/7/ VDI-Wärmeatlas: Berechnungsblätter für den Wärmeübergang. VDI-Fachgruppe Verfahrenstechnik. Düsseldorf: VDI-Verlag 1957.

/8/ Grütz, A.; Hochrainer, A.: Rechnerische Untersuchungen von Leistungsschaltern mit Hilfe einer verallgemeinerten Lichtbogentheorie. ETZ-A 92 (1971), Heft 4, S. 185 - 191.

/9/ Bayreuther, K.: Über das Verhalten von Wechselstromlichtbögen unter dem Einfluß hohen statischen Gasdruckes. XIII. Intern. Wiss. Kolloquium TH Ilmenau 1968, Vortragsreihe "Elektrische Apparate und Anlagen", S. 35 - 44.

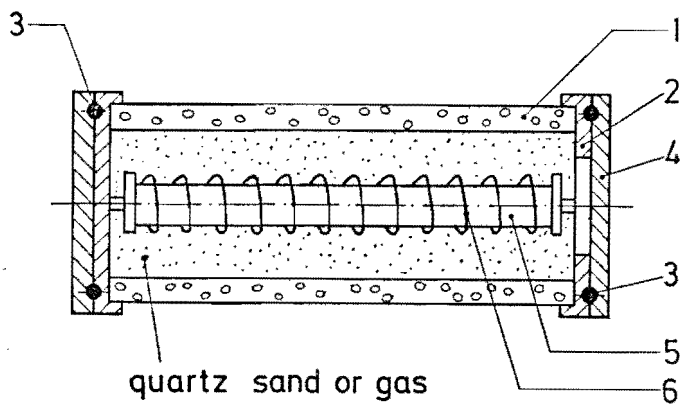

Fig. 1: Test Body

1 epoxy resin tube
2 metal end caps
3 O-rings
4 metal flanges
5 ceramic supporting core
6 fuse-element

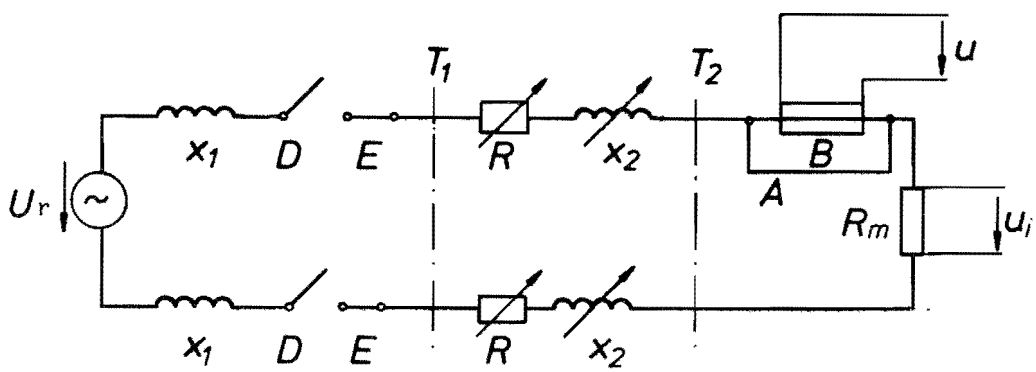

Fig. 2: Simplified equivalent circuit diagram of the test circuit

X_1; X_2	inductances	B	test arrangement
R	resistance	A	removeable short circuiter for regulationof the test current
D; E	circuit-breakers		
T_1; T_2	transformers	R_m	measuring resistance

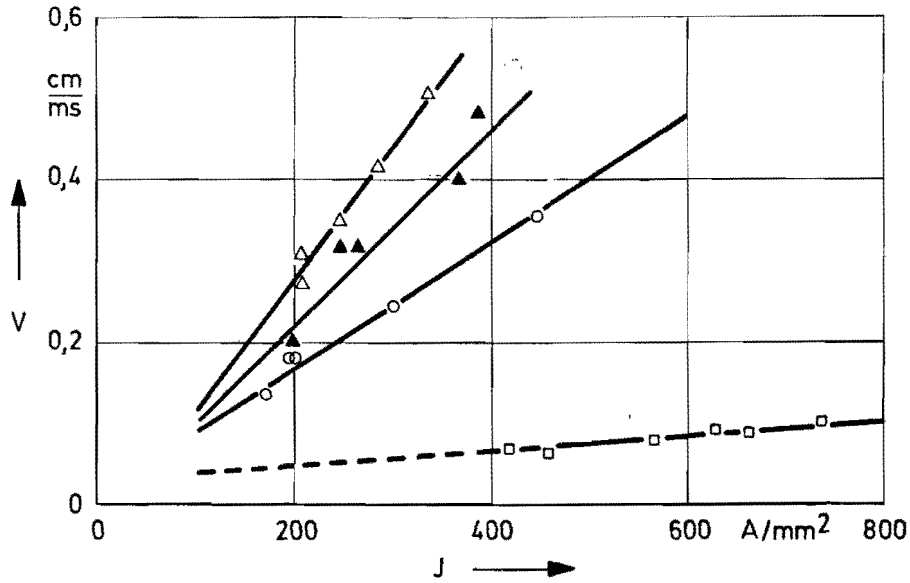

Fig. 3: Burn-back rate of silver wires in dependence of the current density in different filling media

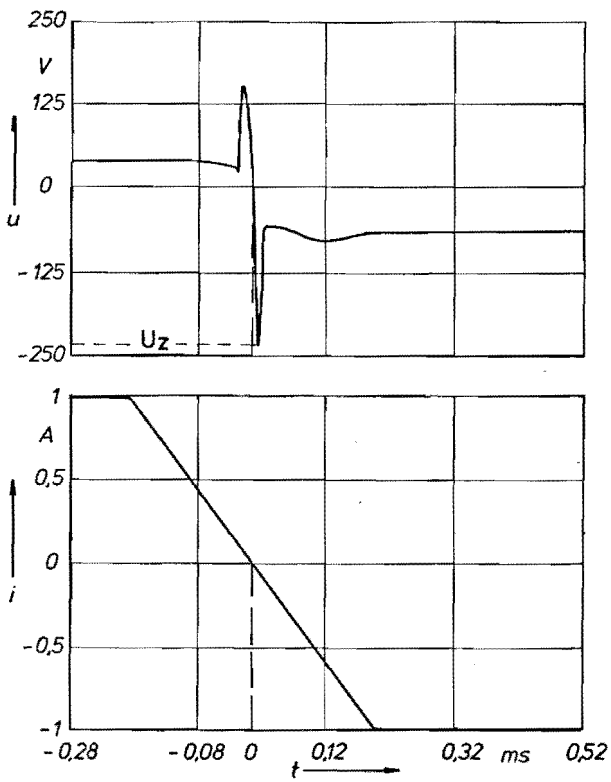

Fig. 4: Voltage and current development of a low overload current restriking arc in quartz sand

I	=	14 A	arc current
U_r	=	20 kV	rated voltage
l	=	10 mm	arc length
du_c/dt	=	220 V/µs	transient recovery voltage
U_Z	=	245 V	ignition voltage (neg. polarity)

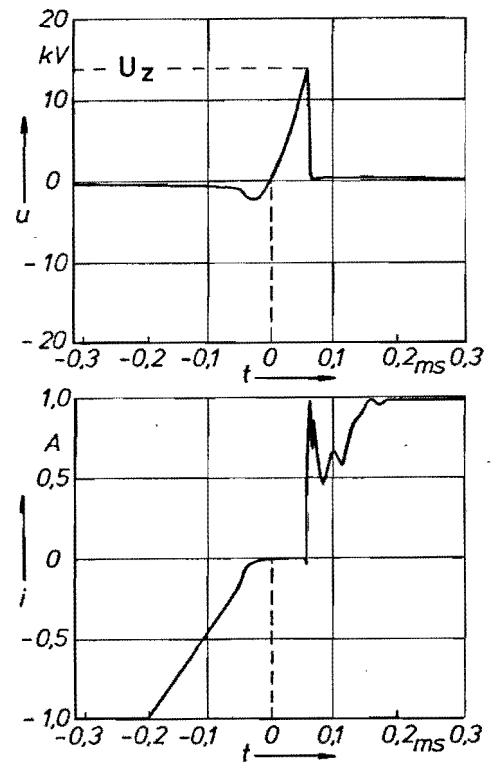

Fig. 5: Voltage and current development of a low overload current restriking arc in SF_6

I	=	14 A	arc current
U_r	=	20 kV	rated voltage
l	=	10 mm	arc length
du_c/dt	=	220 V/µs	transient recovery voltage
p	=	0,3 MPa	pressure of the gas
U_Z	=	14 kV	ignition voltage (pos. polarity)

REFERENCES

/1/ Stenzel, H.-D.: Auswirkungen der Verlustleistungen in Hochspannungs-Hochleistungssicherungen auf den Sicherungskörper bei Betrieb mit kleinem Überlaststrom. Diss. TU Hannover 1972.

/2/ VDE 0670 Teil 4/...79 Entwurf: Wechselstromschaltgeräte für Spannungen über 1 kV - Strombegrenzende Sicherungen. VDE-Verlag GmbH: Berlin 1979.

/3/ Weißgerber, W.: Untersuchungen über die Temperaturfelder von Hochspannungs-Hochleistungs-Sicherungen. Diss. TU Hannover 1971.

/4/ Daalder, J. E.; Hartings, R. M.: The Burn Back Rate of High Voltage Fuses. Fourth International Symposium on Swichting Arc Phenomena Lodz/Poland 1981. Part II: Postconference Materials, S. 158 - 164.

/5/ Kroemer, H.: Der Lichtbogen an Schmelzleitern in Sand. Archiv für Elektrotechnik 36 (1942), Heft 8, S. 455 - 470.

/6/ Mosch, W.; Hauschild, W.: Hochspannungsisolierungen mit Schwefelhexafluorid. Hüting Verlag: Heidelberg, Basel 1978.

/7/ VDI-Wärmeatlas: Berechnungsblätter für den Wärmeübergang. VDI-Fachgruppe Verfahrenstechnik. Düsseldorf: VDI-Verlag 1957.

/8/ Grütz, A.; Hochrainer, A.: Rechnerische Untersuchungen von Leistungsschaltern mit Hilfe einer verallgemeinerten Lichtbogentheorie. ETZ-A 92 (1971), Heft 4, S. 185 - 191.

/9/ Bayreuther, K.: Über das Verhalten von Wechselstromlichtbögen unter dem Einfluß hohen statischen Gasdruckes. XIII. Intern. Wiss. Kolloquium TH Ilmenau 1968, Vortragsreihe "Elektrische Apparate und Anlagen", S. 35 - 44.

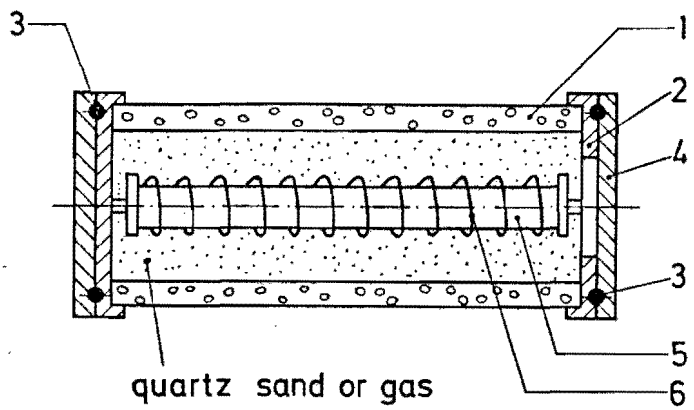

Fig. 1: Test Body

1 epoxy resin tube
2 metal end caps
3 O-rings
4 metal flanges
5 ceramic supporting core
6 fuse-element

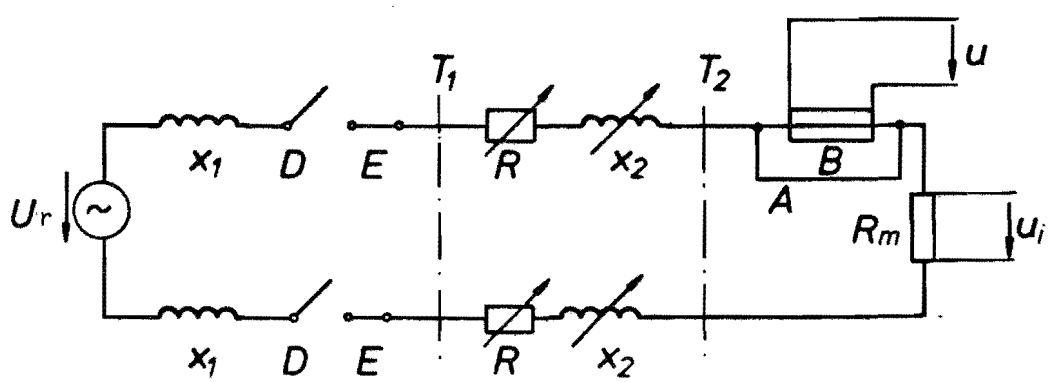

Fig. 2: Simplified equivalent circuit diagram of the test circuit

X_1; X_2	inductances	B	test arrangement
R	resistance	A	removeable short circuiter for regulationof the test current
D; E	circuit-breakers		
T_1; T_2	transformers	R_m	measuring resistance

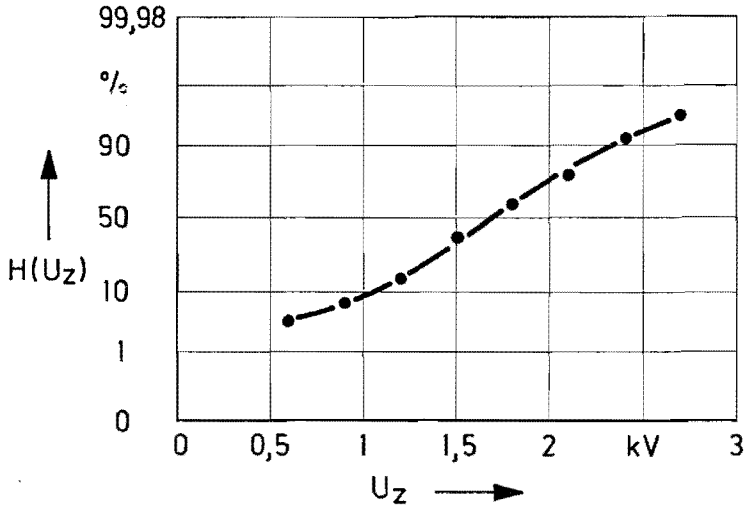

Fig. 6:

Cummulative frequency distribution of the measured ignition voltage of overload current arcs in quartz sand with a current density of $J = 792\ A/mm^2$ and an arc length of $\ell = 10\ mm$

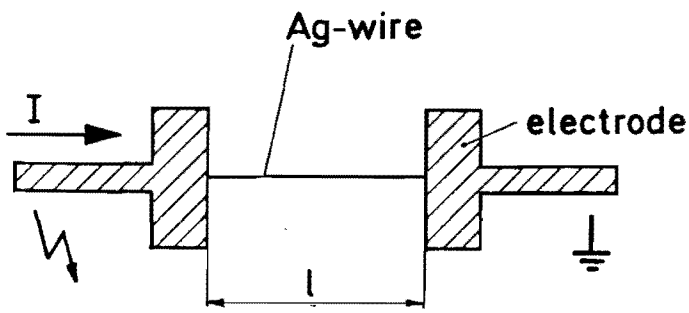

Fig. 7:

Arrangement of the fuse wire for producing a definite arc length in gaseous media

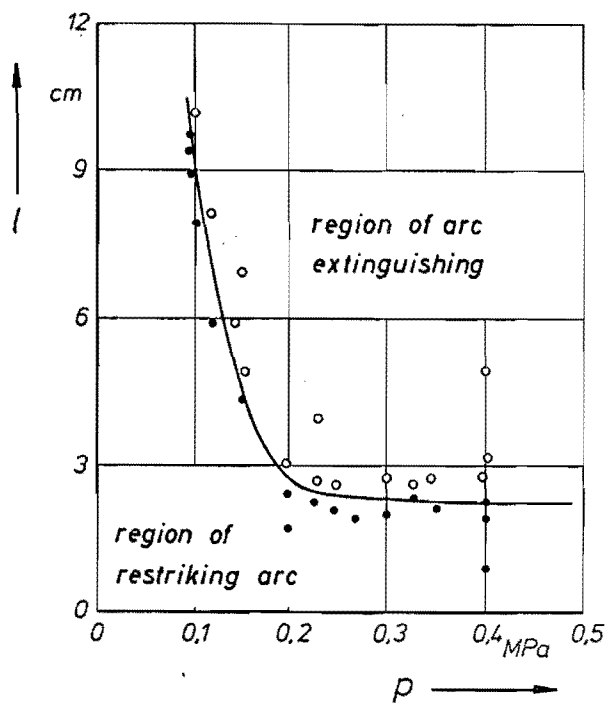

Fig. 8:

Minimum burn-back length of a wire in dependence of the pressure of SF_6

I = 14 A arc current

U_r = 20 kV rated voltage

du_c/dt = 220 V/µs transient recovery voltage

THE EFFECT OF FUSE-ELEMENT SHAPE ON BREAKING PHENOMENA IN a.c CIRCUITS

J. Ossowicki
Electrotechnical Institute, Gdańsk, Poland

ABSTRACT

Description is given of the results of comparative tests on interrupting parameters by fuse-links having an aM time-current characteristic. The tests were carried out at alternating current of 1180 ± 20V on fuse-link models with 0,20mm wide, single and parallel, copper strip elements. The active length of the fuse-elements was 96 mm. The fuse-link insulation bodies were made of Al_2O_3 and had an inside diameter of 43 mm. They were filled with quartz sand of a 0,2 to 0,5mm granulation. The results obtained permit to determine the dependence of the interrupting arc energy and the energy needed for melting $1mm^3$ of the fuse-element upon the width of the element as determined by the number of modules. The analysis comprises the interruption of I_2 critical currents and overload currents selected so that the prearcing times amount to from 20 to 200 sec.

1. INTRODUCTION

Progress in the construction of fuses continues to be dependent on incessant research and development work. Nevertheless, quantitative advantages following from the application of several parallel fusible strips instead of one strip having their summary width are still unknown. Thus, attempts have been made at clarifying this matter partially and tests carried out pertaining to the effect of the strip fuse-element construction on the process of interrupting short circuits and overloads. The interrupting capability of model links with single fusible strips, from 2 to 8 modules wide, was compared with the results obtained with single-module parallel fusible strips arranged in the link so that distances between their surfaces amounted to 5mm approximately. The arc energy, length of the melted elements and the energy needed for melting 1 mm^3 of the element mass were used as criteria for the comparison. The tests were limited to interrupting critical short circuit current I_2 and breaking overload currents selected so that their prearcing time amounted to from 20 to 200 sec. The measurements were taken at alternating current of 1180 ± 20V on copper fuse-elements having a thickness of 0,2 mm and an active length of 96 mm.

2. GENERAL CONSIDERATIONS REGARDING INTERRUPTION BY FUSES

Correctness of interruption by means of fuses is decided, above all, by the amount of energy appearing in the arc and by the fuse-element melting rate. This refers especially to fuses for rated continuous currents of several hundreds of amps and for rated voltages of more than 600 V. Special technical difficulties are encountered at working out designs for high-voltage full range fuses . This is so because of the lack of appropriate information in references, and the available descriptions of the phenomena which accompany the interruption of currents by fuses are in general confined to short circuit conditions and usually they refer merely to fuses with single fusible strips or wire elements. Parallel fusible strips find application nowadays in actual fuses for higher rated currents. In fuses of such a design, however, progressive destruction of the fuse is found to take place at interruption in such cases when, because of any reasons, the parallel fusible strips do not take the same part in the process connected with interrupting the current. The strip at which the largest fulgarite appears, will also have the lowest arc impedance and it will quickly take over the whole interrupting task while the arcs at other elements extinguish. In such cases the arc usually comes up to the end caps, in many cases burning out holes in them, which results in a failure of interrupting the current. Such kind of faulty operation is, according to Rosen [5] , is typical in fuses having their elements of an insufficient length or it takes place when the test is carried out with a smaller current than the minimum fuse-link interrupting current.

3. TEST CONDITIONS

The tests were carried out on fuse-links composed of typical metal element as used in low voltage industrial links with second size blade contacts and with Al_2O_3 bodies, 100mm long, inside diameter 43mm. Quartz filler was used as arc-quenching material having a granulation of 0.2 to 0,5mm and the following basic chemical composition: 99.25% SiO_2; 0.21% Al_2O_3 + TiO_2; 0.05% Fe_2O_3 and 0,1% CaO. While being filled the links were subjected to shaking in order to ensure lowest possible porosity [4] . The tests comprised 340 models of fuse-links with copper strip element having an active length of 96 mm, a thickness of 0.2 $\pm^{0}$0.005 mm and a module width of 3 $\pm$ 0.02mm. The fuse-elements were composed of single strips having n = 1; 2; 3; 4; 5; 6; and 8 modules /Type B/ and of single-module strips /Type C/ placed in the links in parallel with their centre line and welded at both ends to the copper contact blades /Fig.2/. The distances between the single-module strip planes amounted to 5 $\pm$ 0,5 mm each. The melted element length was determined on the basis of X-ray photographs by suming up the particular lengths melted in the fusible strips. While evaluating the melted length areas of the out-outs for forming restrictions as shown in Fig.1 were taken into account. The test circuit in compliance with the IEC requirements [7] was supplied form a single-phase transformer, 15kV/1kV; 3 MVA. Resistors and air-core reactors were used for presetting the values of the current and power factor. The voltage and tests current were measured with an accuracy

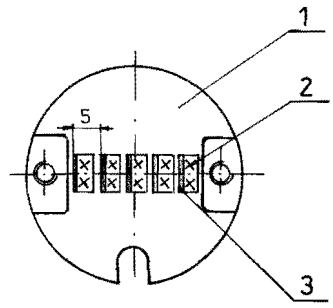

Fig.1. Fuse-link blade contact with arrangement of 5 strips shown. 1-blade contact; 2-fuse-element welding points; 3-fusible strip.

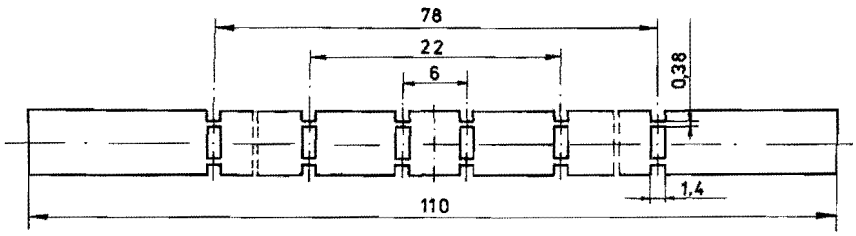

Fig.2. Two-module strip element with an aM characteristic.

of 1,5%, and the Joule's integral /I^2t/ and arc energy /A/ by means of special meters with an estimated accuracy of 5%. The measured values were recorded by a loop oscillograph, in which loops with a resonance frequency of 5 kHz were applied. The recording tape moving speed amounted to 5m/sec. at the short-circuit tests, and 0,5 m/sec. at the overload tests.

Ten measurement were taken per each point of the characteristic, and in doubtful cases even up to 30.

4. INTERRUPTION OF SHORT-CIRCUITS

The tests were carried out at alternating current of 1180 $\pm$ 20V in a circuit with a power factor of 0.22 $\pm$ 0.02. The test current /I_p/ was selected so that the cut-off current /i_o/ values amounted to /0,65 to 0,75/ $\sqrt{2}.I_p$ The current making angle was 0° to 20°el. Subjected to the tests were 60 models with single-strip elements /Type B/ containing 1; 2; 3; 4; and 5 modules respectively and 50 models with elements composed of single one-module strips /Type C/. The dependense A=f /n/ appears to have a straight line form for single and parallel strip elements

$A = a_o + a.n$ /1/ The coefficients in this equation as determined by the above mentioned minimum square deviation method take such values as given in Table 1.

As this may be seen the linear correlation coefficients r^2 are very high in both the cases. This means that the correlation degree between the results calculated according to dependence/1/ and the results of measurements is very high. Thus, it may be concluded that equation /1/ describes the dependence A = f/n/ correctly. In order to check whether are any essential differences between the straight lines 1 and 2 /Fig.3/, the results of the arc energy measurements in the model groups with 2; 3; 4 and 5 module fuse-elements were subjected to a test of essential differences of the mean "t" values. It appeared that it is possible to determine with a 99% probability that there are no essential differences between the results in both these groups. The tests carried out on 110 models of fuse-links at interrupting I_2 currents made it possible to determine at a 0.98 confidence level the energy which is necessary for melting the specific mass of a copper fuse-element. On both the types of element models practically the same value of 53 ± 3,7 J/mm3 was obtained. For the sake of comparison. Table 2 shows the value of energy needed for damaging 1 mm^3 of a copper element as given by several authors.

Table 1. Values of the coefficients in equation/1/

Fuse-link model type	a_o /J/	a /J/	r^2
B	0,31	2,44	0,994
C	0,13	2,66	0,993

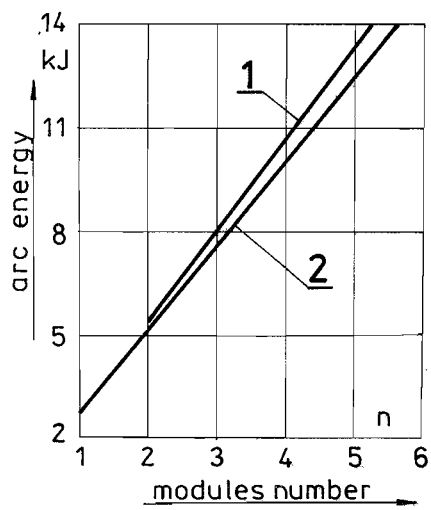

Fig.3. Dependence of short-circuit current interruption arc energy on fuse-element width. 1-single strip element, 2-multi-strip element.

Table 2. Energy needed for damaging $1mm^3$ of copper-element

Source of information	Element melting energy /J/mm^3/
Kohlrausch [2]	53
Johann [1]	46,3
Turner [6]	53,4
author	53 ± 3,7

The relatively high scatter of results obtained by the author is explained by the effect of restrictions on the arc burning process.

5. INTERRUPTION OF OVERLOADS

These tests were carried out at an alternating voltage of 1180 ± 20V in a circuit having a power factor of 0.5 ± 0.05. The test current I_p was selected so that a current value of 75A with a tolerance of 2% corresponded to one module i.e. the test overload to 75·n±2% Amps. This corresponded to the prearcing time, in dependence on the dimensions and shape of the fuse-element, from 20 to 2000 seconds.

Fig.4. shows the dependence of the fuse-element melted lengths on the number of modules in the element as calculated on the basis of measurements. Line 1 /Type B fuse-links/and line 2 /Type C fuse-links/show the courses X = f/n/ as calculated by the minimum square deviation method. Vertical lines have been applied for marking the mean arithmetic values deviation ranges calculated on the confidence level of 0.98. As it may be seen the dependences X = f/n/ have the shape of a straight line. $X = X_o + a \cdot n$ /2/ Nevertheless, the linear correlation coefficients r^2 given in Table 3 have small values, which may be an indication of a relatively low probability of describing correctly the obtained results X = f/n/ by means of the equation /2/.

Nevertheless, it may unambiguously stated that the application of parallel fusible strips in a fuse link instead of one strip with a summary width for interrupting overload currents having a prolonged arcing time from 20 to 200 sec.diminishes by 3 to 3.2 times the mean melted length of the fuse-element. This has a considerable significance in practice in the case of high voltage fuse-links.

Table 3. Values of coefficients in equation /2/

Fuse-link model type	X_o /mm/	a /mm/	r^2
B	78,43	-0,02	0,01
C	30,3	-1,56	0,12

Fig.5. shows the dependences of energy /A/ emitted in the arc at interruption on the number of modules in the fuse-element as calculated on the basis of measurements. Lines 1 and 2 show the courses of A=f/n/ calculated by the minimum square deviation method. The vertical lines have been used for marking the mean arithmetic value deviation ranges, calculated on the confidence of 0.98.It may be easily seen that the dependence A=f/n/ has the shape of a logarithmic curve

$$A = A_o + A_1 \cdot \ln \cdot n \qquad /3/$$

The coefficients in equation /3/ as determined by the above mentioned minimum square deviation method have such values as given in Table 4.

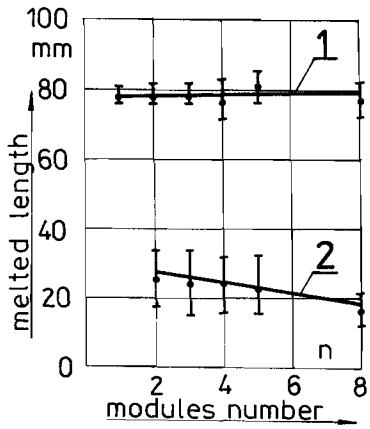

Fig.4. Dependence of the fuse-element melted lengths at interruption of I_2 current on their length.

Table 4. Values of coefficients in equation /3/

Fuse-link model type	A_o /kJ/	A_1 /kJ/	r^2
B	3,8	8,8	0,5
C	0,78	1,05	0,16

As it may be seen the energy emitted at overload interruption by a type B fuse-link with a single element is from 6.1 to 85 times higher than the energy emitted in the C link with an element composed of single one-module strips. This is confirmed to some degree by the arcing times as calculated by the dependence from which it follows that virtual arcing times /t_{Va}/ are in the case of type B models from 4.3 do 7.5 times longer than the times obtained on type C models. The shortening of the arcing time obtained due to division of the strip element into n parallel strips seems to be caused by the fact that the arc usually melts only one of the strips. This means that in the process of interruption migration of the arc takes place. The taking over of the interrupted current by one of the parallel strips in the cause of a current density in that strip, and consequently of a considerable shortening of the arcing time. The arc migration lasts until conditions for the its extinguishing appear. The more so because, according to Onufrienko's investigation [3], the penetration of the arc plasma into the inside of the sand filler does not exceed in practice 2mm at strip thicknesses of not more than 200 μm. The advantages following from subdividing the module strip element in n parallel single-module strips are shown in Fig.6 which gives the dependences of the arc energy magnitude, related to a single module $A' = /\frac{A}{n}/$, on the number of modules in the fuse-element. Another criterion for evaluating the effect of the fuse-element construction on the interruption of overloads consists in a comparison of the energy needed for melting/damaging/ $1mm^3$ the fuse-element in type B and type C fuse-element. The results of measurement and calculation indicate that the values of the energy involved are dependent on the construction of the strip fuse-element and also to same degree on the magnitude of the test current.

$$t_{Va} = \frac{\int i^2 dt}{I_p^2} \qquad /4/$$

Fig.7 shows the results of measurement and calculation of the energy E needed for damaging /melting/ $1mm^3$ of, copper strip elements placed in models of the.B-type /curve 1/and C-type /curve 2/. The lines 1 and 2 show the dependence E = f/n/ as determined by the minimum square deviation method. The vertical lines are used for marking the mean value

deviation ranges calculated on the confidence level of 0.98. It may be concluded from Fig.7 that the dependence E=f/n/ has the form of an exponential curve for both the curves.

$$E = C_0 - C_1 \cdot \ln \cdot n \qquad /4/$$

The coefficients in the above equation as determined by the minimum square deviation method, have such values as compiled in Table 5.

Table 5. Coefficients in equation /4/

Fuse-element type	C_0 /J/mm3/	C_1 /J/mm3/	r^2
B	116,85	21,65	0,18
C	46,15	3,53	0,03

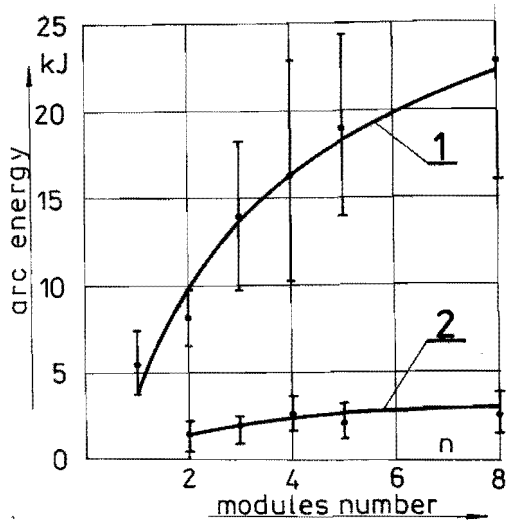

Fig.5. Dependence of overload current interruption arc energy on fuse-element width.
1-single-strip element; 2-multi-strip element

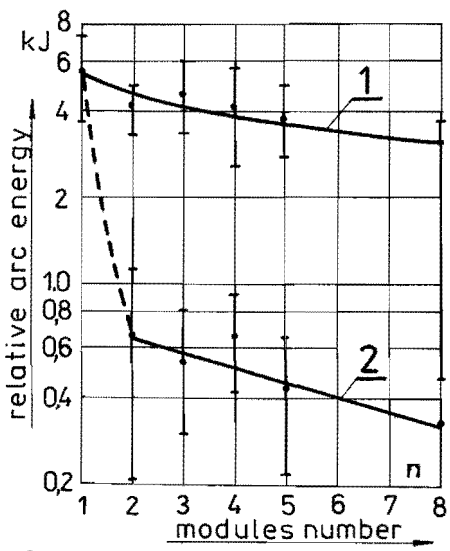

Fig.6. Dependence of overload current interruption arc energy related to a single module upon the width of the fuse-element.
1-single-strip element;
2-multi-strip element

The results of measurement and calculation indicate that value of energy E needed for melting 1 mm^3 of copper in a 0.2mm thick fuse-element surrounded by quartz sand is dependent on the magnitude of the test current and on the construction of the fuse-element. Thus, when interrupting critical fault currents I_2, at alternating voltage, the energy is approximately equal to the values given in references [1, 2, 6] , amouting to abt. 53 J/mm^3. At the interruption of overload currents corresponding to prearcing time of from 20 to 200 sec. the values of that energy is dependent on the construction of the fuse-element to a great degree. For instance, in order to melt 1mm^3 of a 0,2mm thick cooper fuse-element /Fig.1/ composed of from two to eigth single-module strips, 3mm wide each, the values E is nearly completely independent from the number of the strips, amounting to 50 J approximately.

This is a lower value than of 53 J given in references [1, 2, 6] . On the other hand, in the case of a single fuse-element n-module strip the values E is considerably dependent on the width of that strips. Thus, abt. 115 J are needed for melting 1 mm^3 cooper in a 3mm wide single-module strip, and abt. 70 J for a 24mm wide eight - module strip respectively. The explanation is a simple one. The prearcing times are in this case several times longer than at parallel strips, amounting to abt. from 160 msec. for a single-module strip up to abt. 80 msec. for an eigth-module strip. At such long prearcing times a considerable portions of the energy emitted in the fuse-link at interruption is absorbed by the arc-quenching material. Further, the shorter prearcing time as measured in fuse-links having wider elements follows also from the arc does not burn equally at the total length, and only in points moving on the cathode and anode i.e. on the whole width of the strip. The migration of the arc accelerates the melting process i.e. legthening of the arc, and in consequence it results in shortening the arcing time.

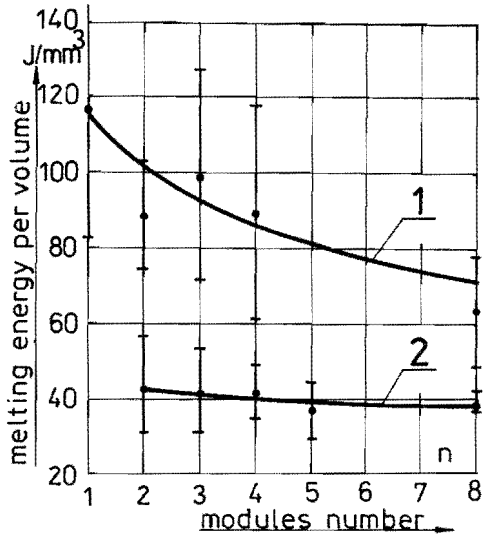

Fig.7. Dependence of copper fuse-element melting energy at interruption of overload current upon the width of fuse-element.
1-single-strip element,
2-multi-strip element.

CONCLUSIONS

The model tests that had been carried out on fuse-links with single and parallel strip elements at alternating voltage of 1180 ± 20V for interrupting critical I_2 short-circuit and overload currents selected so that the prearcing times amounted to from 20 to 200 sec. permit to draw the following conclusions:

/a/. The measured value of energy needed for melting 1mm^3 of a copper strip element at interrupting a critical short-circuit current amounts to 53 ± 3.7 J/mm^3, being in practice the same for single as well as for parallel elements having identical cross-sections.

On the other hand, at interruption of overload currents the value of the energy involved amounts to abt. 40 J/mm^3 for parallel strip elements and in the case of single elements it is dependent on their width, amouting to abt. 115 J/mm^3 for a single-module element and abt. 70 J/mm^3 for an eight-module element.

/b/. The melted length of strip element at the interruption of overload current is 3 to 3.2. times higher in the case of single strip elements than that in the case of parallel elements of the same cross-section.

/c/. The energy emitted at the fuse-link at the interruption of an overload current is 6.1. to 8.5 times higher in the case of links with single-strip elements than in the case of links with parallel strip elements of the same cross-section.

Further, the virtual arcing time time is 4.3 to 7.5 times higher respectively.

REFERENCES

1. Johann H.: Ausschaltlichtbögen in elektrischen sicherungen mit körnigem Löschmittel. Teil 1. Mechanische und thermische Vorgänge. Siemens-Forsch,-u. Entwickl.-Ber. Bd.7/1978/ Nr 4.

2. Kohlrausch F.: Praktische Physik 22. Aufl. Stuttgart: Teubner 1968

3. Onuphrienko Yu.I.: On researches of the arcing process in fuses with filler /sand filled fuses/ Int. Conf. "Elektryczny Łuk Łączeniowy" Łódź 1977

4. Ossowieki J.: Analysis of the fuse elements filling process with quartz sand. Instytut Elektrotechniki, Works 1970, Nr 64, /In Polish/

5. Rosen P.: The optimum disposition of high voltage current limiting fuses of give maximum severity on breaking capacity tests. Inf.Conf."Elektryczny Łuk Łączeniowy"Łódź 1977

6. Turner H.W.,Turner C.:Calculation of the burn-back rate of a fuse element and its relation contact erosion.Int.Conf.:Elektryczny Łuk Łączeniowy" Łódź 1977r.

7. IEC Publ.269-1: Low voltage fuses.Part.1: General requirements, 1986r.

Session IV

ARCING AND DISRUPTION PHENOMENA 2

Chairman: Dr. J. E. Daalder

ARCING PHENOMENA IN A TYPE OF LOW VOLTAGE FULL RANGE FUSES

Wang Ji-mei Meng Xian-zhong

Xi'an Jiaotong University
The People's Republic of China

Abstract

In this paper, the authors give out a kind of full range fuse applying to the low voltage power distribution system, the element structure of which is made of silver or copper metal combined with M-spots and gasing material. The authors explain the experimental results and obtain the main experimental conclusion from the test samples as follows: The element can improve the rupture of low overload currents and high rated breaking current.

1. INTRODUCTION

In recent years, a new kind of fuses have been developed in few countries with full range clearing ability, which could be described as " a current limiting fuse, capable of breaking under specified conditions all currents from the rated breaking current down to the lowest overload current that causes melting of the fuse element " (6).

IEC recommendations requires for standard fuses that the shapes of the time current characteristics lie between definite time current values in the overload and short circuit range, the temperature rise should be below the specified values and the breaking test should finished under the requirements. So all the experiments are according to these recommendations.

2. CONSTRUCTION OF FUSE ELEMENT AND TEST CIRCUIT

The main parts of the fuse element are (shown in Figure 1):
(a) Basic element which is a notched strip is made of silver or copper metal;
(b) M-spots are used to be better off the breaking performance of low overload currents, which are located at the necks of fuse element;
(c) Covered medium (gasing materials) is made of PTEE (polufluortetraethylene) to quench arc and to advance the dielectric recovery strength by producing gases. It is belted on the basic element.

Figure 2 shows the principle of the breaking test circuit with low overload currents. The turn-over time from the subsidary circuit to the main circuit is less than 0.08 second by our automaticall controlled device. The voltage of subsidary circuit is about 10V and the voltage of main circuit is 550V.

The main measuring instruments for low overload breaking test are as follows:
(a) A time counter records the prearcing time and the arcing time;
(b) A tape memory recorder and a light-ray oscillograph both are used measuring the fuse arc voltage and current with low overload.

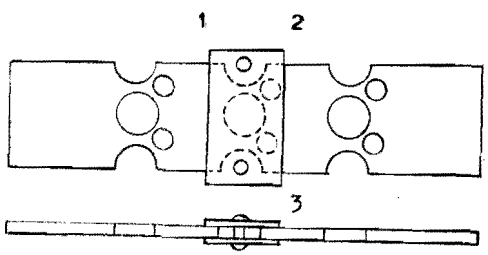

Figure 1. Fuse element
1——M-spots 2——Covered medium
3——Bolt

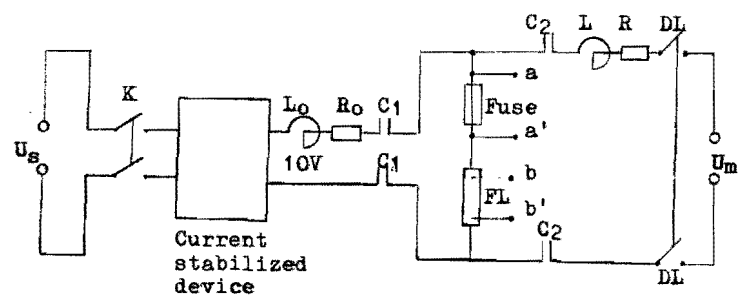

Figure 2. The principle of the breaking test circuit with low overload currents
U_s=220V U_m=550V FL——Shunt C_1,C_2——Contacters

3. EXPERIMENTAL PHENOMENA

3.1 LOW OVERLOAD CURRENT REGION

If it is not specified, the low overload current means the current less than $3I_n$ and more than $1.25I_n$. Low overload current breaking tests prove that the fuse element sometimes multiple reignition take place (arcing, recovery and reignition for a few semiwaves) then clearing.

For copper fuses, if I_p is less than $1.6I_n$, the multiple reignition would occru. The typical curve of this phenomena is shown in Figure 3. Fulgurites are comparatively regular and have black colour near M-spots, red colour among them, white colour in the other region and also clear grains of quartz sand. M-spots in the neck of constrictions except the middle constric-

tion have the melting traces and spots. The total length of arc lumen is not longer than the diameter of siddle holes in the fuse element in normal cases.

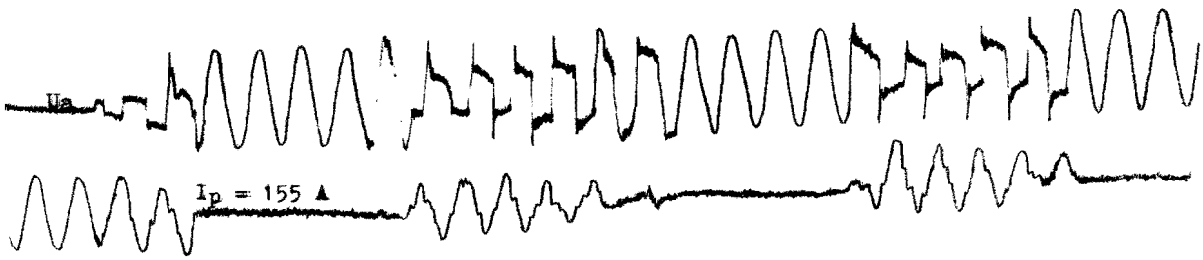

Figure 3. The typical curve of low overload current breaking test (for copper element)

The permanent high frequency oscillation phenomena are observed in the measurement of arc voltage which is flat on the average in the initial 1-2 ms. Near the zero current region, the voltage frequency is about 1 kHz and then the voltage frequency is higher than 1 kHz.

For silver fuses, no multiple reignition is found, under the same conditions as copper fuse test circuit parameters, the arc gap is shorter and the total arcing time is much smaller, the remains of covered materials are more than that of copper. M-spots on the two sides are seen to have subtle melting traces.

3.2 SHORT CIRCUIT CURRENT REGION

For sort circuit current test up to 50kA(r.m.s.) at 550V. Insulation resistances of copper fuses are above 100 KΩ, sometimes up to 2.5 MΩ and insulation resistances of silver fuses are above 100 KΩ too which are satisfied with the IEC recommendations (1). The typical curves of short circuit test with 50kA (cos=0.15) are shown in Figure 4.

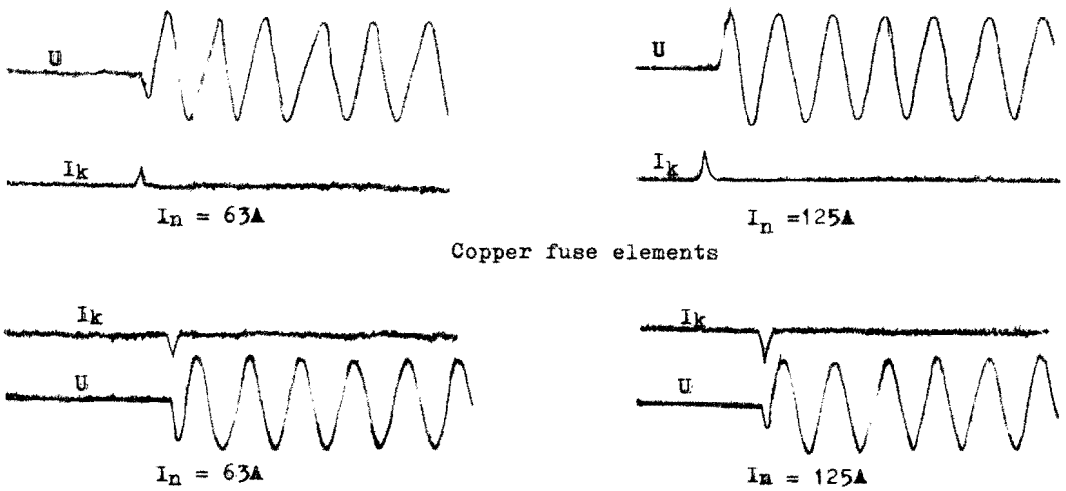

Figure 4. The typical curves of short circuit test

4. M-EFFECT AND G.Q.A. (THE GAS QUENCHING ARC PRINCIPLE)

In recent years, some scholars investigated the fusing and aging behavior of fuse elements with M-spots (9) (10) to indicate the two different patterns of fusing. In our tests, it is observed that the melted tin flows forward to the element neck, until the melted tin reaches to the element neck, the basic element begins to dissolute to the liquid state and it develops more quickly. The dissolution and the penetration are alternatively produced. It makes the electric conductivity and the thermal conductivity of element decreasing. While the surfacial force on the liquid phase can't keep the ballance. The element necks are vapourized and produce arc suddenly. These process may be explained by Figure 5. Figure 5(A) shows the liquid tin contacts the surface of the basic element. Figure 5(B) shows the two materials(tin and copper) occures dissolution and penetration. Figure 5(C) shows the two materials completely dissolution and penetration. Figure 5(D) shows the liquid state of the two materials starts to occur arc. If the quantity of tin M-spots are so small and thin, the liquified time should be delay that means M-spots effect needs to a long time.

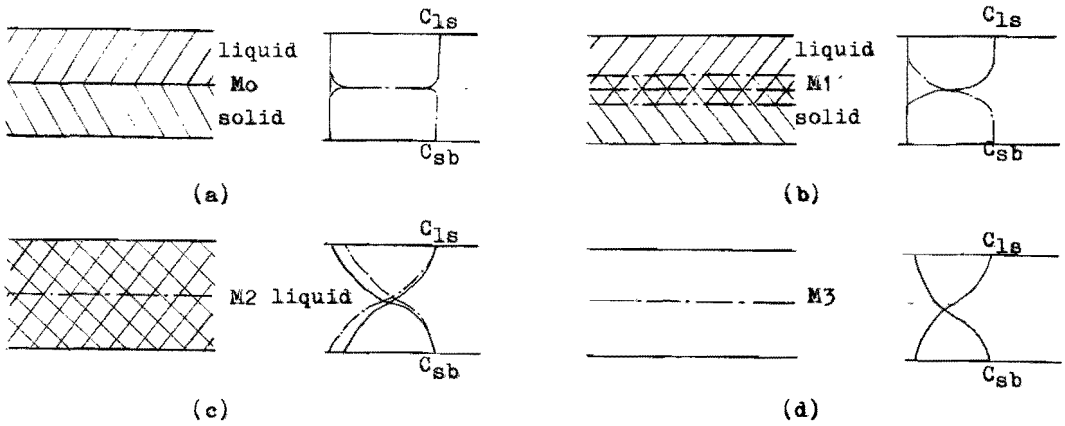

Figure 5. The penetration process of M-effect

The covered material can produce gas and change the dissipated heat state of the fuse-elements, when the elements change into liquid state, the gas promote it to vapourize. The electric conductance becomes insulation state and higher dielectric recovery strenth may be established. What is more, a lot of energy may be consumed by quartz sand to against arc reignition. In this sense, the producing gas is a well condition to quency arc.

As for short circuit current, the discomposition of PTFE is very rapid, according to the theory of high polymer chemistry, when PTFE discomposed, its main products are monomer(≥95%) and a little gaseous hydrogem fluoride. F(fluorine) has the highest electronic attaching ability. The products can attach electrons, decreasing the conductance and promoting the establishment of the dielectric recovery strenth.

5. DISCUSSION

5.1 GENERAL ANALYSIS

The differences of arc phenomena between copper fusea and silver fuses existed, the main reason of which is considered that, in breaking low overload current, during the period of copper fuse rupture, more metal vapour is produced in lumen area, there are more electric conductive particles, this may occur the thermal breakdown sometimes, until the column is cooled enough.Meanwhile more quantity of M-spots materials flow into the column or the lumen area, thus the multiple reignition is easy to occur. For the silver element, by the end of reignition that is kept continuously arcing for several ten ms, because of less metal vapour and column cooling, gas quenching arc, attachment of electrons, enough dielectric recovery strength had been formed, so the multiple reignition couldn't show up. From the viewpoint of energy, it followed that in this circumanstance, there are not enough input energy to maintain the continuous arc so arc put off, and larger gaps eventually created the good conditions for higher dielectric strength.

5.2 FULGURITES

With low overload, the formation of fulgurites depends on mainly the arc energy and the temperature fields of elements, so silver fuses and copper fuses have small fulgurites, but the fulgurites of silver fuses are smaller than those of copper fuses.

Fulgurites of copper fuses after short circuit currents are statistically classified into two kinds: Flat type and tip type.

Flat type hadm't obvious climaxes, the current density $J_1 < J_I$ and $J_2 < J_{Ic}$.

Tip type had striking climames, the current density $J_1 > J_I$ and $J_2 > J_{Ic}$.

These two values J_I and J_{Ic} are taken as the critical values of flat type and tip type, $J_I = 4.5 - 5.6 \times 10^6$ A.cm^{-2} from the prospective short current and $J_{Ic} = 1.6\text{-}2.25 \times 10^6$ A.cm^{-2} from the cutoff current.

The primary conclusion is that the copper fuses would be suitable for make of one, two and three fuse elements.

Figure 6. shows the typical photograph of fuse fulgurite after 80A low overload current test. Figure 7. shows the typical photograph of fuse fulgurite after 50kA short circuit current test.

(80A low overload current test)

Figure 6. The typical photograph of fuse fulgurite.

(50kA short circuit current test)

Figure 7. The typical photograph of fuse fulgurite

6. SUMMARY

(a) The fuse elements with M-spots and covered gasing materials (PTFE) can successfully break low overload current;

(b) In breaking low overload currents, arcing will be multiple reignitions for copper fuses and single reignition for silver fuses;

(c) General description is given about M-effect and G,Q.A.

7. ACKNOWLEDGEMENT

The authors wish to thank Miss Li Yialin, Xi'an Fusegear works and the colleagues in Division of Electrical Apparatus, Xi'an Jiaotong University, China for their supporting in test and the Science Fund of the Chinese National Science Committee for supporting this work.

8. REFERENCES

(1) IEC Publication 269: Low voltage Fuses.

(2) Mikulencky H.W.: Current-limiting fuses with full-range clearing ability. IEEE Trans. on Power Apparatus and System Vol. PAS-84, No12, pp 1107-1116, Dec., 1965

(3) Holec. Corp. : The product sample introduction of h.v. full-range fuses.

(4) P. Rosen: 'Full-range-fusing' ——— a new concept in system protection, Electric Review, 213 No4 July, 1983.

(5) Ofte A. and Rondeel W.: Test procedure and arcing phenomena in h.v. fuselinks near the minimum breaking current. Trondheim. International Conference on Electric Fuses and their Applications. 13-15 June, 1984.

(6) Lipski T.: Lectures on Electric Fuses. Xi'an, China. Sept. 1983.

(7) Van der Scheer D. and Reith H.F.J.: High voltage current-limiting fuselinks capable of breaking all currents that cause melting of the fuse element. Trondheim, Int. Conference on Electric Fuses and Their Applications. 13-15 June, 1984.

INVESTIGATIONS OF THE PRESSURE SHOCK-WAVE GENERATED BY H.B.C. STRIP FUSE ELEMENTS AT THE ARC-IGNITION INSTANT IN SAND FILLED FUSES

J.Hibner, T.Lipski
Gdańsk Technical University, Gdańsk
Własna Strzecha 18 a
Poland

Abstract

The paper describes laboratory investigations of the pressure exploding component generated at the instant of the arc-ignition instant in h.b.c. fuse-elements. 3 different strip shapes of the fuse-elements were applied. Also 4 thicknesses and 5 widths of those strips were used. Tests in a l.v. short-circuit test's rig were carried out using 2 different h.b.c. model fuses. As an arc-quenching medium the standard sand of l.v. fuses was utilized. The test results show some distinct influence of the constiction number, strip length and its width. Test results are illustrated by the oscillograms and the profiles of above mentioned relations. The conclusions end the paper.

1. Introduction

The pressure generation during electrical conductor explosion is known from many years. For example the recorded pressure of order 100 MPa was not so seldom case, if a wire was exploded in the water [5]. Electrical explosion investigators usually are speaking about so-called exploding component [2] of the pressure, because the whole energy delivered to the exploding conductor responsible is for that pressure. On the contrary in h.b.c. fuses , in which a fuse-element is placed in quartz sand during arcing, two pressure components are generated [6]: one, exploding component, at the instant of the arc-initiation due to fuse-element initial explosion (usually in constrictions); second one, arcing component [4] as a result of delivering of the energy to the arc-column. The superposition of those both components is responsible for an exposure of the fuse-link body onto eventual damage due to mechanical failure.

Because both mentioned components are acting in completely different time spans the peak of the superimposed pressures equals to the peak of the one or another component. The time duration of the explosive component is of order hundreds microseconds whereas of the arcing one equals to the arcing-time, say several milliseconds. The explosive component usually is oscillatory one with a strong pronounced damping mainly by sand, while the arcing pressure follows approx. after comulative effect of the liberated arc-energy. The explosive component, upon suggestion given in [6], depends on some power of the current density in the explosion instant. And, of course, due to good damping ability of the sand the pressure magnitude on the fuse-link body is much smaller than that in the exploding constriction.

Published results [3] on the explosive component are dealing with the uniform Cu wire fuse-element of diameter 0.5 mm and length 20 mm streached in the sand. From the manufacturing point of view, however, more interesting should be the pressure behaviour in h.b.c. fuses equipped within strip elements having some constricted parts. This need became the base why since 1977 in our Institute a number of the measurements were done on the pressure in some model h.b.c. fuses with the strip elements. Some results of those investigations limited just to the exploding component are reported hereinafter. Everywhere in the following text speaking about the pressure one shall understand the exploding component of the pressure.

2. Experiments

2.1 Test circuit

To get the most reproducible conditions of the tests using AC current a thyristor making-switch has been used of 1 kA continuous rated current and 2 kV peak reverse rated voltage, shown in Fig.1. A coaxial practically noninductive shunt of 1 or 5 mΩ rated resistance serves to the current measurements. A cathode 5 beam oscillograph of 0.5 MΩ and 40 pF input constants enabled the records of the interested parameters. During check-out procedure of the measuring system a 2 beam oscillograph of 1 MΩ and 40 pF input parameters found an app-

lication.

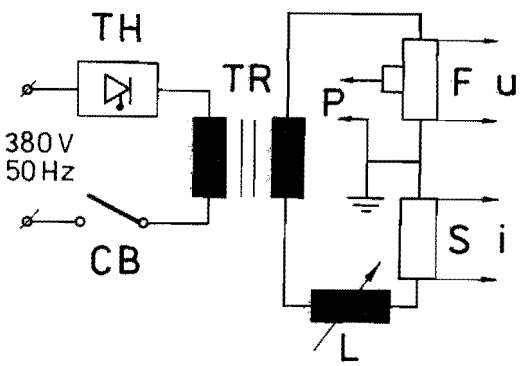

Fig. 1 Simplified test's circuit
TH - making switch, CB - safety circuit-breaker, TR - transformer 380/260 V or 520 V, L - choke, F - tested fuse, S - shunt, u, i, p - recorded voltage, current, pressure

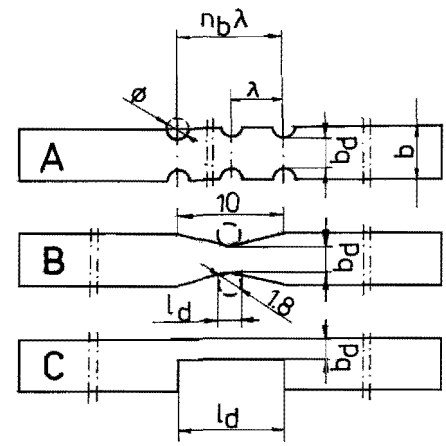

Fig. 2 Tested fuse-elements

2.2 Fuse-elements

The strip fuse-elements of the different shapes shown in Fig.2, of the thicknesses 0.05, 0.1, 0.185 mm and of the widths 3.1, 5, 7.5, 10, 15 mm were applied. The constrictions were distributed rhythmically along the fuse-element within modulus λ. Fuse-element type C has got a rectangular cutting out of the different length.

2.3 Model fuse-links

Two different kinds of the h.b.c. model fuse-links were used, body of which were made from some organic textolite. The body of one was tight, made from one piece (Fig.3a). The fuse-element in this case was soft soldered to the terminals. Arc-quenching chamber ,- 16 mm. The second one (Fig.3b) has got the chamber diameter 26 mm within lengthwise divided body, fastened by 4 screws M5. The fuse-element now is clamped to the terminals by the wedge fasteners. In every case as an arc-quenching medium the quartz sand of 0.3÷0.5 mm granularity has been used. The granularity fractions were : ab. 67 % of 0.385÷0.43 mm and ab. 22 % of 0.43÷0.49 mm. The fuse-elements were situated alongthe cylindrical arc-chamber axis. A standard firm procedure of the sand gave in result ab 16 % of the mass increment in relation to the loose sand in the chamber.

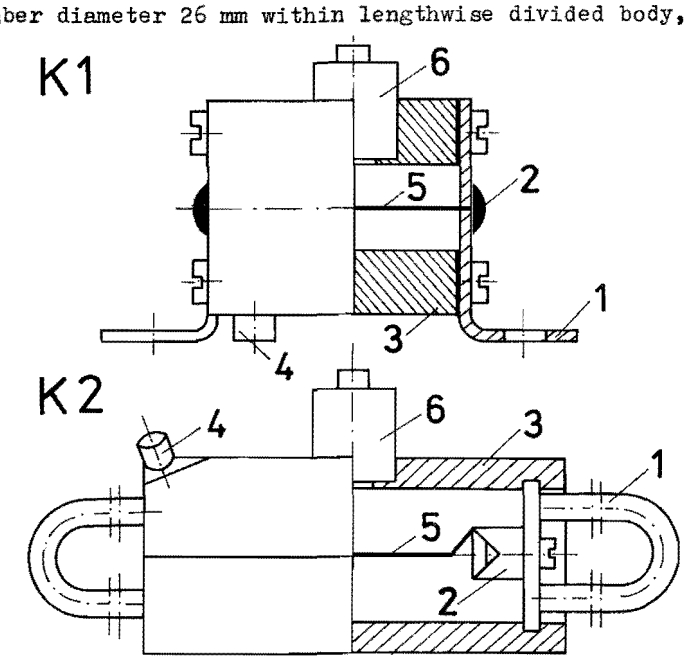

Fig. 3 Tested fuse-liks
K1 - chamber Ø 16 mm, length 42 mm; K2 - chamber Ø 26, length 64 mm; 1 - terminal; 2 - fuse-element connection; 3 - body; 4 - hole for sand strew in closed by nut M8X1 mm; 5 - fuse-element; 6 - p-sensor of Ø 8 mm surface

2.4 Pressure sensor

A piezoelectric sensor has been used of the sensitivity 1.88 V/MPa, self-capacity 900 pF and resistivity 600 GΩ. The measured frequency range up to 100 kHz. A concentric cable of Ø 7 mm and of 5 m length to connect the sensor with oscillograph was applied. The wave resitance of the cable,- 75Ω. The check-out tests of the presure

measuring system has showed no practical influence of the interferences.

3. Test results

Pressure test results show relatively great dispersion, that's why to determine an average magnitude it was necessary to make atleast 10 measurements. Some exemplary results indicated in the Fig.4 show that the exploding pressure component lasts less than 100 μs.

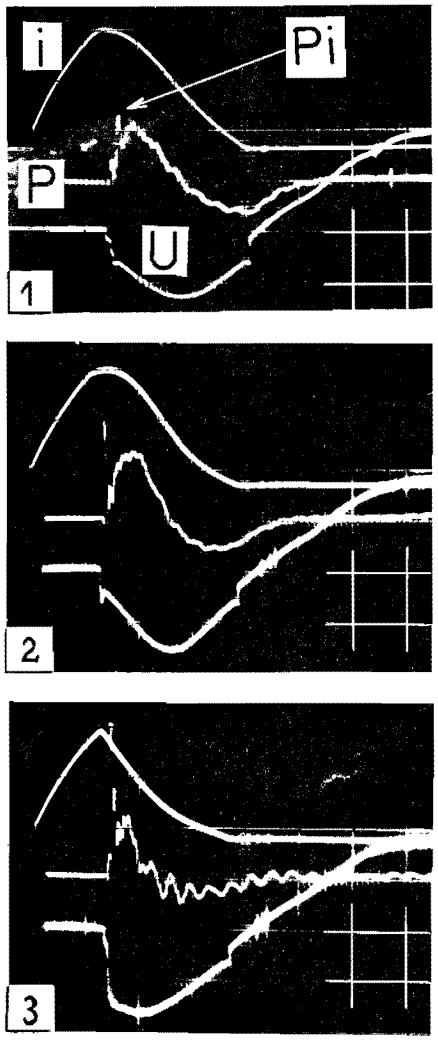

Fig. 4 Exemplary test records of fuse-links K2, circuit conditions 520 V, 50 Hz. 1 -element A, n_b= 3, constrictions Ø 1.8mm, λ = 3 mm; 2 - element C, l_d= 5 mm; 3 - as 2 but l_d= 20 mm. Scale unit 746 A/cm, 216 V/cm, 0.216 MPa/cm, 1.5 ms/cm

Obtained results are summari/zed in the Figs 5 to 9. Given in those Figures exemplary profiles are for this same costriction cross-sectional area. Due to the adiabatic heating conditions kept during the tests in every case the current density at the instant of the arc-initiation was practically this same. From Figures 5 to 8 outcomes that the influence of the parameters n_b, b_d, and l_d on the pressure is weakening with their growing according to the rule

$$p_i = \frac{p_{max}}{1 + \frac{k}{x}} \qquad (1)$$

in which x is one of the variable n_b, b_d, l_d. For example in the case of pressure relation on the length l_d from the experiments follows

$$p_i = \frac{0.8}{1 + \frac{10}{l_d}} \qquad (2)$$

where p_i in MPa, l_d in mm. From (2) it is clear that further the exploding part to the measuring point lesser its influence on the pressure measured. It can be showed that the relation (1) is in agreement with some analytical calculations based on sum of the partial pressures along the fuse element. The profile given in Fig.7 indicates, for instance, that already for $l_d > 25$ mm the pressure in the centre of the fuse-link has got nearly maximum value, but not so much higher than for 10 mm.

Data in Fig.9 suggest that there is not any logical relation. That's why the arc-ignition voltage can not be the base for the pressure calculation, despite that voltage relates to the length l_d and current density as follows

$$u_i = \rho l_d \sqrt{j} \qquad (3)$$

In addition to that it is necessary to admit that given in the Figure 9 magnitudes are practically for this same current density in the instant of explosion. The results show also (Table 1) that despite 1.8 greater current in the instant of explosion the pressure changes are small. This changes are of order of the result dispersion. But to underline is nearly this same current density at that instant. To note is as well that for every couple of results the circumference of the constriction was practically this same. The only change in both results of given couple was the difference of the thicknesses, i.e. 0.1 or 0.2 mm.

Aforementioned results suggest the pressure exploding component can be described as follows

$$p_i = k_p (b_d l_d)^{\beta} j_i^{\alpha} \qquad 2(\alpha-\beta) \qquad (4)$$

where p_i- in MPa; k_p- in $\frac{\text{MPa mm}}{A^{\alpha}}$ depends on the chamber diameter, sand porosity and granularity; b_d, l_d- in mm; j - ^{A}current density in A/mm^2; α, β - some powers.

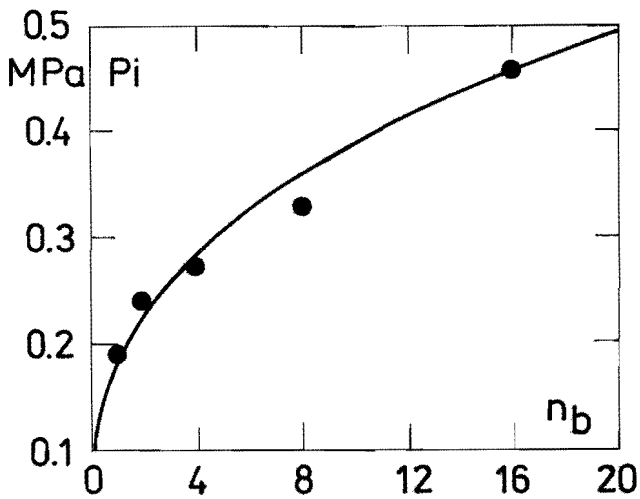

Fig. 5 p_i versus n_b for element A, fuse-link K1, 260 V, 50 Hz

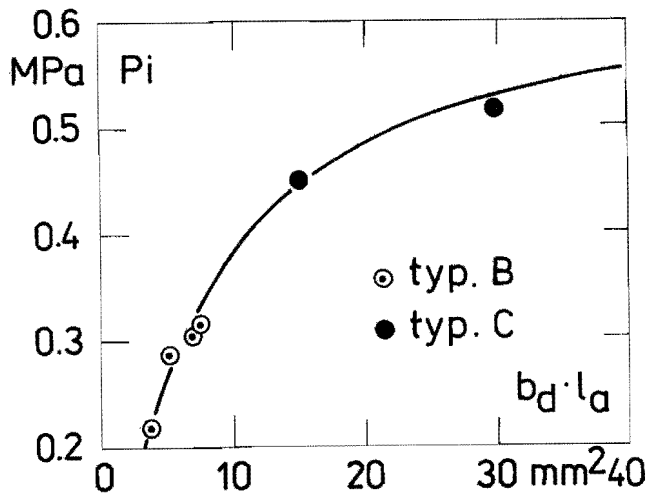

Fig. 8 p_i versus product $b_d \cdot l_d$ for element B and fuse-link K2 and element C and K2, 260 V, 50 Hz

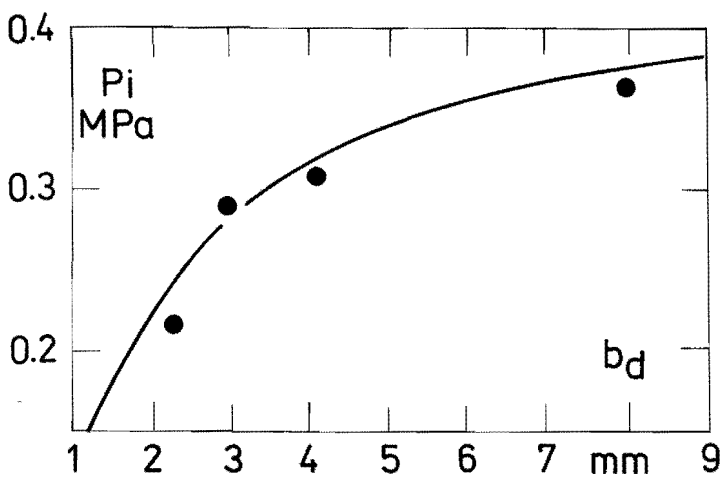

Fig. 6 p_i versus b_d for element B, fuse-link K2, 260 V, 50 Hz

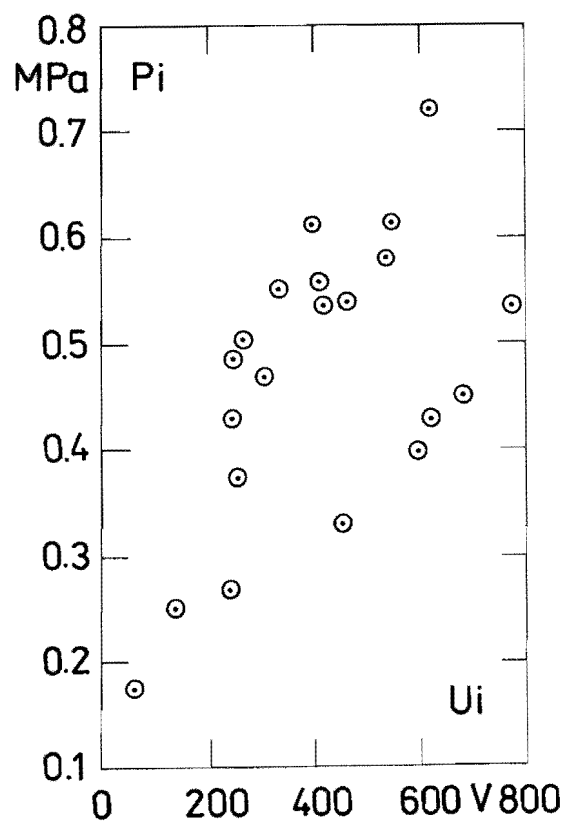

Fig. 9 p_i versus arc-ignition voltage u_i for elements A, B, C, fuse-link K2, 260 V, 50 Hz

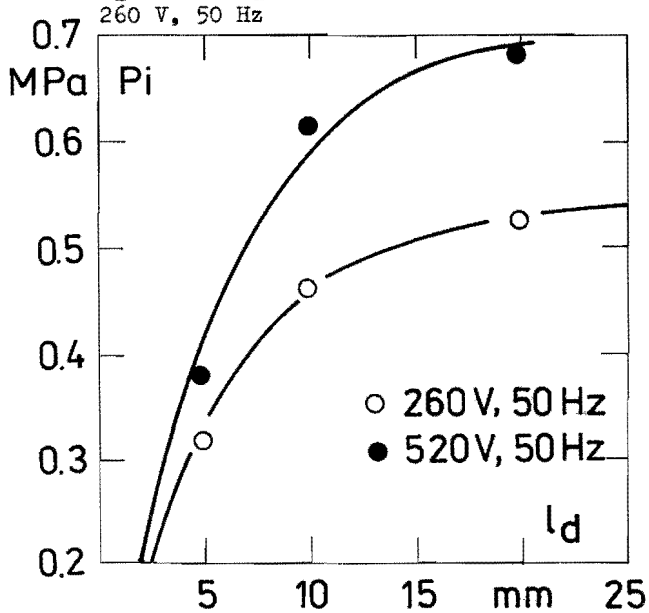

Fig.7 p_i versus l_d for element C, fuse-link K2, 260 V and 520 V, 50 Hz

The relation (4) relates to the tested fuse-link models, applied filler and moreover in the case of fuse-element C to the length l_d = 10 mm and it is valid for single element placed in the fuse-link axis in such a way that the flat surface is parallel to the measuring surface of the pressure sensor.

As the preliminary result it is stated that the powers α , β for those conditions are in the limits 0.5 ÷ 1.0.

Table 1 Influence of i, j, u_i on p_i

λ mm	n_b -	Ø mm	S_{d_2} mm^2	i A	j A/mm^2	u_i V	p_i MPa	p_i %	i %
3	3	1.8	0.15	1603	10686	253	0.328	100	100
3	3	1.8	0.30	2727	9090	250	0.392	120	170
6	3	4.3	0.15	1515	10100	305	0.370	100	100
6	3	4.3	0.30	2727	9090	341	0.455	123	180
6	5	4.3	0.15	1515	10100	538	0.477	100	100
6	5	4.3	0.30	2727	9090	449	0.506	106	180

Note: given in the Table magnitudes are for elements A, fuse-link K1.

4. Conclusions

A. The exploding pressure componenet lasts very short time(range of μs) and appears during explosion.

B. It can be assumed that in given design the exploding component depends on the fuse-element dimensions of its that part which explodes. As a parameter is the current density at the instant of arc-ignition and the circumference of the fuse-element in the place of explosion.

C. When a fuse-element does disintegrate along the whole its length the pressure exploding componenet is a maximum in the middle of the fuse-link. From the relation (2) it can be seen that the influence of some further parts is lesser on the generated pressure.

D. It seems, the exploding pressure component in described measurements depends on the current density rather than current magnitude in the instant of arc-initiation. For example by ab 1.8 times greater current the pressure remains nearly this same by nearly this same current density .

E. It seems, the exploding pressure component does not depends on the arc-ignition voltage. The problem needs some further investigations.

F. The practical calculation of the exploding pressure component, it seems, could be possible from the relation (4). But to get more precise results it is necessary to carry out further investigations to establish appropriate magnitudes of the powers α and β.

5. Acknowledgement

The authors wish to thank Mrs.D.Piotrzkowska, Mr.P.Piotrzkowsi and Mr.A.Bartus for their valuable contributions to the pressure measurements.

6. References

[1] Baxter H.W. 1950, Electric Fuses, Edward Arnold and Co Ed. London.

[2] Exploding Wires. Vol. 1-4, W.G.Chace and H.K.Moore Eds. New York, Plenum 1964.

[3] Gul A., Lipski T.Pressure shock-wave investigations during the wire-element explosion in a h.b.c. fuse. Switching Arc Phenomena Int.Symp. Łódź, Poland, 1985. P.I:Conf Materials p.326-330.

[4] Hibner J. Calculation of the arc-ignition voltage of the fuse-elements with rectangular constriction (in Polish). Przegląd Elektrotechniczny. 1978, No.5, p.204-206.

[5] Krsvage J. In Exploding Wires. Vol. 2, W.G.Chace and Moore Eds. New York, Plenum 1964.

[6] Lipski T. Generation and propagation of the pressure due to the fuse-element disintegration in h.b.c. fuses. Gas Discharges and Their Applications, Int. Conf. Oxford, 1985, p.87-90.

A ONE DIMENSIONAL MATHEMATICAL MODEL FOR THE DYNAMICAL BURNBACK VELOCITY OF SILVER STRIPS

J.G.J. Sloot and V.K.I Kalasek
Department of Electrical Engineering
Eindhoven University of Technology.

J. Sikkenga
Holec Systems & Components
Hengelo

Abstract

This article presents a one dimensional numerical model for the burn-back process, including changes of a metal strip under the influence of an arc.
Special attention is given to the velocity decrease caused by heat conduction and the velocit caused by Joule preheating.

Introduction.

In a short circuit situation, the arc voltage increasement of a fuse is dominated by the burn-back velocity of the metal strip.
Early investigations of Kroemer [1] showed a linear dependence between the velocity v and the current density j of the strip:

$$v = kj \quad \text{with } k = 1.15\ E\text{-}9\ [m3/As] \qquad (1)$$

Daalder [2] suggested an expression for the burning constant k:

$$k = \frac{U}{H_{drop} - H_{begin}} \qquad (2)$$

with

$$H_{begin} = c_s \gamma T_{begin} \qquad (3)$$

$$H_{drop} = c_s \gamma T_{melt} + \gamma L + c_\ell \gamma (T_{drop} - T_{melt}) \qquad (4)$$

In these formulas:

- U: power loss per A arc current to the electrode.
- H_{drop}: the maximal specific enthalpy of a metal part, before it is removed by the arc.
- H_{begin}: the already reached local enthalpy when the arc arrives.
- C_s,C_l: specific heat of the metal in the solid and liquid state.
- γ: specific density in the solid state.
- L: melting heat.
- T_{melt}: melting temperature.
- T_{drop}: temperature of liquid droplets.
- T_{begin}: initial temperature of the metal spot when the arc arrives.
- T_o: room temperature.

Because of Joule heating, T_{begin} can be considerably higher than T_o. For an adiabatic situation, T_{begin} was calculated from:

$$T_{begin} = T_o \exp\left(\frac{j^2 t L_{wf}}{\lambda \gamma c_s}\right) \qquad (5)$$

where $L_{wf} = \frac{\lambda \rho}{T}$ stands for the constant of Wiedemann-Franz, with λ for the thermal conductivity and ρ for the electrical resistivity.

Equation (2) fits a part of the experimental results of Daalder [2] with silver, under the assumption that U = 5.25 V and T_{drop} = 1700 K. However experimental velocities at current densities above 3 kA/mm2 and arcing times of about 5 ms, could not be described with equation (2) as T_{begin} would exceed T_{melt}.
Therefore, our first aim was to extend the validity of equation (2) up to higher current densities.
The most simple extension can be reached by allowing H_{begin} to exceed the product $C_s \gamma T_{melt}$.
In this case the enthapy increasement by Joule heating can be calculated with:

$$\frac{dH}{dt} = \rho j^2 \qquad (6)$$

where for the solid or liquid phase:

$$\frac{dH}{dt} = \gamma c \frac{dT}{dt} \qquad (7)$$

or for the melting phase:

$$\frac{dH}{dt} = \gamma L \frac{df}{dt} \qquad (8)$$

with fraction f<1

We made use of the fact that the resistance factor $A = \frac{\rho}{\gamma c T}$ proves to be constant for silver in the solid or liquid state.
With the resistance factor it follows for the adiabatic Joule heating:

$$T_{begin} = T_o \exp(Aj^2 t) \quad \ldots\ldots\ldots\ldots\ldots\ldots (9)$$

Together with the fractional melting we want to introduce the existence of a not infinitely thin melting layer between the solid and the liquid phase.
Such intermediate layers can occur when internal heat sources are present.

The next aim was to extend the stationary burn back model to a full dynamical model. After the arc initiation it can be expected that especially in the low current range a certain fraction of the arcing power is lost by thermal conduction into the silver before any remarkable burn back takes place; a certain delay time will be the result. At higher values of the arc current or the current period, a fraction of the Joule heat will also escape to the strip ends.

A one dimensional numerical model was developed to calculate the burn back rate including multi-phase effects and non adiabatic heating.

2. General model description.

A thin silver strip is provided with one notch and is fixed at both ends. A constant current starts flowing through the strip at time t=0. A homogeneous current density distribution is assumed. At t=0 the strip has a temperature T_o; the temperature at both ends is considered to be constant (T_o = 300 K) during the whole process. After some time the notch will melt and an arc will be introduced, which will burn back the strip gradually.
It is assumed that the silver material is removed as soon as it reaches the temperature T_{drop} ($T_{drop} > T_{melt}$).
Fig. 1 illustrates that during the burnback process, the part of the strip which has not yet been removed can be divided into three parts:

a. A liquid area with $xl \leq x < xm$.
   At the arcing front x=xl the temperature is maximum $T=T_{drop}$.
b. A melting area with $xm \leq x < xs$.
   Here the temperature is constant $T=T_{melt}$ and the melting heat has not yet been reached: $L < L_{melt}$.
c. A solid area with $xs \leq x < L_{band}$.

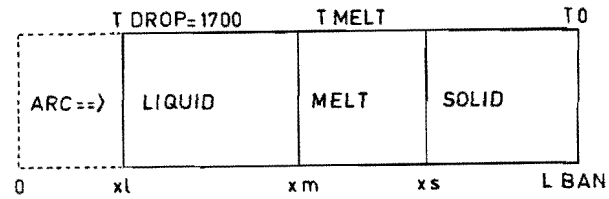

Fig. 1 Multiple phases within the silver strip during the burnback process.

3. The energy balance equations.

The three basic regions can be furher divided into N equal parts with length dx << LBAND.
For the solid and liquid phase the energy balance of an element can be described by the equation:

$$\underbrace{\int_x^{x+dx} c\gamma \left[T_{x'}^{t+dt} - T_{x'}^{t}\right] dx}_{\text{(Heat Content)}} = \underbrace{\int_x^{x+dx}\int_t^{t+dt} \rho j^2 \, dx dt}_{\text{(Joule Heat)}} +$$

$$- \underbrace{\int_t^{t+dt} \lambda \left[\frac{dT}{dx}\right]_x^{t'} dt}_{\text{(Input Heat Cond.)}} + \underbrace{\int_t^{t+dt} \lambda \left[\frac{dT}{dx}\right]_{x+dx}^{t'} dt}_{\text{(Output Heat Cond.)}} \quad \ldots\ldots\ldots\ldots (10)$$

with different values of the specific density γ, specific heat c, thermal conductivity λ and specific resistivity ρ for the solid and liquid phase respectively.

In the situation where the front element is bounded by the arc, the input heat conduction term has to be replaced by Pdt, with P=jU for the effective arcing power input.

For the melting region a similar energy balance can be set up:

$$\int_{xm}^{xm+dx} \gamma \left[H_x^{t+dt} - H_x^{t'}\right] dx = \int_x^{x+dx}\int_t^{t+dt} \rho j^2 \, dx dt +$$

$$- \int_t^{t+dt} \lambda \left[\frac{dT}{dx}\right]_x^{t'} dt + \int_t^{t+dt} \lambda \left[\frac{dT}{dx}\right]_{x+dx}^{t'} dt \quad \ldots\ldots\ldots\ldots (11)$$

In this equation the input heat conduction term has also to be replaced by Pdt in case the front element is bounded by the arc.
Within the melting region the temperature gradient is equal to zero.

4. Discretisation and assumptions.

The elements are numbered N = 1 ..N_{tot}, with $L_{band}=N_{tot}$ dx.

N=1: between x=0 dx and 1 dx
2: ,, 1 dx and 2 dx
N: ,, (N-1)dx and N dx
L: ,, (L-1)dx and L dx, the first liquid element
M: ,, (M-1)dx and M dx, the first melting element
S: ,, (S-1)dx and S dx, the first solid element

The time is also discretized: time t= Kdt, with step number K=0..K_{tot}.

A number of assumptions will be made to transform the set of integral equations into linear equations:

a) As the temperature in the whole element, the mean temperature within an element between x and x+dx is defined:

$$\int_{x=(N-1)dx}^{x+dx} T(x,t)\,dt = T_N^K\,dx \qquad (12)$$

b) For the heat conduction it is assumed:

$$\int_t^{t+dt} \lambda \left[\frac{dT}{dx}\right]_x^{t'} dt = \lambda\,(T_N^K - T_{N-1}^K)\,\frac{dt}{dx} \qquad (13)$$

The temperature dependence of λ is taken into account using different values for the solid, liquid and melting phase with indexes 1,2,3 respectively.

For the integral equation the relevant value at element N-1 is chosen.

c. During the melting the mean enthalpy in an element is taken:

$$\int_x^{x+dx} \gamma H(x,t)\,dx = \gamma H_N^K\,dx \qquad (14)$$

d. The temperature dependence of the specific electrical resistivity is taken into account by the resistivity factor A:

$$A = \frac{\rho}{\gamma c T} \qquad (15)$$

with A=A1 for the solid phase.
A=A2 for the liquid phase.
$\rho=\rho_{melt}$ for the melting phase.

The Joule heat development in an element during dt can be expressed as:

$$\int_t^{t+dt}\int_x^{x+dx} \rho j^2\,dx\,dt = A\gamma c j^2\,dx\,dt\,T_N^K \qquad (16)$$

e. It is assumed that the liquid arc front element is removed on a certain moment t_1 if:

$$\int_{x_1}^{x_1+dx} c\gamma T(x,t_1)\,dx > c\gamma T_{drop}\,dx \qquad (17)$$

If the last but one arc front element has been removed at time t_2, the instantaneous burnback velocity during the time range t_1-t_2 is defined as :

$$v_{mom}\,(t_1,t_2) = dx/(t_1-t_2).$$

f. The melting front element has been melted at time t_1, if:

$$\int_{xm}^{xm+dx} \gamma H(x,t)\,dx > \gamma H_{melt}\,dx \qquad (18)$$

The melting border then moves from xm to xm'=xm+dx.

g. The initial temperature of the silver strip is T_o.

The temperature of the fixed end remains constant $T=T_o$.

5. Sets of linear equations.

The integral equations now can be transformed into a set of linear equations. A number of substitutions will be introduced to reduce the length of the equations:

$$P_1 = \frac{P\,dt}{c\gamma\,dx}$$

$$B_1 = j^2 A_1\,dt \quad B_2 = j^2 A_2\,dt \quad B_3 = \frac{j^2 \rho_{melt}\,dt}{\gamma}$$

$$G_1 = \frac{\lambda_1\,dt}{\gamma c\,dx^2} \quad G_2 = \frac{\lambda_2\,dt}{\gamma c\,dx^2} \quad G_3 = \frac{\lambda_3\,dt}{\gamma c\,dx^2}$$

a. The liquid range with L < N < M.

The energy balance of the liquid front element L now can be described by:

$$T_L^{K+1} = (1 + B_2 - G_2)T_L^K + G_2 T_{L+1}^K + P_1 \qquad (19)$$

and the other liquid elements with L+1 ≤ N < M:

$$T_N^{K+1} = G_2 T_{N-1}^K + (1 + B_2 - 2G_2)T_N^K + G_2 T_{N+1}^K \qquad (20)$$

b. The melting range, with M < N < S.

The element M on the melting front, when it is bounded by the arc:

$$H_M^{K+1} = H_M^K + B_3 + cP_1 - cG_3(T_M^K - T_{M+1}^K) \qquad (21)$$

If the melting front element M is bounded by liquid material:

$$H_M^{K+1} = H_M^K + B_3 + cG_2(T_{M-1}^K - T_M^K) - cG_3(T_M^K - T_{M+1}^K) \quad \ldots\ldots(22)$$

The other elements of the melting range, $M+1 \leq N < S$:

$$H_N^{K+1} = H_N^K + B_3 - cG_3(T_{N-1}^K - 2T_N^K + T_{N+1}^K) \quad \ldots\ldots(23)$$

c. The solid range with $S \leq N < N_{tot}$.

If the solid front element S is bounded by the arc:

$$T_S^{K+1} = (1 + B_1 - G_1)T_S^K + G_1T_{S+1}^K + P_1 \quad \ldots\ldots(24)$$

If the solid front element S is bounded by melting material:

$$T_S^{K+1} = G_3T_{S-1}^K + (1 + B_1 - G_3 - G_1)T_S^K + G_1T_{S+1}^K \quad \ldots(25)$$

If the solid front element S is bounded by liquid material:

$$T_S^{K+1} = G_2T_{S-1}^K + (1 + B_1 - G_2 - G_1)T_S^K + G_1T_{S+1}^K \quad \ldots(26)$$

The other elements in the solid state:

$S+1 \leq N \leq N_{tot}$

$$T_N^{K+1} = G_1T_{N-1}^K + (1 + B_1 - 2G_1)T_N^K + G_1T_{N+1}^K \quad \ldots\ldots(27)$$

metal	: silver		
melting temperature	: T_{melt}	= 1234	[K]
mass density	: γ	= 1.05E4	[kg/m3]
specific heat	: C	= 270	[J/kg]
specific resistivity at T_{melt}	: ρ_{melt}	= 13E-8	[Ω]
resistivity factor below T_{melt}	: A_1	= 2.1E-17	[Ω4/J]
resistivity factor above T_{melt}	: A_2	= 4.4E-17	[Ω4/J]
melting heat	: L_{melt}	= 1.045E5	[J/kg]
thermal conductivity below T_{melt}	: λ_1	= 395	[W/mK]
" " above T_{melt}	: λ_2	= 185	[W/mK]
" " at T_{melt}	: λ_3	= 290	[W/mK]
length of the half of silver strip:	L_{band}	= 40E-3	[m]
power loss per ampere to electrode:	U_{con}	= 5.25	[V]
temperature of liquid droplets	: T_{drop}	= 1700	[K]

Table 1. Variables of the numerical model.

6. Results of the calculations.

The set of linear equations with the distinct conditions were assimilated in a relatively simple computer program, with PASCAL and FORTRAN versions, suitable for personal computers.

Time steps were chosen in accordance with the usual stability limits for the explicit solution method of the diffusion equation. Material properties were chosen in accordance with table 1.

The values for U_{con} and T_{drop} were chosen in according [2], although other combinations are quite possible.

The output results of the program can be characterized by normalized time-distance diagrams like Fig. 2. It shows the physical state history of any silver part; the length coordinate and the time are divided by the strip length and the total current period respectively.

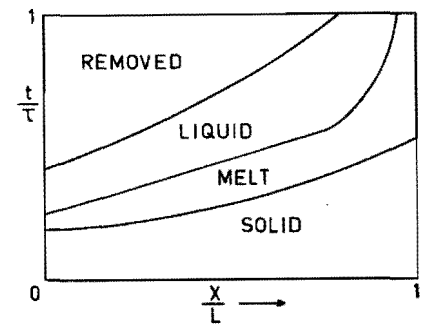

Fig. 2 Normalized diagram of the dynamic burnback process.

To illustrate the influence of the Joule heating and the heat loss by conduction the instantaneous burnback velocity was calculated for several constant current densities during a period of 5-10 ms. Some results are presented in Fig. 3.

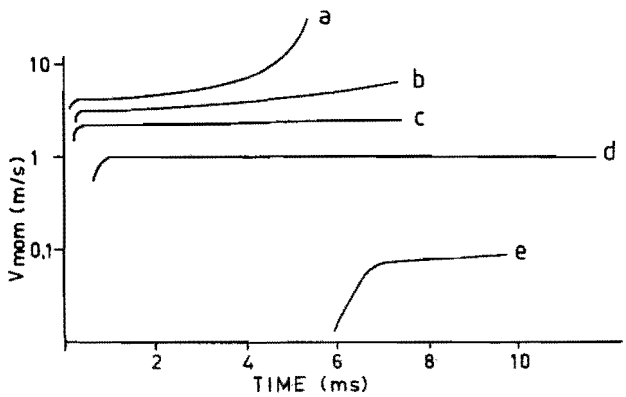

Fig. 3. Calculated dynamical burnback velocities.

current density [kA/mm2]	pre arcing time [ms]
a: 4.04	0.1
b: 3.18	0.2
c: 2.10	0.1
d: 1.02	0.6
e: 0.10	0.0

It is assumed that the arc is initiated after a 'pre-arcing time', during which the Joule heat source is already active. Fig. 3 shows that for the lowest current density (j=0.1 kA/m2), the heat loss by conduction can even prevent the burnback for several ms. In this case non-infinitely thin melting layers occured at the start of the process.

In the intermediate current density range 1-2 kA/mm2, the instantaneous velocity reaches the stationary value within a fraction of a ms.

At higher current densities the Joule heating can cause an exponential increase of the burnback velocity, but this forms no principal limit for the model validity.

Different from the low current situation, melting layers now appeared at the end of the movement process.

Fig. 2 presents instantaneous values, integration is needed when mean velocities have to be considered, which can be compared with experimental results.

In table 2 some experimental and calculated results of Daalder [2] are compared with our numerical program results for the mean velocity.

current density [kA/mm2]	pre-arcing time [ms]	arcing time [ms]	mean velocity exp [2] [m/s]	mean velocity calc [2] [m/s]	mean velocity pro-gram [m/s]
0.10	0.0	10.0	---	0.1	0.04
1.02	0.6	11.8	1.3	1.1	1.1
1.40	0.0	11.6	1.4	1.5	1.5
1.61	0.6	11.8	1.8	1.8	1.8
2.10	0.1	7.4	2.4	2.4	2.3
2.30	0.6	10.9	2.7	3.0	2.9
2.59	0.3	9.3	3.1	3.4	3.3
2.78	0.3	5.5	3.0	3.3	3.2
2.96	0.3	6.0	3.7	3.7	3.6
3.18	0.2	7.2	4.0	*	4.5
3.26	0.3	5.8	4.0	4.4	4.2
3.28	0.2	7.1	3.7	*	5.1
3.64	0.2	5.6	4.7	*	5.4
3.96	0.1	5.4	4.2	*	7.4
4.04	0.1	5.2	4.9	*	7.7

Table 2. Comparison between experiment, mean burnback velocities according [2] and the numerical program results, with N=500 and time step Δt = 1E-6 sec.

For j=0.1 kA/mm2 Table 2 shows that a considerably lower value for the mean velocity is expected with the program, when compared with the result of the stationary equation according [2]. This difference obviously is caused by the retarding influence of the heat loss by conduction. Unfortunately no experimental data were available to test the 0.1 kA/mm result.

An agreement can be noticed for the higher current density range until 3 kA/mm .

For the highest current densities the former calculation [2] is not valid, as T_{begin} exceeds T_{melt}; this is indicated in table 2 by an asterisk (*). The numerical model is not limited by this fact, although the results show systematic upside deviations, compared with the experiments.

Probably the Joule heating has a less dominant effect than it was expected, because the heat loss to the filler material becomes more important in this range.

Therefore a more dimensional model with implicit numerical procedures is under development.
Another approvement of the model is planned by increasing the number of elements, as the convergence limit is not yet been reached in the case of the high current densities.

Conclusions.

The one dimensional numerical model describes the dynamical burnback processes within a wide range of current densities.
It indicates that the heat loss by conduction in the silver has a delaying influence on the burnback velocity, during a fraction of a ms at 1 kA/mm or during several ms at 0.1 kA/mm .
As a consequence, the mean burnback velocity which is determined experimentally after a relatively long arcing time, often will not correspond to the instantaneous velocity obtained after short arcing times.

For current densities above 3 kA/mm the present model predicts an exponential increasement of the burnback velocity, although experiments show that this effect is less dramatic.

Acknowledgement.

The authors want to express their gratitude to Drs. A.J. Geurts of the Department of Mathematics of the Eindhoven University of Technology for his stimulating remarks.

References.

[1] : Kroemer, H.: Der Lichtbogen an Schmelzleitern in Sand.
Arch.Elektrotechn. 36 (1942) 455-470.

[2] : Daalder, J.E. and Schreurs, E.F.: Arcing Phenomena in High Voltage Fuses.
EUT Report 83-E-137. Eindhoven University of Technology (1983).

Session V

DEVELOPMENT AND DESIGN ASPECTS

Chairman: Prof. Dr. T. Lipski

LIMITATION AND ELIMINATION OF ELECTRON FIELD EMISSION OF THE HIGH VOLTAGE FUSE ELEMENT

Cz.Królikowski, M.Stroiński, H.Mościcka-Grzesiak
W.Górczewski, H.Gruszka

Technical University of Poznań
Electrical Engineering Department
Poznań, Poland

Abstract

In a high-voltage vacuum fuse, a disadvantageous phenomenon of the electron field emission from a wire may occur. This phenomenon can be limited by screening the wire as well as by increasing its smoothness. The paper shows the effect of screening the wire by electrodes, according to the size of the electrodes and their spacing. An improvement of the surface of the wire was obtained by electropolishing. It was found that electropolished wires are characterized by a considerably higher voltage, corresponding to the occurrence of the emission current.

INTRODUCTION

There has been a growing interest in the high voltage vacuum fuse lately. Laboratory investigations have shown that the vacuum fuse has a number of characteristic properties [1, 2, 3, 4, 5, 6]. One of them is breaking the current at the first passing of the current sinusoid through zero. As a result there is a lack of overvoltages in the circuit, and a lack of reignitions. The fuse element is short and the fuse chamber is of small dimensions.

The possibility of the phenomenon occurrence of electron field emission, from the surface of the fuse-element wire, is a defect. The field emission phenomenon is inadmissible, because:

- it causes surface roughening of the wire and a rapidly progressing ageing process of the wire,
- narrowings of the wire occur, which may even result in melting the wire,
- X-radiation is a secondary effect of electron field emission.

In the paper, the possiblities of eliminating and of limiting the phenomena of electron field emission will be presented, using two methods:

- screening the wire by means of two electrodes whose dimensions and spacing are properly chosen,

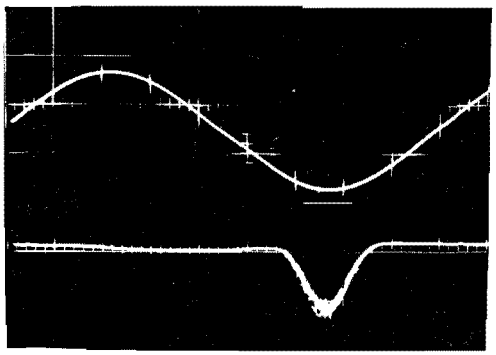

Fig.3. Oscillogram of voltage and emission current from the wire surface

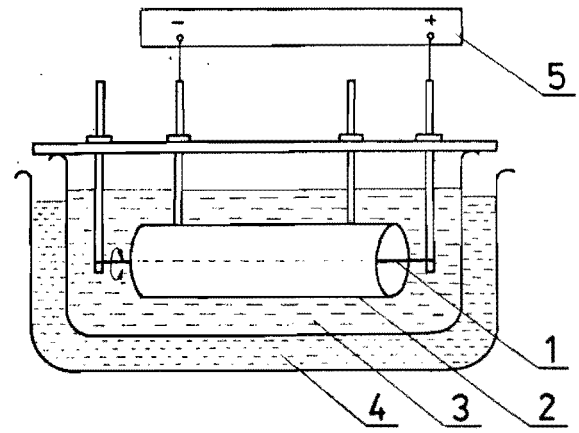

Fig.4. The set for electropolishing the wire, 1-electropolished wire, 2-cylindrical electrode, 3-65% water solution of orthophosphoric acid, 4-water bath, 5-stabilized voltage source

Figure 4 shows a set for electropolishing the wire. Before electropolishing, the wire underwent degreasing in a solution composed of: NaOH - 5g, Na_2CO_3 - 25g, $Na_3PO_4 \cdot 12H_2O$ -25g. The temperature of the solution amounted to 75°C, and the time of the degreasing - 4 minutes. The process of wire electropolishing was carried on in a 65% water salution of orthophosphoric acid /H_3PO_4/ at the temperature of 20°C. The electropolished wire was connected with the positive pole of the source, the voltage amounted to 0,8 V, and the current during the polishing of the copper wire, 0.5 mm in diameter and 90 mm long, amounted to 0.4 A. The time of electropolishing was 30 minutes.

RESULTS

Figure 5 shows the U_e voltage of occurrence of the 1 μA electron emission current, according to the diameter of the copper wire. The surface of the wire was only washed with alcohol. This figure presents the values of the arithmetic mean, calculated for fifteen measuring points as well as the standard deviation.

Figure 6 presents the U_e voltage of occurrence of the electron emission current from the wire, according to the H spacing between the electrodes, for a wire 0.15 mm in diameter and electrodes 22 mm in diameter which have been selected as an example. Figure 7 presents, for the same wire and the same electrodes the values of the arithmetic mean of the U_e voltage as well as standard deviations, according to the H spacing of the electrodes. Figure 8 presents in the common coordinate system the characteristics of U_e voltage, in the function of the H electrode spacing, for five diameters of the wire and for the 34 mm diameter of the electrodes. Figures 9 and 10 show analogical characteristics for the 22 and 14 mm diameters of electrodes. For small spacing of electrodes, equal to 0 - 25 mm, the electron field emission from the wire may not occur , whereas the emission current or breakdown occurs between the disk electrodes and the cylindrical

- improvement of the wire surface roughness, obtained by electropolishing.

EXPERIMENT

Samples

A copper wire 0.07, 0.15, 0.30, and 0.90 mm in diameter was used for the investigations. The wire was washed in alcohol or electropolished. The electrodes, made of electropolished copper, had the shape of disk 14, 22 and 34 mm in diameter.

Measuring systems

Figure 1 shows the investigated object. All the investigations were carried out at alternating voltage of 50 Hz, in the vacuum of the order of 10^{-4} Pa. The current of electron field emission was measured between the wire (1) and the cylindrical electrode (3), using the method of the high voltage unbalanced bridge, shown in Figure 2. Figure 3 shows the oscillogram of the emission current. Emission of electrons from the wire occurs only in the negative half-period of the voltage.

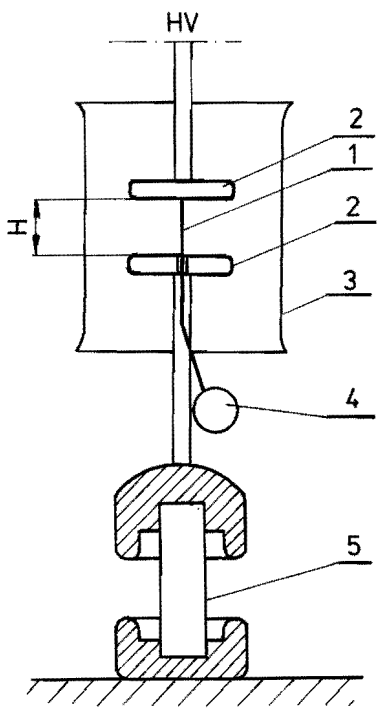

Fig.1. Electrode arrangement
1-investigated wire,
2-screening electrodes,
3-cylindrical electrode,
4-load sphere, 5-insulator

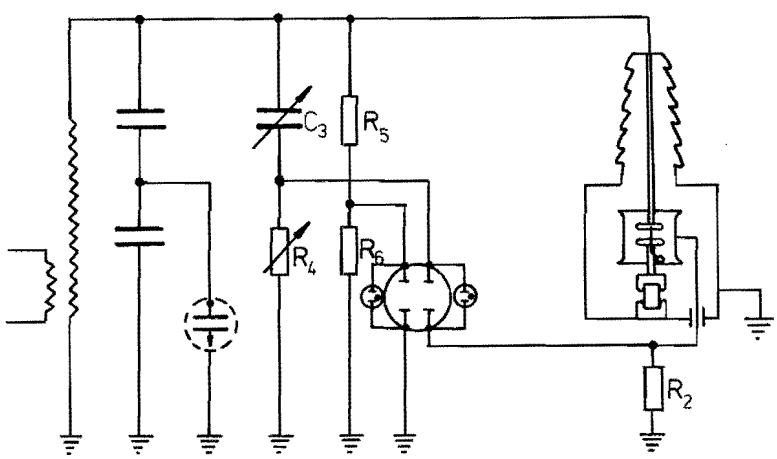

Fig.2. High voltage bridge for measuring the emission current

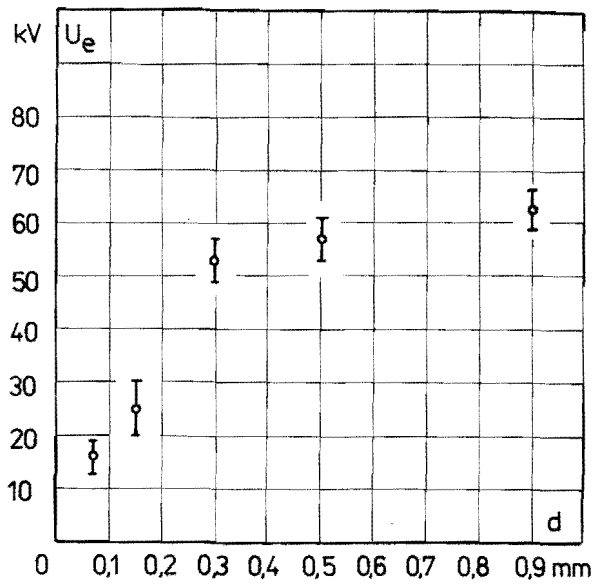

Fig.5. Voltage U_e where the electron emission current equals 1 μA for various diameter of the copper wire

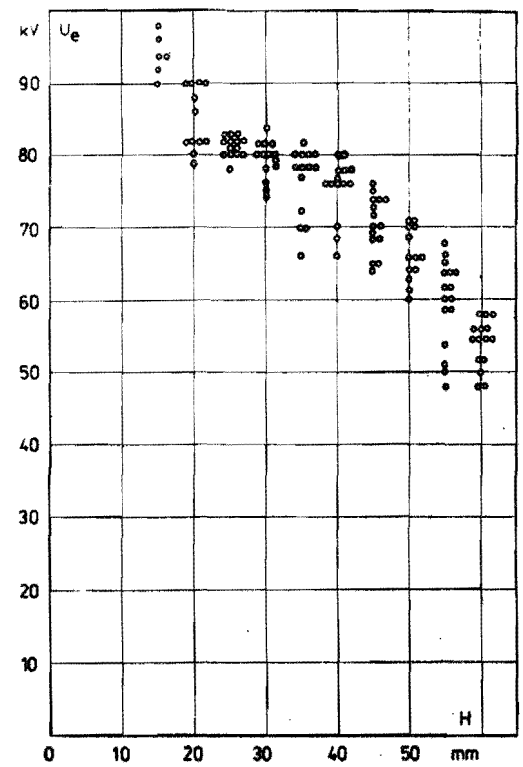

Fig.6. Voltage U_e where the electron emission current equals 1 μA, according to the spacing between the electrodes for a wire of 0.30 mm diameter and for the electrodes of 22 mm in diameter

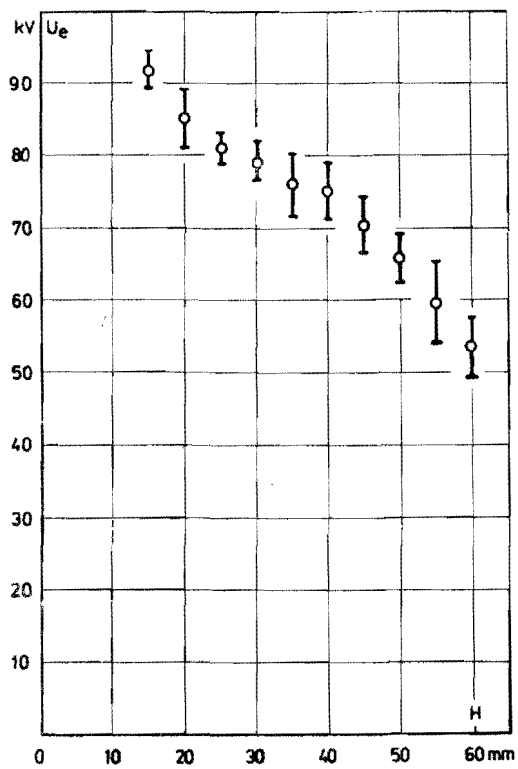

Fig.7. The values of the arithmetic mean of the voltage U_e and standard deviations, according to the spacing H of the electrodes. Wire diameter 0.30 mm electrodes diameter 22 mm

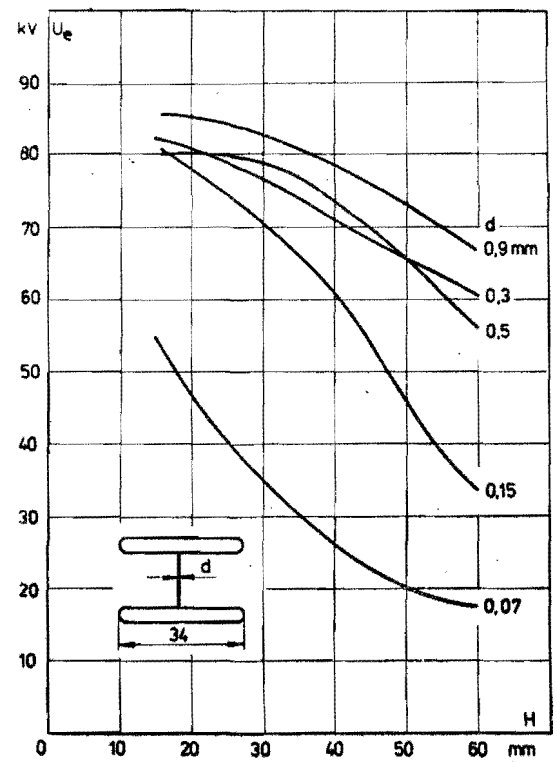

Fig.8. Voltage U_e where the electron emission current equals 1 μA, as a function of the electrode spacing H for five diameters of the wire and for the electrode diameter 34 mm

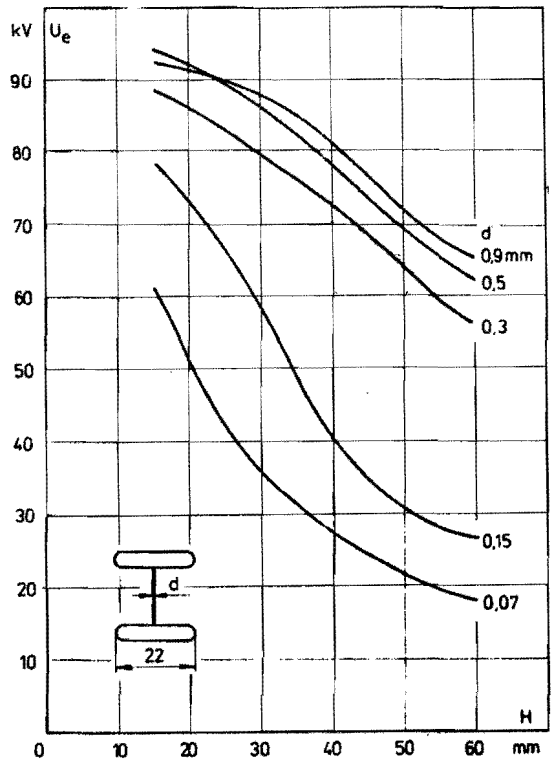

Fig.9. **Voltage U_e where the electron emission current equals 1 μA, as a function of the electrode spacing H for five diameters of the wire and for the electrode diameter 22 mm**

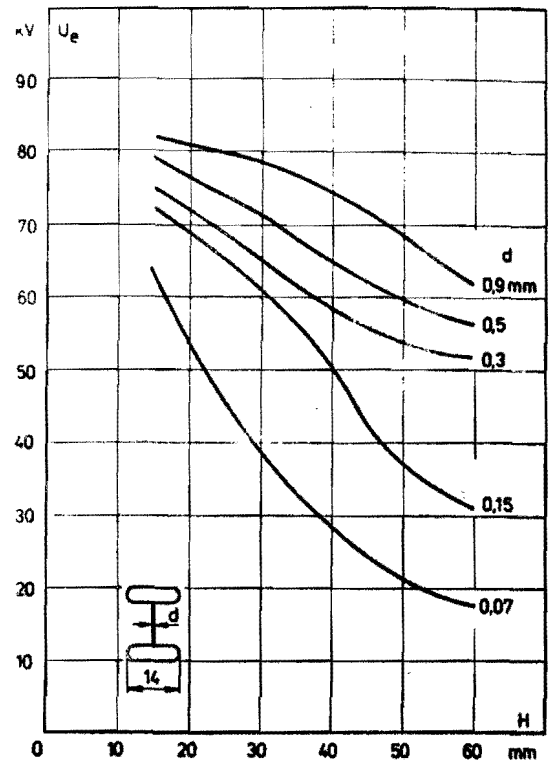

Fig.10. Voltage U_e where the electron emission current equals 1 μA, as a function of the electrode spacing H for five diameters of the wire and for the electrode diameter 14 mm

electrode.

It results from the analysis of characteristics in Figures 8, 9 and 10 that the approaching of electrodes causes a distinct limitation of the field emission phenomenon and increase in the U_e voltage of the occurrence of the electron emission current and this should be associated with the phenomenon of wire screening by electrodes. In the case of electrodes of small diameter (ϕ = 14 mm), the effect of wire screening is less.

In the second part of the experiment, the influence of the technology of wire electropolishing on the phenomenon of the electron field emission from the surface of the wire was investigated. After electropolishing, smoothness of the wire surface increased and the change of the diameter was 0.05 mm. It was found that the U_e voltage of occurrence of the electron emission current from the surface of the electropolished wires is of about 25% higher in comparison with nonelectropolished wires.

CONCLUSION

1. The undesired phenomenon of electron field emission, from a wire in a high voltage vacuum fuse, can be reduced or eliminated by wire screening as well as by electropolishing its surface.

2. The effect of wire screening can be obtained in a simple way by applying electrodes of the shape of disks to its ends. The effect of screening is the greater the bigger the diameter of the electrodes is and the smaller their spacing is.

3. On applying electropolishing of the wire, an increase in about 25% in the voltage of occurrence of the electron field emission current from the surface of the wire was obtained.

REFERENCES

[1] Cz.Królikowski, M.Stroiński, "Determination of arc and arcless current breaking zones by fuse wire under vacuum". Proc. of the VII International Symposium on Discharges and Electrical Insulation in Vacuum. Novosibirsk, 1976, 441.

[2] Cz.Królikowski, H.Mościcka-Grzesiak, M.Stroiński, "Insulation arrangement of vacuum fuse chamber". Proc. of the X International Symposium on Discharges and Electrical Insulation in Vacuum, 1982, Columbia, South Carolina, 256.

[3] Cz.Królikowski, H.Mościcka-Grzesiak, M.Stroiński, "Predischarge phenomena in a concentric wire-cylinder arrangement in vacuum". North-Holland Publishing Company, Physica 104 C, 1981, 233.

[4] T.Lipski, B.Kacprzak, "Badania zdolności wyłączania modelowej próżniowej komory bezpiecznikowej", 1985, opracowanie R.I. 13-01.3.2.

[5] Prof.T.Lipski, Technical University of Gdańsk, private information.

[6] Mc Graw-Edison Company, Power System Division, Apparatus Catalog 240-40.

NEW DESIGN ASPECTS OF SEMICONDUCTOR FUSES

B.Krasuski
Gdańsk Technical University
Poland

Abstract

Some main new design aspects of recently developed Polish semiconductor fuses has been described. Particular attention has been drawn on: fuse-link barrel made now from metal (aluminium), insulating bushings of fuse terminals and gas-evolving elements to improve the arc-quenching ability of small overcurrents. Also the better manufacturing reproducibility of new fuses is underlined. Examples of new fuses, corresponding oscillograms are attached.

1. General informations

The range of recently developed by Institute of High Voltages and Electrical Apparatus Intitute of Gdańsk Technical University new semiconductor fuses type Btd is given in the Table 1. This range is expected to be extended in the future up to 6.3 kV rated voltage and 1000 A rated current. The rated breaking capacity of those fuses is 50 ÷ 100 kA(RMS), depending upon the rated voltage and rated current. The minimum breaking current corresponds to the prearcing time not less than 30 s.

Table 1 SIZES OF Btd FUSES

U (V)	Dimensions [mm]		
	e	l	L
250	80	50	110
400	80	50	110
630	110	80	140
1000	140	110	170
1600	170	140	200
Barrel dimensions [mm]	∅20	∅28	∅36

RATED CURRENT in A

2	10	16	20	32	40	50	80	100	125	200	250	315	400	500	630
W-0		W-I			W-II			W-III			W-IV		W-V		
∅20		∅28			∅36			∅48			∅60		∅76		

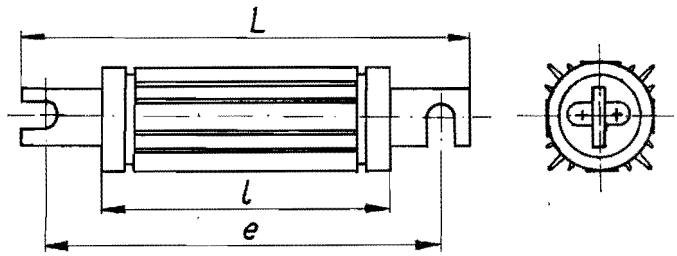

Some of design aspects of Btd fuses are new in comparison to the existing practice and to the inventions known from the patent documents. These aspects makes possible to improve the behaviour of new fuses during manufacturing and in service.

The aim of the paper is to describe mentioned design aspects in contrast to the existing practice.

2. List of new design aspects

Fig.1 shows longitudinal cross-section of Btd fuses just in order to demonstrate main aspects of the design and to point out the following elements which are relatively new in comparison with the known solutions.

2.1 The main new design point is the fuse-link barrel now made from a metalic(in this case

some aluminium alloy) body in the form of a good heat sink. It made possible to elevate the fuse-link rated current of 10÷15 % by this same fuse-element.

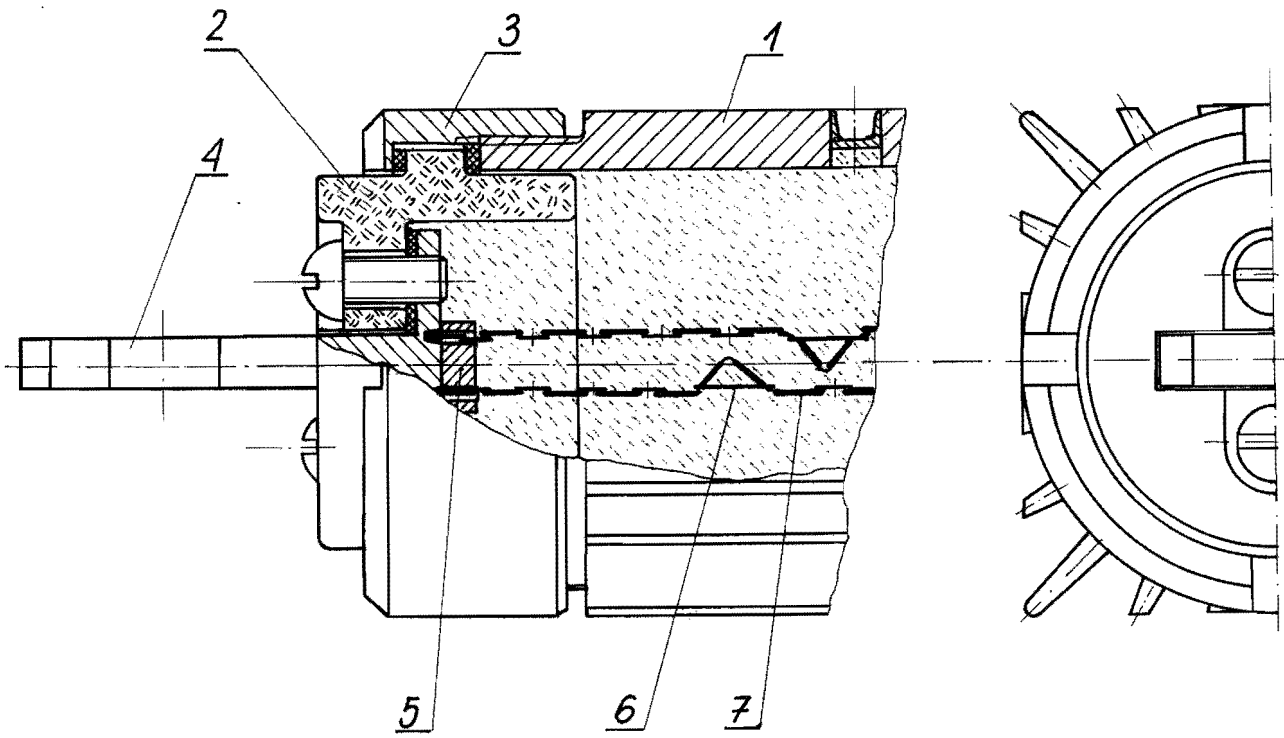

Fig.1 Partial cross-sectional view of Btd fuses
1 - aluminium body, 2 - ceramic bushing, 3 - aluminium nut, 4 - copper terminal,
5 - gas-evolving element, 6 - ring rubber to compensate elongation of fuse-element,
7 - fuse-element

2.2 Electrical insulation between terminals consists from the two ceramic bushings 2 (Fig.1) which replace usuall fuse-link end-caps. The bushings are fastened to the barrel 1 by means of metalic (again this same aluminium alloy) nuts 3.

2.3 The fuse-element 7 is made from silver-copper combination. Constricted parts are from silver, whereas shoulders from copper. The constrictions are partially punched and partially made by groove rolling process.

2.4 The reproducibility of the positioning of fuse-element is done in the following way: the both contacts 4 during manufacturing are connected together by means of two (not indicated in Fig.1) screws which then after assembling are removed. The assembly consisting from two terminals, fuse-element and mentioned screws form a kind of "clockwork" which then is protract through the barrel 1 and then is centred by the bushings 2 and fastened by shown in Fig 1 screws.

2.5 Multi-parallel fuse-element (Fig.2) is so collected that the loops for the elongation compensation 6 are directed inwardly. Shown in Fig 2 element consists from six partial elements with those loops disposed between them. The Figure also shows a magnified view of the fuse-element portion.

2.6 Gas-evolving elements 5 in Fig.1 placed close to the terminals prevent against arc burn-through of those contacts particularly in the region of interruption of small overload currents. The elements can be made from such materials as $Al_2O_3 \cdot 3H_2O$.

2.7 There are moreover some other special points, say like the compensation of fuse-element elongation, connection of the fuse-element to the terminals a.s.o.

Fig.3 gives a general view and Fig.4 a set of the barrels for different rated currents by the same rated voltage. Figs 5 and 6 demonstrate some exemplary oscillograms from the breaking capacity tests of 1000 V rated voltage fuses.

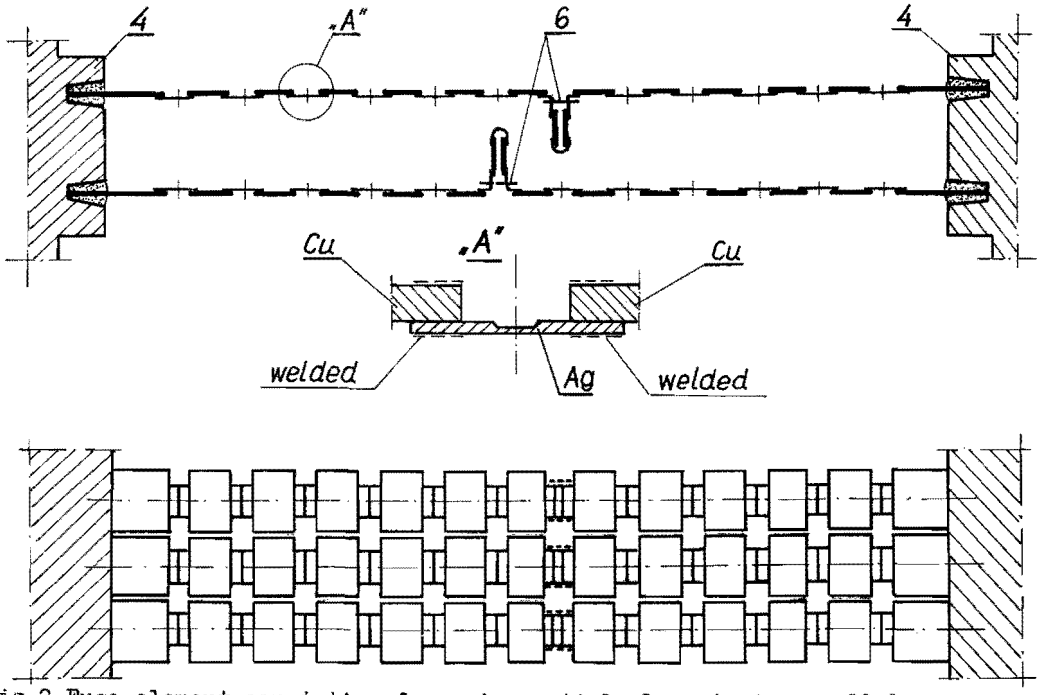

Fig.2 Fuse-element consisting from six partial elements in parallel

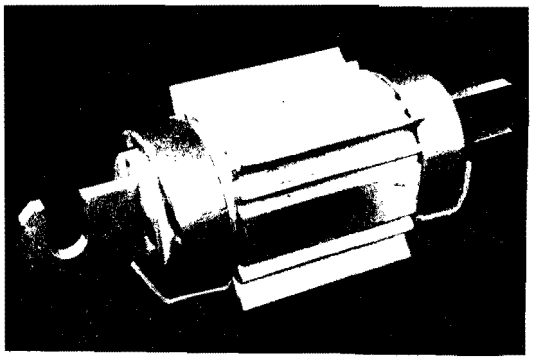

Fig.3 General view of a Btd fuse, 1000 V, 250 A

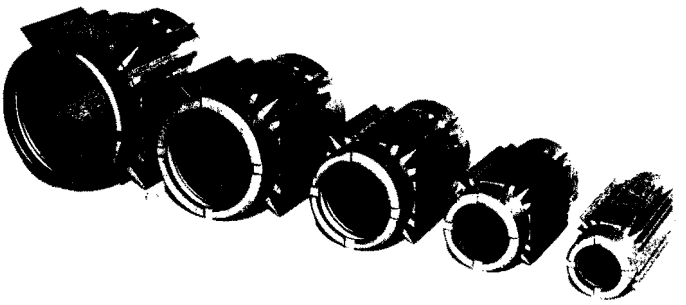

Fig.4 Aluminium barrels, 1000 V, size I÷V

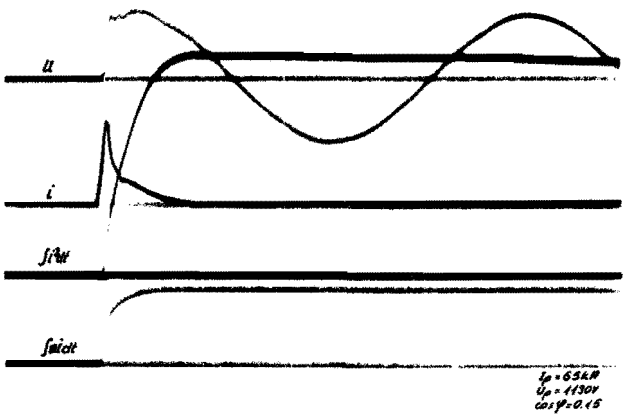

Fig.5 Oscillogram, fuse 1000 V, 250 A, 65 kA

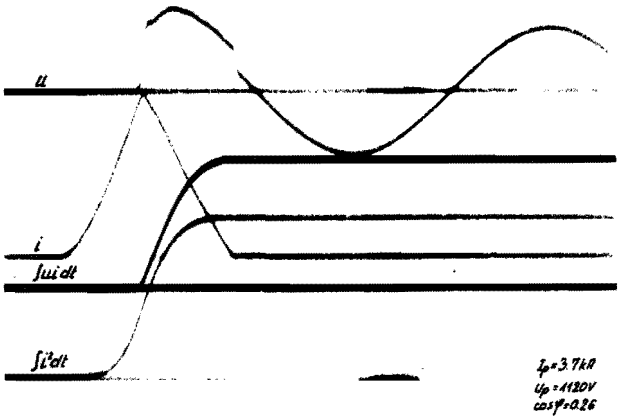

Fig.6 Oscillogram, fuse 1000V, 250 A, 3,7kA

3. Final remarks

Several described points of Btd fuses are claimed by the Polish patent documents. Author is of opinion that given new design aspects demonstrates some progress in the semiconductor fuses development.

Durability Enhancements in Cadmium Element High Voltage Current Limiting Fuses

by: W. R Crooks, A. C. Westrom, and Dr. B. R. Livesay

Abstract

The elements of all fuses but especially those of high voltage current limiting fuses are subject to deterioration by thermal and mechanical cycling due to the variable nature of the loading and overloading in most circuits.

The difference in the nature of this cycling according to the type of distribution system circuit is examined, e.g., short time transients such as transformer inrush currents to long term virtually fixed levels of load such as on shunt capacitors.

The paper describes how the nature of the cyclic loading affects the fusible elements in different ways due to the different mechanical and metallurgical phenomena involved.

Alternate compressive and tensile stresses develop at the widely different temperature occurring during the load cycle which draw special emphasis to the combination of deformation mechanisms which act during each half cycle of a thermal-mechanical fatigue sequence. Grain size is found to be a significant factor for controlling the durability of fuse elements in both load cycling and steady state modes.

Attempts to improve those properties relating to performance as a fuse element are described and the metallurgical reasoning stated together with an examination of the effectiveness of those improvements.

W. R. Crooks and A. C. Westrom are with Kearney Division of Kearney-National, Incorporated, Atlanta, Georgia, USA

Dr. Livesay is with Georgia Tech Research Institute, Atlanta, Georgia, USA

1. Introduction

Very few high voltage current limiting fuses (CLF) are applied such that they carry a steady value of load current. In addition to widely varying values of load current there are transient currents varying in duration from a cycle or two to many seconds which arise from:

1. Energization transients such as magnetizing current inrush of transformers and charging current inrush of capacitors.
2. Hot and cold load pickup.
3. Through faults cleared by a downstream device.

These variations in current cause temperature excursions in the elements from as low as ambient, which may be -40°C, when the fuse has been off load for some hours to high values of perhaps up to 150°C where overload conditions occur.

In CLF's containing elements which have local reductions of cross section these 'bridges' will, under short time transient current conditions, rise in temperature much more rapidly than the bulk parts of the element.

These temperature excursions, either slow changing and uniform throughout the element or quickly changing and local to the reduced areas will cause stresses in the metal of many types including tension and compression, creep forces and fatigue processes.

In addition the various thermo mechanical processes can cause changes in the micro structure of the metal from such phenomena as grain growth, cavitation, grain boundary sliding, twinning, and dislocation networks.

These degradation processes and the effects of additives or dopants have been investigated for some CLF element metals (1) (2) and also for expulsion fuse element metals (3).

As far as is known to your authors no such work has been done on cadmium in connection with fuse elements. The paper describes the experimental work done primarily at Georgia Tech Research Institute in Atlanta, GA and also at the Kearney Research Laboratory in McCook, IL.

2. The Nature of Fuse Loads and Transients

In most devices a steady state load or duty is less demanding than a cyclic load or duty simply because the term steady state implies that nothing is changing.

For h.v. C.L.F.'s this non steady state or cyclic condition is almost without exception the case. Circuits and devices are subject to or the generator of transient currents while changes in connected load and system faults further complicate the picture.

The effect of load changes and transient currents is to produce temperature changes in the elements and since all metals expand with temperature then stresses of one kind and another are generated within the materials and it is necessary to design and apply the fuses such that these stresses remain within the long term capability of the material in the same way that structural materials must be used within well defined limits of stress.

Different effects are produced depending on rates of change of temperature especially in non uniform elements.

In many applications h.v. C.L.F. ratings must be chosen not on the basis of load considerations but such that they are able to repeatedly withstand the transient currents which may be anticipated. These transients have numerous origins and while the pre-arcing time/current or I^2t data for the fuse may be readily available it is more difficult to predict the actual conditions that will occur in the field.

In many cases 'rules of thumb' have developed from a combination of actual measurement and analysis both of which have been tempered by experience. Some of the commonly considered causes of transient current generation together with some commonly accepted quantification are as follows.

2.1 Magnetizing Current Inrush

A commonly used definition of long standing is that the worst case magnetizing current inrush integrates to a value equivalent to $12xI_n$ for 0.1 sec, where I_n is the transformer rated current. Another commonly used rule is that the inrush equates to $25xI_n$ for 0.01 sec.

2.2 Capacitor Charging Inrush

An uncharged capacitor appears as a short circuit at the instant of switching in and the first few loops of current can be very high and at high frequency. Further a capacitor connected to an overhead line protected by a recloser will at the instant the recloser clears the circuit be charged to peak voltage. A fast reclose operation, say .25 seconds, could result in closing at the opposite polarity so that the capacitor would have almost double voltage impressed across it with consequent effect on the current inrush.

The inrush current will also be increased if a capacitor bank is energized in close proximity to an already energized bank.

An oscillogram for a typical charging inrush is shown in Fig. 1, this is for a 7.2kV, 100 kvar capacitor having a rated current of 13.9 amps energized in a circuit having a fault level of 10.2kA. The peak current was 350 amp and the inrush was limited in duration to a few milliseconds.

2.3 Cold Load Pickup

If a loss of supply is of long enough duration all of the load controlled automatically, such as by thermostats, will be switched to the on condition thus causing a loss of diversity. When the supply is restored this situation is very demanding on the distribution system and its components. The effect of cold load pick up has been characterised as equating to $6xI_n$ for 1 sec, $3xI_n$ for 10 sec and $2xI_n$ for 5 min. or 15 min. for winter in a cold climate.

2.4 Overload

In the North American continent it is not uncommon for a transformer to be overloaded to 2 to 2.5 times its normal rating.

2.5. Lightning

There is no consensus, at this time, as to exactly what causes fuses to operate under thunderstorm conditions. However, operate they do and some users choose to have a minimum fuse rating or I^2t withstand to mitigate the problem of fuse operations due to lightning.

2.6. Through Faults

Operation of downstream devices subjects upstream fuses to the effects of the fault current as limited by the downstream device. If the fault levels are known then data should be available to predict the let through I^2t of the downstream device.

3. Effects of Current Changes and Transients

The effect of any of these conditions is to cause the fuse element temperature to change along its complete length or in a non uniform manner.

For load and overload conditions the rate of change of temperature is slow, there is a great proportion of the generated heat lost from the elements and the filler and other fuse components are also subject to a rise in temperature.

Generally the elements will expand to a greater degree than the other components and the accomodation of this expansion may cause localized stress both during the heating period and the subsequent cooling period.

For short time currents such as capacitor charging inrush there will be very little heat transfer from the element and in elements with local sections of reduced cross section there will be little heat transfer from the reduced area into the bulk of the element. Using numerical methods (4) it has been shown that even for a melting period as long as .11 seconds the temperature at the center of a reduced section immediately before melting was 880°C compared with 205°C at a point some distance away from the area of reduced section. Clearly for a shorter melting period the temperature differential would be even more marked.

The effect of the temperature differential is to rapidly expand the area of reduced cross section and consequently set up compressive stresses later to be replaced by tensile stresses as the elements cool.

The effects of expansion and contraction first became evident in silver element fuses used in circuits supplying direct-on-line induction motors where the starting currents of about 6 times the motor rated current exist from about 6 to 60 seconds depending on the nature of the drive. It was found that the expansion produced in the elements tended to be taken up at 1 or 2 locations causing the formation of 'kinks' (5) which could not readily straighten out on cooling causing residual tensile stresses which increased after every subsequent start up of the motor until failure occurred. A solution to this particular aging problem is to manufacture the fuse elements with pre-formed expansion bends distributed along the whole element length, this accommodates the expansion on a per unit length basis and prevents the formation of kinks. Such arrangements have been tested to give the equivalent of 21,000 starts. (5)

4. The Effects of Temperature Excursions

a. Atomic diffusion. The metals employed for fuse elements experience long times at elevated temperatures during normal usage. Metal atoms are well known to diffuse under such condition and thereby alter microstructural characteristics of the elements. Diffusion mechanisms thus affect mechanical behavior and corrosion characteristics. For many fuse metals, recrystallization normally occurs even at room temperature. Thermal diffusion is also a factor in metallic oxidation processes. Elevated temperatures involved here greatly accelerate these processes.

b. Mechanical stresses. First, mechanical stresses may be introduced during thermal excursions by two primary mechanisms. Differences in the temperature coefficients of expansion between the fuse housing and the fuse elements lead to tension, compression and flexure stresses on the relatively soft metallic elements. Second, thermal gradients are induced in the element metals during rapid thermal excursions. This is particularly true for the notch configurations in fuse elements where both higher resistances and lower mass exist in the notch. The power transients of several cycles at high frequencies associated with either capacitive switching or lightning strokes produce high temperature gradients. The high gradients in the notched regions result in high compressive stresses in the fuse element. Mechanical stress concentration factors also cause notched regions to be more susceptible to mechanical damage mechanisms.

c. At temperatures of approximately 0.4 of the melting temperature (on the absolute scale) most metals recrystallize and grain growth can occur. (1) These processes are accelerated with temperature, roughly, according to the Arrhenius expression for reaction kinetics.

5. Metallurgical Mechanisms

A principal consequence of excessive grain growth is a greatly reduced mechanical strength. Grain boundaries are interfaces which retard dislocation motion and thereby provide mechanical strengthening. Pure Cd experiences growth in grain size at temperatures above 100°C so that the grain boundary hardening mechanisms are not effective. Plastic deformation takes place by both slip and stress twinning in Cd. In addition, grain boundary sliding appears in pure Cd filaments under the various thermal and mechanical stress loads applied to fuse materials.

Experiments were conducted to add selected metallic dopants to pure Cd in order to retard grain growth in Cd fuse elements. Such techniques are regularly employed to enhance the mechanical strength of the alloys used in aircraft and other high performance structural systems. Several dopants were considered for Cd to enhance structural performance. Of these, alloys involving Zn and Ag were prepared and evaluated under various laboratory conditions. Intermetallic compounds form from these dopants with Cd. The goal was to inhibit grain growth at temperatures up to 150°C without adversely affecting the fatigue strength of the element metal. Many intermetallics result in internal interfaces which are brittle or otherwise greatly reduce fatigue strength.

The thermal stability of the microstructure in Cd based fuse element materials were evaluated for several compositions of Zn and Ag doped alloys. The forming processes of flat element configurations (rolling, etc) generate small grains. It was the objective to maintain the small grain size.

6. Laboratory Testing of Fuse Materials

The laboratory testing of fuse material included

a. Tensile behavior.

b. Cyclical mechanical testing.

c. Mechanical creep.

d. Microstructural studies.

e. Current cycling experiments.

The stress-strain curves in monotonic tension tests demonstrated increased tensile strength and greatly enhanced thermal stability of the tensile strengths of both Ag and Zn doped alloys of Cd compared to that of pure Cd. These are illustrated in the curves of Figure 2 and Table 1. As expected the tensile strength of pure cadmium decreased to a lower value than that of the alloys after simple oven aging. Stress-strain curves for both Cd2%Ag and pure Cd are shown in Figure 2. Deformation takes place primarily by slip mechanisms in cadmium but deformation twinning also occurs. The small horizontal displacements on the stress-strain curves corresponded to the creation of twins during the test.

Strain controlled fatigue tests to failure were conducted on fuse elements of pure Cd and of the doped alloys. A special microfatigue apparatus was modified to impose mechanical strain cycles on individual fuse elements while they were conducting representative current. Details of the cylical hysteresis curves were monitored for the progress of mechanical degradation mechanisms. Several curves of the force amplitude plotted as a function of the cycle number are provided in Figures 3 & 4. The force amplitude of pure cadmium elements is comparatively small and decreases significantly with both aging time and numbers of cycles. Metallographic examinations demonstrated that the Ag & Zn doped Cd specimens retained the initial small grain structure while pure Cd experienced significant grain size growth with thermal aging. The degradation mechanisms observed in pure Cd links included slip patterns and extensive grain boundary (GB) sliding along with the initiation of microcracks. The small grain size retained in the doped alloys inhibited both extensive slip and GB sliding resulting in the higher force amplitudes. Degradation in the doped Cd specimens was primarily associated with the growth of microcracks. A key factor for the durability of fuse elements shown by Figures 3 & 4 is that, subsequent to thermal aging, the doped alloys retain relatively large force amplitudes while no significant reduction occurs in the numbers of cycles to failure.

The mechanical creep rates of Cd, Cd2%Ag and Cd2.5%Zn are shown in Table II. The creep rates were found to decrease with thermal aging in each case. However, while the differences for pure Cd were not large, those for the alloys were quite significant. The large reduction in creep rates for the alloys is attributed to the segregation of the doping metal in grain boundaries. While grain size greatly increases with thermal aging of pure Cd specimens, that of the doped metals remains stable. Cd demonstrates greater creep at elevated temperatures.

Durability comparisons were also made by subjecting complete fuses to current cycling tests. The test samples were connected in series to ensure exactly similar conditions and the current cycled 'ON' for 4 hours and 'OFF" for 4 hours on a continuous basis. To reach an earlier conclusion the current density was chosen to be approximately double that of a highly loaded in service condition. Resistance values were checked every working day and if sufficient change was noted that could result from an open element the fuse was removed from the circuit. The results of the tests are given in Table III.

On dismantling the test samples it was observed that the elements giving the best performance had self generated expansion bends distributed along their lengths, see Fig. 5. This was similar to observation made in previous research (5) but in that case the elements contained pre-formed expansion bends which changed their size and distribution. The increased strength and creep resistance of the doped material made it more favorable for the elements to form the wave shaped patterns rather than deform by microstructural mechanisms such as slip or grain boundary sliding.

Samples of elements taken from the fuses after the tests were polished and etched to allow examination of the grain structure. While grain growth was evident in the Cd the Cd2%Ag alloy was essentially unchanged from the as rolled condition.

7. Conclusions

The doping of cadmium with both silver and zinc brought significant improvements to the durability of current limiting fuses. Thermal expansion and contraction with current cycling and surges introduces mechanical stress cycling to the fuse metals. The small additions to the cadmium altered melting points by insignificant amounts but greatly affected the mechanical performance of the elements. Alloying provided an effective control to maintain small grain size through long periods of thermal aging. The long aging times are analogous to long term service operating conditions. The principal parameters affected by grain control were the mechanical strength and creep rates. Strain controlled fatigue lifetimes were decreased somewhat with doping but not by a significant amount. The critical objective was to provide sufficient doping to stabilize the microstructure of the metal without significantly degrading the strength during mechanical cycling. The relatively high strength and very low creep rates resulting from doping provided durability for the thermal cycling environment of an operating current limiting fuse.

References

1. Held, W. and Pollemeier, F.J., Internal Fuses in Modern High Voltage Capacitors, Electra No. 33, 1974.

2. Tamaka, T. et al., Metallographic Study of Dual Type Current Limiting Fuse Element. IEEE Trans. Vol. PAS-101, No. 6 June, 1982.

3. Cress, S., Damageability of Fuses - Electro Thermal Damageability of Fusible Elements., Proceedings of International Conference on Distribution Fusing, Montreal, 1981.

4. Leach, J.G., et al., Analysis of High-Rupturing - Capacity Fuse Link Prearcing Phenomena by a Finite Difference Method, Proc. IEE, Vol. 120, No. 9, September, 1973.

5. Arai, S., Deteriorations and Cycles to Failure of HV Current Limiting Fuses Subjected to Cyclic Loading, Proceedings of International Conference on Electric Fuses and their Applications, Trondheim, 1984.

6. Crooks, W.R., The Quality Aspects of HV Current Limiting Fuse Protection, Proceedings of International Conference on Electric Fuses and Their Applications, Liverpool, 1976.

Table I

Mean Tensile Fracture Strengths (grams)

Material	As Received	Aged 96 hrs. at 150°C
Pure Cd	582	441
Cd 2%Ag	988	639
Cd 1%Ag	916	566
Cd 2.5%Zn	790	835
Cd 1.5%Zn	732	790

Samples were 0.050" x 0.0075"

As received: samples taken directly from the manufactured roll

Table II

Comparison of Creep Rates of Cadmium and Alloys

Metal	Creep Rates (mm/hr) As Received	Aged 150°C, 23 hrs
Pure Cd	0.10	0.05
Cd 2%Ag	0.11	0.0025
Cd 2.5%Zn	0.019	0.0034

Table III

Current Cycling Tests

Element Type	No. Cycles to Fracture	Tensile Strength of Samples (gm)
Cd 2%Ag	270, 323	785
Cd 1.5%Zn	95	
Cd 2.5%Zn	131, 139	685
Cd	70, 79	342

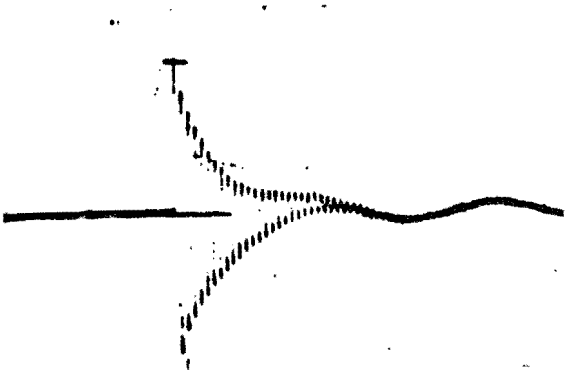

Figure 1. Capacitor charging current inrush

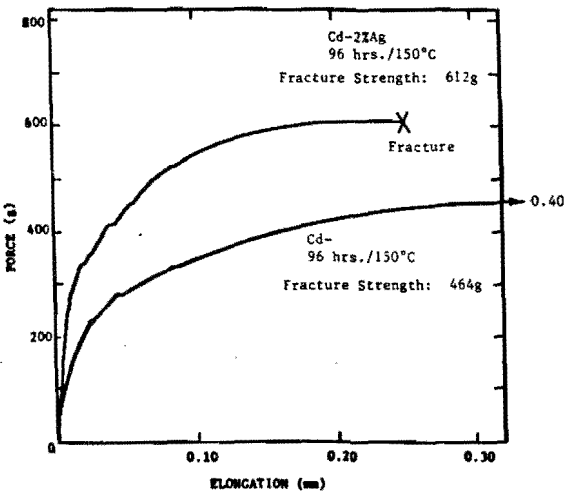

Figure 2. Tensile 'stress-strain' curves for Cd and Cd2%Ag that were annealed at 150°C for 96 hours. The effects of twinning can be noted from the discontinuities in the curves.

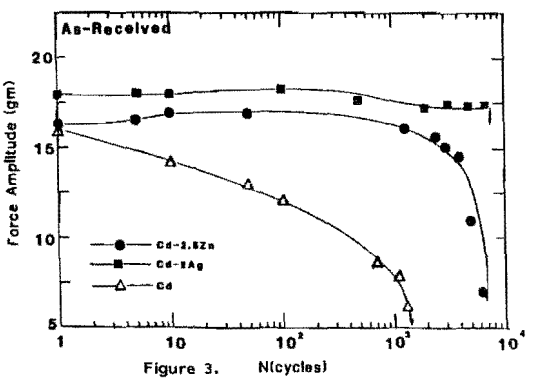

Figure 3.

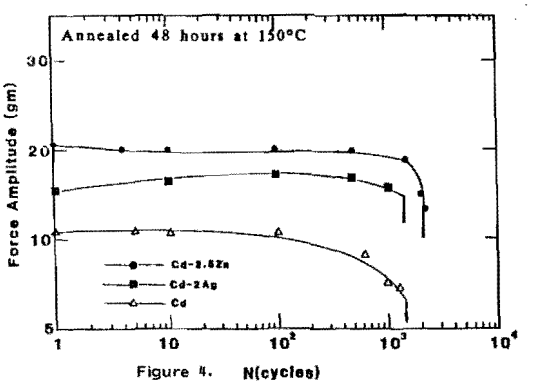

Figure 4.

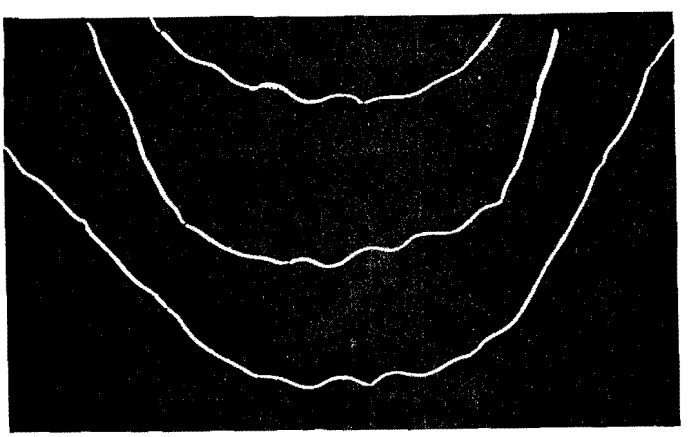

Figure 5 Self generated expansion bends in Cd/Ag elements (edge view) Note sinusoidal type random bands as opposed to sharp kinks at element notches known to occur in pure metal elements.

RESEARCH ON THE TECHNIQUE OF FILLING QUARTZ SAND IN FUSE

CHEN Su-tsing

Shanghai Electrical Apparatus Research Institute
of Ministry of Machine Building,PRC

ABSTRACTS

The performance of fuse can be improved by filling in the cartridge of fuse compactly with quartz sand. The higher filling compactness can be gained, when the fuse link is fixed on the plane of a vibration stand with an inclination of 10 degrees and submitted an impacting vibration in horizontal direction, the vibration frequency should be changed adequately in the course of vibration.

1. INTRODUCTION

Filling in the cartridge of fuse with appropriate quartz sand may provide two effects, first, the quartz sand can be served as an arcing-quenching medium, which would raise the breaking capacity of fuse; second, it is also a heat dissipation medium for lowering the temperature of fuse; The chemical composition, shape and size etc of quartz sand can all effect the performance of fuse. Then the filling compactness of quartz sand can also effect it directly. Generally speaking, the more compactive the quartz sand is filled, then the higher the breaking capacity of fuse will be and the lower the temperature will be.For the same property and breaking capacity of fuse, the more compactive the quartz sand is filled, the more well-knit the volume and structure of fuse can be made and the more the cost can be reduced. So it becomes one of the important techniques of fuse whether the quartz sand is filled compactly or not. What is the best way to fill quartz sand? You can get the answer in this paper.

2. The method of filling quartz sand and its evaluation criterion

The method to fill quartz sand in fuse is to put the fuse link on the vibration stand, and makes it vibrate with the vibration stand continuously, then the quartz sand in the quartz box are poured into the cartridge through the tube and hole until it is full. Obviously, the filling compactness depends on the vibration mode of vibration stand and the mounting mode of fuse link.

2.1 The following four vibration modes are adopted

A. Vibration in horizontal direction

The fuse link vibrates right and left with the vibration stand in the horizontal direction. The amplitude and vibration frequency of vibration stand can be adjusted.

B. Impacting vibration in the horizontal direction

The fuse link vibrates with the stand in horizontal direction, at the same time an impacting force is applied on the fuse link (about 5 kgf) in the horizontal direction.

C. Vibration in vertical direction

The fuse link vibrates up and down with the stand. The amplitude and frequency of the vibration of the stand can be adjusted.

D. Impacting vibration in vertical direction

The fuse link vibrates up and down with the vibration stand, at the same time an impacting force is applied on the stand with a specific frequency.

2.2 The following two mounting modes of fuse link on the vibration stand are adopted

A. Fuse link is fixed vertically on the vibration stand

B. Fuse link is fixed on the plane of the vibration stand at different inclination

Various mothods of filling with quartz sand are established by using the above-mentioned different modes of vibration and mounting,the tests of the compactness of filling with quartz sand in the fuse link have been made one by one and the best method of filling has been found. The vibration amplitude on the vibration stand of the fuse link may be 0.4, 0.3, 0.25, 0.2, 0.15 mm, the frequency may be 55, 52, 50, 48, 45, 40, 30, 20 Hz, the vibration time may

be 2.5 min, the filling hole of fuse link are all covered with quartz sand during the filling. In order to establish a criterion for evaluation of different methods, we adopt a conception of compactness ΔQ:

$$\Delta Q = \frac{Q - Qo}{Qo} \times 100\%$$

where: Qo the weight of filled quartz sand before vibration,
Q the weight of filled quartz sand after vibration.
For defining the weight of quartz sand of every fuse link, the measurement is carried out three times and an average value is adopted. Quartz sand filled by little and little through the filling hole from the tube near the cover. The quartz sand is weighed with the balance of 0.01 g precision. The granule diameter and chemical composition of quartz sand used in the test are indicated in Table 1.

Table 1

Granule Diameter	Chemical Composition and Content %					
mm	SiO_2	Al_2O_3	CaO	MgO	Fe_2O_3	Loss due to burnout
0.2-0.5	99.79	0.08	0.004	0.004	0.01	0.112

3. Results of tests

3.1 Fuse link is fixed vertically on the vibration stand and vibrated in horizontal direction A. As amplitude A=0.2 mm, duration of vibration t=2.5 min, the relations between the compactness of filled quartz sand ΔQ and vibration frequency f are shown in Table 2 and Figure 1.

Table 2

f Hz	45	48	50	52	55
ΔQ %	10.16	16.60	14.12	13.44	12.45

Table 2 and figure 1 show that there is an optimum vibration frequency when fuse link is fixed vertically and vibrated in horizontal direction. When frequency is below or over this optimum frequency, the compactness of filling with quartz sand will reduce obviously. It is better to take 48 Hz here.
B. The relations between the compactness of filled quartz sand ΔQ and the vibration amplitude A under the vibration frequency f=48 Hz and duration of vibration t=2.5 min are shown in Table 3 and Figure 2.

Table 3

A mm	0.10	0.20	0.25	0.30	0.40
ΔQ %	5.58	16.60	16.50	15.46	14.88

It is not appropriate to use an amplitude larger or smaller than (0.2-0.25)mm.

3.2 Fuse link is fixed on the vibration stand with a specific inclination angle and vibrated in horizontal direction.
A. Under amplitude A=2.5 mm, frequency f=48 Hz, duration t=2.5 min, the fuse link is fixed on the vibration stand with an inclination of 10^0 and vibrated in horizontal direction, the compactness ΔQ will be higher than that without inclination. The test results are shown in

Table 4.

Table 4

inclination	0^0	10^0
Δ Q %	16.60	17.11

B. Under the same condition as 3.2.A, the compactness ΔQ will be raised, when 5 kgf impacting force is applied on the fuse link. The test results are shown in Table 5.

Table 5

inclination	0^0	10^0	10^0
condition of impact	without impact force	without impact force	with impact force
Δ Q %	16.60	17.11	17.60

C. Under the same condition as in 3.2.B, if the vibration frequency is reduced adequately at two-thirds of the specified vibration duration, then ΔQ will be brought to an optimum value. The results of the tests are shown in Table 6.

Table 6

inclination	0^0	10^0	10^0	10^0
impact force	without impact force	without impact force	with impact force	with impact force
changing vibration frequency	without	without	without	reduce adequately the frequency at two-thirds of the specified duration of vibration
ΔQ %	16.60	17.11	17.60	19.17

D. Prolonging the duration of vibration in horizontal direction as A=0.2 mm, f=48 Hz, will not obviously raise the ΔQ. The results of the tests are shown in Table 7.

Table 7

t min	2.5	3.5
Δ Q %	16.60	16.70

3.3 Fuse link is fixed on the vibration stand in vertical direction and vibrated in vertical direction.

A. Under amplitude A=0.2 mm, duration of vibration t=2.5 min, the relations between the compactness ΔQ and vibration frequency f are shown in Table 8 and Figure 3.

Table 8

f Hz	20	30	40	50
△Q %	6.38	15.05	13.30	10.60

Table 8 and Figure 3 show that fuse link has also an optimum vibration frequency when it is fixed in vertical direction and vibrated in vertical direction. It is better to adopt 30 Hz here. It is lower than the optimum frequency vibrated in horizontal direction.

B. Under vibration frequency f=30 Hz, duration of vibration t=2.5 min, the relations between the compactness △Q and vibration amplitude A are shown in the Table 9 and Figure 4.

Table 9

A mm	0.15	0.20	0.30	0.40
△Q %	7.31	15.05	14.12	12.50

Table 9 and Figire 4 show that it is better to adopt the amplitude of vibration stand A=0.2 mm here, when fuse link is fixed on the vibration stand and vibrated in vertical direction.

C. Under amplitude A=o.2 mm, vibration frequency f=30 Hz, adequately prolonging the duration of vibration will obviously raise the △Q. It is shown in Table 10.

Table 10

t min	2.5	5
△Q %	15.05	17.47

D. under amplitude A=0.2 mm, vibration frequency f=30 Hz, duration of vibration t=2.5 min. The compactness of filling quartz sand △Q can be raised by continuously impacting the fuse link, but it is not more obvious than that vibrated in horizontal direction. The results of the test are shown in Table 11.

Table 11

Condition of impact	without impact	with impact (300 time/min)	with impact (160 time/min)
△Q %	15.05	15.78	16.28

E. Under the same condition as 3.3.D, the compactness of filling quartz sand △Q can be raised, when the vibration stand is vibrated to a certain time, the vibration frequency is reduced adequately. The results are shown in Table 12.

Table 12

Condi tion of frequency (f)	Constant (f)	Reduced (f)
△Q %	15.05	16.27

3.4 Fuse link is fixed on the vibration stand at different angles and vibrated in vertical direction.
Under amplitude A=0.2 mm, vibration frequency f=30 Hz, duration of vibration t=2.5 min the relation between the compactness of filled quartz sand $\triangle Q$ and the inclination angle α can be abtained by altering the angle between the plane of stand and fuse link,as shown in Table 13.

Table 13

	0^0	5^0	10^0	15^0
$\triangle Q$ %	15.05	15.05	14.96	14.94

Table 13 shows that if it filled sand under vertical vibration, the fuse link can be mounted without inclination.

4. The influence of the compactness of filled quartz sand $\triangle Q$ upon the breaking capacity of fuse.
After a fuse link of rated voltage 415 V ac and rated current 100 A is filled with quartz sand in different ways, the test at the maximum joule integral (I^2t) is performed under the test voltage 460 V ac, current 6.3 kA and $\cos\varphi$=0.29. Results of tests are shown in Table 14.

Table 14

modes of filling quartz sand / results of tests	general	according to the mode of 3.2.C
Pre-arcing $I^2t.10^3$ A^2s	45.3	32
Operating $I^2t.10^3$ A^2s	85.7	64
Peak value of cut-off current kA	6.63	5.92

Table 14 shows that in a certain range, to increase the compactness of filling quartz sand $\triangle Q$ may raise the breaking capacity of fuse. The reason for this is that to raise the compactness of filled quartz sand can increase the thermal capacity of sand in unit volume of cartridge and the capacity sucking up arc energy (2.1 kw.s per gram of quartz sand). At the same time it may limit the expansion of arc diameter and the increase of pressure in arc area, so as to strengthen de-ion of arc area, thus making the arc-quenching easier.

5. Results

5.1 No matter how vibration is performed in horizontal direction or in vertical direction, when the quartz sand is filled, the best vibration amplitude A and frequency f are existed in all cases. So we can gain higher compactness $\triangle Q$ under these circumstances.

5.2 When the quartz sand is filled, no matter how vibration is performed in horizontal direction or in vertical direction, $\triangle Q$ will be raised by reducing the frequency adequately after two-thirds of the specified duration of vibration.

5.3 When the fuse link is fixed on the plane of the vibration stand with a certain inclination, vibration in horizontal direction can raise the compactness of filled quartz sand. But vibration in vertical direction can't obviously increase it.

5.4 Under the same compactness $\triangle Q$ and optimum condition, the duration of vibration in horizontal direction will be one half of that in vertical direction.

5.5 The fuse link is fixed on the plane of the vibration stand with an inclination about 10^0

and vibrated in horizontal direction with impact, the vibration frequency is reduced after a certain appropriately time of vibration the methods can bring the compactness ΔQ to maximum. Besides, the duration of the vibration may be shortened. This method is suitable for using in the factory production.

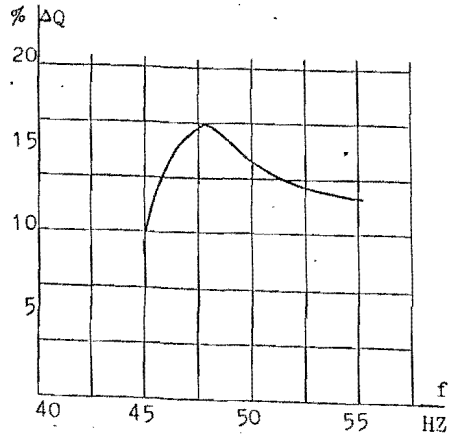

Fig.1 Relation between the compactness ΔQ and frequency f, at amplitude A=0.2 mm duration of vibration t=2.5 min. (in horizontal vibration)

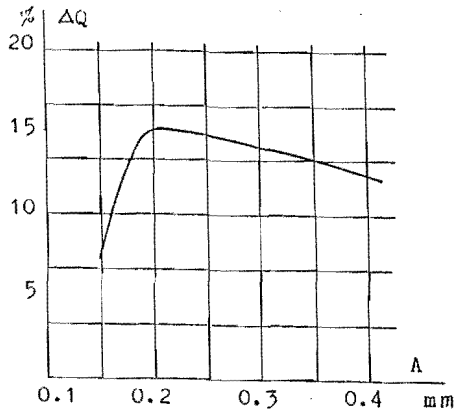

Fig.2 Relation between the compactness ΔQ and amplitude A, at vibration frequency f=48 Hz, duration of vibration t=2.5 min (in horizontal vibration)

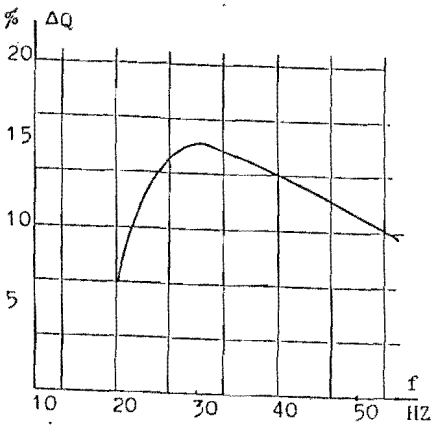

Fig.3 Relation between the compactness ΔQ and frequency f at amplitude A=0.2 mm duration of vibration t=2.5 min (in vertical vibration)

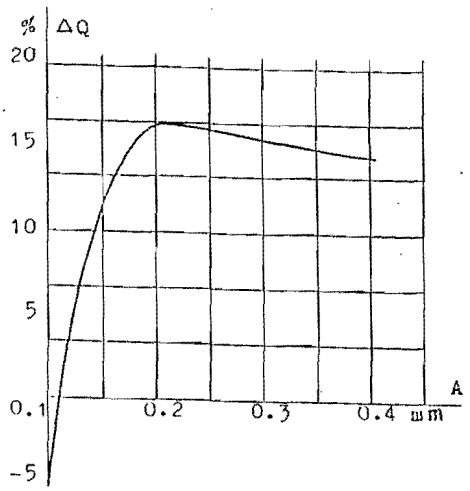

Fig.4 Relation between the compactness ΔQ and amplitude A at vibration frequency f=30 Hz, duration of vibration t=2.5 min (in vertical vibration)

REFERENCES

(1) Namitokov K.K., Chmelnickij R.S., Anikeeva E.N.: Fuses (in Russian). Moskva. Enertgija Ed. 1979
(2) Josef Paukert: Electric Conductivity of arc Extinguishing Media For Low Voltage Fuse. International Conference on Electric Fuses and Their Applications, 1984
(3) Lipski T.: Electric Fuse (in Xian, Chin a) 1984
(4) Chen Su-tsing, Wang Ji-mei: Technique of filling quartz sand in fuse, Low voltage apparatus(China), No.1,1986,p.44-47

Session VI

MINIATURE FUSES 1

Chairman: Mrs. Dr. C. Turner

FUSE WITH ABLATING WALL

S. Ramakrishnan
CSIRO Division of Manufacturing Technology
Preston Victoria 3072
Australia

W. M. C. van den Heuvel
Technische Hogeschool Eindhoven
5600 MB Eindhoven
The Netherlands

ABSTRACT

This paper deals with a study related to the process of short-circuit current interruption in low-voltage fuses which have no sand filling. In such fuses, quenching of the arc column within the fuse is aided by the material ablated from the wall of the fuse.

Experiments have been conducted using tubes of 4 and 6 mm internal diameter made of perspex, pvc and Teflon to measure the transient arc voltage and pressure within the tube after the explosion of the fuse wire for approximate step current pulses of upto 100 A. Fuses with ablative walls have also been tested in a short-circuit test circuit rated to provide 1500 A (prospective) from a 250-V, 50-Hz source.

An algorithm has been developed to solve numerically the time-dependent energy balance equation for the arc column taking into account the ablation of wall material and the consequent pressure rise inside an enclosed fuse. Calculated results agree favourably with the measured values.

The study suggests that the process of current interruption is dictated by the temperature distribution in the arc column immediately after the explosion of the fuse wire. It is found that ablative cooling can contribute significantly to the arc interruption process if the initial formation of the arc is in proximity to the ablating wall.

1. INTRODUCTION

This paper addresses a class of cartridge fuses, called "miniature fuses", which are normally used to protect a single apparatus, an instument or a part of an electrical equipment against fault currents. These fuses are used at a nominal voltage of 250 V and have typical outer dimensions of 5 mm in diameter and 20 mm in length. The present limit on the short-circuit current for these fuses is 1.5 kA which is likely to increase in future. Present dimensions, interruption ratings and test recommendations are covered by IEC Publication 127 [1].

These small fuses consist of a thin metallic wire of tinned copper, silver or nickel stretched inside a tube made of glass, ceramic or suitable plastic. End connections to the fuse wire inside the tube are provided by means of two metallic end caps, which make the fuse a totally-enclosed protective device. When the demand on the interrupting capacity of these fuses is as high as 1.5 kA, the tube is also filled with fine-grain sand to absorb the energy liberated and the pressure developed during the arcing process associated

with the interruption of fault current. The requirement of sand filling inside the tube introduces problems in their manufacture thus increasing the manufacturing cost.

One way to avoid the necessity of sand filling inside the fuse is to make the tube of the fuse out of a suitable plastic material with somewhat reduced inner diameter [2]. The polymer used to make the tube should then meet the following two important requirements: (i) it should have sufficient mechanical strength to withstand the high pressure generated within the tube; and (ii) the vapour ablated from the inner wall of the tube as a result of arcing inside the tube should have have good "arc quenching" properties, comparable with those of sand filling. As fuses of this type rely upon the process of ablation of wall material for current interruption, such fuses can be called "ablation-dominated" fuses. In order to obtain quantitative guide lines for the design of ablation-dominated fuses over a range of currents, it is essential to understand the mechanism of current interruption in the fuse and to be able to estimate the presure rise inside the fuse. Unfortunately, there appears to be little published literature on the behaviour of ablation-dominated fuses. Although there exist a few publications [3-5] on the behaviour of ablation-dominated arcs, these are not directly relevant in the context of fuse behaviour because these publications refer to arcing at very high current densities in tubes with open ends, which allow the plasma in the tube to escape thus reducing the pressure inside the tube.

This paper investigates the process of arcing in an enclosed tube with ablating wall with a view to obtain quantitative estimates of the pressure and voltage of an ablation dominated fuse. Experimental results of the transient pressure and voltage are presented for tubes made of perspex, pvc and Teflon. An attempt is made to develop a quantitative understanding of the fuse behaviour on the basis of a theoretical model derived from physical principles.

2. EXPERIMENTS

The process of arcing in a totally enclosed tube is inherently non-stationary in character because even for a steady arc current, continued wall ablation results in ever increasing pressure inside the tube until a mechanical failure occurs. During the interruption of a short-circuit current, the arc current changes from a high value to zero which introduces additional non-stationary characteristics to the problem of short-circuit current interruption by a fuse and hence increases the complexity in identifying the influence of ablative cooling. Most of the experiments have therefore been conducted [6] using approximate step current pulses which eliminate the non-stationary nature arising from variations in current. A few experiments have also been conducted on fuses with ablating walls in a short-circuit test scheme based on IEC recommendations.

2.1. TESTS WITH CURRENT STEPS

2.1.1. APPARATUS

Experiments were conducted on simulated fuses (Figure 1) using tubes of internal diameters 4 and 6 mm, and 50 mm long. These tubes were made from perspex, pvc and Teflon and had an outer diameter of 12 mm to provide a thick wall to withstand the pressure generated during arcing. Two brass end caps fitted with O-rings were fitted to the end of the tube and were held tight to prevent the leakage of plasma from the tube. The brass end caps also served as electrodes to sustain the arc within the tube. The arc was initiated by stretching a copper wire of 72.5 microns across the brass end caps. The fuse was loaded inside a polycarbonate holder (Figure 1) which held the fuse in position and also allowed the provision of the required pressure on the brass end caps of the fuse.

The pressure inside the tube was measured by drilling a hole of 1 mm diameter on its side which was aligned with a 3 mm hole on the polycarbonate holder. The 3 mm hole was terminated with a Kistler piezo-electric pressure transducer rated for linear operation upto 100 bars. An O-ring seal was provided at the junction between the holes in the fuse and the fuse holder to prevent plasma leakage. The hole linking the pressure transducer to the fuse was filled with glycerin to improve the frequency response of the pressure measuring system and also to

prevent arc products coming into contact with the pressure transducer. The charge developed by the pressure transducer was measured using a charge amplifier calibrated in bars with a bandwidth of 10 kHz.

The arc current for tests using current steps was obtained from a capacitor discharge circuit. The discharge circuit, which had been designed to provide 50 or 70 Hz current circuit, was modified to operate in an overdamped mode by inserting a series resistor. The test circuit provided quasi steady arc current pulses for times upto 10 ms when the fuse was replaced by a short circuit. The presence of the fuse, however, distorted the current waveform, but this distortion was small to affect gross arc properties. In order to prevent a mechanical failure of the arc chamber, the circuit current was diverted away from the arc chamber by triggering a spark gap at the end of nearly 3 ms after the initiation of the arc. The arc current was measured using a 5-milliohm co-axial shunt with a response time of 50 ns. The arc voltage was measured using Tektronix P6015 high-voltage probes.

2.1.2. RESULTS

Typical records of current, voltage and pressure obtained druing tests are shown in Figure 2. It can be seen that immediately after the explosion of the fuse wire, the arc voltage rises sharply to high values and then falls before a further steady and slow increase. The pressure in the simulated fuse increases almost linearly with time while the arc current remains approximately constant. It can also be seen from Figure 2 that the pressure developed in a 4 mm tube is much larger than the pressure in a 6 mm tube.

A comparison of the voltage and pressure obtained with tubes made from perspex, pvc and Teflon having the same internal diameter is made in Figure 3, which shows that for a given arc current, perspex gives the largest voltage and pressure while Teflon gives the lowest values. Results for the rate change of pressure with current for arc currents upto 100 A have also been obtained for the three materials considered.

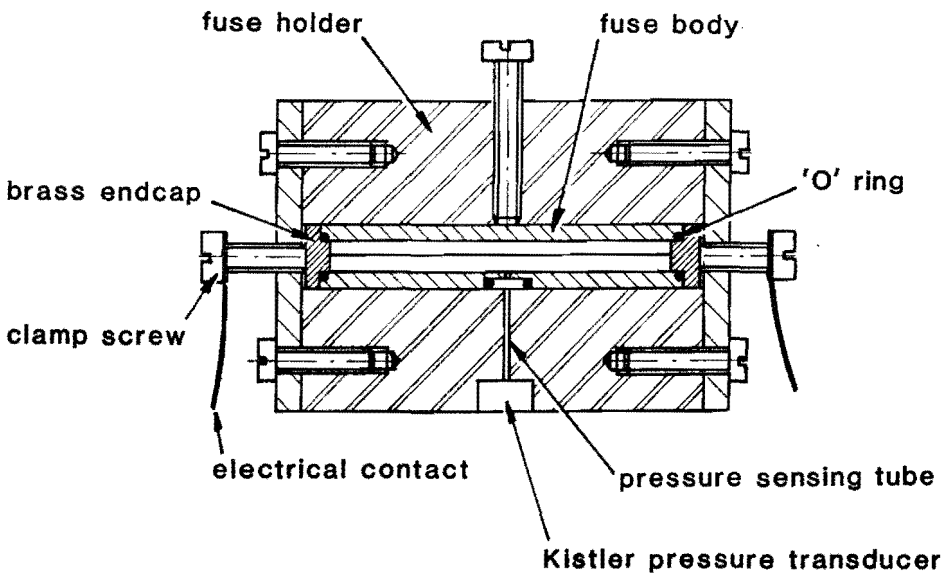

Figure 1 Experimental set-up for fuse studies.

2.2. SHORT-CIRCUIT TESTS

Experiments were also conducted using fuses of standard dimensions in a test circuit built on IEC recommendations [1] to deliver a prospective rms short-circuit current of 1500 A. Although the recommendation of the IEC on the closing angle for initiation of the circuit current relative to the source voltage is in the range of 25 to 35 degrees, the closing angle in the tests was varied from 10 to 45 degrees to investigate the severity of interruption duty.

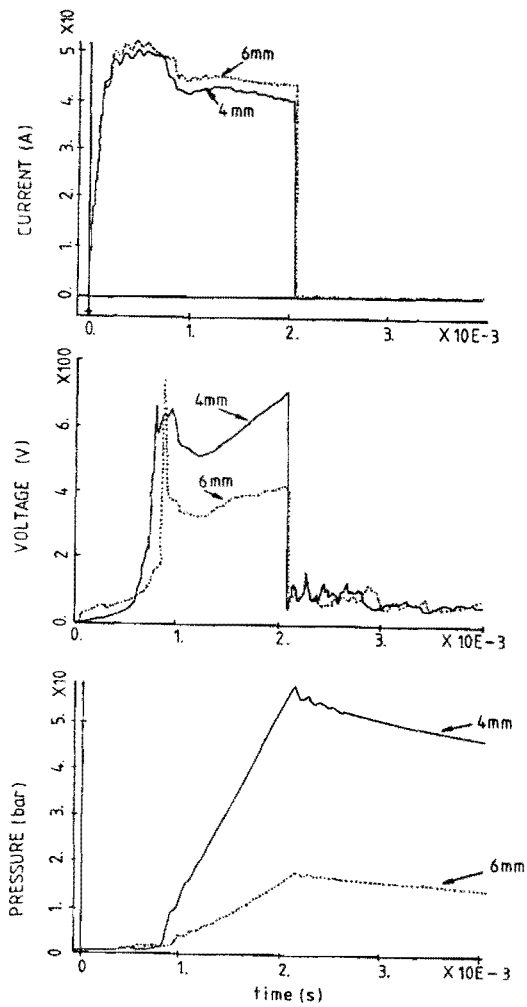

Figure 2 Experimental records showing influence of tube diameter on arc properties. PVC tube and 72.5 microns copper wire.

A typical record of the current and voltage recorded during a test on a fuse of internal diameter of 3 mm with a copper wire of 100 microns is shown in Figure 4. It was found that at a closing angle of 29 degrees, the interruption appeared to be critical. For example, the fuse made out of pvc developed a small hole on one of the end caps although the circuit current was interrupted. Fuses made out of other material showed a small dimple on their end caps which might have resulted in the development of a hole. When the closing angle was increased to 45 degrees, all the fuses failed. In the case of perspex and pvc fuses, the end caps were damaged as a result of arcing and the development of high pressure during arcing. The fuse made out of Teflon was found to explode during the test.

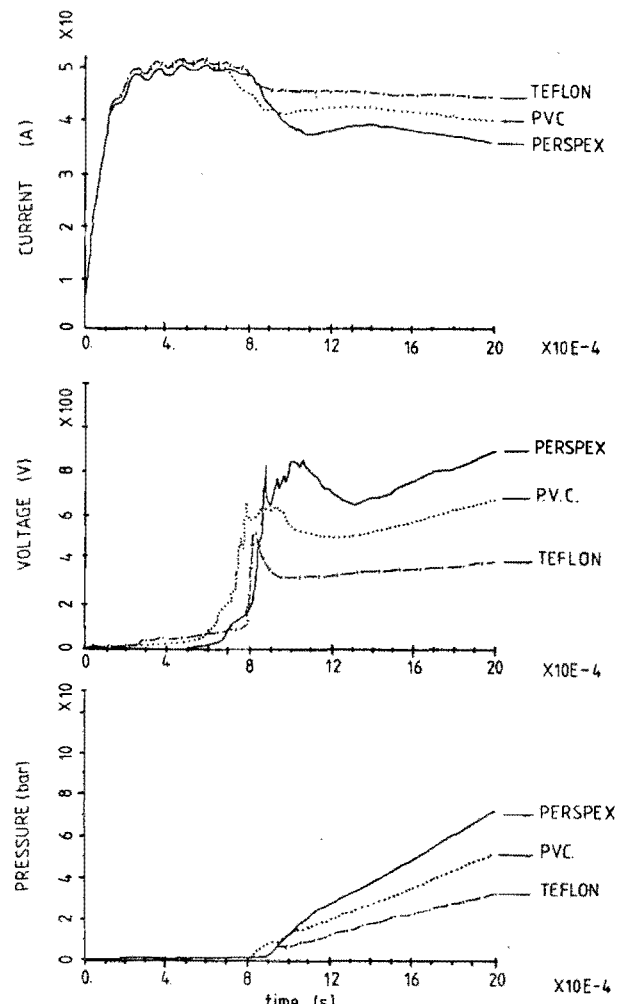

Figure 3 Influence of tube material on arc properties. 4-mm tube and 72.5 microns copper wire.

The tests showed that when the fuses cleared the fault currrent, the current records differed only slightly for the three tube materials. When a failure occurred, it was mainly due to a mechanical failure resulting from arcing at the end caps and high pressure inside the fuse. It was also found from tests with different closing angles that if the cut-off current for a particular closing angle was high due to a high initial rate of rise of current, then the fuse failed to clear the fault. This result shows that the cut-off current or the current at which the fuse wire melts and vapourises has a significant bearing on the arc interruption; the higher the cut-off current the more severe is the short-circuit duty.

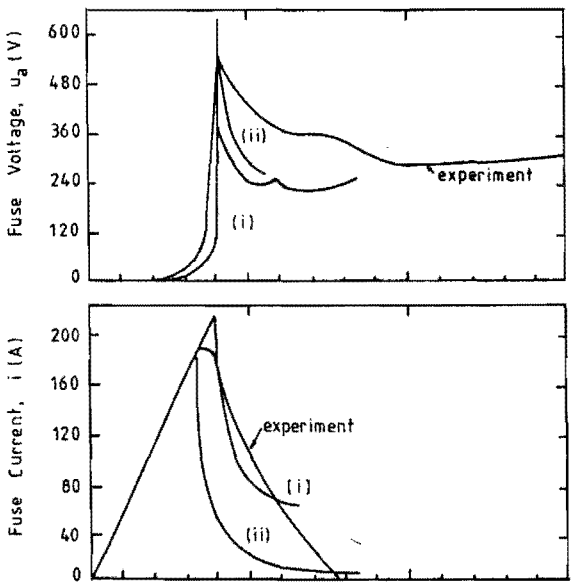

Figure 4 Short-circuit current interruption by a perspex fuse of 3 mm diameter and 20 mm long. Curves (i) and (ii) correspond to theoretical predictions.

3. ARC MODEL

In a fuse of the type shown in Figure 1, when a high current is passed, the fuse wire melts, explodes and an arc column is established within the tube across the end caps. The flow of current through the plasma results in joule heating within the arc plasma which is transported thermal conduction and also by radiation if the temperature of the plasma is sufficiently high. The wall material consequently ablates and gets entrained into the arc column. As the fuse is a totally enclosed tube, the pressure inside the tube increases owing to the addition of wall material as well as the joule heating which raises the plasma temperature. The entrainment of wall material results in a thermal convection directed from the wall to the inner regions of the tube and this thermal convection may be viewed as the energy required to elevate the vapour ablated from the wall to the temperature of the plasma. Thus, ablative cooling of the arc column results.

A detailed modelling of this type of arc should consider all three conservation equations, viz. mass, momentum and energy. As this is extremely difficult, in this study it is assumed that the mass liberated from the wall of tube has negligible inertia and hence distributes itself within the arc column instantaneously. This assumption is equivalent to assuming that the pressure in the radial direction at any instant of time is uniform which allows one to discard the momentum equation.

Further, as the tube is cylindrical in shape, it is assumed that axial variations in plasma properties are negligible. Thus we seek solutions of plasma properties in the radial direction only.

It is to be noted that at the instant the fuse wire explodes, the plasma is made up of the carrier gas, which is a mixture of metal vapour and air. As time progresses, the addition of wall material changes the composition of the plasma in the tube and the ratio of the mass of carrier gas to that of wall gas is a time-dependent function. Calculation of thermodynamic and transport properties of mixtures of gases at different temperatures and pressures is by no means simple. Hence, in this study, only variations in density and heat capacity as a function of gas-mixture ratio are considered at an approximate level. These two material properties contribute considerably towards thermal convective cooling and pressure rise inside the tube.

3.1. ENERGY BALANCE EQUATION

Assuming that the temperature T of the arc column within the tube varies only along the the

radial coordinate r because of cylindrical symmetry, the energy balance equation [7] for the arc column can be written as

$$\rho c_p \frac{\partial T}{\partial t} + \rho c_p v \frac{\partial T}{\partial r} =$$

$$\sigma E^2 + \frac{1}{r}\frac{\partial}{\partial r}\left[r\kappa\frac{\partial T}{\partial r}\right] - u \qquad (1)$$

where E is the axial electric field in the arc column, v the velocity of the plasma in the radial direction induced by the ablation process and t the time. The material functions of the arc plasma are: ρ the density, c_p the heat capacity, σ the electrical conductivity, κ the thermal conductivity and u the net radiation emission from unit volume. The material functions of the plasma are dependent upon temperature, pressure and plasma composition.

The energy balance equation (1) can be interpreted in simple terms as follows: a fraction of the joule heating resulting from the electical power input into the arc column is transported to wall of the tube by thermal conduction; another fraction is transported as radiation; and yet another fraction is expended in heating the ablated wall material to plasma temperature. The remaining power is used up in raising the plasma temperature, as given by the thermal storage $\rho c_p(\partial T/\partial t)$

In order to solve equation (1) two boundary conditions for temperature are required. One of the two boundary conditions is that the heat flux at the axis of a cylindrical arc column is zero. The second boundary condition is determined by the ablation process at the wall. As the wall is continuously ablating during arcing, the temperature at the wall can be taken to be equal to the vapourising temperature of the ablating material [4].

3.2. RATE OF MASS ABLATION

The rate at which the wall material is ablated and entrained into the arc is determined by the rate at which energy is received by the wall from the arc column and the energy required for the wall material to vapourise. If q is the rate at which unit length of wall receives energy in W/m, h_w the energy required to ablate unit mass of wall material in J/kg and $\dot{m}$ the rate at which mass is liberated from unit length of the wall in kg/m s, then

$$q = \dot{m} h_w \qquad (2)$$

The wall of the tube at a radius of r_w receives energy from the arc by means of thermal conduction and transparent radiation. Hence,

$$q = -2\pi r\kappa\left[\frac{\partial T}{\partial r}\right]_{r=r_w} + \int_0^{r_w} u\, 2\pi r dr \qquad (3)$$

and can be estimated using the temperature profile in the arc column.

The value of h_w, which is the energy required to ablate the wall material, is not known accurately. Niemeyer [3] has shown that for both polymer and ceramic materials, the value of h_w lies in the range of 0.3 10^7 to 10^7 J/kg for vapour temperatures in the range of 1000 to 5000 K. Kovitya and Lowke [4] used a value of 0.65 10^7 for their studies on ablation dominated arcs and this value has been used in this study.

3.3. CALCULATION OF PRESSURE RISE

The procedure to calculate the pressure inside the tube at any instant of time should consider pressure changes due to mass addition as a result of wall ablation as well as those due to changes in plasma temperature. The pressure changes due to both these factors can be estimated from the mass conservation equation, which is given by

$$\frac{\partial \rho}{\partial t} + \frac{1}{r}\frac{\partial}{\partial r}\left[r\rho v\right] = 0 \qquad (4)$$

In order to use this equation to estimate the pressure rise, we need to know the dependence of density of the plasma on pressure,temperature and plasma composition, which changes with

time. For the sake of simplicity, we assume that the density of the plasma in the tube is proportional to pressure. That is, if $\rho_0(T)$ is the functional dependence of plasma density on temperature at a reference pressure of p_0, which is taken as one bar, then the density function at any other pressure p is taken as

$$\rho(p,T) = \left[\frac{p}{p_0}\right]\rho_0(T) \tag{5}$$

Multiplying the mass conservation equation (4) by $2\pi r dr$ and integrating from $r=0$ to $r=r_w$, we get

$$\int_0^{r_w} \frac{\partial \rho}{\partial t} 2\pi r dr = -2\pi r_w \ (\rho v)_{r=r_w} \tag{6}$$

The right-hand side of the above equation (6) is equal to the rate at which mass is crossing the boundary at $r=r_w$ at any instant of time and hence should be equal to the rate of mass liberation from the wall which is given by equation (2). Thus, we have

$$\dot{m} = \int_0^{r_w} \frac{\partial \rho}{\partial t} 2\pi r dr \tag{7}$$

If the densities of the carrier and wall gas are equal, then equation (7) can be used together with equation (5) to get an expression [8], which gives the rate of change of pressure with time as a result of mass addition as well as temperature changes. However, it is very unlikely that the mass density of the wall gas will be the same as that of the carrier gas. As it is difficult to estimate the gas density of a complex gas mixture, we use an approximate averaging procedure to calculate the density of the composite plasma consisting of both carrier and wall gases.

We define the density function ρ_0 of the composite plasma at the reference pressure of p_0 of 1 bar as follows:

$$\rho_0(T) = \frac{\rho_c(T) + x\ \rho_w(T)}{1 + x} \tag{8}$$

where $\rho_c(T)$ and $\rho_w(T)$ are the density functions of the carrier and wall gases respectively and x is a ratio which depends upon the relative masses of the gases at any instant of time. The value of the ratio x at any instant of time is evaluated by forcing mass conservation for the two species individually. That is, if m_c and m_w are respectively the masses of carrier and wall gases per unit length of the plasma column at time t, then we require:

$$m_c = \frac{p}{p_0} \int_0^{r_w} \left[\frac{\rho_c(T)}{1 + x}\right] 2\pi r dr \tag{9}$$

$$m_w = \frac{p}{p_0} \int_0^{r_w} \left[\frac{x\rho_w(T)}{1 + x}\right] 2\pi r dr \tag{10}$$

$$m = m_c + m_w = \frac{p}{p_0} \int_0^{r_w} \rho_0(T) 2\pi r dr \tag{11}$$

Knowing the temperature profile in the plasma at time t and also the masses of carrier and wall gases at the same instant, the value of x can be calculated.

The pressure within the tube at any instant of time can be calculated by integrating equation (7) and using the total mass conservation equation (11). The expression given below gives the pressure at time t:

$$p = \frac{m\ p_0}{\int_0^{r_w} \left[\frac{\rho_c(T) + x\rho_w(T)}{1 + x}\right] 2\pi r dr} \tag{12}$$

3.4. CONVECTIVE COOLING

The entrainment of the ablated wall material

into the arc column results in a a radial convection directed from the wall to the axis of the tube. This convection results in a cooling of the outer regions of the arc column and heating the inner regions. Or, it can be viewed as the energy absorbed by the wall gas in being raised from the value of temperature at the wall to the plasma temperature. Assuming that the pressure across the tube to be uniform, the value of ρv at different radial positions can be calculated from the mass conservation equation (4). Integrating equation (4), we get

$$(\rho v)_{r=r'} = -\frac{1}{r'}\frac{\partial}{\partial t}\int_0^{r'} \rho r dr \qquad (13)$$

For $r'=r_w$, the above integral reduces to equations (6) and (7).

3.5. JOULE HEATING

The local joule heating of the plasma is given by term σE^2 in the energy balance equation (1) and is determined by the electrical power input into the plasma from the external test circuit. The current, i, through the arc column is related to the electric field through Ohm's law, which is

$$E = \frac{i}{\int_0^{r_w} \sigma 2\pi r dr} \qquad (14)$$

As the tube is cylindrical, the electric field can be assumed to be uniform axially and hence the voltage seen by the test circuit for a given current can be obtained by multiplying the electric field by the length of the tube.

3.6. MATERIAL FUNCTIONS

The carrier gas is made up of metal vapour from the fuse wire and air. If the fuse wire made of copper, for a 100 microns diameter wire in a 3.2 mm tube, the mass ratio of copper to air is nearly 8. The values of density, heat capacity, thermal conductivity and electrical conductivity for approximately this mass ratio have been taken from the publication of Shayler and Fang [9].

It is assumed that the transport properties, viz. thermal and electrical conductivities for the composite plasma, are assumed to be the same as those for the carrier gas.

It can be seen from the energy balance equation (1) that the most dominant influence of ablation results from thermal convection which is determined by the density and heat capacity of the composite plasma. The density of the composite plasma is determined by the averaging method given by equation (8). The heat capacity of the of the composite plasma is estimated by summing over the two component gases [9], the product of heat capacity and mass fraction of the two components. That is, the heat capacity c_p of the composite plasma is given by

$$c_p = \left[\frac{\rho_c}{\rho_0(1+x)}\right] c_{pc} + \left[\frac{x\rho_w}{\rho_0(1+x)}\right] c_{pw} \qquad (15)$$

where c_{pc} and c_{pw} are the heat capacities of carrier and wall gases respectively.

The values of mass density and heat capacity of wall gases of perspex, pvc and Teflon have been taken from the publication of Kovitya [10].

The values of net emission coefficient u of the composite plasma are taken to be equal to those of nitrogen plasma [11] for temperature above 12000 K. However, calculations showed that if the arc temperature was as high as 12000 K for radiation losses to be dominant then the fuse would not interrupt the current at all.

3.7. NUMERICAL METHOD

An explicit scheme using finite differences was used to solve the energy balance equation (1). The numerical algorithm is basically an integration procedure in time with which we march forward in time to seek solutions of temperature distribution as a function of time, starting from a set of initial conditions. The set of initial conditions correspond to the time when the fuse

wire within the tube explodes to establish an arc column. At this instant, we need to specify the pressure p, the mass of carrier gas m_c, the current i and the temperature distribution in the arc column. The mass of carrier gas at the initial instant was taken to be equal to the sum of the masses of the copper wire and the surrounding gas. The value of the initial pressure was determined from the mass of the carrier gas and the initial temperature distribution. The choice of a suitable initial temperature profile is discussed in the next section.

4. RESULTS AND DISCUSSION

Calculations have been made using the arc model to predict properties of arcs corresponding to the experimental conditions for both step-current tests and short-circuit tests. The calculation procedure relies upon specifying the correct initial conditions for the problem. The important initial conditions are the current at which the fuse wire explodes and the temperature distribution within the arc column immediately after the explosion of the fuse wire. The current at which the fuse wire explodes is determined by the I^2t value for melting of the fuse wire and in the case of step current tests, the value of the current and time which the explosion of the fuse wire takes place is not critical. However, in a short-circuit test, the dynamic interaction of the fuse with the test circuit produces certain inaccuracies in the determination of the current and time. Hence, for short-circuit test calculations, the cut-off current obtained in the experiment was used as the initial condition.

4.1. INITIAL TEMPERATURE PROFILE

The temperature profile of the plasma immediately after the explosion of the fuse wire is not known. Preliminary investigations [12] using high-speed framing photography at 35000 frames/second show that the initial location of the arc column within the tube is somewhat random and very often the arc resides in the form of a core near the wall of the tube. A treatment of this type of arc behaviour requires a two-dimensional treatment in both radial and azimuthal co-ordinates and hence is difficult. The arc model considered in this study assumes azimuthal symmetry as a first-order approximation and to be consistent with this assumption, we have chosen two forms of initial temperature profiles: (i) Elevated core : the arc is assumed to have a very thin core near the axis of the tube and (ii) Elevated wall : the arc is assumed to be an annulas near wall of the tube; this elevated temperature near the wall gives a larger value of electrical conductivity near the wall and can also be viewed as an enhancement of electrical conductivity near the wall of the tube owing to the the presence of copper vapour near the wall.

4.2. ARC BEHAVIOUR FOR STEP CURRENTS

Typical results of current, voltage and pressure obtained using the arc model for a 50 A arc burning in a 4-mm Teflon tube with a 72.5-microns copper wire are compared with the experimental results in Figure 5. In the case of the assumption of elevated core temperature as the initial condition, the calculations show that the temperature at the axis increases initially very rapidly to accommodate the imposed steady current, which produces intense joule heating within the core of the arc column. The temperature at the axis then begins to drop as a result of radiation from the core, but the arc column broadens as time progreses. The broadening of the temperature profile within the tube results in an increase of the conductance of the arc column with a consequent drop in the voltage as shown by Figure 5. The rate at which the broadening of the arc column decreases as time progresses because the ablated mass from the wall not only cools the outer regions of the arc column but also increases the mass and hence the thermal inertial of the arc column. The arc voltage drops significantly initially, but this drop tends to flatten after nearly 0.4 ms as shown by the figure. In the case of the assumption of elevated core, most of the heat received by the wall is due to transparent radiation and hence the rate of mass ablation from the wall is small. Consequently, the calculated pressure rise is smaller than the values determined experimentally. Further, calculations using this initial temperature profile for short-circuit current interruption predict unsuccessful interruption for experiments corresponding to successful interruption. It is therefore concluded that this type of

temperature profile is a very unlikely consequence of the explosion of the fuse wire.

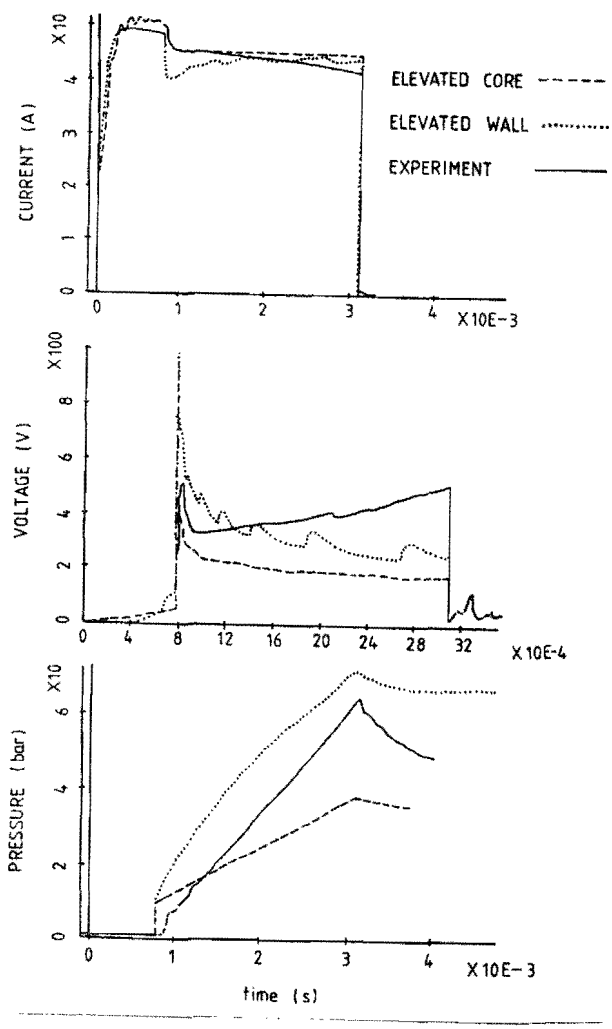

Figure 5 Comparison of experimental and theoretical results obtained for an arc in a 4-mm Teflon tube initiated by a 72.5 microns copper wire.

If joule heating is present near the abalting wall, then very effective cooling of the arc column can take place until heat diffuses to the inner regions of the tube. Calculations based on the initial condition of elevated wall temperature show that entrainment of ablated wall material is larger in this case than in the case of elevated core temperature profile. The results for the elevated wall case compare more favourably with the experimental results as shown in Figure 5. There is however an overestimation of the pressure in the tube because of the assumption that the arc is an annular ring near the wall of the tube which results in an overestimation of the mass ablated from the wall; in practice the heated zone might be more localised than what has been assumed.

The rate of increase of pressure in the tube with time for step currents of different magnitudes is shown in Figure 6. It can be seen that the calculated results agree reasonably with the experimental values for three tube materials considered. Experimental values of (dp/dt) for the 6-mm Teflon tube are much lower than the predicted results. The reason for this discrepancy may be due to the abalting characteristics of Teflon which exhibits highly localised vapourisation resulting in craters instead of uniform ablation over the surface when exposed to electric arcs.

4.3. FUSE BEHAVIOUR UNDER SHORT-CIRCUIT TESTS

In order to predict the behaviour fuses under short-circuit test conditions, the arc model was linked with the equations describing the test circuit bassed on IEC recommendations [8]. Calculated results of current and voltage as a function of time are compared with the experimental results for a fuse made of perspex tube of inner diameter of 3 mm and having a fuse wire of 100 microns in diameter (Figure 4). Case (i) in Figure 4 corresponds to the case where the cut-off current is estimated from the I^2t value for melting for the fuse wire. As the cut-off current in this case is higher than the experimental value, the arc model predicts intense heating of the arc column immediately after the explosion of the fuse wire followed by a failure of the fuse to interrupt the current. In case (ii), we have used the cut-off current obtained in the experiment for calculations, which show that successful interruption is possible. These calculations show that the current at which the fuse wire melts has a significant bearing on the interruption of current by the fuse in the test circuit.

Results were also obtained for current interruption by a pespex fuse with a copper wire of 100 microns in diameter at a closing angle of 10 degees of the test circuit. In this case, as the

inital rate of rise of current is lower than the value at a closing angle of 29 degees, the cut-off current is lower and hence a successful interruption is predicted by the arc model. These results confirm our experimental results that while the fuse cleared the fault current at a closing angle of 9.4 degrees, it failed to clear the fault current at 45 degrees.

Calculated results of current, voltage and pressure for fuses made of 3-mm diameter, 20-mm long perspex tubes with fuse wires of different diameter are shown in Figure 8. The values of cut-off current for these calculations have been estimated on the basis of I^2t values. It can be seen that the interruption of current gets more critical as the diameter of the wire is increased.

4.4. DISCUSSION

Results obtained from experiments and theoretical calculations show that for step currents, perspex gives the largest pressure and voltage for a given magnitude of the current while Teflon gives the smallest values. The reason for this can be attributed to the fact that perspex vapour has a lower value of mass density and a higher value of heat capacity. The addition into the tube of a wall gas which has a lower mass density reduces the density of the composite plasma inside the tube and hence results in an increased pressure for a given amount of gas within the tube. If the heat capacity of the wall gas is larger then larger amount of heat is absorbed by the wall gas from the arc column thereby reducing the plasma temperature. A reduction in plasma temperature results in a reduction in the conductance of the arc column and hence an increase in the arc voltage.

This study shows that although ablative cooling of the arc column in fuses can be used to aid current interruption, prolonged arcing in the presence of wall ablation results in an increased mass inside the fuse which can have the two following detrimental effects : (i) the pressure inside the tube increases to very high values and can cause a mechanical failure and (ii) the increased mass inside the fuse increases the thermal inertia of the arc column and hence the plasma cools much more slowly than when no wall ablation is present.

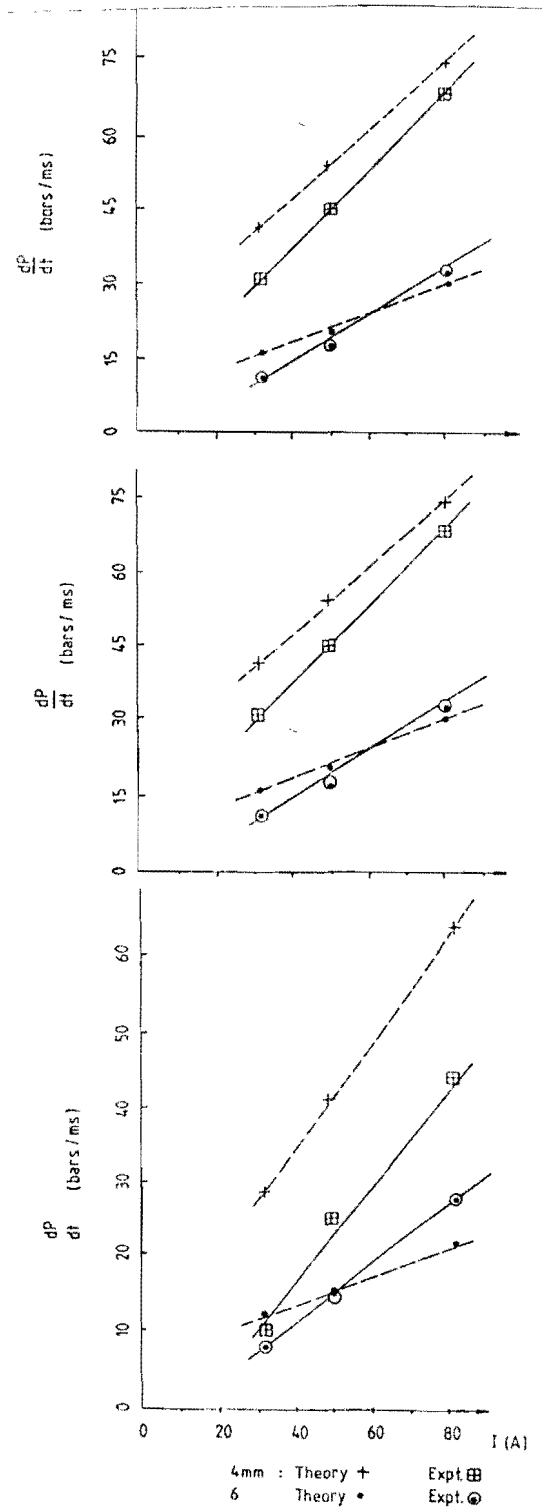

Figure 6 Dependence of rate of increase of pressure with time on arc current. Top: perspex, middle: pvc and bottom: Teflon.

This study also reveals that the current at which the fuse wire explodes has an imporatant bearing on current interruption. Immediately after the explosion of the fuse wire, most of the joule heating is balanced by wall ablation. For a tube of radius r_w, the joule heating is proportional to $(1/r_w^2)$ or is a volume effect whereas ablative cooling is a surface effect which is proportional to r_w. Consequently, a large initial current increases the plasma temperature considerably. Since ablative coling is dominant only near the outer periphery of the arc column, if considerable heating of the inner region the arc column is caused by a large initial current, the interruption of fault current will not result.

We have assumed in this study that the temperature profile inside the arc column immediately after the explosion of the fuse wire is one that offers enhanced conductivity near the ablating wall of the fuse so that most of the joule heating occurs near the wall initially. It is necessary to investigate the initial period of arc development within the fuse to improve our arc model.

5. CONCLUSION

A numerical model has been developed to study the behaviuor of arcs in enclosed tubes and the process of current interruption in small fuses whose wall ablates as a consequence of arcing within the fuse. Results of current, voltage and pressure within the fuse obtained using the model are in approximate agreement with experimental results.

One of the main difficulties of the model stems from the lack of knowledge of the temperature profile inside the arc column immediately after the explosion of the fuse wire. It is found from a comparison of the calculated results with experiments that most of the joule heating should occur near the ablating the wall of the fuse.

In order to produce strong ablative cooling of the arc column during a current interruption process, it is essential that the surface area of the arc column is large and that the arc column lies close to the ablating surface.

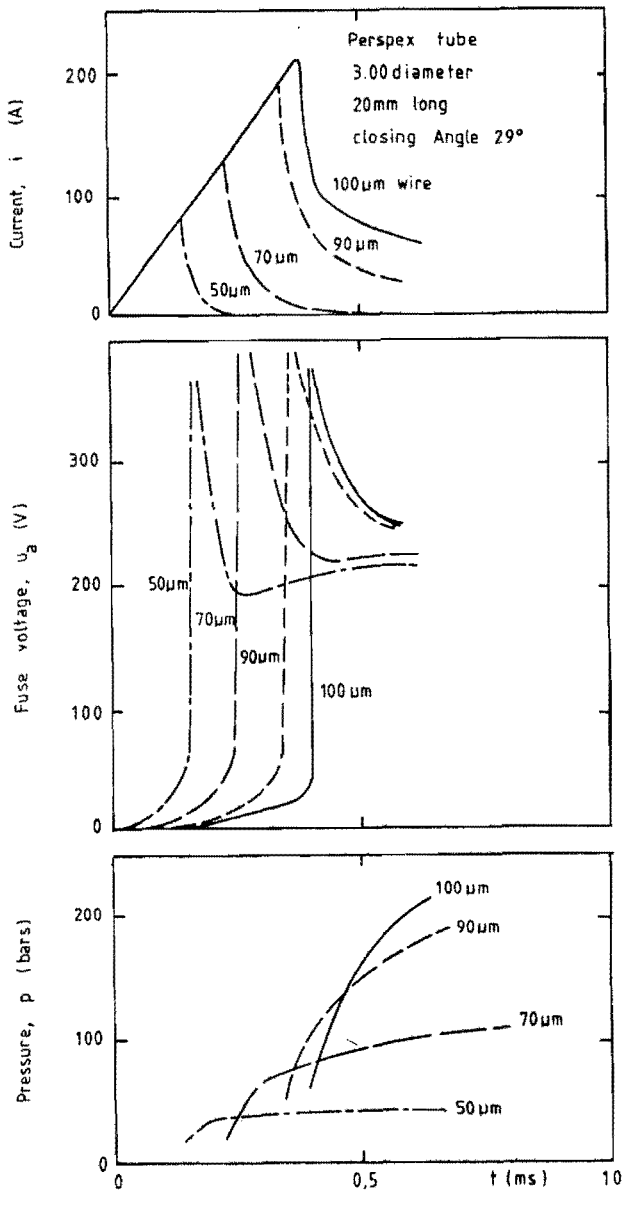

Figure 7 Theoretical predictions of interruption behaviour of a fuse with ablating wall.

ACKNOWLEDGMENTS

We wish to thank Ms. M. Clemson for doing some of the work reported here. Stimulating discussions with Dr. L. Vermij are gratefully acknowledged. Most of this work was carried out when one of the authors (SR) was with the Eindhoven University of Technology on a study leave from the University of Sydney.

REFERENCES

[1] IEC Publication 127 (1974) : Cartridge Fuse-Links for Miniature Fuses Geneva : International Electrotechnical Commission.

[2] Vermij, L. (1971) Holetechniek, vol. 1, p.32-36.

[3] Niemeyer, L. (1978) IEEE Trans. Power App. & Sys., vol. PAS-97, p 950- 58.

[4] Kovitya, P and Lowke, J.J. (1984) J. Phys. D: Appl. Phys., vol 17 p 1197-1212.

[5] Ibrahim, E.Z. (1980) J. Phys. D: Appl. Phys., vol 13, p 2045-65.

[6] Clemson, M. (1985) B.E. (Honours) Thesis, School of Electrical Engineering, The University of Sydney.

[7] Jones, G.R. and Fang, M.T.C. (1980) Rep. Prog. Phys., vol 43 p 1415-65.

[8] Ramakrishnan, S. and van den Heuvel, W.M.C. (1985) EUT Report 85-E-151, Department of Electrical Engineering, Eindhoven University of Technology, The Netherlands.

[9] Shayler, P.J. and Fang, M.T.C. (1976) Report ULAP-T45, Department of Electrical Engineering and Electronics, University of Liverpool, U.K.

[10] Kovitya, P. (1984) IEEE Trans. Plasma Sci., vol PS-12, p 38-42.

[11] Ernst, K.A., Kopainsky, J.G. and Maecker, H.H. (1973) IEEE Trans. Plasma Sci., vol. PS-4, p 3-16.

[12] Kansel, R. (1984) Practical Work Report EG2.85.s.05, Electrical Energy Techniques Group, Department of Electrical Engineering, Eindhoven University of Technology, The Netherlands.

"ABLATIVE MATERIALS AS A NEW POSSIBILITY FOR THE DESIGN OF MINIATURE FUSES"

A.J.M. Mattheij, L. Vermij, Littelfuse Tracor, Utrecht, The Netherlands

ABSTRACT

In principle the use of ablative material as an arc-extinguishing medium is not new;they were used before in, for example, circuitbreakers. However their typical properties make them ideal for the design of miniature fuses. In this paper we will give some results of breaking capacity tests and some physical aspects will be discussed. The use of new materials for miniature fuses makes additional tests necessary. A proposal for new test methods will be given.

1. INTRODUCTION

IEC-publication 127 requires for miniature high breaking capacity fuses an interrupting ability of 1500A, but in practice also higher interrupting abilities are required, e.g. 5 to 6kA. Moreover, it may be expected that in future a greater demand for such fuses will be there. It is current practice to obtain such a high breaking capacity by using a filler material, normally quartz sand. This sand-filling of fuses however introduces manufacturing-problems and thus increased manufacturing costs. A way to avoid sand-filling of fuses is the use of an ablative material for the fuse body.

2. THE POSSIBILITY OF MAKING HBC-FUSES WITHOUT SAND FILLER

From past experience we already knew that it is in principle possible to make HBC-fuses without sand filler [1]. The condition is that the discharge after blowing the fuse element should be enclosed in a hole of relatively small dimensions. Under this condition the behaviour of such a fuse during the arcing period is comparable with those of a sand-filled fuse. Further it has been shown in [1] that blowing a fuse element in a small hole in an epoxy-resin tube gives rise to higher arc-voltages compared with the arc-voltage in a ceramic of equal dimensions. Further it has been demonstrated that the obtained experimental results can be rather well explained theoretically.

The above mentioned condition for the space left to the discharge after blowing the fuse element can be realised in miniature fuses rather easily. Moreover, the relatively moderate requirements with respect to the interrupting capacity of miniature fuses create not too severe conditions regarding pressures arising in the volume where the arc is burning. So, in developing HBC-fuses without sand filler, the most obvious first step is the development of HBC-miniature fuses without sand filler. This is the more so because the sand-filling process is a rather serious complication in an automatic fuse manufacturing process of miniature fuses.

3. BENEFITS OF THE USE OF ABLATIVE MATERIALS

Ablative materials have the property that gasses are evolved due to arcing. This means that rather large energies are required for desintegration of the inner layer of the fuse body material. Moreover the desintegration products of an ablative material assist in quenching the arc.

A lot of common polymeric materials are known which have more or less good arc-interrupting and gas-evolving characteristics [2]. Polymeric materials also have the advantage that they are insulating materials and they can easily be moulded. The moulding process allows for a greater freedom in shaping the fuse body, meaning that also other designs are possible to make these fuse types better suitable for automatic production technologies. Making use of ablative materials for fuses, however, requires special plastic materials which should withstand relatively high temperatures and which should have sufficient mechanical strength to be able to withstand the relatively high pressures inside the fuse body during arcing. Fortunately the materials which can be used, have sufficient mechanical strength and elasticity to withstand the high pressures. In fact, they perform better in this respect than glass or ceramic, the materials used in common practice.

The fact that polymeric materials can be moulded, makes it easy to design the bodies in such a way that fastening the caps to the body can be done in an easy way; glueing and/ or soldering is not necessary anymore.

Fig. 1 shows a possible design of a miniature fuse using an ablative material. The caps are crimped on, attaching these firmly to the body in a way which is better able to withstand pressures than caps attaching by glueing or otherwise.

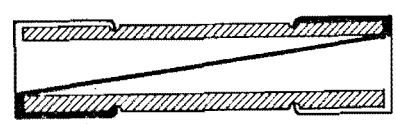

Fig. 1 Design of a miniature fuse using a plastic body and no sand filler.

Another advantage to choose for polymeric materials instead of glass or ceramic is the fact that fuse bodies of different manufacturing batches have less deviation in their dimensions. This reduces manufacturing problems. Plastic materials also weigh less than glass or ceramic; this reduces transportation costs for bulk packages. As a remark, a European patent has been filed for HBC miniature fuses without sand filler, using ablative materials [3].

4. RESULTS OF BREAKING CAPACITY TESTS

In reference [4] a computer simulation is described of the current interruption in a miniature fuse with an ablative inner wall. It is found that in case of short-circuit the current is reduced to a small value very rapidly. This conforms with experimental results of short-circuit tests which were carried out at Eindhoven University of Technology.

Some breaking capacity tests were done in a circuit for high breaking capacity tests according to IEC publication 127. Fig. 2 shows an oscillogram of a fuse with a rated current of 1A and a body made of an ablative material. The fuse had no sand filler. The voltage across and current through the fuse were measured with a digital recording system. (CAMAC, LeCroy) From the measured voltage and current traces, the arc power and arc energy as a function of time could be calculated.

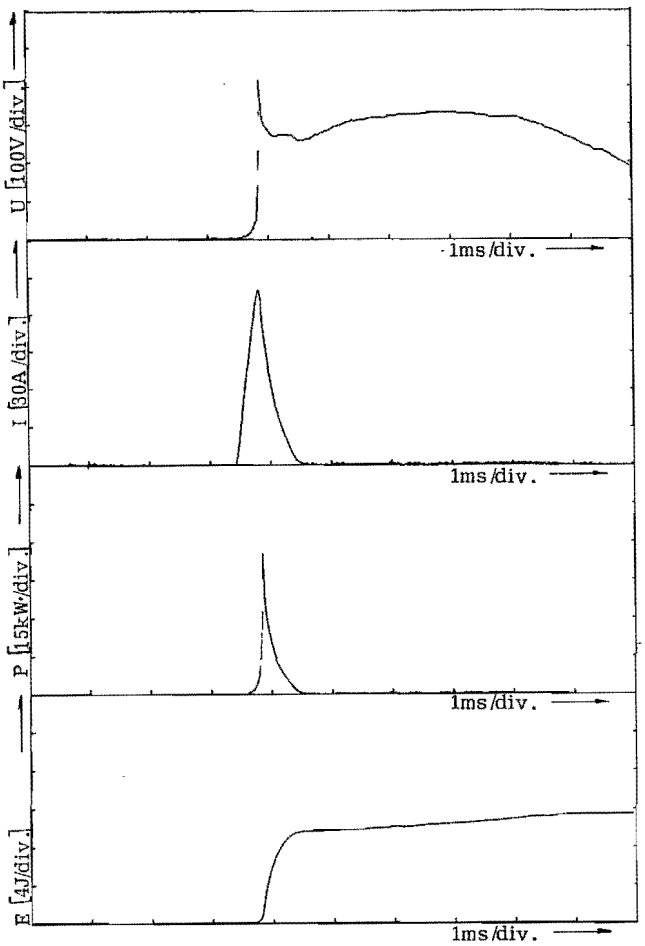

Fig. 2

Breaking capacity test on a miniature fuse (rated current of 1A) with ablative body.

U : voltage across the fuse.

I : current through the fuse.

P : arc power.

E : arc energy.

5. TESTING OF ABLATIVE FUSES

On miniature fuses with dimensions 5 x 20mm and 6.3 x 32mm IEC publication 127 is applicable. So it is obvious that a fuse with a body made of an ablative material must fulfil all the requirements mentioned in this IEC publication. For the new ablative fuses most attention should be paid to the breaking capacity test and the endurance test. As for the breaking capacity test, the fuse body has enough mechanical strength to withstand the high pressures which occur during arcing. Most attention has to be paid to the caps and their fastening to the body.

The problems which might arise during the endurance test are not the diffusion of tin out of the solder into the wire, because the wire is not soldered to the caps. In our case the endurance test is a test of the material which is used for the fuse body. When an inferior plastic is used, the wire will cut into the body due to the cyclical heating up and cooling down of the wire during the endurance test. This will lead to at least a bad electrical contact between wire and cap; it might even result in a premature interruption (no contact at all between wire and cap) of the fuse before the test is done.

As stated before, the fuse has to fulfil all the requirements mentioned in IEC publication 127. The use of polymeric materials for miniature fuses, however, makes additional tests necessary. Especially in the overcurrent range of a certain fuse, the body has to withstand relatively high temperatures; temperatures at which most common polymeric materials will melt or deform. So it is obvious that some sort of "high temperature test" has to be done. A possibility is to apply the so-called "step-test" or "current-test" which is mentioned in the proposed ISO standard for blade type electric fuse links [5] and the draft specification DIN 72581, part 3 [6]. These standards aim at car fuses for which the use of polymeric materials is already common practice. We think however that the "current-test" is also applicable to miniature fuses using ablative material. From experience with testing blade fuses for automotive applications it is well known that, based on such a "current-step-test", a rather quick and reliable judgement can be made regarding the quality of the fuse body. The test is described as follows :

"A current equivalent in value to the rating of the fuse link on test shall first be applied for a duration of 5 minutes. The current value shall then be increased in steps of 2.5% of the fuse link rating each 5 minutes until the element melts and the current flow is interrupted."

As miniature fuses have a higher fusing factor (1.5 - 1.7) than the blade fuse to which the above mentioned ISO standard is applicable (1.1 - 1.2), we suggest to start the "current-test" or "step-test" at a higher current value. Our experience is that a value of 1.4 times the rated current is a good starting point. (see fig. 3)

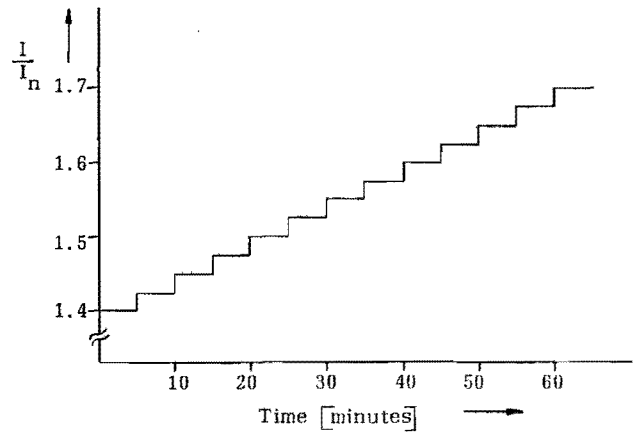

Fig. 3 : "step-test" or "current-test" I_n is rated current.

During this test the highest temperature which might occur, is reached. A fuse may pass this test when it can be easily withdrawn from the test holder and no serious deformation or holes in the fuse body do occur. (deformation can be checked by carrying out the alignment test mentioned in IEC publication 127)

Another test wich should be done, is some sort of environmental test. It is a well-known fact that some polymeric materials are sensitive to fluctuations in ambient temperature and humidity. A test which might be of use is also described in the above mentioned proposed ISO standard. According to this standard the fuses are put into a climate chamber in which the relative humidity and temperature are varied between the boundaries as indicated by the shaded areas in fig. 4. The complete environmental test lasts for 10 cycles. (10 days)

A fuse may pass this test when the voltage drop measured at rated current did not increase by more than 10% of the value measured before the test.

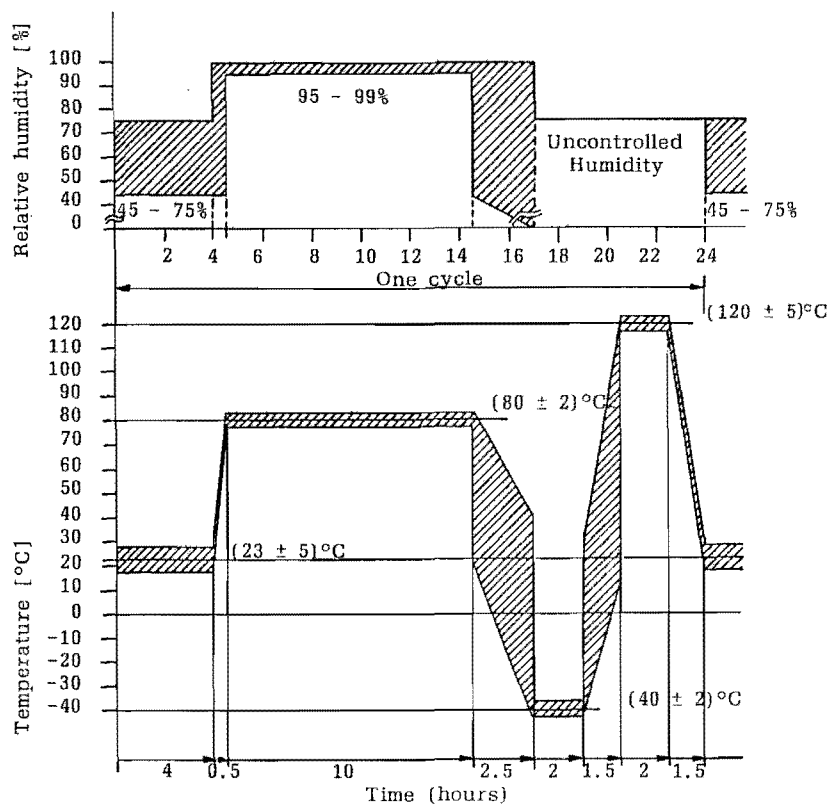

Fig. 4 : temperature and humidity cycle test. The test continues for 10 cycles.

6. CONCLUSIONS AND SUGGESTIONS

Our experimental results show that the use of ablative material is a possibility in miniature fuse technology. However, the materials used have to come up to meet special requirements. Especially high temperature behaviour is an important matter. This high temperature behaviour can be checked by two tests; the so-called "step-test" and a temperature cycle test. The temperature cycle test seems to be a (too) severe test; an ambient temperature of 120°C is probably never reached in common practice. However, this test is meant as an accelerated ageing test.

REFERENCES

[1] L. Vermij : "Electrical behaviour of fuse elements."
Thesis Eindhoven University, 1969

[2] P.F. Hettwer : "Arc interruption and gas evolution characteristics of common polymeric materials."
Trans IEEE PAS-101, 6, (1982), 1689-96

[3] European patent application no. 86 200 571.7

[4] S. Ramakrishnan, W.M.C. van den Heuvel : "A study of the process of short-circuit current interruption in a low voltage fuse with ablating walls."
EUT Report 85-E-151, (1985)

[5] Proposed ISO standard for blade type electric fuse links
ISO/ DP XXXX/ 1
ISO/ TC 22/ SC 3/ WG 5/ N 81, May 2, 1984

[6] Entwurf DIN 72581 Teil 3 : Sicherungen für Kleinspannungsanlagen, Flachsicherungseinsätze, Januar 1986

Session VII

MINIATURE FUSES 2

Chairman: Prof. Dr. W. M. C. van den Heuvel

SOME PROBLEMS IN THE MODELLING OF MINIATURE FUSES

R. Wilkins, Consultant, 18 Speedwell Drive, Heswall, Wirral, U.K.

Abstract

Realistic modelling of the thermal behaviour of miniature fuses requires primarily the estimation of heat losses from the fuse element, and the way in which these losses are affected by the element dimensions, fuse body size, type of test clip, and the nature of the filler if used. In the paper the heat loss mechanisms are discussed and some experimental correlations for the heat-loss coefficients are given. Solution methods for the resulting non-linear set of equations are then described. Arcing phenomena for fuses with and without filler are then reviewed and a general approach to the modelling of arcing is presented. Deficiencies in existing knowledge are highlighted as areas for possible future research.

LIST OF SYMBOLS

m = density of element material
c = specific heat of element material
S = element cross-sectional area
T = $T(x,t)$ = temperature rise of fuse element
I = element current
ρ_o = specific resistivity of element material
α = temperature coefficient of resistivity
K = thermal conductivity of element
d = diameter of wire element
h = wire surface heat-loss coefficient
x = axial position along element
t = time
N = number of element sections
$[Q]$ = (N+1) x (N+1) matrix for steady-state solutions
$[R]$ = (N+1) x 1 matrix for steady-state solutions
$[T]$ = (N+1) x 1 matrix of unknown temperature rises
C = coefficient in wire heat-loss correlation
C_b = coefficient in body heat-loss correlation
C_e = coefficient in end thermal resistance correlation
L = fuse length
D_1 = inner diameter of body
D_2 = outer diameter of body
T_b = outer body temperature
T_e = endcap temperature rise
f = fraction of element touching body wall
θ = arctan (D1/L)
γ = coefficient of expansion of element
T_{av} = average element temperature rise
g_f = filler thermal resistance per unit length
g_b = body thermal resistance per unit length
g_{ext} = external thermal resistance per unit length
k_f = filler thermal conductivity
k_b = body thermal conductivity
R = element resistance per unit length
R' = spiral element resistance per unit axial distance
ϕ = characteristic angle of helix
$[A]$ = (N+1) x (N+1) matrix for transient solution
$[B]$ = (N+1) x 1 matrix for transient solution
T_{ms} = average temperature rise of M-blob
R_{ms} = effective thermal resistance of M-blob
C_{ms} = effective thermal capacitance of M-blob
t_d = disruption time, t_r = voltage rise time
K_d, K_r = coefficients associated with t_d and t_r
j = instantaneous current density

INTRODUCTION

Computer modelling of fuse behaviour and the simulation of fuse testing plays an increasingly important part in the fuse design process. While there have been several accounts of modelling procedures for sand-filled power fuses, there is very little information available on similar procedures for miniature fuses.

Many miniature fuse designs use wire elements in air, the elements being cooled by natural convection, which is probably the most difficult heat-loss process to model. Some very simplified formulae, such as "Preece's Law" have been commonly used, but these are not sufficiently accurate for design purposes. In practice the effects of elementgeometry and material, body size, and end assembly need to be represented. In this paper thermal modelling is discussed in some detail, and then some initial ideas on the modelling of arcing behaviour are presented.

The fundamental thermal behaviour of a fine-wire fuse element can be accurately represented by the partial differential equation below, which was originally formulated by Verdet [1].

$$mcS\frac{\partial T}{\partial t} = \frac{I^2\rho_o(1+\alpha T)}{S} + KS\frac{\partial^2 T}{\partial x^2} - \pi dhT \qquad (1)$$

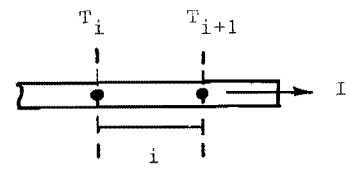

Fig.1 Division of wire element into finite sections.

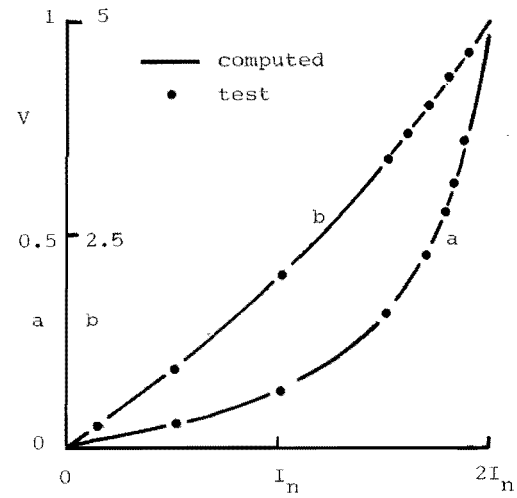

Fig.2 Comparison of test results and computed results with h independent of temperature.

(i) 1A fuse, silver element

(ii) 0.1A fuse, "nickel-silver" element

This equation is a heat balance at point x on the element in terms of the power per unit length. The first term on the right-hand side is the rate of internal heat generation due to the flow of current. The second term on the r.h.s. represents the axial heat loss by thermal conduction along the wire, while the third term is the loss from the wire surface to the surrounding medium. Any imbalance of the terms on the r.h.s. gives rise to a change in internal energy (and temperature), which is given by the term on the l.h.s.

The key to the accurate solution of (1) is knowledge of the surface heat-loss term h, as all the other terms in the equations are known quite precisely.

STEADY-STATE THERMAL SOLUTIONS

By putting $\partial T/\partial t=0$ in (1) we obtain an ordinary differential equation governing the steady thermal state, in which the heat generated is just balanced by the heat losses. This equation can be solved by wholly numerical methods using for example finite differences but there are great difficulties in obtaining satisfactory convergence [2]. If for the moment we assume that h is constant an analytical solution can be found. This solution is given fully in reference [2] which shows that the axial temperature distribution for a finite-length element with constant cross section and properties may be governed by hyperbolic functions (flat-topped - at low currents) or by trigonometric functions (at higher currents). If the current is too high no steady-state solution exists. Equations are also given in [2] for the heat transferred by conduction to the ends of such a finite-length element. This permits an element to be represented by N sections as shown in Fig.1. A model in which the properties of the element vary with x can then be used.

By equating the heat transfer by conduction at the interfaces between sections the following matrix equation is obtained:

$$[Q]\ [T] = [R] \qquad (2)$$

which can be solved for the unknown temperatures [T]. The first and last equations in the set are different from all others in that in these cases the heat transferred by conduction has to be equated to the heat lost to, for example, the test-clips in a temperature-rise test. Rules for assembly of the matrices are given in [2].

In practice the heat-loss coefficients are not constant but are weakly temperature dependent. To allow for this an iterative process is needed. An initial estimate of the heat-loss coefficient is made, after which (2) is solved for the temperatures. From these values better estimates of the heat-loss coefficients may be obtained, (2) is re-solved, and so on, until the process converges, under-relaxation being necessary to ensure convergence.

This iterative analytical method is very fast, as (2) is a tridiagonal matrix equation which permits efficient solutions for the temperatures.

HEAT-LOSS COEFFICIENTS

Given the above model and solution method it was necessary to find an expression for the surface heat-loss coefficient h for a fine wire enclosed in a glass tube without filler. Problems in heat transfer by natural convection are solved by establishing a functional correlation between the Nusselt and Rayleigh numbers, which then permits h to be found for given conditions [3]. Over a given range of Rayleigh number the functional correlation can be modelled as a power-law, with h shown to vary with the physical dimensions of the object losing heat and the temperature difference between the object and its surroundings. There are published data for wires in free air but with a miniature fuse the situation is different, in that the flow of air around the wire is restricted. A 3-dimensional pattern of circulation will be established within the fuse which differs significantly from that which occurs in free air.

Experiments have been conducted to determine the power laws governing (a) the wire surface heat-loss coefficient, (b) the outer body surface heat-loss coefficient, and (c) the thermal resistance of a standard IEC127 test-clip.

(a) wire surface heat-loss coefficient h

First the dependence of h upon wire temperature and diameter was studied by analysing test data on m.f.c.'s , mV drops, and temperature rises for miniature fuses with fixed body size (20mm x 5mm). Fuses with different wire materials, and wire diameters from 0.01mm up to 0.2mm were considered.

It was found that there was no detectable dependence of h upon the wire temperature. Thus for a given fuse geometry, use of a constant value of h gave results predicted by the solution of (1) which fitted the test results very well. Fig.2 shows a comparison of the computed and measured variations of mV drop with current for two different fuses using a constant value of h. If temperature-dependence of h was included using power laws typical of those found for wires in free air [3] the computed results could not be matched to the test data. This result is fortunate as it means that in the iterative solution previously described the alteration of h on the basis on temperature is not necessary, giving faster and more sure convergence.

There was however found to be a weak dependence of h upon the wire diameter, h being found to be approximately inversely proportional to d raised to the power 0.25. This is similar to the dependence of h upon d for wires in free air, and also is in broad agreement with experience over many years with the use of Preece's Law for the minimum fusing current of a wire in air. If (1) is solved in the steady-state for a long wire ($\partial^2T/\partial x^2=0$) with h independent of d we obtain Preece's Law, i.e. minimum fusing current varies with d raised to the power 1.5. If however h is assumed to vary inversely with d to the power 0.25, the index in Preece's Law falls from 1.5 to 1.375. This trend is evident also in revised versions of Preece's Law which have been published. See for example, reference [4].

Having determined the weak correlation just described, the effect of varying the body size was investigated. This was expected to have a

strong influence upon h since the size of the volume of air within the fuse will affect its circulation pattern and hence the value of h. A series of tests was conducted on fuses with varying lengths (up to 32mm) and internal body diameters (3mm to 4.7mm) and in each case a value of h was found by trial and error, which when used in (1) gave the best correlation with the test results. The total series of test results was then analysed to find the indexes in the power-law relating h to the fuse body dimensions. A least-squares best fit gave the following results:

$$h = \frac{C}{d^{0.25}} \left[\frac{20}{L}\right] \cdot \left[\frac{3}{D1}\right]^{0.4} \quad W / mm^2 / degC$$

where C=3.06 x 10-4 with the dimension in mm.

(b) outer body surface heat-loss coefficient

After (1) has been solved the heat lost radially through the fuse body can be calculated by subtracting the power lost to the element ends (by conduction) from the total generated power. This permits an estimate of the temperature rise of the outer fuse body if the body surface heat-loss coefficient is known. Values of h_b which gave agreement with the test values were found and then a least-squares fit gave the correlation:

$$h_b = \frac{C_b}{D2^{0.584}} \left[T_b\right]^{0.079} \left[\frac{D2}{L}\right]^{0.8} \quad W / mm^2 / degC$$

where C_b=23.5 x 10-5 with the dimension in mm. This correlation is similar in form to standard formulae for the heat loss from finite horizontal cylinders [3], with a weak dependence of h_b upon temperature.

(c) thermal resistance of test-clip

Heat transferred to the fuse elements ends by thermal conduction along the element is then lost by conduction along the test-clip and by convection and radiation from the surface of the test-clip and the fuse endcap. Again by using similar analytical procedures the thermal resistance viewed from the element ends was found to be governed by the correlation.

$$G_e = \frac{C_e}{(T_e)^{.129}(D2)^{.339}} \quad deg\ C / W$$

where C_e=294.0. G_e decreases with temperature T_e because of the effect of loss by convection and radiation from the surface of the test clip and the fuse endcaps, while the variation with D2 indicates the relative importance of the losses from the surface of the endcaps.

The three correlations given above represent the major factors which influence the heat loss from an enclosed fuse element in air. There are minor influences also, particularly the effect of wall thickness and endcap length and thickness but the scatter in test data was too large to enable these effects to be isolated.

Nevertheless, using the three correlations above and the iterative analytical solution method, the correlation coefficients relating the computed values of mV drop, body temperature, and endcap temperature to the test values were 98.9%, 92.9% and 97.6% respectively.

EFFECT OF WIRE EXPANSION

When calculating the steady-state thermal performance it is necessary to consider the possibility that owing to thermal expansion the fuse element may defect laterally and touch the inside of the body wall. When this occurs (mostly with longer fuses) the part of the element in contact with the body wall is subject to additional cooling, which typically can lead to an increase of around 15% in the minimum fusing current, together with a localised hotspot on the outer surface of the body near the point of contact. A rough correction for the effect of wire expansion can be made by assuming that the wire deflects in the shape of a parabola [5], and if the expansion, which is proportional to the average wire temperature, exceeds a critical value, the wire will touch the inner wall. If the critical average temperature is exceeded it can easily be shown that the fraction of the wire length in contact with the body is given by:

$$f = 1 - \frac{2}{3} \cdot \frac{\tan^2\theta}{\gamma T_{av}} \qquad (3)$$

If the wire was originally centrally located within the fuse, in which case the fraction in contact will be around the centre of the wire. On the other hand, if the element was originally diagonally wired the element will be pressed up against the body at the ends, and the fraction in contact will be given by:

$$f = 1 - \frac{2}{3} \cdot \frac{\tan^2\theta \ \cos\theta}{(1 - \cos\theta + \gamma T_{av})} \qquad (4)$$

The angle θ is a constant for a particular fuse design. Solution of (3) or (4) with f=0 gives the critical average element temperature for touching.

This model can be incorporated in the iterative solution algorithm as follows. After the element temperatures have been initially computed a check is made to see whether the average temperature is greater than the critical value T_c. If so all elements sections are assumed to be touching and the temperature distribution is recomputed. The fraction f is then reduced after each iteration until the average temperature is just sufficient to cause the assumed value of f. The process is then terminated. For any section of the element in contact with the body the heat-loss coefficient is simply increased by a factor K. Experience indicates that a value of 1.33 typically gives the required correction.

Sometimes after the first iteration it may appear that no steady-state solution exists, the cooling being insufficient for the level of test current applied. If this situation occurs it is necessary to continue the iteration assuming the wire is touching the body, since this may have been the reason for the failure to obtain a solution at the first iteration.

Attempts to model this process with more accuracy met with a difficulty. Sometimes during the computation the wire would expand, touch the body, be cooled, then contract away from contact with the body, setting up a stable oscillation. (This may be possibly occur in some fuses).

However the effect of wire touching the body is a second-order effect and the simple model described can give a reasonable correction to the solution which would otherwise be obtained.

FUSES WITH FILLER

If the fuse is filled the heat loss from the element is by conduction through the filler and body and thence by convection and radiation to the ambient. The solution process described in [2] may be used, which includes a correction for axial heat-flow through the filler and body to the endcaps.

The effective wire surface heat-loss coefficient is then given in terms of the radial thermal resistances, as:

$$h = \frac{1}{\pi d\,(g_f + g_b + g_{ext})}$$

where

$$g_f = \frac{1}{2\pi k_f} \ln \frac{D1}{d}\ ;\quad g_b = \frac{1}{2\pi k_b} \ln \frac{D2}{D1}\ ;\quad g_{ext} = \frac{1}{\pi D2\, h_b}$$

The appropriate value of h_b is used after each iteration to find the new body temperature and to correct the value of g_{ext} and then h. Otherwise the model is as described in [2].

SPIRALLY-WOUND ELEMENTS

These are commonly used in miniature fuses to achieve anti-surge performance and can be modelled by a very simple variation to the methods described as for plain wire fuses. If the resistance per unit length of the would element is R' per unit length compared with R for the plain wire then

$$\frac{R'}{R} = \frac{1}{\cos\phi} \qquad (5)$$

where ϕ is the characteristic angle of the helix. If the spiral element is regarded as a composite conductor the internal heat generation per unit length and the stored energy are increased by $(1/\cos\phi)$ times compared with a plain straight wire, while the axial thermal conduction is reduced by a factor coso because of the longer axial heat flow path. Using these factors in Verdet's equation (1) it is apparent that the effect of spiral winding can be represented by:

(i) dividing the element thermal capacity by $(\cos\phi)^2$

(ii) multiplying the element cross-section by $\cos\phi$

With these simple alterations the thermal equations for the spiral element became identical with those for the plain element, and the same solutions subroutines can be used. The only extra requirements are that (a) in calculating the heat-loss coefficient for the composite conductor the effective overall diameter of the wound element needs to be used, rather than the wire diameter, (b) a further component must be added to the heat-loss term to account for heat losses from the element to the core of the helix. These losses are only present for transient conditions and are best modelled by representing the core by a lumped thermal reistance-capacitance model.

TRANSIENT THERMAL CALCULATIONS

In this case no analytical solutions of (1) are possible and so numerical methods must be used. The most successful method has been to represent the element by a series of finite sections as shown in Fig.1 and then to develop for these sections a finite-difference equation equivalent to (1) using the Crank-Nicholson technique applied to every term in (1). This results in a tridiagonal matrix equation

$$[A]\ [T] = [B] \qquad (6)$$

which has to be solved at each time step for the transient temperature of the element sections. Some of the elements of the matrices [A] and [B] have to be adjusted at each time-step to allow for temperature-dependence of heat-loss coefficients.

There is little information on the time-dependence of convective loss coefficients but for fuse simulations there is little error in using the steady-state values throughout. This is because the heat-loss terms make very little difference to the thermal response at high currents, where the element heating may be regarded as adiabatic, or for times of the order of 1 sec, where heat losses by conduction to the ends, which is automatically taken into account, is dominant. The main area of difficulty in modelling is for response times of the order of hundreds to thousands of seconds where accurate representation of the temperature variations are currently not possible.

An important practical consideration in automatic computation of thermal transients is the choice of time-step. This must be small enough to give accuracy but large enough to minimise computing time. The following method has been found to give good all-round performance:

(i) Initially compute the melting time neglecting axial heat conduction and using estimates for the heat loss coefficients based upon some convenient temperature rise, say 100°C. This melting time is obtained by a simple analytical solution of (1) with $\partial^2 T/\partial x^2 = 0$.

(ii) Begin the computation with a time step of 1/20th of the "long-wire" melting time, and if melting has not occured after 20 time steps the time step is increased by 50%. This procedure is repeated every 20 time steps.

In the case of filled fuses the above increase of time step is not possible if the transient conduction loss to the filler is computed as this places a limit on the maximum possible time step. However for the simpler model used here based upon the use of an effective value of h to represent the heat loss from the element, the above algorithm has been found satisfactory.

M-EFFECT

Minature fuses often use wire elements with a blob of low melting-point material to achieve M-effect. The thermal mass of this blob is

large compared with that of the element to which it is attached, so there is an appreciable thermal lag. Heat is conducted from the element to the M-blob, and the rise in temperature of the M-blob may be modelled as a simple thermal lag, i.e.

$$\frac{dT_{ms}}{dt} = \frac{1}{R_{ms}C_{ms}} (T_i - T_{ms}) \qquad (7)$$

where T_i is the temperature of the element section to which the M-blob is attached. If Tm_s exceeds the eutectic temperature of the M-blob/element interface, it is assumed that diffusion begins and using the square-root law the eventual breaking time can be estimated [2].

Fuses which use plated-wire to achieve the M-effect are difficult to represent. The only effective way available at present is to treat the wire as a composite with appropriately weighted values for all the thermophysical properties, and a hypothetical M-spot to represent the diffusion which will take place at the interface of the plating with the substrate material.

ARCING PHENOMENA

For breaking-capacity tests on miniature fuses the element melting times will be roughly in the range 0.1ms to 1ms, which gives current densities at melting of 43-13 kA/mm^2 (inductive circuit) or 25-7 kA/mm^2 (resistive circuit). The physical phenomena which occur in this range of current density have been studied by Vermij [6] and Arai [7]. In this range striated disintegration of the element occurs, there being insufficient time for the formation of unduloids.

In order to model the behaviour it is necessary to calculate the fuse voltage at any instant. This is much more difficult than with power fuses, which usually use notched elements in sand, giving arcs with relatively well-defined geometries. For wire elements a large number of small arcs is initially produced and after a very short time these arcs coalesce to form a single arc. This process of coalescence occurs at a crucial phase in the breaking process and more information is needed for satisfactory modelling. The overall breaking time may be divided into four stages:

(a) prearcing phase

The transient temperature response can be obtained using the methods already given. At each time step the fuse voltage is calculated by adding the voltage drops across all the element sections. The effect of element resistance during the prearcing period can very significantly alter the prospective current wave. The prearcing period ends when the element material reaches its melting-point.

(b) disruption phase

In this phase the wire deforms mechanically and eventually breaks. This phase is terminated when the first arc appears. Arai's experiments showed that the disruption time in air was inversely proportional to the current density i.e. $t_d=Kd/j$ with K_d=0.27 A-s/mm^2. For wires in air the disruption time was longer, and Arai attributed this to the effect of sand grains touching the wire surface and somehow accelerating the disruption process. Vermij also found that disruption times in air were about 50% longer than in sand.

If the disruption process were simply determined by the input energy we might expect t_d to be proportional to $1/j^2$, but if there are mechanical delays in accelerating liquid metal, then for increasing current densities the time required would be longer than that needed simply on the basis of energy input. This implies a dependence of t_d upon j with a power less than 2, as predicted by Arai.

(c) voltage rise phase

This phase has been investigated by Vermij [6] for fuse elements in air and was found to be characterised by a rapid rise in fuse voltage to a value V_0. It is believed that during this phase the voltage builds up in a series of steps as multiple arcs are formed. The peak voltage V_0 at the end of this period can be predicted for wires in sand by the use of Hibner's empirical formula [8]. For wires in air the initial voltage is only about 30% of this value.

The voltage rise time was found to by Vermji to be given by $t_r=K_r/j$ with K_r about 0.2 for wires in air and 0.4 for wires in sand.

These simple rise times can be easily incorporated in computer models see e.g. reference [9], but as the rise times are very short there is little effect upon the results for highly-inductive circuits, in which the circuit current can be taken to constant during the disruption and voltage-rise phases. However many miniature fuse tests are done near to unity power factor, for which a true dynamic representation is needed. In this case the circuit current falls rapidly as the voltage rises thus invalidating Hibner's formula, and (possibly) altering the overall rise time. One method which has been found to give reasonable results is to assume that the fuse resistance builds up during the rise time t_r (rather than the voltage). With this model the 'saturation' effect noted by Baxter [10] can be correctly predicted. (i.e. the fact that the peak voltage reaches a fixed level as the circuit inductance is increased). Nevertheless much more information is needed upon the factors which affect the build-up of fuse resistance, particularly the effect of element material, since miniature fuses use a much wider variety of materials than have been used in the experiments upon which these models have been based.

(d) arcing period

In this period the multiple arcs first coalesce and then a single arc is produced which burns until the current is reduced to zero. For sand-filled fuses an adaptation of the models already used for power fuses can be used, but for wires in air the situation is much more problematical. Some assumptions have to be made about the way in which the initial arc expands to fill the tube. This is another area where much more experimental data is needed. Once the tube is filled we have a wall-stablilised arc with well-defined geometry and which can be modelled much more accurately [9].

CONCLUSIONS

The paper has discussed some of the problems in modelling the behaviour of miniature fuses, and described some solutions which have been found most effective.

General-purpose software for miniature-fuse design has been developed based upon the models described here. In some cases the models used are precise while in others they are based upon 'educated guesswork'. In the latter cases the availability of properly-structured software mean that improvements in modelling can be incorporated as more knowledge is forthcoming as a result of experimental research. It is important to note that assessment of the quality of a certain model is much easier when the software is already available into which the new model may 'plugged' and tested. This leads to the interesting conclusion that the development of software in this area is useful even if all the processes cannot be modelled adequately.

Outstanding areas for miniature-fuse research appear to be: (i) the thermal models for long-duration transients (ii) dynamic investigation of the initial phases of arcing for wires in air, and (iii) further investigation of the melting behaviour of plated wires.

ACKNOWLEDGEMENTS

The author is grateful to Beswick Division of Dubilier PLC for their support of this work, and particularly to R. Brown and T. Dry for help with the experiments.

REFERENCES

[1] Carslaw H.S. and Jaeger J.C.: "Conduction of heat in solids", (2nd edition, Oxford 1959)

[2] Wilkins R.: "Simulation of fuselink temperature-rise tests", Int. Conf. on Electric Fuses and their Applications, NTH, Trondheim, Norway, 13-15 June 1984, pp24-33

[3] Incropera F.P. and De Witt D.P.: "Fundamentals of heat transfer", (Wiley 1981)

[4] Fowler W.H.: Electrical engineers pocket book, (Scientific Publishing Company 1958)

[5] Morley A.: "Strength of materials", (Longmans-Green 1956)

[6] Vermij L.: "Electrical behaviour of fuse elements", Ph.D. thesis, TU Eindhoven, 1969

[7] Arai S.: "Deformation and disruption of silver wires", Int. Conf. on Electric Fuses and their Applications, Liverpool Polytechnic, 7-9 April 1976, pp50-58

[8] Hibner J.: Discussion contribution. 2nd Int. Symp. on Switching Arc Phenomena, TU Lodz, Poland, 1973

[9] Gnanalingam S. and Wilkins R.: "Digital simulation of fuse breaking tests", Proc IEE, vol 127, 1980, pp434-440

[10] Baxter H.W.: "Electric fuses", (E. Arnold 1950)

TIME-CURRENT CHARACTERISTICS OF MINIATURE FUSES

L. Vermij, A.J.M. Mattheij, Littelfuse Tracor B.V., Utrecht, Netherlands

ABSTRACT

Miniature fuses are made in a very large variety of designs and types, and for diversity of applications, resulting in a large number of different requirements with respect to dimensions, electrical characteristics, a.s.o. Several different standards exist for miniature fuses as e.g. IEC and UL standards for fuses for use in electronic and household appliances, ISO for automotive applications a.s.o. This great variety of types and designs as well as the existance of different standards create some specific problems with respect to the design and manufacturing of miniature fuses. On the other hand, a comparison of requirements and standards results in some interesting conclusions, as will be shown in the paper. Special attention will be given on the time-current characteristics of miniature fuses, not only from a viewpoint of standards, but also influencing parameters will be discussed. A method of computing the It-characteristic from the minimum fusing current up till the higher overcurrents will be presented briefly as well as comparison with experimental results.

1. INTRODUCTION

Due to the large number of different requirements with respect to dimensions, electrical characteristics a.s.o., miniature fuses are made in a large variety of designs and types and for a diversity of applications. Several standards exist for miniature fuses, each specifying their own requirements with respect to, amongst others, time-current characteristics. First of all the current IEC-publication 127 [1] should be mentioned. This specifies several kinds of 5 x 20mm and 6.3 x 32mm catridge fuses, whereas the draft IEC-publication 127 part 3 specifies requirements for sub-miniature fuses. UL-document 198G [2] gives also requirements for miniature fuses but they differ remarkably from IEC-requirements. Moreover, for automotive applications USA-standards exist as well as the DIN 72581 and at this moment a draft ISO standard.

This large variety in standards and applications poses an interesting challenge to the fuse designer to meet all these different electrical requirements in fuses with different shaping and dimensions. (see fig. 1) It is of course not pratical to make all these designs for all the current ratings required purely on the basis of experience, trial and error. This paper will show some basic design tools in a simplified way. (in order to keep this paper within reasonable length) Not all characteristics will be discussed, we confine ourselve to the time-current (It)characteristics.

2. A FIGURE OF MERIT FOR THE It-CHARACTERISTIC

Many miniature fuses are of a simple design, allowing for a not too complicated description of the pre-arcing behaviour by means of the well-known energy balance equation [3] :

$$\lambda \cdot \frac{\partial^2 T}{\partial x^2} + J^2 \rho_o (1+\beta T) - GT = c_v \gamma \frac{\partial T}{\partial t} \qquad (2.1)$$

Where :

- λ : heat conductivity of the fuse element material. $[Wm^{-1} K^{-1}]$
- T : temperature of the fuse element [K] T = T(x)
- J : current density $[Am^{-2}]$
- ρ_o: specific resistance at ambient temperature. [Ωm]
- β : temperature coefficient of the specific resistance . $[K^{-1}]$
- G : total heat flux per deg C in radial direction to the surrounding of the conductor. $[Wm^{-3}K^{-1}]$

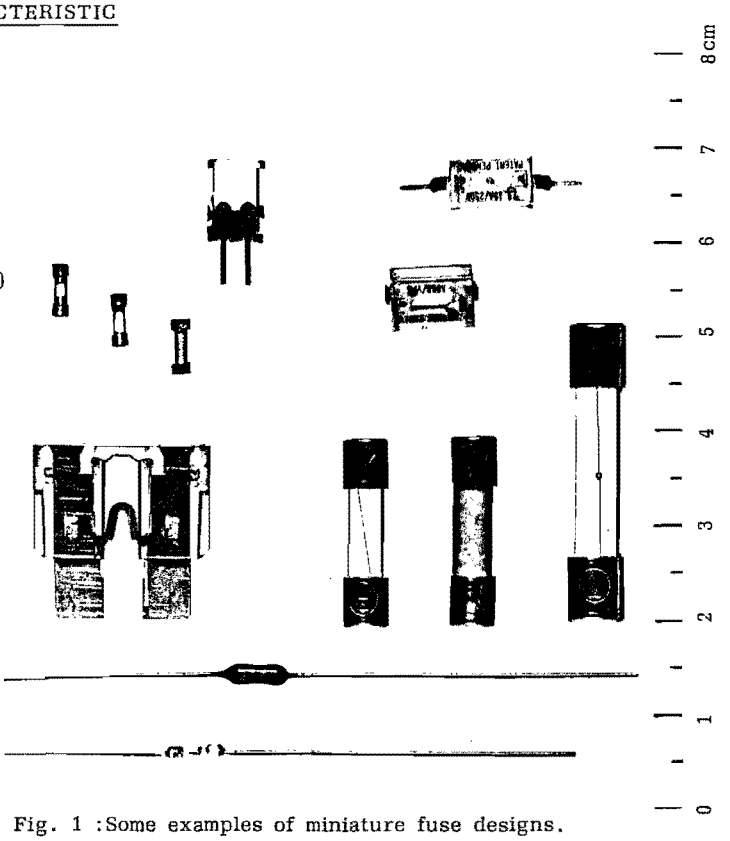

Fig. 1 :Some examples of miniature fuse designs.

c_v : specific heat of the fuse element material. [$Jkg^{-1}K^{-1}$]

λ : specific mass of the fuse element material. [$kg\ m^{-1}$]

t : time

x : coordinate as shown in fig. 2.

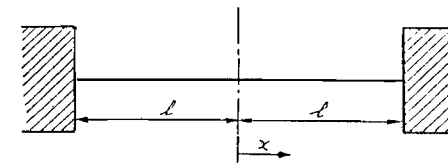

Fig. 2

Equation (2.1) is valid for a stretched and solid fuse element, see fig. 2. Solving this equation will lead to the It-characteristic for this particular case. The heat transfer factor G, which depends mainly on the geometry of the fuse element, its environment and on fuse dimensions, can be determined via experiments. We will return to this later in this text. Although it is in principle possible to compute the It-characteristics, it is not so easy to do this. However, it is less difficult to arrive at some insights with respect to influencing parameters and to define a kind of "Figure of Merit" for the It-characteristic, starting from equation (2.1). For that purpose, we will discuss some special cases.

* For a long wire (that means the temperature in the middle of the wire, thus at x = 0 is not influenced by axial heat transfer) and under steady state conditions, so $\frac{\partial T}{\partial t} = 0$, it follows from e.g. (2.1) :

$$J^2 = \frac{GT}{\rho_o(1 + \beta T_m)} \qquad (2.2a)$$

* Introducing the melting temperature T_m we find a simple expression for the minimum fusing current $I_s = J_s A$, where A is the cross-section of the fuse element :

$$I_s^2 = A^2 \frac{GT_m}{\rho_o(1 + \beta T_m)} \qquad (2.2)$$

* The case of adiabatic heating, thus neglecting heat transfer to the surroundings of the fuse element, leads to the well-known Meyer's equation :

$$M = \int i^2 dt = \frac{A^2 \gamma c_v}{\beta \rho_o} \ln(1 + \beta T_m) \qquad (2.3)$$

This equation is valid for the larger overcurrents.

Equation (2.2) is represented by vertical lines in the It-graph, examples are given in fig. 3 and indicated as I_{s_1} and I_{s_2}.

Under IEC 127 testing conditions, equation (2.3) is represented by straight lines on a log-log-scale, as shown in fig. 3. (lines M_1 and M_2)

The quotient $\frac{M}{I_s^2}$ is a measure how the two lines for I_s and M are situated with respect to each other. The value of G is in a certain fuse design and fuse geometry pratically a constant. So determining the quotient :

$$K = \frac{M \cdot G}{I_s^2} = \frac{\gamma c_v}{\beta T_m}(1 + \beta T_m) \ln(1 + \beta T_m) \qquad (2.4)$$

gives a value K which is independant of the cross-section A and is only determined by physical parameters of the fuse element material. So K can be computed easily.

The parameter K has the character of a Figure of Merit for the It-characteristic: the smaller K is, the more fast-acting the fuse will be.

Table 1 shows the computed values of some fuse element materials. From this table the conclusion can be drawn that Ag gives a more fast-acting fuse than a Ni wire, complying with the experience.

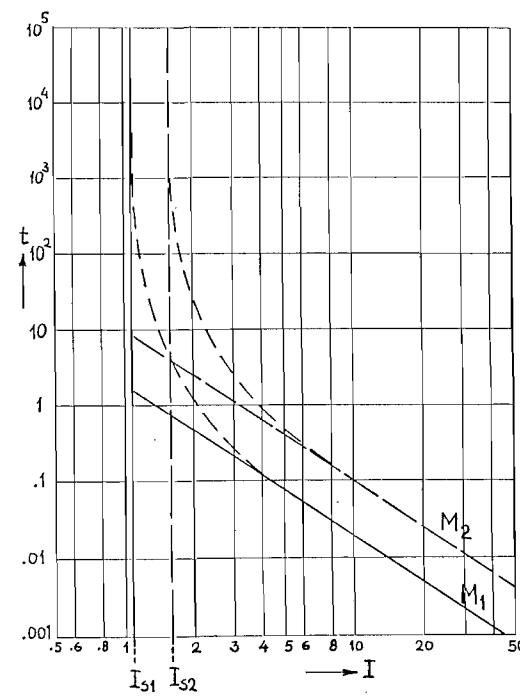

Fig. 3. Asympthotes of the It-characteristic being the minimum fusing current I_s and the line representing Meyer's integral M. The dotted line shows examples of actual It-characteristics with different value of I_s and M (the current I is given in arbitrary values)

Table 1

	T_m (°C)	$\beta(K^{-1})$	$J(kg\ m^{-3})\ 10^3$	$c_v(J\ kg^{-1}K^{-1})10^3$	K
Ag	960	4,3	10,49	0,234	5,0
Zn	420	4,2	7,13	0,35	4,0
Ni	1453	6,8	8,9	0,439	10,3

It should be kept in mind that conclusions like this are only valid for pure, solid, stretched and long metal conductors in a given configuration (G constant), so the effects of plating, M-effect, etc, are not taken into consideration. The K-value, as mentioned above, has only a value for the comparison of the effect on the It-characteristic of different fuse element materials. However, other parameters can be taken into account as well.
As an example, the length of a fuse element may have an influence on the minimum fusing current I_c of a fuse, which can also be computed from equation (2.1) For short fuse elements, the radial heat transfer (the factor G) is negligible, compared with the axial heat transfer via the ends of the fuse element. Then, under steady state conditions it follows from (2.1) :

$$\lambda\frac{d^2T}{dx^2} + J^2\rho_o(1 + \beta T) = 0$$

with the solution for T at x = 0, viz T_o :

$$\cos \ell J \frac{\beta\rho_o}{\lambda} = \frac{1}{1 + \beta T_o} \qquad (2.5)$$

Introducing $T_o = T_m$ and consequently $J = J_S$, we have an expression for the minimum fusing current density J_S as an function of the length $l = \frac{1}{2}L$ of the fuse element and for a given metal conductor.

For a specific case (a non-filled, 5x20mm glass-fuse) the value of G is in the order of $G \approx 10^7\ Wm^{-3}\ K^{-1}$. With this value the minimum fusing current density for a long wire, neglecting the axial heat transfer, (denoted by $J_{S\infty}$) can be computed from equation (2.2A) So, from equations (2.2a) and (2.5), the relation between J_S (for short fuse elements) and $J_{S\infty}$ can be computed. The result of such computations is shown in fig. 4 for the metals Ag, Ni and Zn.

From this graph it can be seen that a silver element of certain cross-section in a 5 x 20mm fuse, having in many cases a fuse element with a length of 17 - 18mm in it (due to solder joints), will result in an increase of the minimum fusing current by 10-20% compared with a fuse with a much longer fuse element in it. This is the case with Ag, but not with Ni and Zn. (Cu behaves pratically in the same way as Ag in this respect) The value of M (eq. 2.3) does, however, not change. So it follows that the Figure of Merit K will decrease by10-20% using silver fuse elements in a 5 x 20mm fuse.

This example shows that the conclusion which could be drawn from table 1, viz, that a Zn-element would give a more fast-acting fuse compared with a Ag-element, may not be justified. Nevertheless, a Figure of Merit $K = MG/I^2_S$ can be defined also in the case of short fuse wires. The graphs of fig. 4 indicate also that a certain spread in the value of K (and consequently in the It-characteristic) may easily occur using high-conductivity metals like Ag and Cu. This is due to variations in the length of the fuse element which may result from small variations in production process parameters. This is the more so when producing in large quantities the smaller-sized fuses like miniature fuses.

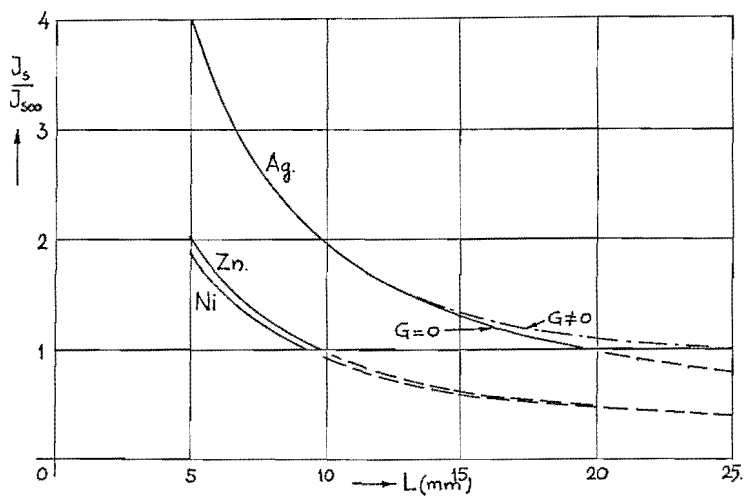

Fig. 4

The minimum fusing current density J_S of short fuse element, related to the minimun fusing current density $J_{S\infty}$ of very long fuse elements, as a function of the total length L of a streched fuse element of constant cross-section.

3. THE DETERMINATION OF THE It-CHARACTERISTIC

In the previous chapter a characterisation of the It-characteristic is presented, based on two parameters:

- the minimum fusing current I_s
- the figure of Merit K

These two parameters determine the two asymptotes of the It-characteristic. This is shown in fig. 3. As a remark, in stead of I_s, also the rated current I_n can be taken as a parameter after introducing the fusing factor $f = I_s / I_n$.

The full computation of the It-characteristic can be done by solving the energy balance equation as given in equation (2.1) for a somewhat simplified situation. The problem in solving this equation is the determination of the value of G in each situation. (fuse design, fuse element shaping, a.s.o.) In principle the value of G can be experimentally determined in the following way :

If a current $I < I_s$ is flowing through a fuse, then under steady state conditions the following must be valid:

$$I^2 r_o (1 + \beta T) = G_t T$$

Where r_o is the fuse resistance at ambient temperature. The temperature T now has the meaning of an average across the fuse-length, whereas $G_t [WK^{-1}]$ is the total heat transfer from the fuse element to its surroundings. Introducing $r_T = r_o(1 + \beta T)$ (the resistance at temperature T at current I), then

$$G_T = \frac{I^2 r_T}{T} = \frac{I u_v}{T} \qquad (3.1)$$

where u_v is the voltage drop at current I, which can be measured easily. For long and short fuse elements a relation can be derived from the energy balance equation (2.1) between J/J_s and T_o/T_m, where T_o is the temperature at x = 0 [3].
This relationship for the metals Ag, Zn and Ni is shown in fig. 5.

The temperature distribution under steady state conditions can also be computed, so the average temperature is also computable. This means that from a simple measurement in principle a value of G can be found, taking into account also dimensional aspects. For these calculations a computer program has been designed.

For the computer calculations use was made of voltage drop measurements as shown in fig. 6.

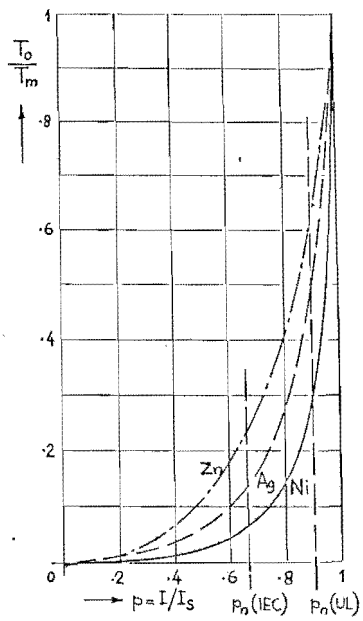

Fig 5 :The temperature T_o at x = 0 related to the melting temperature T_m, as a function of $\rho = I/I_s$ ($I \leq I_s$), for the metals Ag, Ni and Zn for the streched fuse element of constant cross-section.

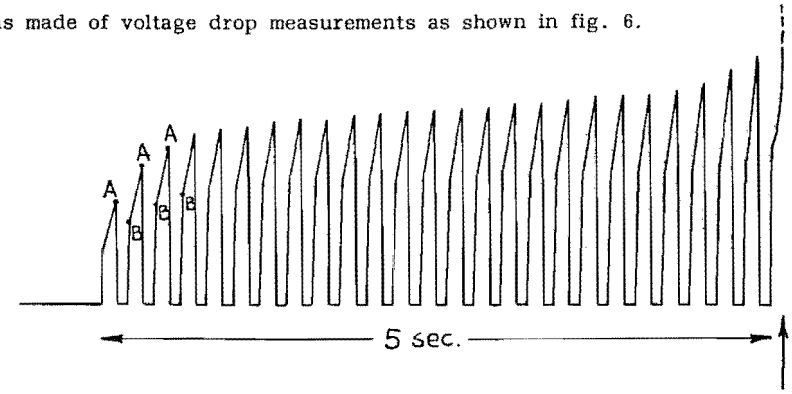

Fig : 6 The voltage across a 5 x 20mm fuse with a rated current of 1 Amp. as a result of a train of rectangular current pulses through the fuse each pulse having a amplitude of 2.5 Amp.

A train of current pulses was passed through the fuse during which the voltage drops A and B during each pulse were measured and fed into the computer. These voltage drop measurements allowed for the calculation of a value G. With this value it is possible to solve equation (3.1) for that particular case.

Fig. 7 shows one of the results, together with a number of measuring points which are obtained by blowing a number of fuses in normal test equipment, following IEC test rules. Voltage drop measurements were also carried out using the test fuse holder as specified in IEC-publication 127.

As will be seen from fig. 7, the measured points fit very well with the computed curve for this particular fuse.

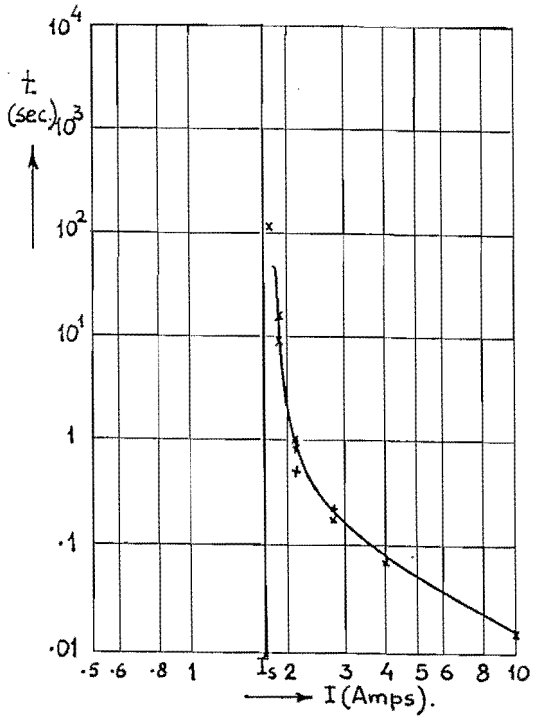

The preliminary indicates only the principles of the computational methods, it is beyond the scope of this paper to describe the computational process in details. It might, however, demonstrate that a full computation of the total It-characteristic is a possibility, serving the following aims :

* It might reduce development work on miniature fuses considerably because computation gives a quick impression of the It-characteristic of a newly developed fuse, using only a few samples.

* It opens the possibility to study the character of the parameter G as a function of element geometry, dimensioning of the body and other parameters. After gaining such a quantitive knowledge of G, it is even possible to compute the It-characteristic of new designs without having samples available.

We like to point out that the above mentioned gives only a simplified treatment which is to a certain extend only valid for the most simple fuse designs. However, the authors are convinced that the achievements gained so far contributes to a fuse designing process for miniature fuses with better possibilities for optimisation and a better understanding of the influencing parameters on fuse characteristics, departing further from trial and error methods.

Fig. 7 : Calculated It-characteristic of a fast-acting, 1 Amp., 5 x 20mm fuse. The crosses indicate measured values. The line indicating the minimum fusing current I_s is the computed value.

ACKNOWLEDGEMENT

The authors like to express their sincere thanks to Mr. J. Jaspers, who has given a very important contribution to the development of the computer model and who has carried out much of the computations. He has done this work in partial fulfilment of requirements for his MSc-degree at the University of Technology in Eindhoven, the Netherlands.

LITTERATURE

[1] IEC-publication 127B, (1985)
"Catridge fuse-links of miniature fuses"

[2] UL 198G, (1985)
"Fuses for supplementary overcurrent protection"

[3] L. Vermij, H.C.W. Grundlach
"Current-limiting capability and energy dissipation of high-voltage fuses"
International Conference on Electric fuses and their applications, April 1976, Liverpool

SURGE PERFORMANCE OF MINIATURE FUSES
A Study of the Influencing Factors

R. Brown, B.Eng., M.Phil.
Dubilier-Beswick, Frome, Somerset, England, BA11 1PP.

ABSTRACT

This paper identifies the parameters which have an influence on the surge performance of miniature fuses, so that fuses with superior time-lag properties to those presently available can be developed. A measure of surge performance is described called the thermal time constant of the fuse, τ, with the dimension of time. After developing an equation for τ, it is shown how each term of the equation may be maximised theoretically and practically to give high surge performance. An indirect method of measuring τ is explained and the correlation between measured and calculated values for two types of fuses given.

LIST OF SYMBOLS

α = Temperature coeff. of resistivity, k^{-1}
c = Specific heat capacity, $J\,kg^{-1}k^{-1}$
d = Diameter, m
d.f. = Delay factor
h = Radial heat loss coefficient, $W\,m^{-2}k^{-1}$
I = Current, A
I_a = Adiabatic melting current, A
I_m = Minimum fusing current, A
K = Thermal conductivity, $W\,m^{-1}k^{-1}$
m = Density, $kg\,m^{-3}$
P = Perimeter, m
ρ_o = Specific resistivity, Ω m
S = Cross-sectional area, m^2
t = Time, s
t_a = Adiabatic melting time, s
τ = Thermal time constant, s
T = Temperature, k
T_M = Adiabatic melting point, k
T_m = Steady-state melting point, k
x = Axial displacement, m

1. INTRODUCTION

Throughout the history of the miniature fuse the performance demanded from its diminutive package has always been increasing. The fuse designer has had to meet this demand by careful engineering and not a little ingenuity as energy sensitive semiconductors and circuits with high inrush currents have proliferated, all requiring reliable and cheap protection. This is unlikely to alter in the future as the telecommunications industry joins the foray with requirements, at the subscriber line interfaces of its exchanges, for miniature fuses which blow at continuous overload currents of as little as 200mA and yet can carry 60A for 1ms.

It is the behaviour of a miniature fuse when subjected to these high overload, short duration surges which is of great importance when choosing overcurrent protection for a given application. In fact, fuses are broadly classified according to their response to such stimuli, for example quick-acting, time-lag etc.[1]. This paper is concerned with the factors which influence this particular fuse characteristic. These may be divided into three types:-

(1) the thermophysical properties of the fuse element material,
(2) geometrical factors and
(3) techniques which alter the fuse element's inherent properties e.g. Metcalf-effect.

By studying the fundamental equation which governs the heating of a fuse wire it is possible to determine, in detail, how each of these may be optimised to give a fuse with a required surge performance.

The emphasis will be on those aspects of the fuse which give it the ability to withstand such surges i.e. its time-lag properties. This is because a simple straight fuse wire is inherently quick-acting and so a large amount of design effort is expended on developing time-lag types. Figure 1 shows typical operating curves for time-lag and quick-acting miniature fuses. The time-lag fuse takes longer to operate at high overload currents.

In order to optimise the time-lag properties of a miniature fuse it is first necessary to develop some measure of this particular attribute. One way of doing this is to define a 'delay factor', d.f. as the ratio between a high overload current and the minimum fusing current:-

$$d.f. = I_a / I_m \qquad (1)$$

The problem with equation 1 is that the adiabatic melting current, I_a must be associated with a certain adiabatic blowing time e.g. 1ms or 10ms. This means that a single fuse can have a multitude of delay factors dependent on the blowing time chosen for fixing I_a.

Alternatively, it is possible to obtain a 'thermal time constant', τ, for the fuse which has a direct relationship to d.f. but is independent of the adiabatic blowing time and so has a unique value for a particular type and rating of fuse.[2] This is the approach which will be taken here.

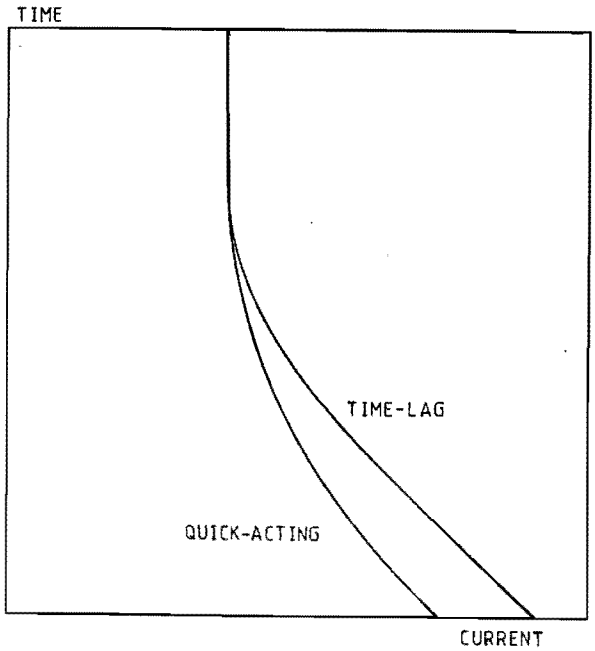

Figure 1

Typical time/current curves

2. THE THERMAL TIME CONSTANT

The operation of a fuse is governed by the delicate balance between Joule heating of the element and heat loss to the environment by the mechanisms of conduction, convection and radiation. This may be represented by an energy-balance equation, first developed by Verdet in 1872:-

$$mcS.\frac{\partial T}{\partial t} = \frac{I^2\rho_o(1+\alpha T)}{S} + KS.\frac{\partial^2 T}{\partial x^2} - PhT \qquad (2)$$

In this equation, the term on the left is the rate of increase of internal energy, the first term on the right is the Joule heating, the second is the axial conduction loss and the third is the radial loss which is due to convection and radiation combined. This last term is represented as a simple function of the wire perimeter and its temperature although in reality it has a complicated dependence due to the 3-dimensional convective fields existing within the fuse body. However, empirical results have shown that this simplification is reasonable when applying the equation to miniature fuses.[3] All the quantities in (2) are calculated per unit length of the element.

2.1 Adiabatic Condition.
When a fuse is subjected to very high overload currents it heats and melts before any appreciable heat loss can occur. The process is thus adiabatic and (2) can be simplified as follows:-

$$\frac{dT}{dt} = \frac{I^2\rho_o(1+\alpha T)}{mcS^2} \qquad (3)$$

By separation of variables and then integrating we obtain:-

$$I_a^2 t_a = \frac{mcS^2}{\rho_o\alpha}.\ln(1+\alpha T_M) \qquad (4)$$

which shows that for high currents the pre-arcing I^2t is constant, as we would expect.

2.2 Steady-state Condition.
If a current is applied to the fuse which is just less than I_m the element temperature will increase until heat loss exactly balances the heat input. In this instance equation (2) reduces to:-

$$\frac{I^2\rho_o(1+\alpha T)}{S} + KS.\frac{d^2T}{dx^2} = PhT \qquad (5)$$

since dT/dt=0. This is difficult to evaluate for I but can be made considerably easier if axial heat loss is small compared to the radial loss. This is reasonable when considering wires which have a large length/perimeter ratio as is usually the case with miniature fuses. In this instance (5) becomes:-

$$\frac{I^2\rho_o(1+\alpha T)}{S} = PhT \qquad (6)$$

Putting $T=T_m$ we can equate $I=I_m$ giving:-

$$I_m^2 = \frac{PhT_mS}{\rho_o(1+\alpha T_m)} \qquad (7)$$

2.3 Equation for τ
Having formulated equations involving I_a and I_m it is now possible to define τ. Dividing (4) by (7):-

$$\frac{I_a^2 t}{I_m^2} = \frac{mcS.[(1+\alpha T_M).\ln(1+\alpha T_m)]}{Ph\alpha T_m} = \tau \qquad (8)$$

The factor τ has the dimension of time and can be thought of as the thermal time constant of the fuse. It can be seen to be directly related to d.f. as follows:-

$$\tau = (d.f.)^2.t_a \qquad (9)$$

where t_a is the adiabatic blowing time. We can now separate (8) into a number of factors which can be studied individually to see how τ can be maximised:-

$$\tau = \left[\frac{(1+\alpha T_m).\ln(1+\alpha T_M)}{\alpha T_m}\right] \times \frac{1}{h} \times \frac{S}{P} \times mc \qquad (10)$$

2.4 Maximising τ
Taking the square bracket first, this may be considered as the 'trigger effect' bracket since it shows how τ is affected by using a mechanism which triggers the element to melt at a lower temperature under steady-state conditions than under adiabatic conditions. This is essentially the process behind M-effect and spring type anti-surge fuses. Figure 2 shows how the value of this bracket varies with T_m and T_M (keeping α constant). It can be seen that it is slightly advantageous to use a high melting point material if no trigger effect is employed, but the real gains are obtained when a large separation between T_m and T_M can be achieved.

The first of the geometrical factors is the term 1/h, the radial heat loss term, and is obviously maximised when the surface heat loss coefficient, h is a minimum. In practical terms this means that the element should be thermally insulated.

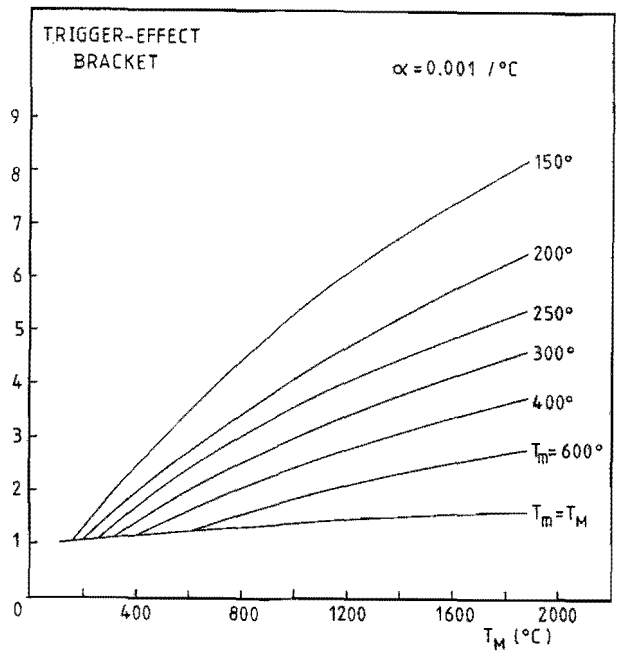

Figure 2
Value of trigger effect bracket

The second geometrical term is S/P, the ratio of cross-sectional area to perimeter. This is a maximum when the element is a solid, circular wire and in this case has the value d/4. Therefore, it should be of the largest possible diameter, which is why, for a given element material, surge withstand performance increases with I_n (the rated current). The corollary of this idea is that, for a given I_n, the resistivity of the element material should be maximised. This is to be achieved within the constraints of the internal dimensions of the fuse body and the breaking capacity required.

The final term (mc) is the product of the density and specific heat capacity of the element material, sometimes called the thermal mass. For a given volume, substances with a high thermal mass require a large amount of heat energy to raise their temperature appreciably. This term should be maximised.

3. PRACTICAL METHODS OF INCREASING τ

Now we know how τ, and hence surge performance is affected by each of terms in equation (10) it should be possible to determine practical ways of incorporating those features which increase τ in the design of a time-lag fuse.

The most obvious practical example of increasing the value of the trigger effect bracket is by using an M-effect blob on the fuse wire. With a tin/lead solder blob on a silver wire the value of the bracket increases from 1.99 to 3.73 (making T_m equal the eutectic temperature of 60/40 tin/lead solder). Alternatively, the wire may be tin-plated causing the M-effect to take place along the entire length of the element.

Another way the value of this term is increased is by using a copper or copper-containing wire. At low overloads, the elevated temperature causes the copper to slowly oxidise, increasing the element resistance and effectively causing it to blow at a much reduced temperature.

A more versatile way of implementing the trigger effect would be to employ a pyrotechnic compound in place of the solder. With a well defined ignition temperature and sufficient heat output, such a compound could be used in conjunction with <u>any</u> metal, causing it to melt at a temperature well below T_M.

The thermal insulation of the fuse element is difficult to improve unless evacuating the fuse body is considered, since air itself is such a good insulator. Experiments have shown that introducing ordinary thermal insulators into the fuse body, such as fibre glass, has the effect of increasing the heat loss from the element because the internal dimensions are so small. However, there is thermal insulation available which can be used to some advantage and this is based on the microporous principle where the material consists of small cells with a diameter less than the mean free path of an air molecule. Using this technique it has been possible to increase τ by approximately 1.5 times.

The S/d term can be increased by using a high resistivity material, thereby increasing the element diameter. An indirect method of doing this is presently used in the helical type fuse where a wire is wound on an insulating core. This effectively increases the resistivity provided the turns do not touch. Obviously, the core diameter should be as small as possible in relation to the outside diameter of the helix so that S/d is maximised.

Data relating to the thermal mass of various metals is shown in figure 3. It shows that the traditional fuse element material, silver has a fairly low value of 2.47×10^6 J kg^{-1} K^{-1} while some of the high resistivity alloys are around 4×10^6 J kg^{-1} K^{-1}. Bearing in mind the comments concerning resistivity in the previous paragraph, for time-lag applications it would appear that such alloys are ideal.

The emphasis in this section has been on metallic fuse elements but the theory does not exclude non-metals which make available a much wider range of thermophysical properties, provided that they can be realised in a form suitable for inclusion in a miniature fuse.[2,4]

4. THEORETICAL AND EXPERIMENTAL VALUES FOR τ

It is possible to show that τ is the time taken for the centre of the fuse element, when carrying I_m, to reach 63% of T_m.[2] So, to evaluate τ directly is almost impossible because of the difficulty in measuring the element temperature inside the fuse body. However, it is possible to obtain a value for τ <u>indirectly</u> from I^2t data as follows. Using equation (9):-

$$\tau = (d.f.)^2 . t_a$$

$$\tau = (I_a/I_m)^2 . t_a \qquad (11)$$

METAL	mc x 10^6 ($Jm^{-3}k^{-1}$)
NICKEL	4.09
STAINLESS STEEL	4.04
INVAR	4.02
WROUGHT IRON	3.77
COBALT	3.74
CONSTANTAN	3.73
PURE IRON	3.59
NICKEL SILVER	3.48
COPPER	3.44
MANGANIN	3.40
MILD STEEL	3.30
BRONZE	3.17
BRASS	3.15
PLATINUM	2.92
ZINC	2.75
GOLD	2.55
SILVER	2.47
ALUMINIUM	2.47
TITANIUM	2.37
TIN	1.65
SOFT SOLDER	1.58
LEAD	1.43
ANTIMONY	1.37
BISMUTH	1.23
SODIUM	1.20
MAGNESIUM	0.43

Figure 3

Thermal mass of various metals

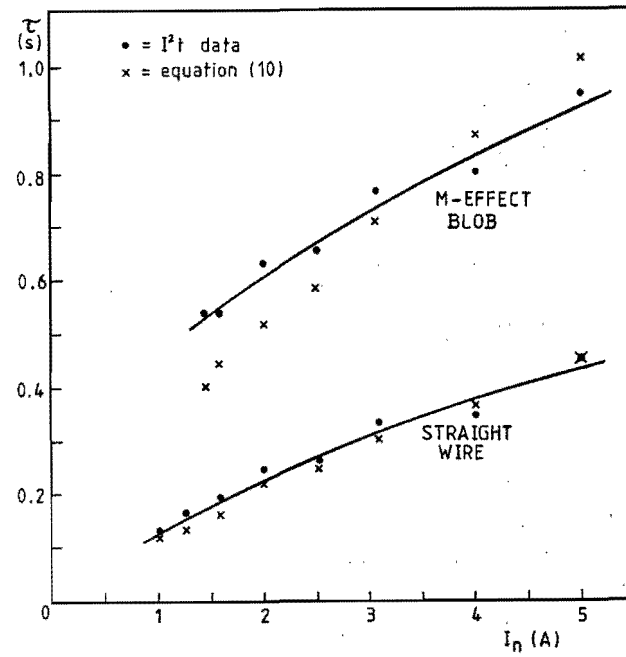

Figure 4

Values of τ for two types of fuses

Since I^2t is constant for high overloads we can chose t_a and therefore find I_a. Estimating I_m from known non-blowing and blowing conditions, τ can be found from (11). Figure 4 shows the results obtained in this way for two types of 20mm x 5mm glass bodied fuses, one a straight silver wire and the other a silver wire with an M-effect solder blob. It can be seen that the M-effect fuse has a considerably higher value of τ than the simple straight wire type. This is confirmed by the former being classed as time-lag according to IEC 127:1974, while the latter is quick-acting.

Also plotted in the figure are values of τ obtained by evaluating equation (10), substituting the appropriate values for each term (see appendix 1). These are in fairly close agreement, particularly for the quick-acting type.

5. CONCLUSIONS

The paper has indicated how the surge performance of miniature fuses can be improved by designing the fuse to include certain key features. It has shown how a measure of the surge withstand capability can be obtained by defining a thermal time constant, τ which has the dimension of time only. The influences on τ of varying the adiabatic and steady-state melting temperatures, the radial heat loss, the ratio of cross-sectional area to perimeter and the thermal mass of the element have been investigated and practical realisations have been suggested of how each may be maximised. Some of these techniques are being used at present in the development of new types of miniature fuses.

To summarise, for good time-lag properties the fuse element should be of circular section and be solid. It should have a high thermal mass and high resistivity and be thermally insulated from the environment. If a trigger effect can be employed, then the largest possible separation between T_M and T_m should be aimed for. Generally, a high melting point material is preferred.

There are obviously other constraints which must be considered such as power dissipation, volt drop, constructional difficulties etc. which will not allow all these to be fully exploited, but it does indicate the areas which should be given careful consideration when designing time-lag fuses.

APPENDIX 1.

I_n (A)	I^2t (A^2s)	I_a (A)	I_m (A)	τ (s)
Quick-acting				
1.0	0.47	21.7	1.90	0.13
1.25	0.94	30.7	2.38	0.17
1.6	1.79	42.3	3.04	0.19
2.0	3.50	59.2	3.80	0.24
2.5	5.82	76.3	4.75	0.26
3.15	11.9	109	5.99	0.33
4.0	20	141	7.60	0.34
5.0	41	202	9.50	0.45
6.3	75	274	12.0	0.52
Time-lag				
1.4	3.80	61.6	2.66	0.54
1.6	5.00	70.7	3.04	0.54
2.0	9.10	95.4	3.80	0.63
2.5	15.0	122	4.75	0.66
3.15	27.8	166	5.99	0.77
4.0	46.2	215	7.60	0.80
5.0	85.0	292	9.50	0.94
6.3	137	370	12.0	0.95

From I^2t Data

NOTES: 1) t_a = 0.001s
2) I_m based on $1.9I_n$

I_n (A)	d (mm)	1/h (mkW^{-1})	d/4 (m)	τ (s)
Quick-acting				
1.0	0.059	1.61×10^{-3}	1.48×10^{-3}	0.12
1.25	0.066	1.66	1.65	0.13
1.6	0.076	1.72	1.90	0.16
2.0	0.097	1.82	2.43	0.22
2.5	0.107	1.87	2.68	0.25
3.15	0.127	1.95	3.18	0.30
4.0	0.145	2.02	3.63	0.36
5.0	0.173	2.11	4.33	0.45
6.3	0.198	2.18	4.95	0.53
Time-lag				
1.4	0.095	1.81×10^{-3}	2.38×10^{-3}	0.40
1.6	0.103	1.85	2.58	0.44
2.0	0.118	1.92	2.95	0.52
2.5	0.129	1.96	3.23	0.58
3.15	0.152	2.04	3.80	0.71
4.0	0.178	2.12	4.45	0.87
5.0	0.200	2.19	5.00	1.01
6.3	0.229	2.26	5.73	1.19

From equation (10)

NOTES:
1) mc = 2.47×10^{6} $Jm^{-3}k^{-1}$ (silver element)
2) Time-lag fuse had a 60/40 Sn/Pb blob
3) Trigger effect bracket
= 1.99 for quick-acting fuse
= 3.72 for time-lag fuse
4) h calculated using $h = 54.4/d^{0.28}$ (ref. 3)

REFERENCES

1. International Electrotechnical Commission
Publication 127:1974 "Cartridge Fuse Links for Miniature Fuses"
2. Cook,R.J.
"Very Long Delay-Factor Fuses using Non-Metallic Elements."
Internal report, Dubilier-Beswick, June 1986.
3. Wilkins,R.
"Time-Current Characteristics of Miniature Fuses - a study of modelling methods."
Internal report, Dubilier-Beswick, undated.
4. Brown,R.
"A Study of Non-Metallic Conductors in relation to Miniature Fuses."
M. Phil. Thesis, Liverpool Polytechnic, July 1985.

THE CONTROL OF VOLTAGE-DROP IN MINIATURE FUSES

J.D. Flindall

Dubilier plc, Beswick Division

ABSTRACT

Voltage-drop is an aspect of performance uniquely significant in miniature fuse design and specification. This paper endeavours to explain the reasons for this importance, and to describe the treatment of voltage-drop and the associated power dissipation in miniature fuse Standards. Techniques for satisfactory design are discussed.

INTRODUCTION

In larger fuses, the voltage-drop is usually only regarded as important in that it is an indication of power dissipation, and therefore of circuit loss, and of excess heat generation.

While these factors are also important in a miniature fuse, voltage-drop is of fundamental concern for other reasons.

When the voltage-drop at the minimum fusing current approaches the system voltage, there is danger that the fuse will fail to operate correctly. This is particularly important where circuits operate on a supply of 5V or less, and where normal currents may be of tens of milliamps.

Balanced telecommunications line applications require not only that fuse impedance be limited, but also that for a given type and rating the range of voltage-drop values be closely controlled.

International Standards have for many years recognised voltage-drop as an important factor in specification. More recently it has become of prime importance in the requirements of quality control as an indicator of possible degradation of the fuse. Specifications for power dissipation and acceptance have had to be introduced to enable safe co-ordination of fuse-link and fuse-holder.

Much can be done in design and material selection to influence voltage-drop. However, there have inevitably to be compromises in other areas of fuse performance.

USER REQUIREMENTS

Minimum Operating Voltage V_o

It is obvious that if the voltage applied to a fuse under fault conditions (nearly always the system voltage) is less than the maximum value of voltage-drop attained before operation at the fault current applied, then there is a danger of the fuse failing to operate, or operating in a much longer time than is usual. This is a danger unique to miniature fuses, which are frequently used in systems operating well below V_n.

Unfortunately, the only specification point given in International Standards or in manufacturers' literature is a maximum of voltage-drop at rated current. It has for many years been a 'rule-of-thumb' that a fuse should not be used where the system voltage is less than twice the maximum expected voltage-drop. If this (somewhat unreliable) rule is followed, then Fig. 1 shows the relationship between I_n and the minimum operating voltage for fuses with values of voltage-drop corresponding to the maxima allowed by IEC 127 : 1974, and also for representative realistic fuse types.

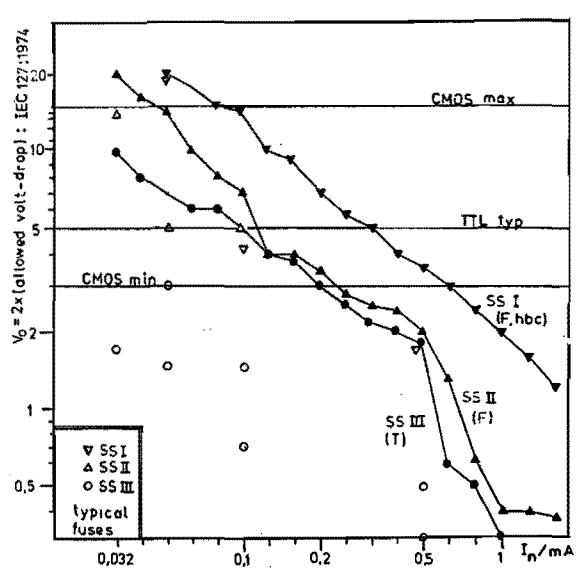

Fig. 1 I_n : Minimum operating voltage at twice IEC127 voltage-drop limits.

It can be seen that the problem is at its worst at very low values of I_n. It is unfortunate that, with the emphasis on low power consumption in all types of equipment, this is an area of immediate importance.

For reference, minimum and maximum power supply voltage values and indications of typical circuit currents for a number of recognised electronic circuit configurations are given in Fig. 2.

Industrial Standards	
9V	battery operated consumer equipment
12V	military. typical RS232
15V	industrial analogue equipment
24V	DIN industrial standard
Semiconductor Families	
≈1.2V	I^2L devices
2-6V	74HC logic
3-15V	4000 series CMOS
5V	nominal TTL and LSI supply
12.5V 21V 25V	EPROM programming.

Fig. 2 Typical power supply specifications.

Power Dissipation P_d

The importance of correct design of terminations to enable adequate and controlled dissipation of generated heat has long been recognised in power fuses (Wright and Newbery[1] state that up to 75% of the heat generated by a fuse-link is dissipated through the end connections, and Wilkins et al[2] point out the importance of the heat-generating contribution of fuse endcaps and connecting cables in modelling fuse performance). I^2R heat and its dissipation are of equal importance in miniature fuse design, for two reasons:

1) As Fig. 3 shows, for fuselinks of relatively high rated current, the design of termination systems has a significant effect on the low-overload performance and volt-drop. The comparison here is between fuse-links mounted in a) the test-fixture specified in IEC 127, and b) a commercial chassis-mounting fuse-clip.

Fuse-link type: 20x5mm to UL198G	
Rated current: 5A	
Conditions: 1.35 I_n operation	
a) Using IEC 127 test-clip:	
Operating time =	mean: 13.8s
	σ : 2.1s
b) Using commercial fuse-clip (as used in testing by UL)	
Operating time =	mean: 9.2s
	σ : 0.9s

2) If a fuse-link is mounted in a fuse-holder of inadequate design, possibly with poor electrical and mechanical connections to the system, then it is all too possible for the total heat generated by the fuse and its connections even at rated current to cause damage to the fuse-link, the fuse-holder and the terminations. Typically, if the fuse-link to fuse-holder terminal contact is maintained by a compression spring, this may anneal and thus cause a decrease in contact pressure. The contacts and terminations inside and outside the fuse- holder may become oxidised, and the fuse-link itself, after a prolonged period of operation at, effectively, an abnormally high ambient temperature, may suffer deterioration causing a high inherent resistance, and possibly a potential failure to operate normally. The result is a thermal runaway situation, and unless the fuse eventually operates, the outcome will be a fire in combustible parts of the fuse-holder or its connections. The author knows of such a case systematically occurring in consumer equipment, which in the short term caused a number of fires in public buildings, and in the long term a large claim for damages and compensation!

Matching and tolerance of voltage-drop values.

In telecoms line applications, fuses are often required to be placed between outside line equipment and sensitive amplifying and switching circuits inside the telephone exchange. Here, in conjunction with parallel-connected over-voltage protectors they protect the exchange circuits against the effects of accidental mains connection to the telephone lines.

In this position, the fuse necessarily forms a part of the termination network of the balanced line. Therefore its impedance must be closely controlled. In circuits in current use, only the resistive component of the impedance is significant; in future systems, the inductance may also be important.

A typical interface circuit is shown in Fig. 4., and a typical specification for a matched pair of line fuses in Fig. 5. In this particular case the fuse is also required to have a nominal resistance of 1.15Ω; this is rather higher than the minimum achievable value for the fuse characteristic. The requirement that, in order to maintain line balance, the resistance of the two fuse elements must be matched to ±7.5%, after one of the elements has been subjected to 10 x 1.5kV pulses of 10/700μs waveform, is very difficult to meet on a mass-production device.

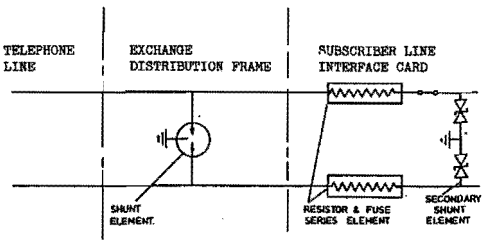

Fig 4. Typical telecoms line protection circuit.

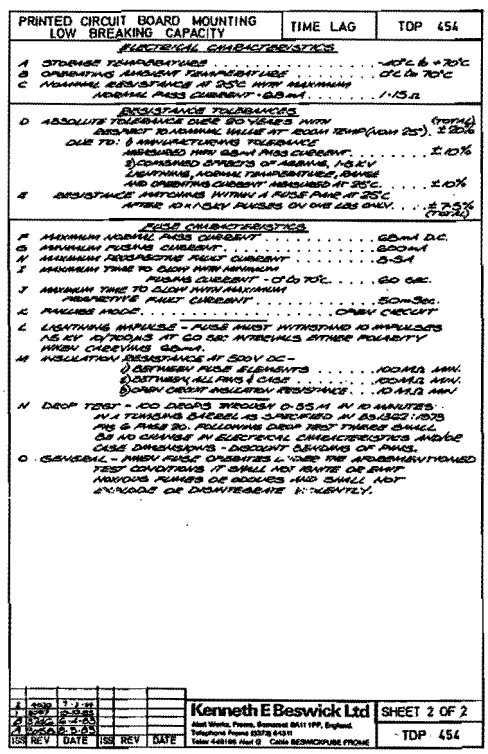

Fig. 5. Specification for telecoms line fuses: balanced pair.

INTERNATIONAL STANDARDS REQUIREMENTS

1. IEC Standards have until recently not specified (or even defined) power dissipation for fuse-links. Since 1980, IEC 257[4] has required manufacturers to provide in their catalogues the accepted power (P_a) of their fuse-holders; this figure is verified by a temperature rise test using a 5Ω power resistor in place of the fuse-link, at a current of, typically, 900mA. In fact, the requirement to publish P_a has been rarely been obeyed.

Furthermore there has been no definition or test for the power dissipation of fuse-links in IEC 127[5]; nor has a temperature-rise test been specified. The only relevant parameter specified has been the maximum allowed voltage-drop.

More recently, the Working Groups of IEC Technical Sub-committee SC 32C have prepared specifications for the power acceptance of fuse-holders and for the maximum sustained dissipation of fuse-links (tabulated against I_n), together with test requirements. These parameters are both arranged in preferred values of 1.6, 2.5 and 4 watts to enable users easily to specify safe combinations of fuse-links and -holders. These requirements will be incorporated in the forthcoming complete revision of IEC 127, which will become a multi-part document covering a comprehensive range of miniature fuse-links types.

Also included will be a warning note on the subject of minimum operating voltage: this is to be published first as an Amendment to the existing document. It will probably be necessary to include tabulated limits of minimum operating voltage for some sub-miniature fuses in the new Standard.

2. The UL Standard on miniature fuses, UL198G[6], contains no requirements on voltage-drop. There is, however, a limit of temperature rise, tested at 1.1 I_n (or for some types 1 I_n).

UL[3] require a fuse-holder to be tested for temperature-rise at its rated current (ie the maximum rated current of a fuse-link with which it is intended to be used), using a copper slug of negligible resistance in place of the fuse-link; this test can only determine the current-carrying capacity of the fuse-holder and fuse-link contact system, and not the susceptibility of the fuse-holder to heat input from the fuse-link.

IEC[4], on the other hand, have since 1980 required equivalent tests to be carried out using a power resistor of similar dissipation to a typical fuse-link, but at a small fraction of the rated current, thus testing the heat withstand of the fuse-holder but not the current-carrying capacity of the contacts. This clearly gives rise to a potential situation of dangerous misapplication; this is one of the areas of conflict between the two standards systems which the IEC Committees have been trying for many years to resolve (but so far, without success).

MATERIALS AND DESIGN

Choice of materials

In many cases element materials of the lowest possible resistivity may be used (i.e. silver or copper), and in the shortest practicable length (i.e., essentially the length between the terminations. Two constraints may cause the designer to choose another material:

1. The practical requirements of handling make it impossible to use these materials in sizes smaller than, e.g. 40 micron diameter unless physically supported. Such materials as nichrome can be handled unsupported down to about 6 micron; by special techniques, for example platinum is used in sub-micron sizes.

2. Long experience, and recent analytical work, show that the time-delay characteristic of a simple fuse element is strongly dependent upon its length and the resistivity of its material. Increasing the length of a miniature fuse element by forming the conductor as a helix is common practice, as is the use of metals or alloys of relatively high resistance such as silver/copper, brass, zinc or tin/zinc. Unfortunately such designs tend to increase the voltage-drop and dissipation of the fuse. Also, when a filler is used to increase breaking capacity it may be necessary to use another material to compensate for the change in characteristic caused by the cooling effect of the filler.

Design considerations

The following are among the techniques in design which have yielded improvements in voltage-drop:

1. Reducing element length.

This also gives a faster-operating fuse, which may be undesirable, and will adversely affect breaking-capacity. It has been achieved by, for example:

-Using a helical element[7], which is then dipped in solder to leave a short, central, operating area.

-Using a fine wire element supported on a paper former, which is then coated with conducting material[8], leaving a central operating section.

-Using a design of fuse for printed wiring board mounting, with parallel connecting pins. The element length is defined by the pitch of these pins, and provided the spacing is sufficient for the working voltage when the p.w.b. is assembled, the user can choose a fuse with the combined benefits of minimum size and minimum voltage-drop.

-Using a compound element of the spring and blob type. To achieve a reduction in voltage-drop it is necessary to shunt the spring with a flexible conductor: this may not be possible at low values of I_n where the heat generated in the spring is important to ensure operation at low overloads.

2. Use of 'Metcalfe Effect'.

This is usually considered as a technique for lowering the minimum fusing current, and thereby giving a time-delay characteristic. However, it has also been used as an expedient allowing a significant increase in element wire diameter, and thereby reducing voltage-drop and dissipation. In one particular case it was found possible to meet a UL temperature-rise specification for a non-time-delay fuse only by this method; rather than the 'M-blob", a continuous tin coating was used, giving a further slight reduction in voltage-drop.

3. Use of insulating filler.

In a paper presented at this Conference, R. Brown[9] describes the use of microporous insulation to decrease the radial heat loss from the fuse element, decreasing the minimum fusing current and thereby increasing the delay of the fuse. This also has the advantage of enabling a larger element cross-section to be used for a given rated current, thus reducing the voltage-drop and dissipation.

CONCLUSIONS

Although voltage-drop, matching and dissipation have always been important parameters in specifications agreed between suppliers and users of miniature fuses, it is only recently that this importance has been reflected in the drafting and co-ordination of International Standards.

There are useful techniques available for the minimisation or control of voltage-drop, although these invariably have effects on other aspects of performance. There remains much to be done in exploring the limits of performance of miniature fuses, and voltage-drop will be an important prime parameter in this development.

REFERENCES

1. A. Wright and P.G. Newbery. "Electric Fuses". Peter Peregrinus Ltd. / IEE, 1982.

2. Wilkins R., Wade S. and Floyd J.S. "A suite of interactive programs for fuse design and development". I.C.E.F.A., Trondheim, 1984.

3. UL 512 "Standard for fuseholders" Seventh Edition, 1975, and Amendments

4. IEC 257: 1968. "Fuse-holders for miniature fuse-links". Also Amendment No. 1 (December 1980)

5. IEC 127: 1974. "Cartridge fuse-links for miniature fuses", and Amendments.

6. UL 198G "Fuses for supplementary overcurrent protection", and Amendments.

7. U.K. Patent No. 1 545 205, filed 1975: "Improvements relating to electric fuse-links", D.G.E. Beswick and S. Wright.

8. U.K. Patent No. 2 068 657, filed 1980: "Method of manufacturing electrical cartridge fuselinks", K.W. Woznica.

9. R. Brown. "Surge performance of miniature fuses". I.C.E.F.A., Eindhoven, 1987.

Session VIII

APPLICATION ASPECTS

Chairman: Mr. B. Noordhuis

3-PHASE OPERATION OF CURRENT-LIMITING POWER FUSES

R. Wilkins, Consultant, 18 Speedwell Drive, Heswall, Wirral, U.K.

Abstract

The breaking capacity of power fuses is usually verifed in single-phase tests but in service fuses are very often used in three-phase power systems. In the paper the relative severity of fuse testing is discussed, using computations based upon a relatively simple fuse model. The sequence of fuse operation in 3-phase systems is illustrated and the worst cases are highlighted. The maximum arc energy is shown to be dependent upon system neutral earthing, as well as the test voltage and closing angle. Normalised characteristics are presented showing the circuit severities in terms of arc energy, and the results are discussed in the light of fuse testing standards. The practice of using only two fuses in an unearthed 3-phase system is shown to produce exceptionally severe stresses on the fuses.

LIST OF SYMBOLS

E	= r.m.s line to neutral voltage
e_a	= $\sqrt{2}$ E sin (wt + θ)
e_b	= $\sqrt{2}$ E sin (wt + θ - 120°)
e_c	= $\sqrt{2}$ E sin (wt + θ - 240°)
i_a	= instantaneous current in phase 'a'
i_b	= instantaneous current in phase 'b'
i_c	= instantaneous current in phase 'c'
I_o	= half-cycle melting current
L	= source-circuit inductance
R	= source-circuit resistance
v_o, r_o	= constants in Hirose's fuse model
vf_a	= instantaneous voltage for fuse 'a'
vf_b	= instantaneous voltage for fuse 'b'
vf_c	= instantaneous voltage for fuse 'c'
v_p	= instantaneous voltage at fault point
θ	= circuit closing angle with respect to e_a
w	= supply angular frequency

INTRODUCTION

Although the breaking-capacity of current-limiting fuses is normally verified in a single phase test circuit, in service fuses are very often used in 3-phase systems, in which the fuses may interact with one another in some way when interrupting a short-circuit fault current. There is some disagreement and confusion about the relative severity of the stresses imposed upon fuses in a 3-phase situation, compared to those produced in a single-phase test. For example the IEC high-voltage current-limiting fuse specification allows fusesto be tested at 87% of the intended 3-phase line voltage, whereas many users insist that the fuse should be tested at the full line voltage. For circuit breakers which clear at a current zero the first phase to clear has to do so against a source voltage of 1.5 times the line-to-neutral voltage, which is 0.866 times the line voltage. Gibson [1] has discussed this problem, pointing out that a current-limiting fuse operates in a manner which is fundamentally different from that of a circuit breaker, and that the correspondence between the 87% test for fuses and the 0.866 value used for circuit breakers is a coincidence.

In this paper this problem is discussed qualitatively by describing the sequence of fuse operation in 3-phase circuits, and quantitatively using Hirose's fuse model [2].

The results, which are illustrated with normalised arc-energy characteristics for a typical fuse, are only relevant to the testing of fuses when they operate in the current-limiting mode (I_1 and I_2 tests).

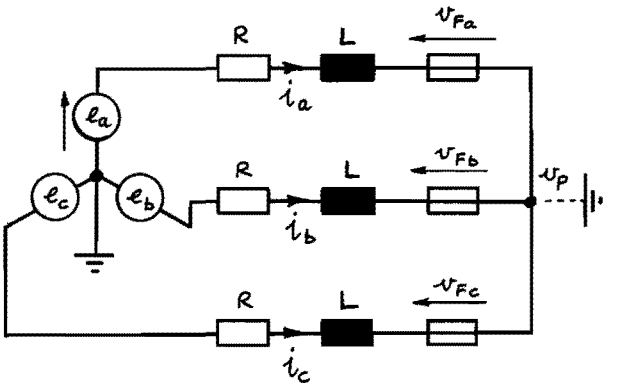

Fig.1 Circuit arrangement.

CIRCUIT MODELS

Fig.1 shows a typical 3-phase power system fitted with 3 fuses during the interruption of a 3-phase fault by the current-limiting action of the fuses. If the 3-phase fault involves earth and the supply neutral is earthed the circuit can be regarded as three single-phase circuits which operate independently of one another, and the fuses will be stressed at the same levels that would obtain in a single-phase test at the line-to-neutral voltage E. If however the fault does not involve earth the fuses will interact with one another. This situation will be referred to as the "unearthed" case, and it would also arise if the supply neutral is unearthed when the fault involves earth.

The general case can be treated by letting the voltage at the fault point be v_p. The circuit currents at any instant in time can then be found by solution of the three differential equations below:

$$\frac{di_a}{dt} = \frac{e_a - Ri_a - vf_a - v_p}{L}$$

$$\frac{di_b}{dt} = \frac{e_b - Ri_b - vf_b - v_p}{L} \qquad (1)$$

$$\frac{di_c}{dt} = \frac{e_c - Ri_c - vf_c - v_p}{L}$$

The equations (1) may be solved by numerical integration. It is convenient to use normalised values for all the variables [3]. In this system all voltages are expressed as multiples of E while all currents are expressed as multiples of the one-half-cycle melting current. The fuse voltages were modelled as follows:

(i) Prearcing state

$$vf_i = 0$$

(ii) Arcing state

$$vf_i = v_o + r_o |i|$$

This is Hirose's model [2] which gives a more realistic voltage than the more commonly-used 'rectangular' arc voltage profile.

Solution of (1) also requires v_p to be computed at each time step. This can be done as follows:

(i) Earthed system

$$v_p = 0$$

(ii) Unearthed system

since $i_a + i_b + i_c = 0$ it follows that

$$\frac{di_a}{dt} + \frac{di_b}{dt} + \frac{di_c}{dt} = 0 \qquad (2)$$

(a) All fuses intact

Using (1) and (2) we obtain for v_p

$$v_p = -\frac{1}{3}(vf_a + vf_b + vf_c)$$

(b) After 1st fuse has cleared

If, say, fuse 'a' clears first and thereafter present an infinite impedance, using (1) and (2) we obtain

$$v_p = \frac{1}{2}(e_b + e_c - vf_b - vf_c)$$

Cyclically similar expression may be derived for v_p if fuse 'b' or fuse 'c' clears first.

The solution procedure requires that after each time step the 'states' of all three fuses are checked to see whether a change of state has occurred. There are 3 possible states - (1) intact (the initial setting), (2) arcing, and (3) blown. Transition from state 1 to state 2 occurs if the integral of i^2 for that fuse exceeds the prearcing I^2t value (0.01 using normalised currents and a 10 ms half-cycle time). Transition from state 2 to state 3 occurs if the fuse is already in the arcing state and current was forced to pass through zero during the previous time-step. The appropriate value for v_p is used at each time step and the computation is terminated (i) when all fuses have blown if the system is earthed, or (ii) when any two fuses have blown if the system is unearthed.

The numerical integration procedure as well as giving the phase currents by solution of (1), is also used to calculate the i^2t integral for each fuse and the arc energy liberated in each fuse (the integral of $v_f.i.dt$).

ADEQUACY OF FUSE MODEL

Use of complex dynamic fuse models such as that described previously [4] requires excessive computation for the present purpose, since hundreds of simulations are necessary to investigate the variation of arc energy with point-on-wave, prospective current, test voltage and circuit arrangement for all 3 phases. For this reason Hirose's simpler model was used.

It is required in this case that the model should adequately represent the way in which maximum arc energy varies with test voltage. Some test results have been published by Hirose [5]. Use of the dynamic fuse model for this purpose [6] shows that for a typical fuse arc energy increases with test voltage raised to the power 1.93. Similar results have been obtained with the simple Hirose model. Indexes of 1.7 - 1.9 were found for the values of v_o and r_o given below. These values are representative of those obtained from tests on a typical low-voltage fuse and a typical high-voltage fuse. [1]

	v_o	r_o
LV	0.60	0.70
HV	0.35	0.45

The lower values for the high-voltage fuses suggest that this type is more sensitive to increase in test voltage. This has been found to be the case.

In order to restrict the number of variables the power factor of the test circuit was set to 0.1 for all simulations.

TYPICAL WAVEFORMS

The precise sequence of fuse melting and of arc extinction for all 3 phases varies considerably with the test current, closing angle and test voltage relative to the fuse arc voltage. Some typical examples only are given here to illustrate the way in which the fuses can interact with one another when the system is not "fully" earthed.

Figs 2 and 3 show the sequence of fuse operation for earthed and unearthed systems at a current close to the critical current for phase 'a'. The circuit closing angle here was set at 0° which gives a high arc energy for the fuse in phase 'a'. The results shown here and in Figs 4 and 5 are for the typical high-voltage type.

Detailed analysis of Figs 2 and 3 reveal the following:

Fig 2 (Earthed)

At circuit closing phase 'b' voltage is near its negative maximum. The initial rate-of rise of current is therefore highest for fuse 'b' which melts first, followed by 'c' then 'a'. All fuses operate independently. Fuse 'c' clears first (minor loop) followed by 'b' then 'a'.

Fig.3 (Unearthed)

Until fuse 'b' melts the currents are the same as in the previous case. However when fuse 'b' melts it produces an arc voltage which acts in opposition to the source voltages in phases 'a' and 'c' and which thus delays the melting of fuses 'a' and 'c'. Fuse 'b' clears first, after which arcing continues in 'a' and 'c' in series against the line-to-line voltage, until eventual clearance by 'a' and 'c' simultaneously. Note that the duration of arcing in fuse 'a' is prolonged compared with Fig.2.

EFFECT OF OMITTING FUSE 'C'

In some systems with unearthed neutral it is practice to fit only 2 fuses, the third being replaced by a link. Since the phase-to-earth fault current is zero in these systems, high short-circuit currents only occur when more than one phase is involved, so the fault will always be detected by at least one of the two fuses. This circuit connection has also been occasionally used for fuse testing. [1]

However in this case very severe stresses can be imposed on the fuses as can be seen from Fig.4, which has been drawn for a closing angle of 0° for phase 'a' for ease of comparison with Figs.2 and 3. A closing angle of 0° is not the worst condition: if only two fuses are fitted the worst condition is near a closing angle of 90° for phase 'a', producing the maximum stress on fuse 'b'. (Since the circuit is not cyclically symmetric, random variation of closing angle produces a different range of stresses on the 2 fuses - this is quite different from Figs.2 and 3 where a random variation of closing angle in the range 0-60° produces an equal range of stresses upon the 3 fuses). The responses for a closing angle of 90° are shown in Fig.5.

Detailed analyses of Figs.4 and 5 reveal the following:

Fig.4 (Unearthed)
(2 fuses, θ=0°)

Initially the situation develops as in Fig.3 but after fuse 'b' has cleared fuse 'a' is left alone to clear against the line-to-line voltage ($V_a - V_c$) with no assistance from an arc voltage in phase 'c', just as the phase 'c' voltage is approaching its maximum. Arcing is prolonged in phase 'a' at a high current level.

Fig.5 (Unearthed)
(2 fuses, θ=90°)

In this case the phase 'a' voltage is at its maximum so fuse 'a' melts and clears first. The arc voltage of fuse 'a' forces the current in fuse 'b' from a negative minor loop to a positive value. The melting of fuse 'b' is thus accelerated and after 'a' has cleared fuse 'b' is left alone in circuit in the arcing state and early in the rising half-cycle of the phase 'b' voltage. Arcing is thus prolonged in phase 'b'.

ARC ENERGY CHARACTERISTICS

Fig.6 shows the variation of arc energy as a function of prospective current for various test circuit arrangements. In every case the values shown are the maximum possible i.e. the effect of the closing angle has been eliminated by plotting for every test current only the highest value of arc energy, (which occurs at different closing angles for different levels of current). The normalised arc energy is expressed as a multiple of the base value $EI_o t_o$.

The curves show the well-known maxima in arc energy but there are large differences between the values. The lowest energy is obtained for the "earthed" case, which corresponds to a single-phase test at the line-to-neutral voltage. The relative severities for various test arrangements are shown below.

Circuit	Maximum arc energy, p.u.		Relative severity	
	HV	LV	HV	LV
Single phase	1.96	1.38	1.0	1.0
3-phase unearthed	2.38	2.21	1.21	1.60
Single-phase at 87% of line voltage	4.26	2.80	2.17	2.03
Single-phase at 100% of line voltage	5.72	3.61	2.92	2.62
Unearthed with only 2 fuses. Fuse 'b' value.	6.10	3.95	3.11	2.86

The results above show that the arc energy for a 3-phase fault not involving earth may be 1.21-1.60 times the value obtained in a single phase test at the normal line-to-neutral voltage. However the arc energies obtained at 87% of the line voltage (i.e. 1.5 times the line-to neutral voltage) are significantly higher (2.03-2.17). This shows that the 87% test is more than adequate to verify the breaking capacity for the types of fault simulated. Tests at the full line voltage give an unrealistically high stress on the fuse. The only justification for testing at the full line voltage would be that it is desired to protect against a 'cross-country' fault e.g. where the load side of one fuse is shorted to the supply-side of a fuse in an adjacent phase, which results in the full line voltage appearing across the first fuse.

It is also clear from the results that the manner and sequence of the fuse operation in a 3-phase system is quite different from that obtained with zero-awaiting devices and therefore the 87% level which appears in the standard has no special significance.

The use of only 2 fuses in an unearthed 3-phase system means that both fuses will be subjected to exceptionally high arc energies, especially if the prospective current is high (see Fig.6). Furthermore, the computer simulations show that very high recovery voltages may appear across the first fuse to clear, increasing possible restriking problems.

UNBALANCED FAULTS

The above analyses have been restricted to 3-phase faults. Unbalanced faults will generally give stresses on current-limiting

fuses which are no greater than those produced by 3-phase faults. The source power factor may be affected by the type of fault but it is unlikely to be lower than the values used in fuse testing. If the sequence impedances have the same X/R ratio the maximum possible arc energies for single and double line-to-earth faults will be the same as for the three-phase earthed case. For phase-to-phase faults the arc energy will be lower as two fuses will be acting in series against an effective source voltage of 1.732 times normal.

CONCLUSIONS

The transient variation of phase currents for fuses operating in a 3-phase system have been computed and the maximum stresses upon each of the fuses have been obtained by numerical integration.

For normal faults the stresses are slightly lower than those obtained in a single-phase test at 87% of the line voltage and very much lower than those in a test at the full line voltage, particularly for high-voltage fuses.

The practice which is sometimes adopted, of using only fuses in an unearthed 3-phase system is shown to produce very high stresses on the fuses, higher than those obtained in a single-phase test at the full line voltage.

ACKNOWLEDGEMENTS

The author is grateful to GEC Installation Equipment Ltd. for their support of this work.

REFERENCES

[1] Gibson J.W., Reply to discussions. Int. Conf. on Electric Fuses and their Applications. Liverpool Polytechnic, April 7-9 1976

[2] Hirose A : "Mathematical analysis of breaking performance of current-limiting fuses", ibid, pp182-191

[3] Wilkins R : "Generalised short-circuit characteristics for h.r.c. fuses", Proc IEE, 1975, vol 122, pp1289 - 1294

[4] Wilkins R : "A suite of interactive programs for fuse design and developement", Int. Conf. on Electric Fuses and their Applications, NTH, Trohdheim, 13-15 June 1984, pp227-235

[5] Hirose A : "Maximum arc energy of low-voltage fuses in terms of their voltage", 5th Int. Symp. on Switching Arc Phenomena, TU Lodz, 1985, pp341-345

[6] Wilkins R : Discussion contribution on reference [4], ibid, part II, pp126-127

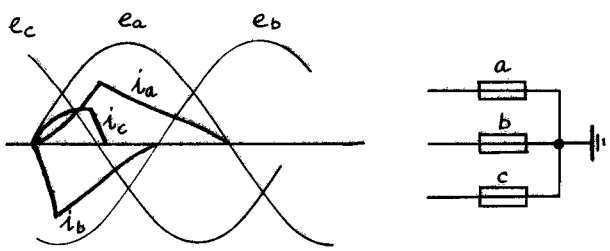

Fig.2 Fault current transients. (Earthed, θ = 0°)

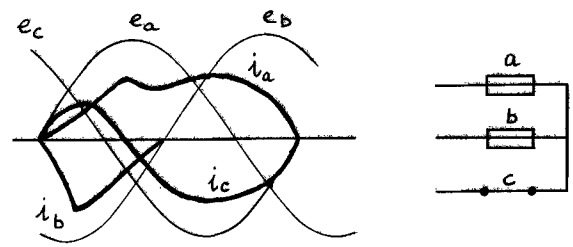

Fig.4 Fault current transients. (2 fuses, unearthed, θ = 0°)

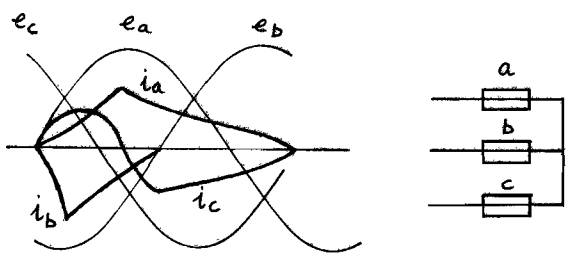

Fig.3 Fault current transients. (Unearthed, θ = 0°)

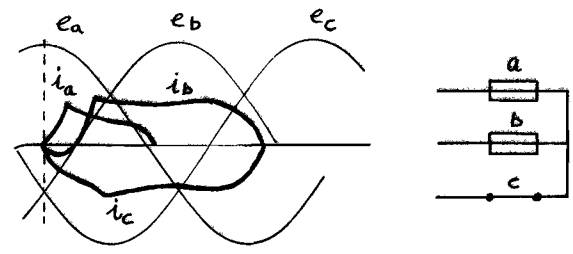

Fig.5 Fault current transients. (2 fuses, unearthed, θ = 90°)

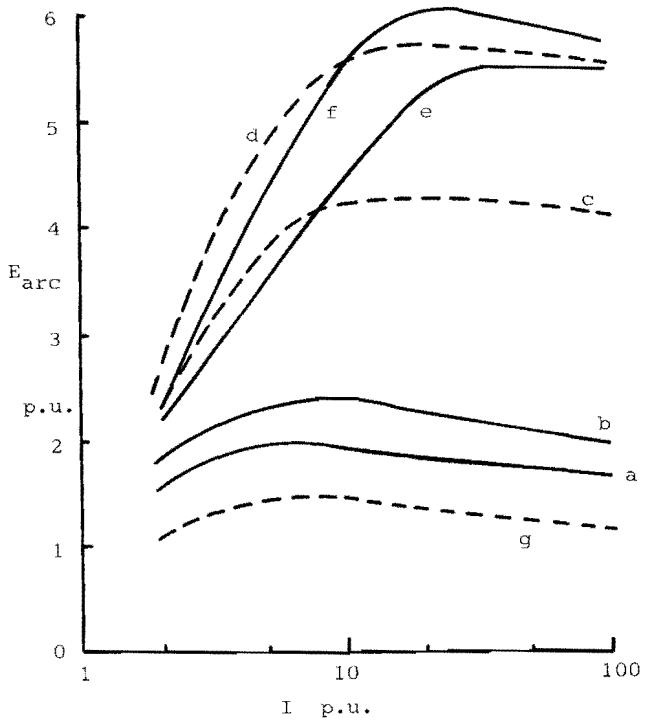

Fig.6 Arc energy characteristics for fuse HV.

a. Earthed
b. Unearthed
c. Earthed, 87% of line voltage
d. Earthed, 100% of line voltage
e. Unearthed, only 2 fuses, fuse 'a'
f. Unearthed, only 2 fuses, fuse 'b'
g. Phase-to-phase fault

OPTIMISATION OF H.V. FUSE-LINK CONTACTOR COMBINATIONS BY STUDY OF THE EFFECTS OF CIRCUIT CONDITIONS AND FUSE-LINK MANUFACTURING TOLERANCES ON TIME-CURRENT CURVES FOR TIMES LESS THAN 0.1 SECONDS.

A J CRANSHAW

ABSTRACT

Industry has seen a significant change from the use of H.V. circuit breakers to fuse-link/ contactor combinations. The inherent advantages in the use of fuse-links for short circuit protection can be fully exploited in minimising the cost of the total installation, due to reduction in maximum current and energy. To give maximum economic benefit, the contactor capability must be matched to the highest possible fuse-link rating. This requires a better understanding of the way in which circuit conditions and manufacturing tolerances affect nominal time/current curves of fuse-links.

A computer programme has been used to predict the effect of power factor, point on wave, and manufacturing tolerances on the nominal time/current curve of a particular high voltage fuse-link, for operating times less than .1 seconds. The results allow certain general comments to be made, and are also used to examine a particular fuse-link-vacuum switch combination.

GEC INSTALLATION EQUIPMENT LTD
EAST LANCASHIRE ROAD,
LIVERPOOL L10 5HB
ENGLAND.

OPTIMISATION OF H.V. FUSE-LINK CONTACTOR COMBINATIONS BY STUDY OF THE EFFECTS OF CIRCUIT CONDITIONS AND FUSE-LINK MANUFACTURING TOLERANCES ON TIME-CURRENT CURVES FOR TIMES LESS THAN 0.1 SECONDS.

INTRODUCTION

This investigation arose from a desire to show that a particular 3.6kV 250A fuse-link could be satisfactorily used in conjunction with a vacuum switch with an interrupting rating of 5.5kA to BS.5311 Duties 4 and 5. The latched opening time of the vacuum switch is 25mS and the time current point of 5.5kA/25mS is close to the nominal time/current curve of the 250A fuse-link. Whilst IEC.282-1 allows a tolerance of ±20% on the current ordinate of the curve most manufacturers claim a maximum tolerance of ±10% for currents giving operating times down to 0.1 seconds. Below this level the effects of current asymmetry may be expected to increase the tolerance, but even the use of +10% would result in the proposed fuse-link/vacuum switch combination being declared unsatisfactory. It was thus decided to conduct a study on the variations in time/current characteristics which would be brought about both by the effects of manufacturing tolerances and current asymmetry for operating times less than 0.1 seconds. Virtual time/current curves have been used to take account of the latter but their accuracy is in some doubt and virtual time cannot be related to real time situations.

METHOD OF INVESTIGATION

A computer programme for fuse-link performance prediction was used to obtain actual time/current points for a 250A fuse-link. Circuit conditions were 3.3kV applied voltage, 50 HZ, and differing values of prospective current, power factor and making angle. Manufacturing tolerances for both element and element material were also taken into account to provide the longest and shortest operating times for given circuit conditions. The computer predicted pre-arcing times are based upon evaluating fuse-link element temperature rise from a nominal 20°C ambient. The pre-arcing time is that required to reach 940°C rise for the silver elements in use in the particular fuse-link. For each combination of prospective current and power factor the range of making angle from 0° to 180° was covered. The computer predicted time/current points were plotted against the nominal time/current curve as published.

RESULTS

Figures 1 to 6 show the computer predicted time/current points for power factors of .15, .6 and .99 for maximum and minimum manufacturing tolerances. It is clear that at .15 power factor the time zones of operation at a given current are discontinuous when pre-arcing extends beyond 17 milliseconds. The phenomena reduces as power factor increases and is not evident at all at .99 power factor. The individual time zones have been highlighted by joining together the appropriate points with a vertical line. The reasons for such discontinuities can be better understood by examination of a typical temperature-time graph and the associated instantaneous current-time graph as shown in Figures 7 and 8. These are for a current of 3.7kA with making angles of 9° and 10° respectively. For the latter, when the melting temperature is missed at the first peak of an asyymetric current waveform it is a further 50 milliseconds before melting point is reached. The condition is of course dependent upon element temperature at onset of fault current.

Although the position of the time step in relation to making angle will alter with 'pre-conditions' the phenomena will still be evident.

In considering computer predicted time/current point tolerances based upon a current variation from the curve as drawn, and for times between 20 milliseconds and 100 milliseconds, the following is arrived at:-

POWER FACTOR	MAXIMUM TOLERANCE	MINIMUM TOLERANCE
.15	+6%	-21%
.60	+6%	-12½%
.99	+10%	-12½%

TABLE 1.

Since time/current curves are usually determined from Laboratory tests carried out at low voltage and high power factor the computer predicted points for .99 power factor are in close agreement with the generally accept ±10% tolerance. This gives credance to the accuracy of both the computer programme used and the time/current curve as published. The computer predicted results then indicate that as power factor reduces the operating time of the fuse-link becomes faster. However a positive tolerance on the curve is still evident at .15 power factor but then only 6%.

SPECIFIC COMMENT ON THE PARTICULAR FUSE-LINK - VACUUM SWITCH COMBINATION.

Further examination of Figure 1 indicates a positive gap in the pre-arcing time, roughly centred around 20 milliseconds and being at its minimum at 5.5kA with a gap from 17 milliseconds up to 25 milliseconds. Hence if specific computer predicted pre-arcing times are examined for 5.5kA a different picture energes to that of Table 1. This can be seen in Figure 9, which shows that the pre-arcing time of 25 milliseconds is only exceeded where the fuse-link is manufactured to worst case conditions and the power factor is .6 or higher. At .6 power factor the maximum time is 26 milliseconds and at .99 power factor the maximum time is 31 milliseconds.

Thus for the particular combination of fuse-link and vacuum switch it cannot be said that the fuse-link will always operate with a pre-arcing time of less than the required 25 milliseconds under all conditions. However for practical purposes the combination could be deemed acceptable.

Without the use of a computer study, and a lesser understanding of the way tolerances on time/current characteristics vary with manufacturing tolerances and circuit parameters, it would be necessary to adopt a more conservative approach to this type of co-ordination problem. Such action would result in either the use of a more expensive vacuum switch with higher breaking capability, or downrating of the equipment by the use of a fuse-link of lower current rating.

REFERENCES

1. A suite of interactive programs for fuse design and development.
R. Wilkins, S Wade, J. S. Floyd. INT CONF. on Electric fuses - Trondheim 1984.

2. Operating times at low short circuit currents - Sven Lindgren
INT. CONF. on Electric fuses - Trondheim 1984.

COMPUTER PREDICTED TIME-CURRENT POINTS - 3·6KV; 250A FUSELINK

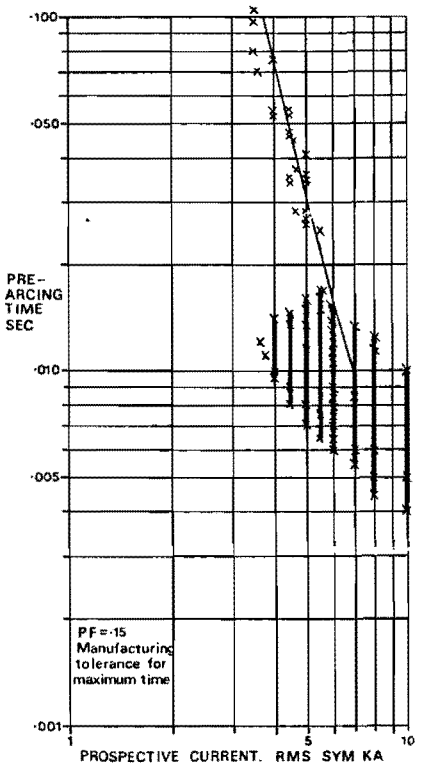

FIGURE 1

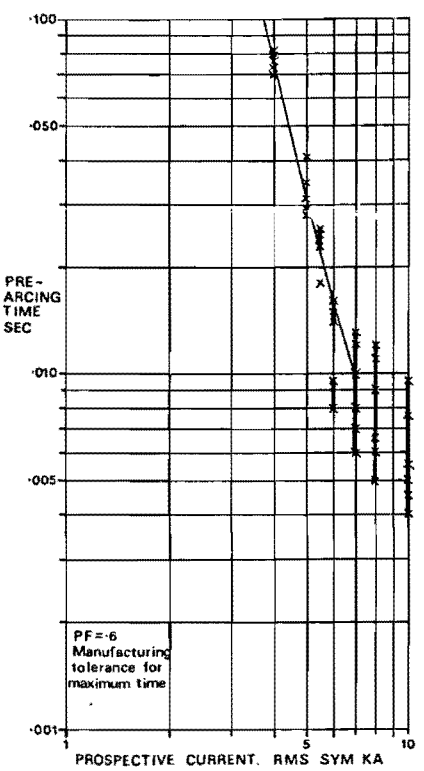

FIGURE 3

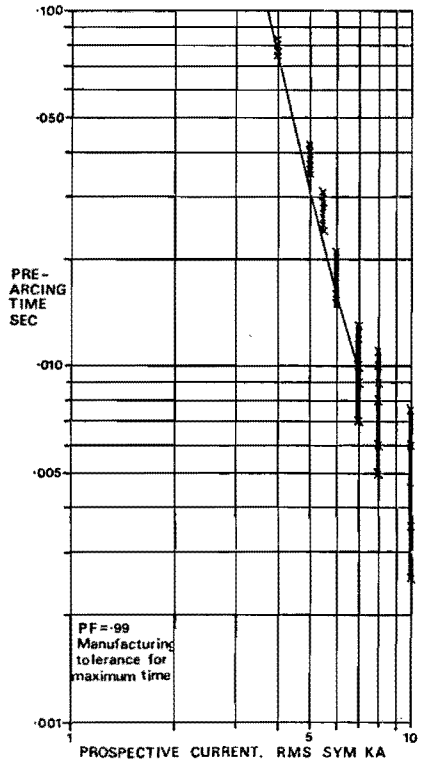

FIGURE 5

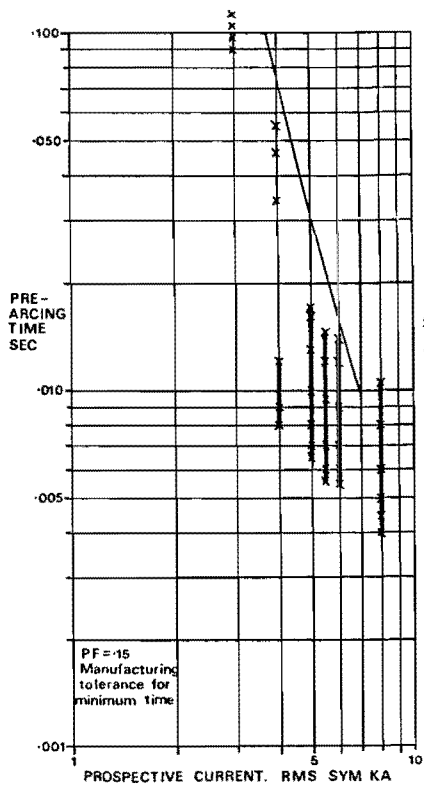

FIGURE 2

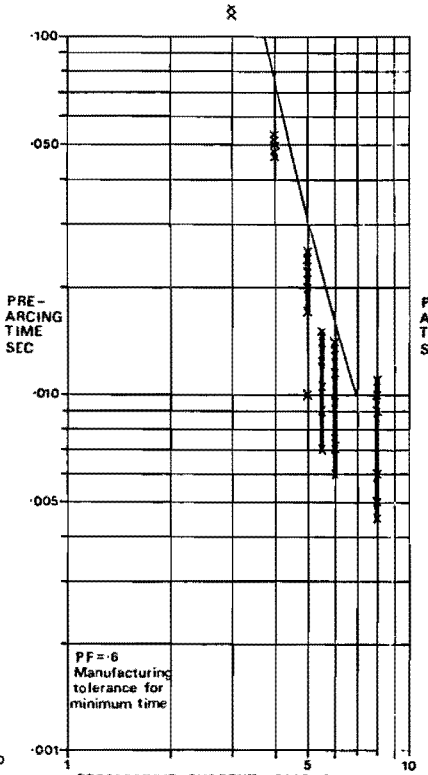

FIGURE 4

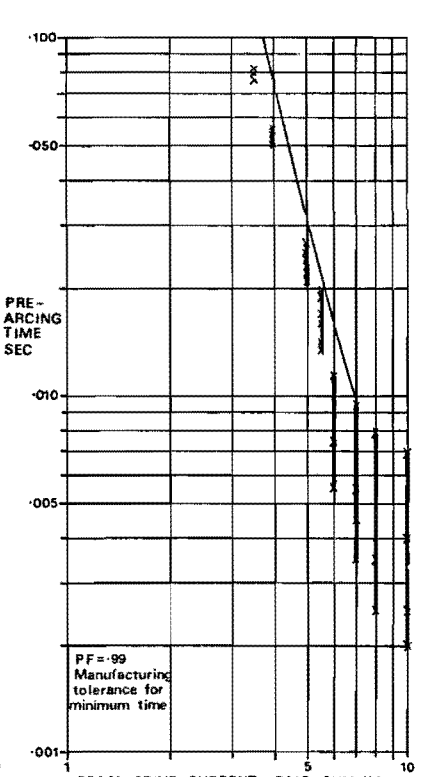

FIGURE 6

CURRENT/TIME AND TEMPERATURE/TIME GRAPHS
3.6kV/250A FUSE-LINK 3.7kA RMS SYM./.15 P.F.

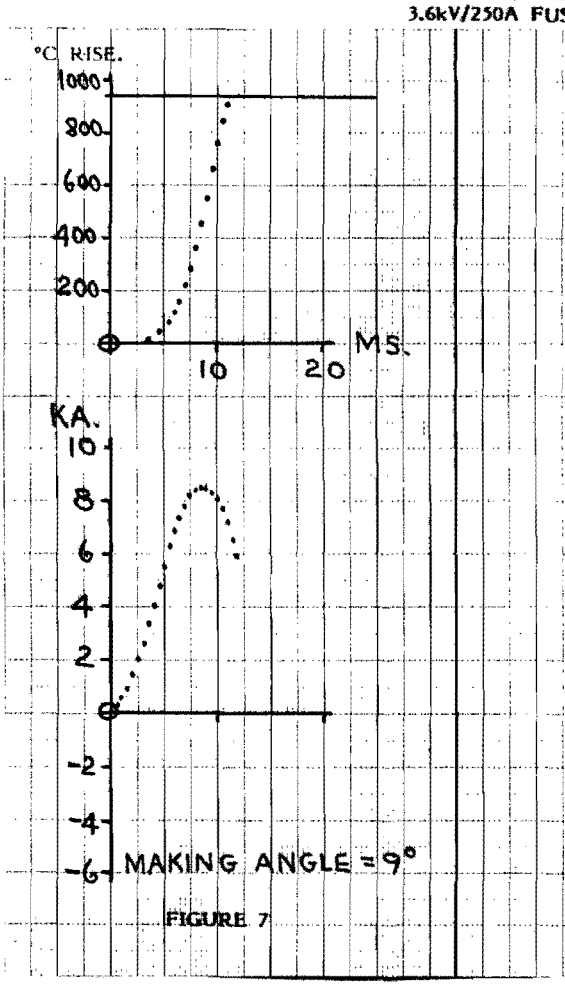

FIGURE 7

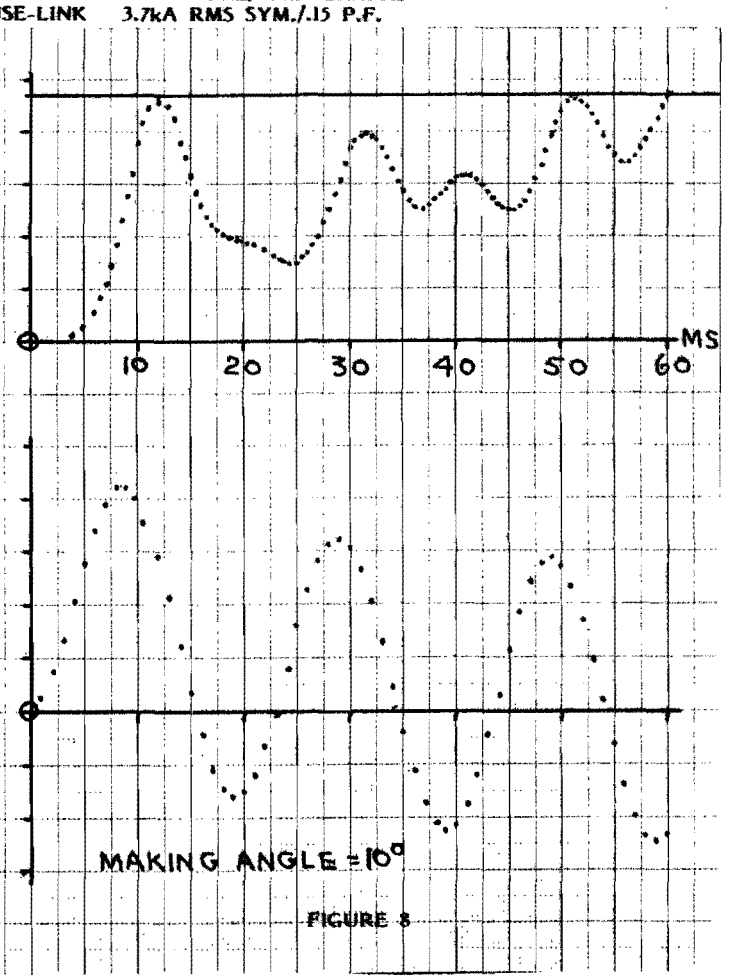

FIGURE 8

COMPUTER PREDICTED OPERATING BANDS AT 5.5kA.

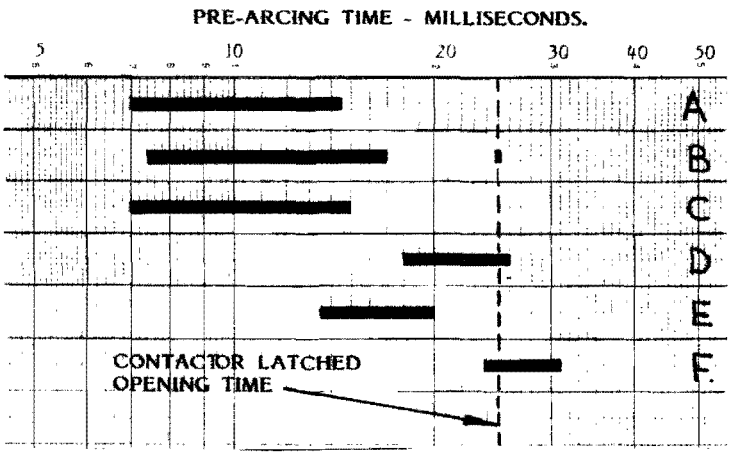

	POWER FACTOR	MANUFACTURING TOLERANCES
A	.15	MINIMUM
B	.15	MAXIMUM
C	.60	MINIMUM
D	.60	MAXIMUM
E	.99	MINIMUM
F	.99	MAXIMUM

FIGURE 9.

CRITICAL PARAMETERS INFLUENCING THE CO-ORDINATION OF FUSES AND SWITCHING DEVICES

H W Turner, Dr C Turner and Dr D J A Williams

ABSTRACT

A switching device in series with a protective fuse when properly co-ordinated is required to disconnect all currents up to its breaking capacity, provided the duration is not above the withstand of the protected circuit. All higher levels must be disconnected by the fuse. The let-through of the fuse passes between the contacts, and there are three critical regions:

(1) The maximum short-circuit level, at which contacts may be flung apart, resulting in severe arc erosion to the contacts.

(2) Intermediate levels at which the contact system is close to the minimum throw-off force at the cut-off of the fuse, which may result in welding of the contacts.

(3) Lower overcurrents exceeding the breaking capacity of the switching device, but in a region of long pre-arcing time.

These problems influence the choice of time/current characteristic for fuses protecting motor starters, analysed in this paper with reference to the fuses available in IEC Publication 269 (Second Edition 1986).

1 INTRODUCTION

Switching devices of limited breaking capacity such as contactors require fuse back-up to protect the switching device and the circuit when fault currents occur above the breaking capacity of the switching device.

The fuse is the most effective limiter of high fault currents, but a period of time, though very small at large overcurrents, is always necessary to fuse the element and clear the circuit, and high cut-off currents may be attained in this period.

At small overcurrents the pre-arcing time becomes much longer and this is the region where the time/current characteristic of the fuse will cross the time/current characteristic of an overload relay in a protected motor-starter.

We identify here a third critical region where the cut-off current of the fuselink is close to the throw-off current of the contacts of the switching device.

This problem was recognised in IEC Publication 292-1A where tests are specified for the co-ordination of low voltage motor-starters with short-circuit protection devices. The tests specified were at test currents 'p' equal to 0.75 I_c and 1.25 I_c where I_c is the crossover current. A further test was specified at test current 'q' not less than the maximum short-circuit current associated with the type of co-ordination needed. The tests conditions specified were as in Publication 157-1 for three phase tests, which is less severe than the single-phase conditions of test specified for the fuses in Publication 269, but sufficiently close to enable a choice to be made of a suitable fuselink on the basis of catalogue data derived during tests to IEC 269.

Up to now, however, it has been necessary to specify in many cases the type, rating, and manufacturer of the protective fuselink to ensure performance as good as in the type test, because of the wide spread of characteristics permitted in the first edition of Publication 269. With the advent of the latest edition of Publication 269 recently published this position is greatly improved Internationally, and the substitution of another general purpose fuse of the same rating has become much more practical.

2 THREE CRITICAL REGIONS OF CURRENT FOR CO-ORDINATION

Three critical regions are identified:

(1) The maximum short-circuit level, at which contacts may be flung apart, resulting in severe arc erosion to the contacts.

(2) Intermediate levels at which the contact system is close to the minimum throw-off force at the cut-off of the fuse, which may result in welding of the contacts.

(3) Lower overcurrents exceeding the breaking capacity of the switching device, but in a region of long pre-arcing time.

We now consider each region individually.

H W Turner, Dr C Turner and Dr D J A Williams are with ERA Technology Ltd, Leatherhead, UK.

2.1 Maximum Short-Circuit Level

The current through the fuse protected circuit at the maximum short-circuit level rises to a peak cut-off value near the end of the pre-arcing time which will vary with the point-on-wave of closing as indicated in Fig. 1.

To obtain an approximate estimate of the maximum cut-off current and actual pre-arcing time, knowing the value of the pre-arcing I^2t of the fuse, a maximum rate of rise can be taken to be that corresponding to peak applied voltage. This would be 1.4 E/L where E is the r.m.s. voltage appropriate to the phase in which the fuse is situated and L the inductance in the circuit. From the integration of this linear rate of rise and the known value of the pre-arcing I^2t the approximate cut-off current and time may be easily calculated.

The accelerating force f produced by a current i causing the contacts to be thrown off is then given (Ref. 1) by the equation:

$$f = 10^{-7} i^2 (l_n B/a - k) - p \qquad (1)$$

Where B is the radius of the end face of the contacts, a the radius of the area in physical contact, k the constant corresponding to any hold-on force provided by the design of the contact system and p the force exerted by the contact spring.

For simple switching devices with butt contacts k is negligible and the throw-off of the contacts may be calculated from the Newtonian laws of motion. Detail of these calculations is not appropriate in this context but it can be reported that calculation and experience (Ref. 2) show that for most contactors under these conditions the contacts are flung apart resulting in arcing at high current which is extinguished by the fuse before the contacts re-close. In that time they generally have cooled to a sufficient extent to avoid welding together on reclosure.

However, the contacts can be seriously eroded by the high current arc burning between the contacts, the rate of erosion being approximately proportional to the time multiplied by the current raised to the power 1.6. When the contacts are thrown-off well before cut-off, the degree of erosion produced when protected by a given fuselink may then be approximately assessed by its let-through I^2t.

When the contactor is closed on to the short-circuit current, there is a further complication if there is any bounce of the contacts prior to reaching the throw-off level, because any such bounce action will cause the contacts to open momentarily and then reclose onto the arc so initiated. This may cause dynamic welding of the contacts. This phenomenon is also troublesome when closing onto lower fault currents where high peak currents may be attained during a contact bounce separation. To permit calculations to be made in this region a new Appendix C has been added to IEC 269-1 in which a method is given for the calculation of cut-off current/time characteristics. An example of the typical results of such calculations is shown in Fig. 2 for the fuselinks of a well known British manufacturer based on data derived from the catalogue. With the much closer limits of time/current characteristics, and the limits on the joule integral now specified in IEC 269 it is possible to draw bands covering a substantial international range of fuselinks which should ease the burden of the controlgear designer in the International market.

2.2 Intermediate Region

This is the most sensitive region for the likely welding of the contacts.

Throw-off force may be evaluated by equation (1) as before, but as the cut-off current is reduced from the value at maximum prospective short-circuit current, a value of current is approached at which f = 0.

Near this condition, the contacts will be either briefly separated at the peak high current, or lightly touching with a tiny area of silver in contact which will be melted by the through current peak. Any such melting can cause an increase in the value of 'a' in equation (1) causing the contacts to 'sink-in' to the molten area as the current passes the peak value.

Either of these conditions is likely to produce severe welding of the contacts.

Using the same methods of calculation and further contact theory related to the temperature of contact areas at high current density, it is possible to make calculations of critical parameters related to contactor design which can improve performance in this area. The effects are seen in Section 2.1 above to be directly related to the I^2t values of the fuselinks studied.

In order to make these calculations however, the designer needs precise fuse data, and with the first edition of Publication 269-1 the variations of time/current characteristic were too wide and there were no limits set to the joule integral values which made an Internationally applicable calculation practically impossible. Now that these aspects have been greatly improved in the new Edition, and closer limits set to permissible variations, designers are enabled to take cognisance of the likely behaviour of fuselinks worldwide.

2.3 Lower Overcurrent Region

At low overcurrents of the order of 10 times the rated current of the fuse, the contacts of the motor starter are subjected to the thermal effects of the overcurrent for a much longer time, especially since the pre-arcing joule integral is much larger in this region than in the short-circuit region. Due to the usual practice of using a fuse of higher current rating than the AC3 or AC4 rating of the contactor, a current of 10 times the fuse rating may be of the order of 15 times the contactor rating, which is in excess of the breaking capacity of the contactor.

During this period the contactor may trip and arcing will then commence at its contacts at a current above the breaking capacity reducing the current and causing the first fuse to take longer to blow. When the first fuse blows, the current drops to 87% as was reported by S Lindgren (Ref. 3). The pre-arcing time of the next fuse is extended to a time corresponding to this reduced current, causing the arcing to persist. It was pointed out that this problem would arise in practice with a fault at the terminals of a motor fed by long cables.

The form of the fuse time/current characteristic best suited to deal with this problem is still very much a matter for debate.

Two forms of characteristic are shown in Fig. 3, 3a being the type of general purpose characteristic found in the gG types standardised in the new IEC 269, and 3b being representative of the dual-element types available as an alternative choice in the USA.

At first sight the type 3b appears to have advantages operating with the breaking current above the point 'A' on the time/current characteristic, due to the very fast operating time at this level compared with the type 3a.

However, when the current is reduced as indicated above, the very steep inflection at current 'A' can result in a very much longer pre-arcing time for currents between 'A' and 'B' when the first fuse blows and the current drops into that region. In fact, the problem reported by Lindgren was precisely at a similar inflection (but less steep) in the characteristic of the gI fuses with which he was experiencing problems. A more shallow characteristic as in 3a is clearly better in this region giving a more nearly constant joule integral and therefore a more consistent performance, although needing a design of contactor capable of a limited withstand of currents above its normal breaking capacity.

This matter is at present under discussion in 32B WG8. There ae strong arguments for both forms of characteristic depending partly on National established practices, and these will need much further debating in the IEC before a rationalised International policy can be established.

3 THE NEW IEC REQUIREMENTS AND THE IMPROVEMENTS IN ACHIEVING CO-ORDINATION

The new requirements for IEC 269 have reduced the spread of available characteristics and also set limits to the range of pre-arcing I^2t of all general purpose fuses Internationally. No limits were set for I^2t in the earlier specifications.

These pre-arcing I^2t values are standardised at a pre-arcing time of 0.01 seconds and the values for the calculation of conditions considered in 2.1 above will in general be lower than these values, giving a margin of safety if calculations are made on the basis of the IEC values.

If a contactor is designed to meet these maximum levels, it should be possible to use any other replacement fuselink of the same rating made to IEC 269 requirements when the new standard is fully implemented without running into new problems in regions (1) and (2).

The situation in region (3) should also be improved, as is shown in Table 1 where the range of current corresponding to a pre-arcing time of 0.1 seconds is seen to be considerably reduced in the new standard. This was the region where trouble was experienced in the past.

4 CONCLUSIONS

(1) Problems with co-ordination of fuses with switching devices are of a different character at different levels of overcurrent.

(2) Three critical levels of current have been identified:

  (i) Maximum breaking capacity;

  (ii) Critical throw-off current;

  (iii) Small overcurrents exceeding the breaking capacity of the contactor.

(3) Potential problems of fuselink replacement will be greatly reduced when the new edition of IEC Publication 269 is fully implemented.

REFERENCES

(1) Holm, R: 'Electric contacts' published by Springer, 1967 page 57.

(2) Turner, H W, and Turner, C: 'Phenomena relating to temperature rise and welding in high current electric contacts', 4th International Research Symposium on Electric Contact Phenomenon, pp 168-171.

(3) Lindgren, S: 'Operating times at low short-circuit currents', International Conference on Electric Fuses and their Applications, Trondheim, 1984, pp 134-138.

TABLE 1

Comparison of the Specification of the Zone of Current for a Prearcing Time of 0.1 Seconds by IEC Publication 269 in 1973 and 1986

Rated Current (A)	gI and gII (1975)		gG (1986)	
	I_{min} (0.1 S) (A)	I_{max} (0.1 S) (A)	I_{min} (0.1 S) (A)	I_{max} (0.1 S) (A)
16	77	240	85	150
20	100	300	110	200
25	135	380	150	260
32	175	480	200	350
40	220	600	260	450
50	285	780	350	610
63	370	980	450	820
80	550	1,240	610	1,100
100	760	1,600	820	1,450
125	970	2,100	1,100	1,910
160	1,240	2,600	1,450	2,590
200	1,600	3,500	1,910	3,420
250	2,100	4,550	2,590	4,500
315	2,600	6,000	3,420	6,000
400	3,500	7,750	4,500	8,060
500	4,550	9,800	6,000	10,600
630	6,000	15,000	8,060	14,140
800	7,750	20,000	10,600	19,000
1,000	9,800	25,000	14,140	24,000
1,250	-	-	19,000	35,000

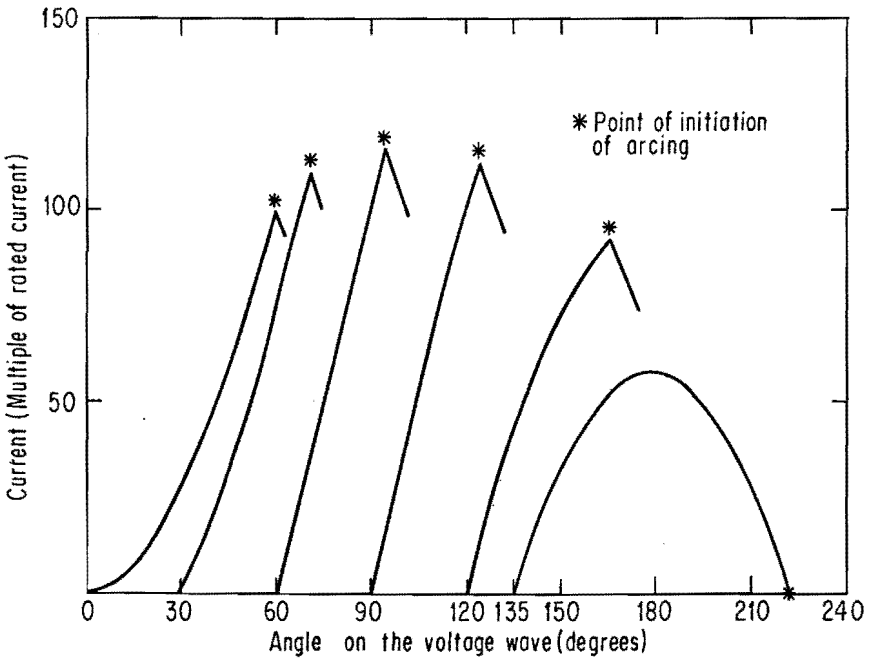

FIG1 CURRENT AS A FUNCTION OF TIME FOR A TYPICAL FUSELINK AT A PROSPECTIVE CURRENT APPROACHING MAXIMUM BREAKING CAPACITY AT 0·1 POWER FACTOR, ILLUSTRATING THE VARIATION WITH CLOSING ANGLE OF CUTOFF CURRENT AND ARCING ANGLE

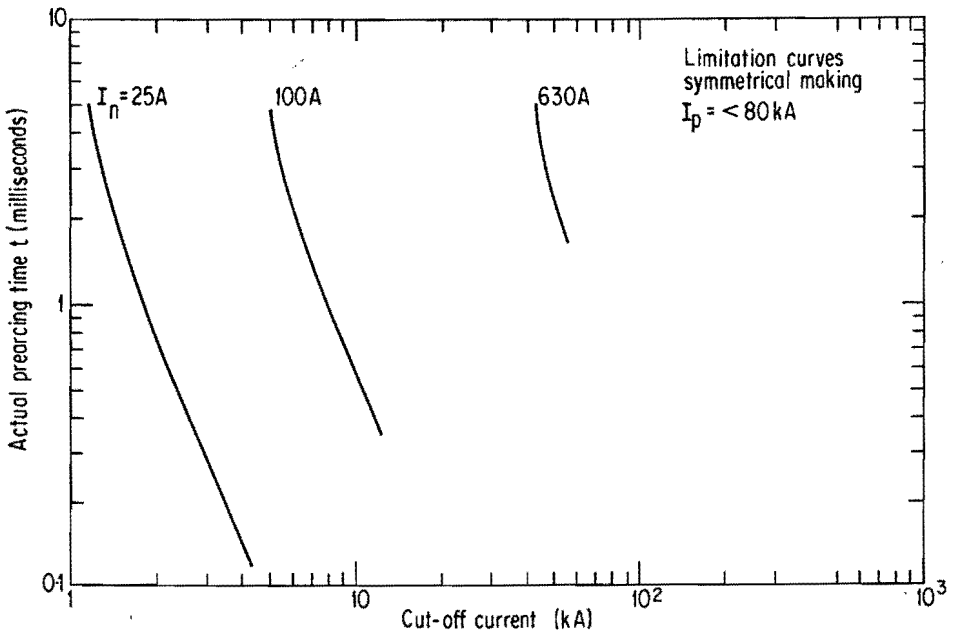

FIG. 2. CALCULATED CURVES OF CUT-OFF CURRENT AS A FUNCTION OF ACTUAL PREARCING TIME FOR A WELL KNOWN BRITISH MANUFACTURER

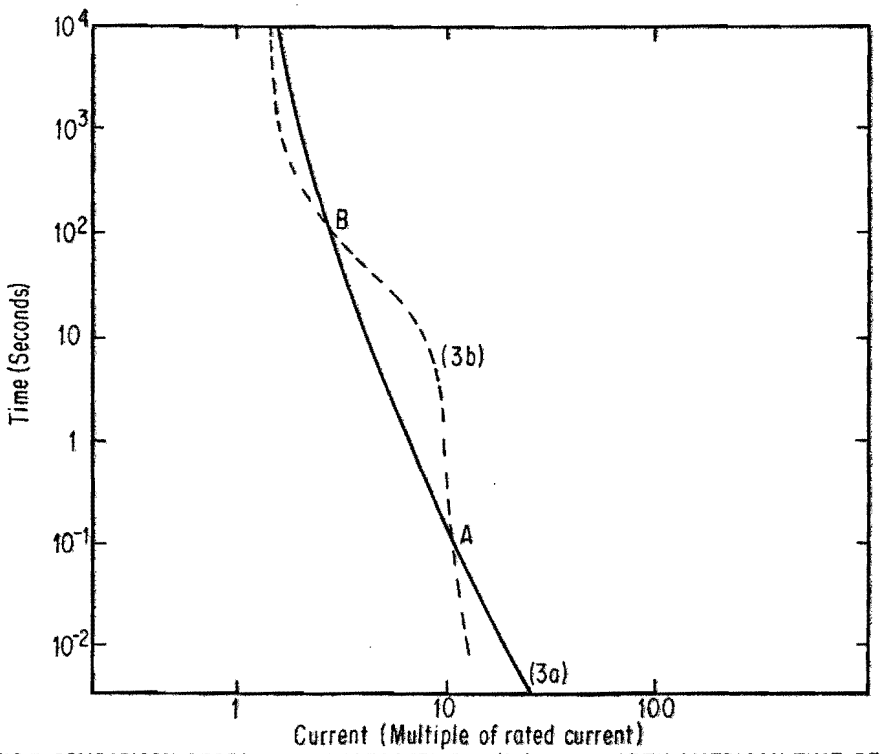

FIG 3. COMPARISON OF IEC gG/gM CHARACTERISTIC(3a) WITH NORTH AMERICAN TIME DELAY TYPE(3b)

BACK-UP PROTECTION OF VACUUM CONTACTORS

Andrzej CEWE, Józef OSSOWICKI
Electrotechnical Institute, Gdańsk

ABSTRACT

Fuses are suitable for preventing excessive damage to the contactor under short-circuit conditions. Relatively high interrupling capability of vacuum contactor allows to create fuse-contactor combination having an operating characteristic like that of a circuit-breaker. The combination may be assemblied on the basis of the coordination principles given in this paper. Defined also was a new parameter: contactor withstand on cut-off current pulses, which allows to estimate a breaking capacity of the combination. These coordination principles were confirmed in 1000V a.c. combination interrupling tests. In take-over current region the breaking task is shared between contactor and fuses, resulting the interruption of a two-phase fault by the contactor. It may to lead to revision of coordination principles.

INTRODUCTION

In the last decade vacuum contactors have been succesfully replacing conventional air-break ones, mainly in 1000V and 6000V a.c. motor circuits. However, these contactors exhibit the ability to perform very well under normal operating conditions and higher, than air-break ones, capacity for withstanding the fault currents, their application in industrial installations at fault level above abt. 10kA is restricted. To extend application of vacuum contactors, special H.R.C. back-up fuses are used to protect them against high-level faults. Placed ahead of a contactor or a panel of contactors, the fuses should be coordinated with the contactors to act only on those faults that exceed withstand or interrupting rating of the contactor.

The fuse - vacuum contactor combinations are intended to be applied as an operating as well as protecting devices simultaneously. These combinations find their application specially in underground installations 1000/1140V and 6000 V in mining industry.

In the paper the problems of creating of the fuse-vacuum contactor combination is discussed and some experimental results are given.

COORDINATION CRITERIA AND SELECTION OF COMBINATION ELEMENTS

The time current characteristics of realy-operated fuse-contactor combinations are presented in Figs.1a/ and b/.

The Fig. 1a/ presents the characteristic of the combination in which opening of the contactor can be initiated by an overload /inverse time/ relay. In Fig. 1b/ opening of the contactor can be initiated by the overload or short-circuit /instantaneous/ relay. The basic difference between these both characteristics are the current ranges at which the contactor operates alone, preventing fuse to melt.The upper limit of this range depends on breaking capability of the contactor. For this reason in the first combination /Fig. 1a/ are as a rule used air-break contactors and in the second /Fig. 1b/ vacuum ones. It is commonly known that breaking capability of vacuum contactors is several times higher than of the air-break ones. This ability of the vacuum contactors allows to create a combination of which performaces and characteristic are the same as those of a fuse-circuit-breaker combination /Fig. 1b/. As a back-up protection of vacuum contactors are applied "aM" fuse-links /up to 1000 V a.c./ [1] or h.v. fuses for motor applications [2] which are generally used to provide short-circuit protection only-in current region above interrupting capacity of the contactor conjuncted with. The contactor is designed to interrupt overload currents up to its breaking current. The short-circuit current in practice have less likelihood to occur in case of fault. The above mentioned combination may be of interest from economical point o view since it allows taking better

advantage of the vacuum contactor interrupting performances.

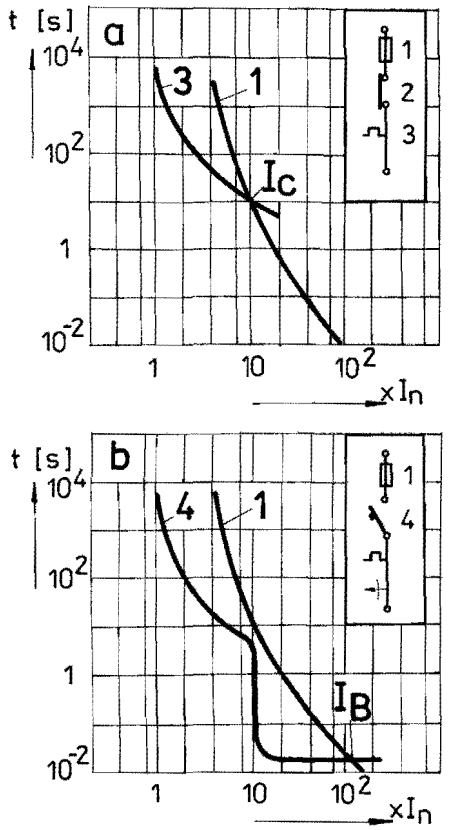

Fig.1. Time-current characteristic of fuse - vacuum contactor combinations

a/ contactor with an inverse time relay only
b/ contactor with inverse time and instaneous relays
1 - fuse; 2 - vacuum contactor; 3 - inverse time /overload/ relay; 4 - vacuum contactor/or c.b./ with overload and short-circuit relay; I_B, I_c - take-over currents; I_n - contactor continuous current /overload relay current setting/.

In Fig.2 are presented time-current zones of a fuse - vacuum contactor /overload and short-circuit - operated/ combination.

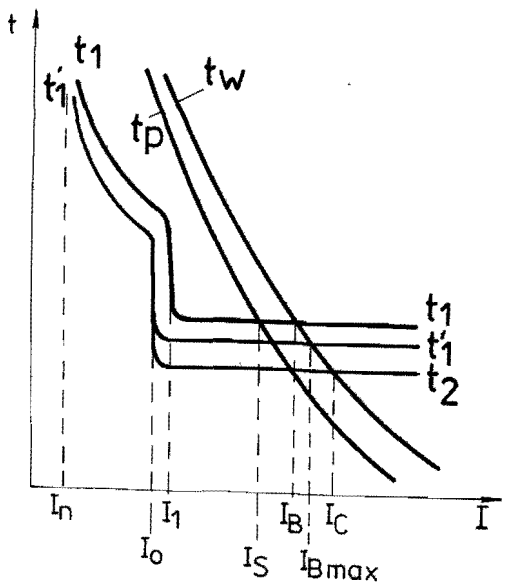

Fig.2. Time-current zones of a fuse-vacuum contactor combination type Fig.1b
t_1, t'_1 - maximum and minimum operating times of contactor-relay assembly; t_2-contactor minimum pre-arcing time; t_w-maximum operating time of a fuse; t_p-minimum pre-arcing time of a fuse; I_n-current setting of an overload relay; I_0-I_1 - current setting zone of a short-circuit relay; I_B-take-over current; I_C-current limit above which a fuse is entrusted with the task of current interrupting.

At currents up to and not exceeding I_S/selectivity current [3] / the contactor operates alone preventing the fuse-link to melt. A take-over current value I_B is determined after I.EC Publ.for c.b combinations [3] . In some standards e.g. Polish Standard the take-over current is defined in point I_{Bmax} /Fig.2 /. Taking into account the width allowed by the fuse standard zone, if the take-over current is defined in point I_{Bmax}, one cannot to create the combination [4,5] . Note that value I_B in Fig.2 is equal to the I_{Smax}, for which the ordinate is upper limit of a pre-arcing time t_{pmax} /not shown in

Fig.2/. For longer times, about 40-80 ms , the pre-arcing time is nearly equal to the operating time value /$t_{pmax} = t_w$/. Within the current range $I_S - I_C$ the breaking task may be shared between relay-operated contactor and fuse, or one of these apparatuses may be entrusted alone with the task of interrupting the fault current only. Closer to the current I_S more probable is operation of the contactor alone but closer to the I_C more probable is breaking by the fuse only. The I_B current value should be lower than interrupting capacity of the contactor. The I_{Bmax} value is concerned with the operating time zone of relay-contactor assembly; the width of this zone depends on quality of both aparatuses. The best practice is when components of the combination can be assemblied togather by one manufacturer which is able to guarantee that the combination will operate satisfactorily. Nevertheless, in some cases as a rule in Polish practice/ the combination components may be grouped togather by system desinger or user who must change the fuse to another one, or to one made by other manufacturer.
For this purpose the following data are needed:

a/ relay-vacuum contactor assembly:
- breaking current I_w
- peak withstand current /without fuse/ i_{sz}
- pulse withstand current /with fuse/ i_p
- maximum time-current characteristic $t_1 = f/I/$

b/ fuse data
- time-current zone $t_p - t_w = f/I/$
- cut-off current characteristic $i_o = f/I/$

The value i_{sz} is given by the contactor manufacturer as an electrodynamic withstand. When the contactor is used with fuse, the contactor withstand value varies greatly. After authors' investigations the pulse withstand value of Polish SV type vacuum contactors i_p is 1.5 - 2 times higher than peak one i_{sz}. Similar value is also given by Saputo [6].
The combination coordination principles can be described by means of the following relations:

/1/ $\quad I \overset{\wedge}{\leqslant} I_S \qquad /t_1 < t_p/$

/2/ $\quad I_B \overset{\wedge}{\leqslant} I_w \;;\; \overset{\vee}{I = I_B} \qquad /t_1 = t_w/$

/3/ $\quad I \overset{\wedge}{>} I_B \qquad /t_1 > t_w/$

/4/ $\quad t_w \overset{\wedge}{\geqslant} 10ms \qquad /i_{sz} \geqslant i_u/$

/5/ $\quad t_w \overset{\wedge}{<} 10ms \qquad /i_p \geqslant i_o/$

where: i_u - peak short-circuit current
i_o - cut-off current of a fuse-link
for other symbols - see Fig.1.

When the value i_p for a contactor is not given in the relation /5/ one substitutes instead of i_p the i_{sz} current value. In such case the breaking capacity of combination will be lower /Fig.3/
The relation /1/ evaluates a minimum rated current of the fuse-link, and the relations /2/-/5/ the maximum rating of the fuse-link. The intention of designer is to select the fuse-link rated with so great current as it is possible.
Breaking capacity of combination may be found from characteristics shown in Fig.3. In this Figure are assemblied time - and cut-off current characteristics. Having time-current characteristic and contactor breaking capacity the breaking capacity of

combination I_{wz} may be estimated and inverserly: if the I_{wz} value has been fixed, the main gates for time - current characteristic, needed by fuse-links designer, may be estimated from Fig.3.

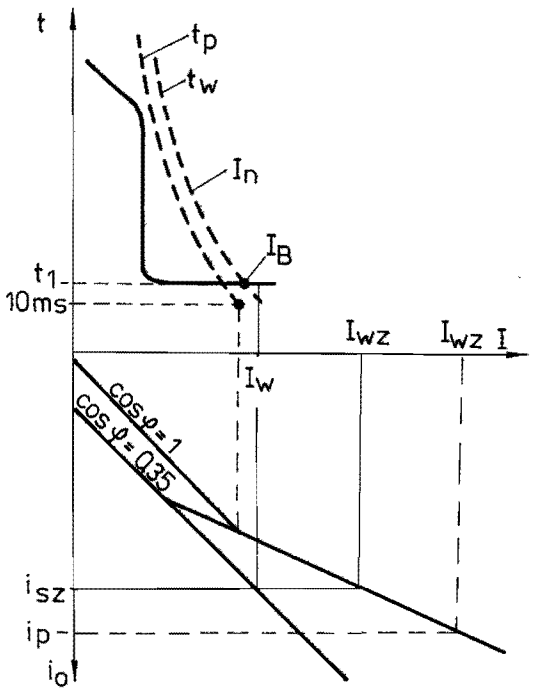

Fig.3. Evaluation of a combination breaking capacity from a fuse and contactor characteristics

for t_1, t_p, t_w and I_B - see Fig.2; I_n - t-I zone and cut-off characteristic of the I_n-rated fuse; i_{sz}, i_p peak and pulse withstand currents of a contactor; I_w -contactor short-circuit breaking capacity; I_{wz}-combination short-circuit breaking capacity.

BACK - UP FUSES

In the Gdańsk Branch of Electrotechnical Institute new low power-loss fuse-links for back-up protection of vacuum contactors 1000 V and 6000 V a.c. have been designed.

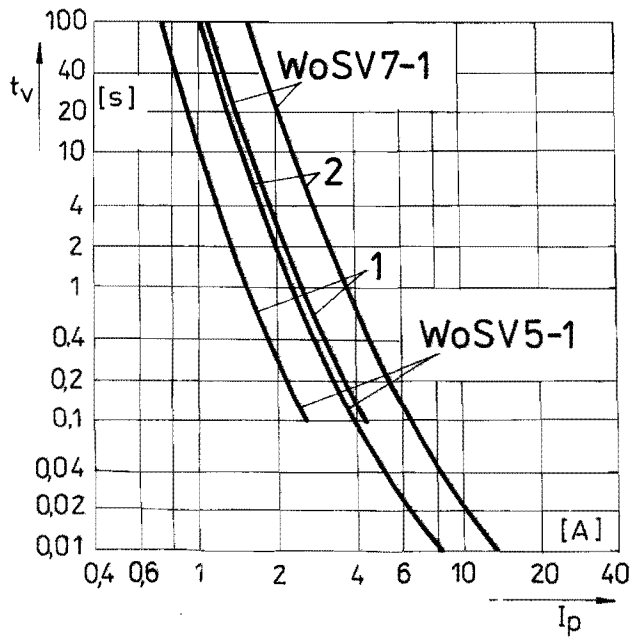

Fig.4. Time-current zones of aM fuses for back-up protection of 1000V a.c. vacuum contactors types SV5 and SV7

The 1000/1140V "aM" category fuse-links /Fig.4/ type WoSV5-1: rated 125, 160 and 200A, type WoSV7-1: rated 200, 250 and 315 A, are capable of interrupting fault currents up to 50kA. The power-losses of these fuse-links are very low i.e.: below 23W for 200A fuse-links and 41W for 315A fuse-links. A maximum temperature-rise on fuse terminals is not

higher than 40K. This is particularly important for coal-mine switch-gears in which the fuse-contactor combinations are in special explosion-proof casings. Environment temperature inside of the casing is often above 50°C. The new fuse-links have substantially high current - limiting ability /Fig.5/ and resistance to pulse overloads i.e.:

a/ Copper strip fuse elements -
- 50 pulses with test current $k_1.I_n/4I_n/$, pulse duration 15s, interval between pulsas 450s; /after new VDE [7] /

b/ silver strip fuse elements - 80 pulses with current value and duration same as a/, interval between pulses 90s.

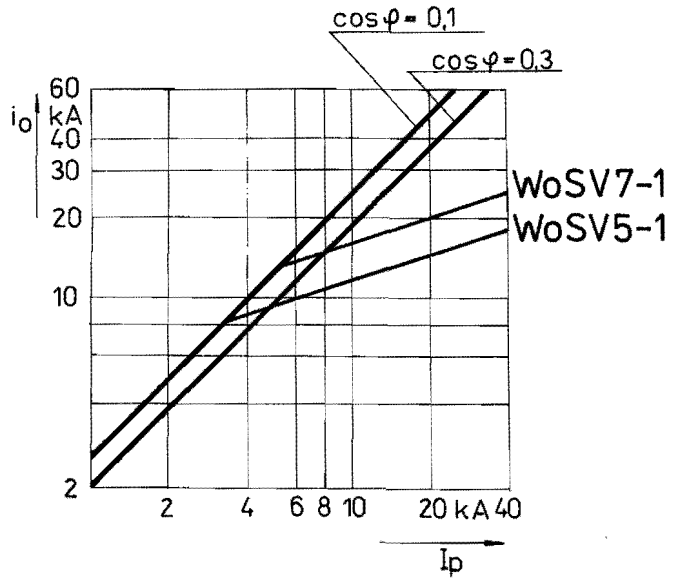

Fig.5. Cut-off current characteristic of 100V a.c. back-up fuses for SV5 and SV7 types contactors

The copper fuse - elements fulfil the requirements for "aM" fuses of normal execution, the silver ones fulfil more severe requirements for mining execution.
New designed h.v.-fuse-links type WoHSV7-1 for motor circuits /partial range/ /Fig.6/, rated 160, 200, 225 and 250A fulfil requirements of IEC Publ. 644 [2] ,

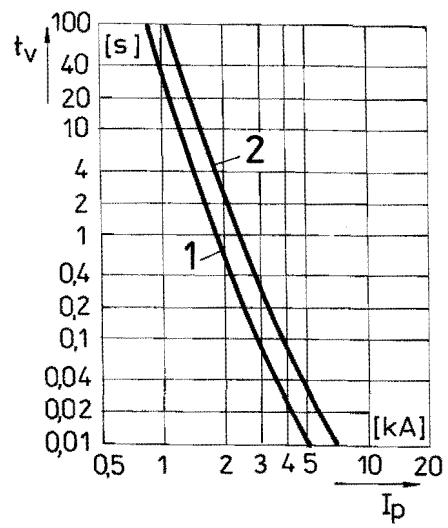

Fig.6. Time-current zone of partial range fuses for back-up protection of 6000V a.c. vacuum contactors type HSV7.

The fuse-elements of these fuses may be of silver or copper strips. Coefficient K, estimated after IEC Publ 644 [2] , specifies overload curve. After this curve, the fuse-link when submitted to overload cyclic pulses should not operate. The K value for copper strip-elements is 0,62, and for the silver ones: 0,66.

The WoHSV7-1 type fuse-links are destinated for industrial and coal-mine power systems with fault power up to 400 MVA. Current - limiting properties of these fuse-links are shown in Fig.7.

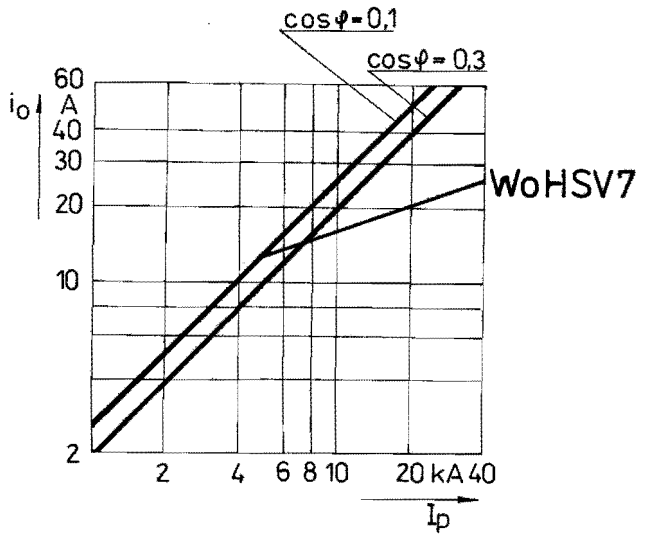

Fig.7. Cut-off current characteristic of 6000V a.c. back-up fuses for HSV7 type contactors.

/Their maximum interrupting capability, up to now has not been verified/. The power losses of these fuse-links are relatively low, i.e.: 100 W for 160A and 150 W for 225A fuse-links; temperature rises on terminals - 20K and 28K respectively.

FUSE AND VACUUM CONTACTOR COORDINTATION IN FAULT CONDITIONS

In order to verify the coordination principles /relation 1-5/ short-circuit tests of 1000V a.c. combinations have been carried out. These tests contained also verification of short-circuit withstands /without and with fuse/ of vacuum contactors [6] . A current flowing through the closed contacts of contactor causes an electrodynamic force to act in the opposite direction to the mechanical force to maintain contacts. This leads to sepation of contactor contacts and can develop substantial arcing and heat which cause contacts welding. The electrodynamic force acting between contacts is proportional to the square of the current; the energy converted to heat in the vicinity of the separated contacts, when arcing, is proportional to the time duration. For this reason the value of I^2t was taken as a characteristic parameter of contacts welding phenomena.
The Table 1 presents withstands of vacuum contactors types SV5 and SV7.

Table 1. Results of short-circuit withstand tests of vacuum contactors

Type	Rated current, I_n	Breaking capacity, I_w	Power factor, $\cos\varphi$	el.dynamic withstand		Let-through Joule's integral, I^2t_w
				without fuse, i_{sz}	with fuse, i_p	
-	A	kA r.m.s.	-	kA peak	kA peak	x $10^5 A^2s$
SV5	100	2,5	0,35	9	15	15
SV7	250	4,0	0,35	12	43	40

Taking into account the i_p current values given in the Table 1, from the Fig.5, the short - circuit breaking capacity of the combination I_{wz} / see relation /5/ and Fig.2/ may be estimated as follows:
SV5 combination: abt. 24kA r.m.s.
SV7 combination: above 60kA r.m.s.
The present fault current level in Polish coal-mine 1000V power systems is not higher

than 11kA, for this reason the combinations as above were verified with the test current up to 15kA only.
The short-circuit tests in take-over current region $I_S - I_C$, Fig.2, have shown that the performences of the contactor are much better than could be expected on the basis of Fig.2. The characteristic in Fig.2 is for single-phase symmetrical current [4,5] .
In a three-phase fault circuit, at least in the two-phases asymmetrical current is flowing. Hence the operating Joule's integral of the fuse in these two phases differs from the one where symmetrical current occurs. This why in a three-phase circuit the shorter operating time, than in time-current characteristic, may be expected.
Maximum and minimum possible relative r.m.s. values of asymmetrical current I_z/I versus time are presented in Fig.8:

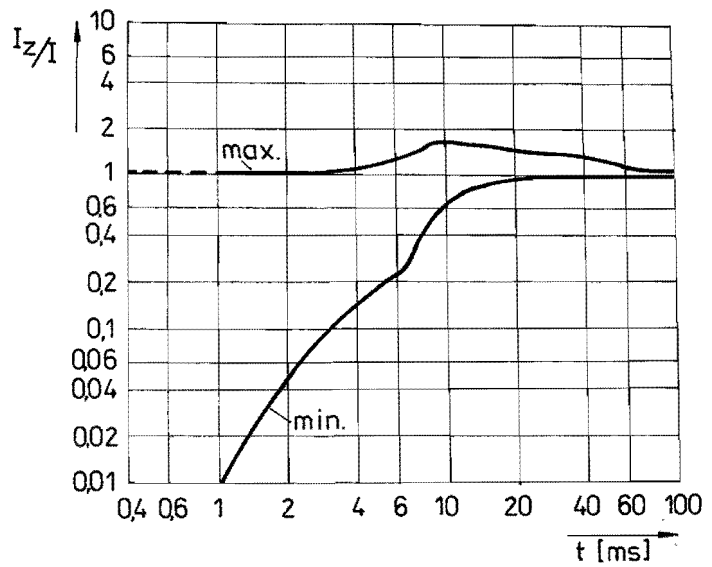

Fig.8. Maximum and minimum possible r.m.s.,values of asymmetrical current I_z/I in three-phase circuit.
t - time measured from a fault instant

/6/ $$I_z/I = \sqrt{\int i_a^2\,dt / \int i_s^2 dt}$$

where: I_z - r.m.s. asymmetrical current
I - r.m.s. symmetrical current
i_a - instantaneous asymmetrical current
i_s - instantaneous symmetrical current

From Fig.8 the possible walues of take-over current can be obtained i.e.:
For contactor operating time t_1 = 40ms the take-over current may be within limits /1-1,5/ I_B; for t_1 = 1ms the take-over current may be /0,01-1/I_B.
When $I_z > I$, in one of the phases the fuse operates as the first, then the three-phase fault inverts into a two-phase fault. The latter may be easily interrupted by a contactor-two contacts operate in series. This explains that if even the coordination criterion /2/ is not fulfiled, i.e. $I_B > I_w$, the contactor is able to interrupt the take-over current satisfactorily. It leads to the conclusion that in the relation /2/, instead of the breaking capacity value I_w, e.g after [3] , other value may be used, estimated in two-phase interrupting tests, as this is recommended by Polish Standard [8].

CONCLUSIONS

- The fuse-vacuum contactor combinations may be used in power circuits at fault power of 400 MVA /1000 volts/ and 250MVA /6000 volts/, respectively. The majority of faults may be interrupted by contactor, what is very important for a continuity of service
- The combination above may be applied as an operating and short-circuit protective device, and in this case no additional circuit-breaker is needed.

- On the basis of the given coordination principles the breaking-capacity of the combination can be evaluated by the designer. The additional contactor parameter has been introduced: the contactor withstant for cut-off current pulse.
- The tests and analysis of fuse-contactor coordination method in region of take-over current, shows that the breaking current value, which is compared with the take-over current , may be verified /higher/ on the basis of the contactor two-phase interrupting tests. It leads to a higher coordinated fuse rating.

BIBLIOGRAPHY

1. IEC Publication 269-1 /1986/: Low-voltage fuses
   Par t 1: General requirements

2. IEC Publication 644 /1979/ Specification for high voltage fuse-links for motor application

3. IEC 17B /CO/127, February 1985. Low voltage switchgear and controlgear. Circuit breakers

4. Toniolo S.B., Cantarella G., Carrescia V.: Improvement of over-current protection in l.v. distribution system L'Elettroteonica, 1976, pp 1479-1483

5. Lipski T.: On coordination of L.v. c.b.s. with separate fuses associated in the same circuit. IV Int.Conf. Switching Arc Phenomena , Lódź 1981, Poland.

6. Saputo V.: Contactor - fuse assemblies for control and protection of high voltage loads. Merlin Gerin Technical News 8, booklet 1

7. VDE 0636 Teil 22: Niederspannungssicherungen NH-System; NH-Anlagen schutzsicherungen bis 1250A und ~ 1000V aM, g Tr, gB. VDE Bestimmung/

8. Polish Standard PN-76/E-06182. Low voltage fuse-circuit breaker combinations. General requirements and tests,/Original Polish/

Session IX

TESTING AND STANDARDISATION

Chairman: Mr. A. Th. Maissan

AUTOMATIC TESTING OF MINIATURE FUSES

P.J. van Rietschoten, H.J. van Altena, Littelfuse Tracor B.V., Utrecht, The Netherlands

ABSTRACT

Miniature fuses involve very large production quantities and in connection herewith very large quantities of fuses have to be tested. Instead of 100% testing, samples are taken to check the quality level of the whole lot. This sample testing still involves large quantities, so it is obvious that automatic testing is considered to be able to guarantee a certain quality level. However, some problems have to be overcome to bring automatic testing into reality. These problems are related with requirements in the relevant IEC 127 standards. In the next paragraphs these problems will be discussed.

1. THE NEED FOR AUTOMATIC TESTING

The newly proposed part 5 of IEC publication 127 (Quality assessement of miniature fuse links) specifies requirements for lot-by-lot inspection. These requirements are divided into two categories, viz :

* Primary characteristics, that means non-destructive testing on marking, mechanical parameters (length, diameter, alignment, cap adherence, cracked insulation tube) and cold resistance.
* Time-current characteristics, that means destructive testing at $1.5I_n$, $2.1I_n$, $2.75I_n$, $4I_n$ and $10I_n$.

For each category inspection levels according to IEC 410 have been specified, as well as AQL-figures. For primary characteristics, inspection level II has been specified. This means that, as an average, appr. 1% of all fuses produced should be tested. So per million fuses produced, 10.000 pieces should be tested. (Production of one million fuses per week is not a very large production volume for this kind of fuses.) Doing the required inspection by hand and one by one should required more than 10 people per million fuses per week. For the time-current characteristics, inspection level S4 has been specified. This means that, as an average, appr. 0.1% of all produced fuses should be tested. This is 1000 fuses per million fuses produced. The requirement is that 40% of these fuses must be tested at $2.1I_n$. The blowing time at this current value may be up till 30 minutes. Assuming an average testing time of 15 minutes and the test will be done by hand and one by one, then only the $2.1I_n$ test requires 100 hours per million fuses.

From the above it might be clear that in an automatic production facility, the inspection by hand involves a number of people which is comparable with those producing the fuses. So the gain may get lost by introducing IEC 127, part 5. Therefore, automatic testing is a need. It should be kept in mind that the IEC requirements are directed to final inspection, all sorts of in-process inspection, patrol inspection and the like, are not taken into account.

2. PROBLEMS FOR AUTOMATIC TESTING AS ORIGINATING FROM IEC 127

Electrical continuity (cold resistance) as well as the time-current characteristic have to be checked using the test fuse holder as specified in IEC 127. (see fig. 1)

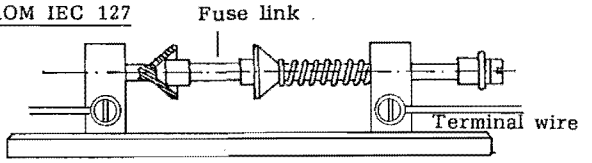

Fig. 1 Test fuse holder according to IEC 127.

Apart from the fact that it is rather difficult to make a reliable mechanism for automatic loading with fuses of such a fuse holder, an even more important factor is that this type of fuse holder requires much maintainance to keep contact pressure and contact resistance within specified limits. The same is valid for the cap adherence test: the requirements and equipment as specified make it not easy to automate such a testing process. In addition to this, cap adherence is to a large extend determined by the process parameters during production. If production is well under control and a good patrol inspection during production takes place, it is questionable why such large quantities should be subjected to an adherence test during final inspection.

Another problem for automatic testing, originating from IEC 127, is that fuse links should be sujected to a so-called modified endurance test. This means: passing a current of 1.5 times rated current through the fuse during one hour and measuring the voltage drop before and after this one hour test. (The voltage drop values of one particular fuse may not change by more than 10%) The voltage drop measurement must be carried out after thermal equilibrium, taking appr. 5 minutes for each measurement. So the total modified endurance test of one fuse takes appr. 1.25 hours. It is specified that 10% of the destructive test category should be subjected to this test. This means that approximately 100 fuses per million fuses produced should be tested. It takes 125 hours when they are tested one by one. Automation cannot reduce this testing time because the testing time is determined by the test requirements. Simultaneous testing can solve this problem only partly.

When there is a production of one million fuses per week but devided over 25 different fuse types and current ratings, then in the average only 4 fuses per fuse type should be subjected to the modified endurance test per million fuses per week. So in this situation the minimum testing time with one equipment suitable for testing 4 or more fuses simultaneously, is in the average $\frac{125}{4} \approx 31$ hours per million fuses per week.

A final problem we like to mention is the fact the determination of the time-current characteristic should be carried out using a DC-source, whereas, according to IEC 127, for the continuity test AC should be used. This condition makes it more difficult to use the same equipment for full electrical testing in one automatic test cycle.

POSSIBILITIES FOR AUTOMATIC TESTING

In the rest of this paper we will not discuss testing of mechanical parameters, we confine ourselves to electrical testing. From the preliminary it became evident that many fuses should be tested simultaneously in order to keep track of production volumes. This is especially true for the more time-consuming tests to determine the time-current characteristic. In principle two possibilities exist for simultaneous testing, viz :

* Parallel testing (see fig. 2) which requires as much current sources as there are fuses to be tested.

* Testing a number of fuses connected in series (see fig. 3) requiring the short-circuiting of each fuse at the instant that the particular fuse blows.

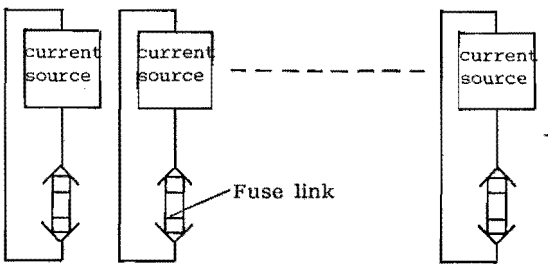

Fig. 2 Parallel testing of fuse links.

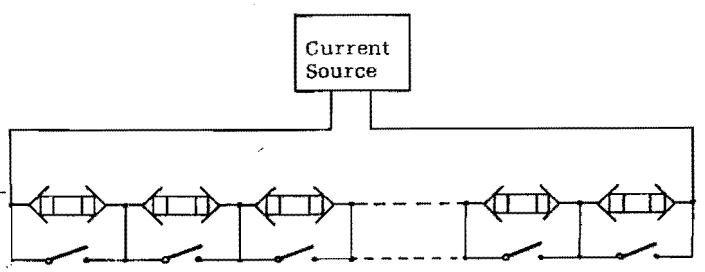

Fig. 3 Serial tesing of fuse links.

In our laboratory we designed and built an automatic testing machine with which a combination of serial testing and one by one testing is realised. Serial testing is carried out for those tests which take a long testing time. (especially the modified endurance test and the $2.1I_n$ test.) Testing times at the remaining current values for the determination of the time-current characteristic are much shorter. (down to max. 20ms at $10I_n$) So one by one testing, but testing a number of fuses in an automatic sequence, is in this case more pratical. Fig. 4 shows the basic concept of the testing machine.

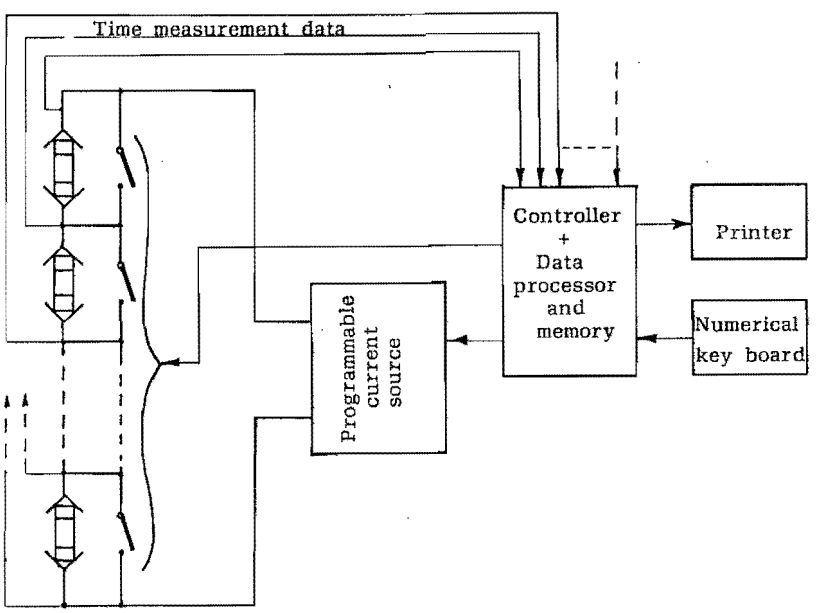

Fig. 4 Basic lay-out automatic testing machine.

In the case of serial tests all fuses connected in series must be monitored constanly. When a fuse blows, the blowing time of that fuse has to be recorded and this particular fuse must be short-circuited, in order to restore current flowing in the rest of the circuit. This short-circuiting should be performed in a very short time (in the order of 0.1 ms) in order not to influence test results by the fuse interruption. (see fig. 5)
Care should be taken not to introduce transient overvoltages (spikes) in the test circuit, which may arise from switching actions while short-circuiting blows fuses.

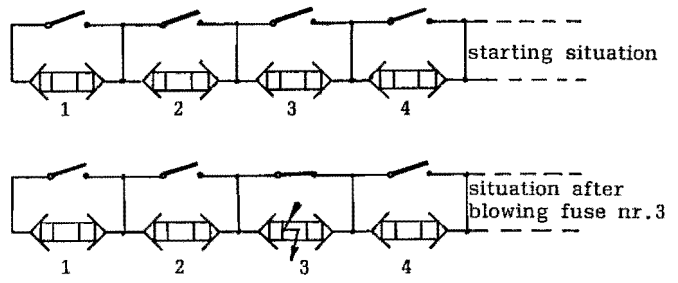

Fig. 5 : Serial testing

The basic idea of sequential one by one testing, in use for the higher current set values, is illustrated in fig. 6.

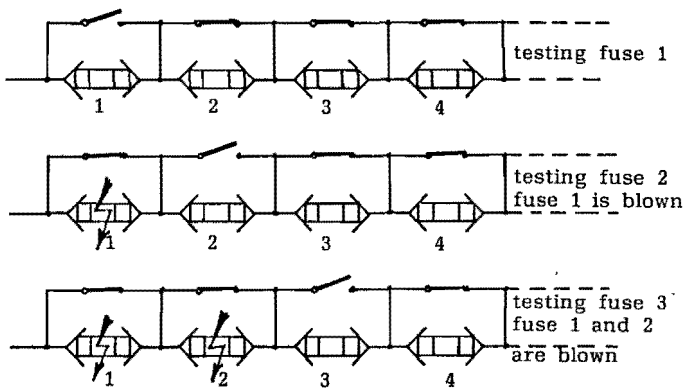

Fig. 6 : Sequential one-by-one testing

The above described functions have been realised in the automatic testing machine. The basic design is shown chematically in fig. 4. With such an equipment it is of course also easily possible to manipulate the test data, for instance determining mean values, standards deviations, etc. per batch.

4. CONCLUSIONS

From the preliminary it may be clear that full automatic testing, following the test duties as specified in IEC 127, part 5, is not simple, due to test requirements as specified in IEC 127, part 1 and 2. A testing machine as described above can, in pratical situations, only be used for final inspection and not for in-process inspection. This is mainly due to testing times which are too long to give an adequate feed-back in the production process.

Quality has to be built-in during the production process and cannot be "tested-in" afterwards. So testing in accordance with IEC 127, part 5 is an additional testing, giving only a final proof of the quality. Testing in this way has no value at all for obtaining a good quality level. The automatic testing machine cannot replace any testing or quality inspection during the production process. The only advantage may be that better reliability figures per batch of finished fuses can be provided.

COMPARISON OF SYNTHETIC AND DIRECT TESTING OF MINIATURE FUSES

L. Vermij, A.J.M. Mattheij, Littelfuse Tracor B.V., Utrecht, Netherlands
A. Th. Maissan, L. van der Sluis, KEMA, Arnhem, Netherlands

ABSTRACT

According to IEC publication 127 the breaking capacity of miniature fuses should be tested using a voltage source of sufficient power. In the past proposals have been made and experiments have been carried out to test the breaking capacity of such fuses in an LC-circuit. It can be argued that relevant conditions in an LC-circuit differ from those as experienced in a direct test method, especially during the arcing period.

Starting from a simplified arcing model the paper presents arguments based on which it becomes conceivable that direct testing may result in different conditions in both test methods, which may lead to test results which are not comparable with each other.

1. INTRODUCTION

The breaking capacity of a miniature fuse is at least determined by two criteria, viz [1]

1-1 The maximum arc power which in general is developed at the instant of fusing.
1-2 The arc energy W_b generated in the fuse during the arcing period.

In this paper a comparison will be made between two methods of testing the breaking capacity of miniature fuses, viz, direct testing according to IEC publication 127, and synthetic testing in an LRC-circuit, as proposed several times in litterature e.g. by Winter at all [2]. Assuming the validity of both above mentioned criteria then the two testing methods should result in equal results with respect to the criteria mentioned and under otherwise comparable circumstances as e.g. pre-arcing conditions.

So we confine ourselve to the arcing period and to the question whether a synthetic test circuit can be defined which will give equal test results regarding the above mentioned criteria as compared with the direct test circuit specified in IEC 127 for HBC miniature fuses. (1500A prospective current in a 250VAC circuit with $\cos\varphi \approx 0.8$) In trying to find an answer on this question we assume that pre-arcing conditions are comparable. This means that for one specific fuse type to be tested the $\int i^2 dt$ value and the instantaneous value of the current at the instant of fusing are equal in both test circuits.

2. THE ARC MODEL

For a theoretical approval of the above mentioned question we start from the resistance - step - model for an arc in a fuse as developed earlier [3] [4] and which has proven to give an acceptable explanation of arcing behaviour in a fuse. Very briefly the resistance - step - model contains the following :

In case of short circuit the arc voltage coming into existance at the instant of fusing can be understood by the action of a resistance step with amplitude R_f at the instant of fusing t_1. The value of R_f is typical for a given fuse design and may also depend to some extend on the value of the current I_1 at the instant t_1. (see fig. 1) The self-inductance, present in any circuit in practice, opposes a sudden variation of current at the instant R_f arises, which means that at $t = t_1$ a voltage E_f across the fuse will arise, the value of which is determined by $E_f = I_1 R_f$. The power P_f at the instant $t = t_1$ is equal to $P_f = I_1 E_f = I_1^2 R_f$, which normally shows a maximal value at $t = t_1$. This means that the criterium for maximum arc power P_f includes a criterium for I_1, meaning that also conditions resulting from the pre-arcing period are taken into account.

In many cases in practice an increase of the arc-resistance during a certain period of time Δ will occur. Such an increase can be approximated by a linear increase during Δ, so R_f may show a time function as indicated in fig. 2. This will be the case as a consequence of multiple arcing and/or burning back of the fuse element. The existance of a rise time Δ may lower the maximum value of the peak voltage to a value $e_{fmax} < E_f$. This is especially the case if the rise-time Δ is not very small compared with the time constant τ of the circuit from which the fuse forms a part.

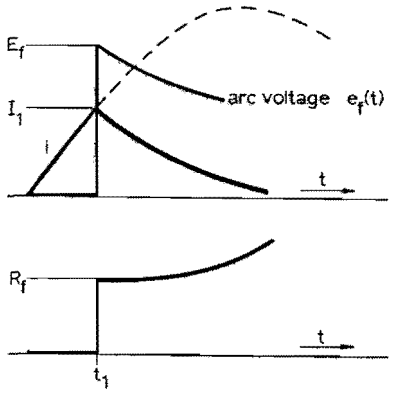

Fig. 1 : Arc voltage current and resistance wave forms of a fuse in case of short circuit.

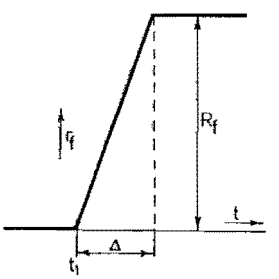

Fig. 2 : Arc resistance model

3. THE MAXIMUM ARC-POWER IN BOTH TESTING CIRCUITS

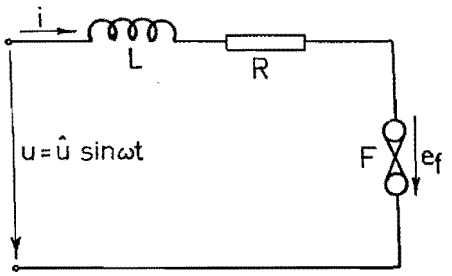

Fig. 3

Direct testing circuit

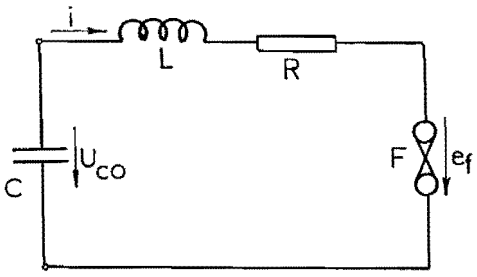

Fig. 4

Synthetic testing circuit

Fig. 3 shows, somewhat simplified, the direct testing circuit as specified in IEC 127 for the breaking capacity test for HBC-miniature fuses, whereas fig. 4 shows the synthetic test circuit using a capacitor as a current source.

A computer simulation has been made for the computation of the maximum arc voltage e_{fmax} in relation to the maximum possible arc voltage $E_f = I_1 R_f$ in both circuits, and using the arc model as shown in fig. 2.

For the circuit of fig. 3 the circuit parameters as derived from the IEC test circuit have been taken. The circuit parameters of fig. 4 have been chosen such that in both cases the pre-arcing conditions ($\int i^2 dt$-value and the value of I_1) are equal.

Fig. 5 shows some computational results. In this graph e_{fmax} / E_f has been plotted as a function of Δ / τ_L, where τ_L is the circuit time constant in both circuits $\tau_L = L/R$. As a remark the capacitance in the synthetic circuit results in a time-constant $\tau_L = RC$ for which is valid $\tau_c >> \tau_L$.

From the graph of fig. 5 it can be seen that there is no big difference in values of e_{fmax} / E_f as a function of Δ / τ_L in both circuits. However, plotting e_{fmax}/E_f as a function of Δ and with relevant values of τ_L in both cases, a remarkable difference between the two circuits becomes visible. (see fig. 6) In the example of fig. 6, comparable results with respect to e_{fmax} are only possible using a charging voltage of the capacitor which is considerable lower than required, according to IEC 127.

As a remark, it has been shown in the past that good conformity exists between theoretical curves for the circuit of fig. 3, as shown in fig. 5, and experimental results [5]. Further, we remark that values of Δ at which a remarkable lowering of the peak arc voltage will occur, are quite normal values for miniature fuses at relevant values of short-circuit current to be interrupted.

So as a conclusion one may state that a difference between the peak arc voltage in both testing circuits is quite conceivable, meaning also that the maximum power P_f in both cases may differ remarkably from each other. Similar results with respect to P_f may be obtained if $\tau_L = L/R$ is equal in both testing circuits, but this condition will create a serious complication concerning equal pre-arcing conditions in both testing circuits.

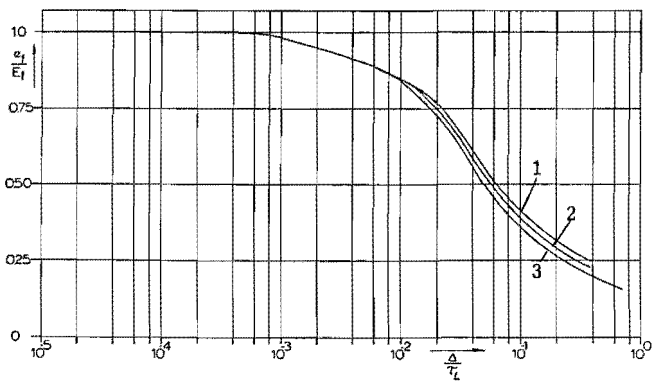

Fig. 5 : Lowering of the peak voltage as a function of $\frac{\Delta}{\tau_L}$.

1 : direct

2 : L = 420μH, E = 225V

3 : L = 230μH, E = 143V

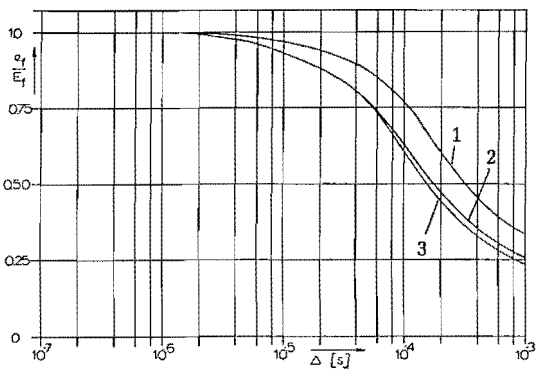

Fig. 6 : Lowering of the peak arc voltage as a function of Δ.

1 : $\hat{E} = 250\sqrt{2} = 353V$; $\tau_L = 4,44ms$

2 : direct, $\hat{E} = 250\sqrt{2}V$; $\tau_L = 2,63ms$

3 : $\hat{E} = 225V$; $\tau_L = 2,63ms$

4. THE ARC ENERGY IN BOTH TESTING CIRCUITS

In principle the behaviour of the arc in a fuse during the arcing period can be described by two simultaneous differential equations, viz :

- The energy balance equation of the arc in the fuse.
- The equation of the circuit from which the fuse is a part.

Solving both equations together may result in an expression for the arc energy in a given situation, providing that all physical and electrical parameters are known in sufficient detail. This leads to the conclusion that the arc energy is not only determined by the fuse parameters, but also greatly influenced by the parameters of the circuit from which it forms a part.

One can wonder if it is in principle possible to create in a totally different circuit equal conditions with respect to arc energy. This is the more so because a synthetic circuit (LRC-circuit), in contrary to the direct testing circuit, may show two different states (an aperiodic and a periodic state) which both may come into existance during testing of one fuse. It has been shown theoretically and proven experimentally [3] [6] that during fuse operation an LRC-circuit may be in the periodic state during the pre-arcing period, whereas during the arcing period the LRC-circuit may be in the aperiodic state. This will be the case if the fuse resistance R_f is larger than the critical resistance $R_c = 2\sqrt{\frac{L}{C}}$ of the circuit. So adjusting the LRC-circuit such as to create similar pre-arcing conditions does not garantee at all that during the arcing period also similar conditions occur.

This statement can be made more plausible by having a somewhat closer look at the differential equations describing the circuits of figures 3 and 4. For both circuits is valid :

$$u(t) = L\frac{di}{dt} + Ri + e_f(t)$$

Where $e_f(t)$ is determined by $e_f(t) = ir_f(t)$ and $r_f(t)$ is governed by the energy balance equation of the arc. For the arc-energy dW_b during the time interval dt is valid : $dW_b = e_f(t)i\,dt$, resulting in :

$$dW_b(t) = u(t)dt - Li(t)\frac{di}{dt} - Ri^2(t)dt$$

The voltage u(t) in fig. 3 is given by the expression :

$$u(t) = \hat{U}\sin(\omega t + \varphi)$$

whereas for fig. 4 is valid :

$$u(t) = \frac{1}{C}\int i(t)dt$$

which in general will result in different expressions for dW_b and, consequently, for $W_b = \int_{t_1}^{t_2} dW_b$ for both circuits.

It can be shown that in general for the circuit of fig. 3 the following is valid :

$$W_b = q_3\,\hat{U}\,\hat{I}$$

whereas for the circuit of fig. 4 we have :

$$W_b = q_4\,U_{co}\,\hat{I}$$

where $\hat{I}$ and $\hat{U}$ are maximum values of current and voltage respectively and U_{co} is the charging voltage of the capacitor of fig. 4. The parameters q_3 and q_4 are rather complicated functions of circuit parameters, closing angle, $\varphi_f(t)$, a.s.o. It is tempting to analyse these functions further, but the outcome is rather strong dependant on the amplied arc model for such an analysis, so the pratical value of such an analysis is questionable.

As a remark we like to mention that Boehne [7] already arrived at an expression for q_1, assuming that at $t = t_1$ a constant arc-voltage E_f comes into existance. To give somewhat more evidence of possible differences in arcing behaviour in both testing circuits, the current and voltage wave forms in both cases are shown schematically in figures 7 and 8, for the circuits of figures 3 and 4 respectively.

Fig. 8 shows the transition from the periodic state (for $t < t_1$) to the aperiodic state (for $t > t_1$), that means a transition from i_p to i_a in fig. 8. This will happen if for $t < t_1$ the resistance R is smaller than the critical resistance $R_c = 2\sqrt{\frac{L}{C}}$ of the circuit, whereas for $t > t_1$ is valid $R + R_f > R_c$. In pratical cases, the time constant $\tau = (R + R_f)C$ (assuming a constant fuse resistance R_f during the arcing period) which determines the rate of aperiodic discharge of the capacitor, is always far greater than the time constant $\tau_{f1} = L/(R+R_f)$ which determines the transient phenomena as indicated by the shaded area of fig. 8. In most pratical cases the initial fuse voltage $E_f = I_1 R_f$ is much greater than the capacitor voltage U_{c1} at $t = t_1$. If this is so, it can be easily derived, introducing $R_f = nR_c (n > 1)$, :

$$I_a = \frac{U_1}{nR_c} << I_1$$

That means that the magnitude I_a of the aperiodic current (see fig. 8) is considerably less than the current I_1 at $t = t_1$. Further it means that the value of I_a and $i_a(t)$ depends on the voltage U_1 at the instant of fusing. Such a dependancy does not exist in the case of the circuit for direct testing as shown in fig. 3.

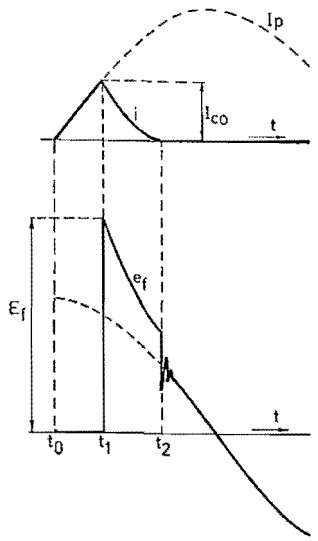

Fig. 7 : Current and voltage traces in a direct testing circuit.

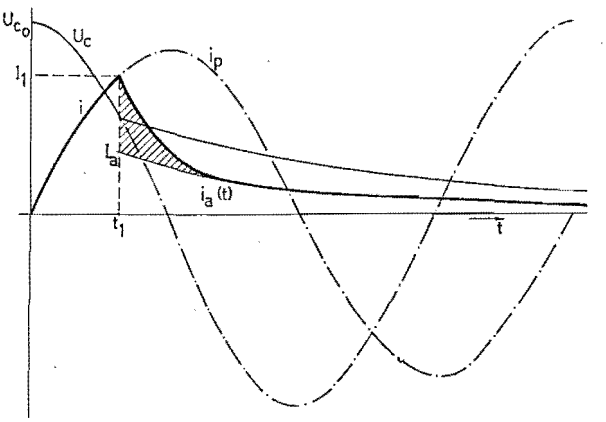

Fig. 8 : Current and voltage traces in a synthetic testing circuit.

5. CONCLUSIONS

In the preliminary some comparison has been made between the conditions for testing of miniature fuses in two different testing circuits. This comparison has been made, based on two criteria for the arcing period only, so it is assumed that equal test conditions occur with respect to the pre-arcing period. It is argued that equal conditions regarding the pre-arcing period in a direct testing circuit according to IEC 127 and a synthetic LRC testing circuit, does not necessarily mean that during the arcing period also equal conditions are present. Arguments are given for the statement that it is unlikely that both testing circuits will give comparable results with respect to the breaking capacity of fuses.

LITTERATURE

[1] J.W. Gibson :The high-rupturing capacity catridge fuse.
Journal IEE 88 pt. II (1941) 2.

[2] D.F. Winter, W.C. Reinhardt, M.M. Dorn :Synthetic test facility for distribution types of apparatus, Part I, development.
Trans. IEEE, PAS 97 (1978)5, 1842.

[3] L. Vermij : Interaction between Exploding wires and the Electrical Circuit.
Z. angew. Physik 25 (1968)6, 350.

[4] L. Vermij : The Voltage Across a Fuse During the Current Interruption Process
Trans. IEEE, PS-8 (1980)4, 460.

[5] L. Vermij : Electrical Behaviour of Fuse Elements
D.Sc. Thesis, University Eindhoven, 1969.

[6] L. Vermij : Fuse Elements as Part of an LC-Circuit
Holectechniek 2 (1972)1, 20.

[7] E.W. Boehne : Performance criteria for current limiting power fuses.
Trans. AIEE 65 (1946) 1034.

BREAKING CAPACITY OF MINIATURE FUSES AND THE TESTING OF A HOMOGENEOUS SERIES

H W Turner, Dr C Turner and Dr D J A Williams

ABSTRACT

The closing angle is specified in the breaking capacity test in IEC Publication 127. The tests analysed in this paper demonstrate that this situation is unsatisfactory for ratings above a critical level. The arcing angle should be specified. Alternatively, the correct closing angle is shown to be calculable if suitable pre-arcing data are provided when fuses are submitted for test.

The proposed introduction of homogeneous series testing of miniature fuse-links makes it more necessary to correct this situation, because a successful breaking capacity test on the highest rating is then considered to be proof that lower ratings of the same design are also satisfactory.

1 INTRODUCTION

IEC Publication 127 specifies breaking capacity tests for miniature fuse-links which are carried out at a prospective current of 1500 A ac rms 50 Hz at a power factor of 0.7 for high breaking capacity fuse-links, and 35 A or 10 times rated current (whichever is the greater) for low breaking capacity types. To attempt to ensure repeatibility of the tests, a closing angle of 30 $\pm$ 5 degrees on the voltage wave is specified.

In the United States, no closing angle is specified, random switching being employed. The tests described below verify the long held suspicion that neither of these methods of breaking capacity testing is completely satisfactory.

It is well established for other types of fuse-link that the arcing angle is the factor which determines the severity of a test on a fuse-link, and the results outlined below verify that this is also the case for miniature fuse-links. A fuse which successfully clears the circuit when arcing commences at an angle near to the next voltage zero will not necessarily perform satisfactorily when arcing commences just before voltage maximum.

Miniature fuse-links are a low-cost item. This is a reason why the cost of testing must be kept to the minimum consistent with safety, and there are at present moves to reduce these costs by introduction of the principles of homogeneous testing of series of fuse-links of similar construction, differing only in the dimensions which determine the current rating. In this technique the maximum number of tests is carried out on the highest rating in a series, and the results are considered to apply to lower ratings without further test. This development has focussed attention on the breaking capacity test which is most unreliable for the larger ratings in the low breaking capacity types.

The present test specification requires the breaking capacity test to be performed on every rating, and thus unsatisfactory designs can be eliminated when they fail to complete the breaking capacity test on ratings less than the maximum in the series, where the arcing commences near voltage maximum.

For fuse-links of very low ratings (eg up to 100 mA) the arcing angle is extremely close to the closing angle, and thus there is no need to depart from the practice of specifying a closing angle. The range of ratings over which this applies varies with the type of fuse-link, and can be calculated, as is shown below.

2 RANGE OVER WHICH THE PRESENT SYSTEM IS SATISFACTORY

The range may be assessed by consideration of the maximum values of pre-arcing I^2t specified in Publication 127 calculated from the gates specified at 10 times rated current. This will give a margin of safety, since the pre-arcing joule integral tends to be lower at higher prospective currents. The mathematical problem is then to find the arcing angle corresponding to the given closing angle for the value of joule integral thus determined.

H W Turner, Dr C Turner and Dr D J A Williams are with ERA Technology Ltd, Leatherhead, UK.

The problem was solved by consideration of the equation for the I^2t dissipated in an inductive circuit which is given by the following equation:

$$\int i^2dt = 2I_p^2 \int_{t_1}^{t_2} \{\sin(\omega t_2 - \phi) - \exp(-R\,(t_2 - t_1)/L).\sin(\omega t_1 - \phi)\}^2\,dt \qquad (1)$$

Where I_p = rms prospective current

ω = the angular velocity

t_1 = closing instant after voltage zero (sec)

t_2 = instantaneous time from voltage zero (sec)

ϕ = phase angle

R = resistance

L = inductance

The solution to this equation is as follows:

$$\int i^2dt = I_p^2[t_2 - t_1 - (\sin(2C_2) - \sin(2C_1))/2\omega + (4\omega L^2/Z^2.\sin(C_1)\,.\,(F_2 - F_3) + F_4)] \qquad (2)$$

Where C_1 = $(\omega t_1 - \phi)$, $C_2 = (\omega t_2 - \phi)$ and $Z^2 = R^2 + \omega^2 L^2$

F_2 = $\exp(-R(t_2 - t_1)/L)).(R/\omega L.\sin(C_2) + \cos(C_2))$

F_3 = $R/\omega L \sin(C_1) + \cos(C_1)$

F_4 = $L/R.\sin^2(C_1).(1 - \exp(-2R(t_2 - t_1)/L))$

With the aid of a computer, the arcing angle was evaluated from equation (2) by means of an iterative program which identified the conditions for the nearest match to the given joule integral. It is proposed below that the same technique be used to predict the correct closing angle when the higher levels of current rating are being tested and thus obtain the desired arcing angle.

On the basis of tests on all types of miniature fuses, confirmed by the tests described below it can be seen to be desirable that the arcing angle should be between 30 and 90 degrees in the breaking capacity tests, if the present specification of a 30 degree closing angle is sustained.

Miniature fuse-links are classified in IEC 127 in four different types, details of which are given in the standard sheets of the specification. For the standard sheet I fuse-links the maximum rating is 6.3 A with a maximum pre-arcing time of 0.02 sec at 63 A. This implies a maximum pre-arcing joule integral of 79 amp squared seconds under these conditions. By substituting the above value in equation (2) we found that on the basis of the criterion of an arcing angle below 90 degrees, there is no problem with the high breaking capacity types. However the results of tests (Fig. 1 is an example) showed that the arc energies peaked at arcing angles near voltage maximum, and there could thus be an argument for some increase in the specified closing angle. Comparability between different sources and current ratings is however very good with the 30 degree closing angle.

Standard Sheet II fuse-links are low breaking capacity types having a maximum pre-arcing time of 20 milliseconds at 10 times rated current. The pre-arcing joule integral is thus equal to 2 x (rated current)^2 amp squared seconds. Substituting this value in the equation and putting the prospective current at 35 A we find that on the basis of the above arcing angle criterion, no problem is likely for rated currents of 1.6 A and below.

Standard Sheet III fuse-links are time-lag types with a pre-arcing time of up to 0.3 seconds which corresponds to a joule integral of thirty times the square of the rated current. Substituting in the equation as before, we see that problems are only likely to arise for rated currents exceeding 400 mA.

All the above fuse-link types are of the 5 x 20 mm dimensions, but Standard Sheet IV is a 6.3 x 32 mm type with a maximum of 0.08 sec at 10 times rated current. Similar calculations reveal that on the basis of the above criterion, there should be no problem for fuse-links of ratings below 800 mA.

3 TEST RESULTS

The test results indicate the extent of the problem at present.

Figure 2 is a graph of the arc energies measured for a range of fuse-links 5 x 20 mm of European manufacture of rated currents from 0.63 A to 4 A tested at their breaking capacity current and rated voltage. The current was set by adding resistance to the test circuit. The test source was a large laboratory test transformer, but of lower power than that normally used in standard testing, so that the severity of the test was slightly greater than that specified for type testing.

It can be seen that the arc energy peaks in the region around 90 degrees and that all the failures were at arcing angles between 55 and 120 degrees.

On the basis of these tests, and the criteria applied in testing other types of fuse-link we propose that the arcing should commence near 90 degrees on the voltage wave.

4 MEANS OF ACHIEVING THE CORRECT ARCING ANGLE

The expense of measuring and recording arcing angles has been quoted as a major objection to specifying arcing angle in the past. However if the average pre-arcing joule integral is stated by the manufacturer (or obtained from the test of time/current characteristic at 10 times rated current), then equation (2) gives adequate accuracy for the calculation of the correct closing angle to obtain arc initiation in the desired range.

Figures 3, 4 and 5 illustrate the degree of accuracy obtained using this technique, for typical fuse-links to standard sheets I, II and III. The circles represent the calculated values using the average value of pre-arcing joule integral for each type and the crosses show the experimental results, with a solid line which was drawn through the experimental points before the calculations were made.

5 CONCLUSIONS

1) The breaking capacity test specified in the present IEC Publication 127 based upon a specified closing angle will not always produce the most onerous conditions particularly for fuse-links of higher rated current of low breaking capacity.

2) Calculations show that there is likely to be no problem of this kind for fuse-links below 400 mA rated current, and that for fast acting fuse-links 5 x 20 mm there is no problem up to ratings of 1.6 A.

3) The arcing angle should be specified instead of the closing angle.

4) The closing angle corresponding to the required arcing angle may be readily calculated if the average value is known of the pre-arcing joule integral corresponding to the test current, and calculation of the closing angle from the average joule integral gives a result sufficiently accurate for miniature fuse breaking capacity tests.

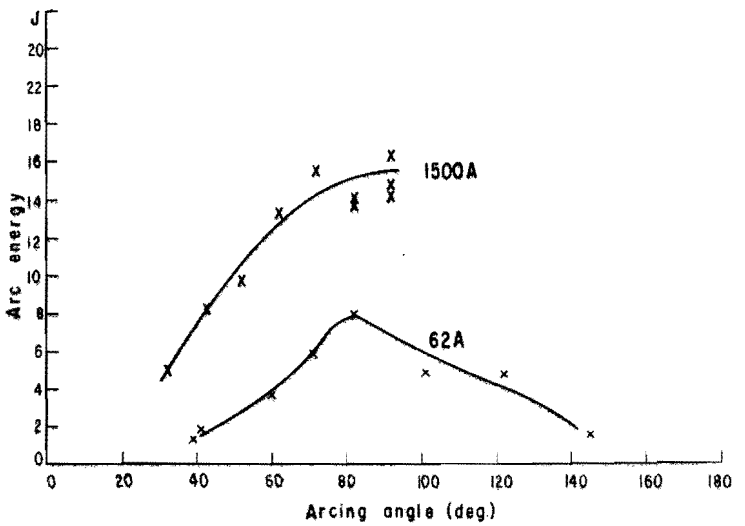

Fig. 1 Arc energy as a function of arcing angle for Standard Sheet I fuse-links I_n = 0.63 A. Tested at 62 A prospective current (no added inductance) and at maximum breaking capacity.

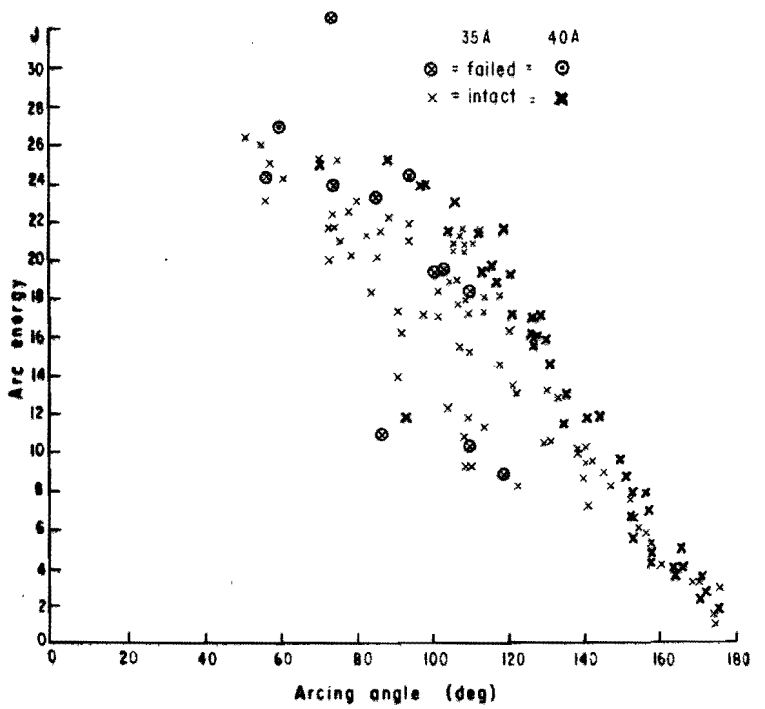

Fig. 2 Arc energy as a function of arcing angle for low breaking capacity fuse-links of differing current ratings, designs and time delay characteristics. Tested at 35-40 A with no added inductance.

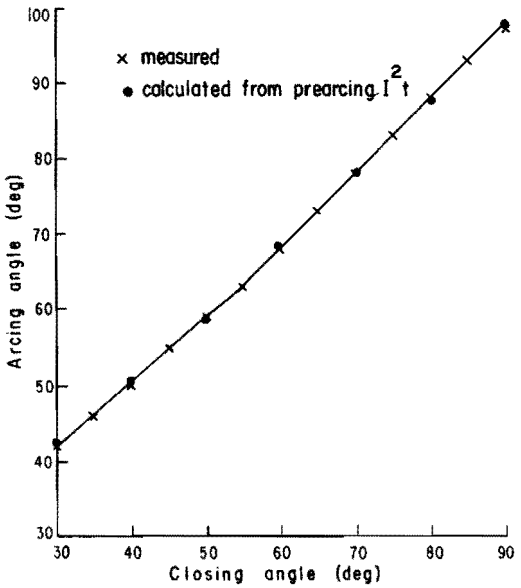

Fig. 3 Arcing angle as a function of closing angle for Standard Sheet I fuse-links I_n = 6.3 A.

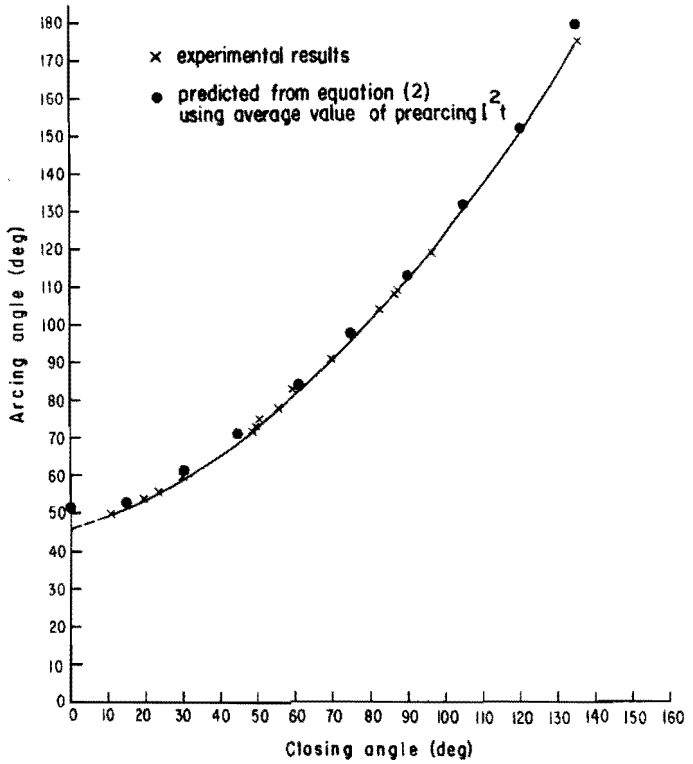

Fig. 4 Arcing angle as a function of closing angle for Standard Sheet II fuse-link I_n = 0.63 A. Tested at 35 A with no added inductance.

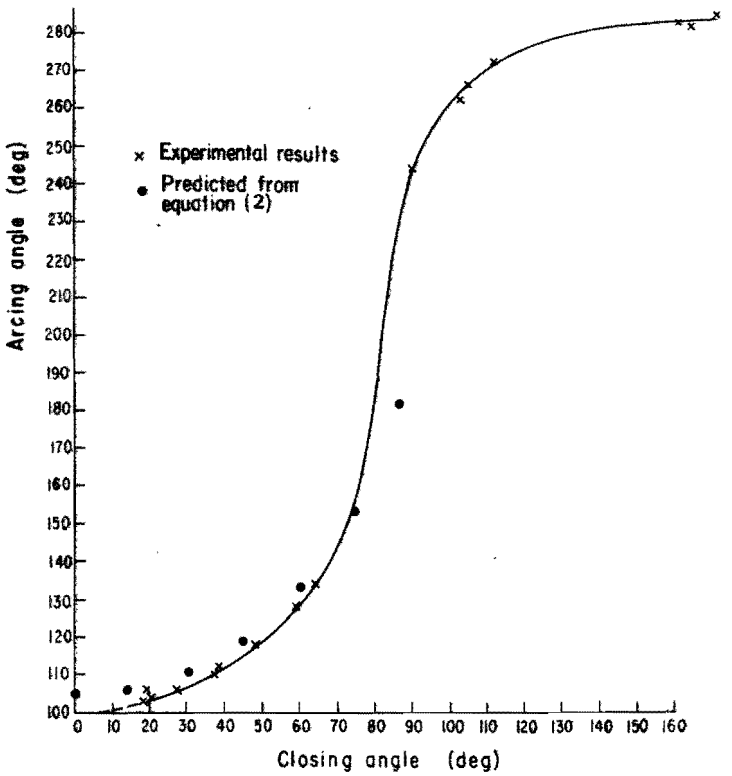

Fig. 5 Arcing angle as a function of closing angle for Standard Sheet III fuse-links I_n = 1 A. Note: The virtual impossibility of achieving arcing angles between 180 and 240 degrees (0-60 degrees).

STATE OF THE ART OF IEC WORK WITH RESPECT TO FUSES

G.J. Deelman, G.R. Hoekema, B. Noordhuis

INTRODUCTION

In present-day electrical installations the current-limiting fuse forms an integral component, with an excellent price-performance ratio. As a result, the International Electrotechnical Commission pays wide and active attention to the various aspects of fuses.In this paper a review is given of the present situation of the IEC-standardization work concerning high-voltage fuses, low-voltage fuses and miniature fuses.
For each group of these fuses, first will be summarized which standards are available now and which will be available shortly.
Further will be reported on the main items which, in the near future, will probably lead to amendments to the standards. Thirdly, some information is given concerning the future activities of the relevant Working Groups.

COMMITTEES

Within the IEC, electrical fuses are considered by the Technical Committee 32. This TC has three Sub-Committees:

- SC 32A: High-voltage fuses
- SC 32B: Low-voltage fuses, and
- SC 32C: Miniature fuses.

Each SC is assisted by one or more Working Groups, composed of specialists from various countries.

Since 1980 the Technical Committee and its Sub-Committees have met three times: in Montreux, Tokyo, Brussels (32A and C) and Orlando (32B).
For SC 32C the next meeting is scheduled in Prague in 1987.
Usually the Working Groups meet twice a year.

HIGH-VOLTAGE FUSES

Available IEC Publications.

The main document for high-voltage fuses is IEC Publication 282. This standard consists of three parts:

282-1 (1985): Current limiting fuses.
Applies to all types of high-voltage current limiting fuses.
The third edition issued in 1985 is based on the edition of 1974 and a number of amendments issued since.

282-2 (1970): Expulsion and similar fuses.
Applies to high-voltage fuses in which the arc is extinguished by the expulsion effect of the gases produced by the arc.
The first edition of 1970 is still valid. In 1978 one amendment has been issued, dealing with revised requirements for the insulation level. On this subject no further work has been undertaken since by the IEC.

282-3 (1976): Determination of short-circuit power factor for testing current-limiting fuses and expulsion and similar fuses.
IEC sub-committee 32A decided that, in order to harmonize the determination of power factors in test laboratories, some guidance is required. This matter was not considered by other Technical Committees and as a consequence this document was issued under responsability of SC 32A.

For specific applications of high-voltage fuses three more standards have been issued:

549 (1976) : High-voltage fuses for the external protection of shunt power capacitors.
The document gives some requirements with respect to the performance of fuses for this application and it specifies the type tests to be carried out.

644 (1979) : Specification for high-voltage fuse-links for motor circuit applications.
This standard mentions limits for the pre-arcing time-current characteristics. It also defines an overload factor K to which a fuse-link may repeatedly be subjected to without deterioration, due to the specific behaviour of high-voltage motors.
It further specifies withstand tests and it gives guidance with respect to proper selection of fuse-links.

G.J. Deelman - Electrical Engineering Consultant, Eindhoven, The Netherlands
G.R. Hoekema - KEMA, Arnhem, The Netherlands
B. Noordhuis - Holec, Hengelo, The Netherlands

787 (1983) : Application Guide for the selection of fuse-links of high-voltage fuses for transformer circuit applications.
Apart from some considerations of the fuse-link's time-current characteristics, the document elucidates on the co-ordination of fuse-links on the primary side of a transformer and the protective devices at the load side.
An amendment to this standard requires that the manufacturer of this type of fuse-links makes available recommendations for ratings of fuse-links for given kVA ratings of transformers.

Documents in final stage

In april 1986 a number of documents under the Six Months' Rule have been issued.

32A (Central Office) 80 deals with testing of strikers. An improved method of the operation tests is described.
These tests are intended to demonstrate that the action of the striker in every service situation is sufficiently rapid to ensure correct operations of striker tripped fuse-switch combinations.
(IEC Publication 420).

32A (CO) 81 proposes an amendment to the Application Guide for fuses in a three -phase isolated neutral or resonant earthed system. It refers to IEC Publication 265-1: "High-Voltage switches" for tests in earth fault conditions.

32A (CO) 82 concerns another addition to the Application Guide of Publication 282-1, namely to the paragraph where it is stated that fuse-links should be handled very carefully. If fuse-links during normal installation and service are subject to severe mechanical stresses, it should be verified that the fuse-links can withstand such stresses without damage or deterioration.

32A (CO) 83 gives an alternative test method for test duty 3:
Verification of operation with low overcurrents.
This method is particularly of interest if has to be proved that the fuse operates correcly if the pre-arcing time is longer than one hour. It permits the melting of all main fuse elements in a low-voltage circuit, before the high-voltage circuit is switched on.
This method is considered to be more severe than the existing method in which the switch-over has to take place during the arcing period.

32A (CO) 84 describes the waterproof test.
In IEC Publication 282-1 the list of special tests did not mention a test with respect to ingress of moisture for fuses intended to be used outdoors. As the dryness of the arc-quenching medium is an important condition for correct operation, this requirement had to be added.

32A (CO) 85 proposes an enhanced limit for the switching voltage for fuse-links with a low rated current, intended for protection of for example voltage transformers. For this kind of fuses the switching voltage may exceed the limits mentioned in the existing standard, however, only during less than 0.2 ms and up to a level which averages 1.4 times the actual limit.

32A (CO) 86 proposes the introduction of another appendix to the standard, giving technical information for test laboratories how to calculate circuit data in case the test method using two power factors is used for test duty 3.

Work under consideration

For preparation of draft documents Sub Committee 32A is assisted by one Working Group (WG 3) with a general scope.
At the moment the following items are under consideration:

Classification and designation of current-limiting fuse-links.
For high-voltage fuses two classes have been recognized in Publication 282-1, according to the range in which they can be used:" back-up" fuses and" general-purpose" fuses. Actually a third category of fuse-links is on the market: so called" full range" fuses. One of the Secretariat Documents prepared by WG 3 proposes to delete the known classes from the standard, however, to retain the terms in the Application Guide and to determine the fuses by their minimum breaking currents.

Simplification of the rules for homogeneous series of fuse-links.
At present these rules in Publication 282-1 are complex and lengthy. The aim of the Working Group is to reassess these rules and to combine the experience of manufacturers and testing authorities to arrive at simple, however, correct requirements.

Additional test duty for fuse-links which depend for their breaking performance on more than one arc quenching principle.
In the region of the so called take-over current, where one arc interruption system takes over from the other, additional tests are now under consideration.

For the near future IEC Sub Committee 32A may consider further standardization work on new developments such as SF_6 fuses and vacuum fuses. Another type of equipment for which no standard exists are the hybrid overcurrent protection system consisting of a fast explosion actuated zero-voltage disconnector in parallel with a current-limiting fuse.

LOW-VOLTAGE FUSES

Available IEC-Publications:

For low-voltage fuses following IEC publications are available:

241 (1968) : Fuses for domestic and similar purposes.(Report)
Applies to non-interchangeable fuses of ceramic material with cartridge fuse-links for domestic and similar general purposes, with a rated voltage not exceeding 500 V and a rated current not exceeding 200 A, intended for the protection of wiring, provided that the prospective breaking current is within limits indicated in the specification.

The main document for low-voltage fuses is IEC publication 269, applying to:
Fuses intended for protecting power-frequency a.c. circuits of nominal voltages not exceeding 1000 V or d.c. circuits of nominal voltages not exceeding 1500 V.
This standard consists of several subsequent parts.

269-1 (1986): General requirements.
Establishes the characteristics of fuses or parts of fuses in such a way that they can be replaced by other fuses or parts thereof having the same characteristics provided that they are interchangeble as far as their dimensions are concerned.

269-2 (1986): Supplementary requirements for fuses for use by authorized persons (fuses mainly for industrial application).
Specifies, in addition to Part 1, the characteristics of these fuses.

269-2A(1975): First supplement to Part 2: Appendix A(with amendment no. 1.)
Examples of standardized fuses for industrial application.
Contains data sheets for fuses with blade contacts, for fuses with bolted connections and fuses having cylindrical contact caps.

269-3 (1973): Supplementary requirements for fuses for domestic and similar applications. (With amendment no. 1).
Specifies in addition to Part 1: rated voltages, maximum power losses, time/current characteristics and conventional currents, rated breaking capacities, markings, standard conditions for construction, and tests.

269-3A(1978): First supplement to Part 3: Appendix A.
Examples of standardized fuses for domestic and similar applications.
Contains data sheets for screw type fuses, cylindrical fuse-links and pin type fuses.

269-4 (1980): Supplementary requirements for fuse-links for the protection of semiconductor devices.
Establishes characteristics of semiconductor fuse-links in such a way that they can be replaced by other fuse-links having the same characteristics provided that their dimensions are identical. Defines standard conditions for operation in service, characteristics of fuses, markings, standard conditions for construction,and tests.

Documents in final stage

The revision of the Publications 269-2A, 269-3 and 269-3A is in the final stage.

- The new draft of Publication 269-2A is printed now and issued as publication 269-2-1.

- The revision of Publication 269-3 is also finished and issued as Publication 269-3-1987.

- The revision of Publication 269-3A is in the final stage of considering under the Six Months' Rule. At issue it will be numbered 269-3-1.

Work under consideration

IEC sub-committee 32B has set up a number of Working Groups:

WG 7 was formed to prepare supplementary requirements for semiconductor fuses.

WG 8 has the general task to prepare the documents concerning the various items for further discussion in the National Committees. Special work within WG 8 is done at present in three ad hoc groups.

- Ad hoc group "non-deterioration of contacts".
  A German proposal for inclusion of non-deterioration tests in Publication 269-2-1 has been sent to the National Committees. The necessity of such tests for domestic fuses is also under consideration.

- Ad hoc group "IEC-UL characteristics".
  This group has made a reconnaissance concerning the possibilities first and will in due course make proposals for integration of the UL time delay fuse class J in IEC Publication 269-1 and 269-2.

- Ad hoc group "co-ordination between contactors and fuses"
  By the end of 1985 this group was set up to study the problems which arise concerning the co-ordination between contactors with their relays and fuses.
  These problems mainly occur due to the large spread of the operating time of the fuses in the region of 15-30 times the rated current of the contactors.
  In the second meeting of the group is was decided to collect more details of the contactors and relays involved.
  This work has to be done in conjunction with WG2 of sub-committee 17B.

In february 1986 an administrative circular has been sent to all National Committees to notify the set up of Working Group 13 to study "The feasibility of achieving a world-wide low-voltage fuse". This WG has to define the problems, to consider the conditions and to propose ways for feasible solutions. Furthermore a time schedule has to be made. The WG has to report about its results at the next Sub-Committee meeting. The SC will decide then whether and how the work will be continued. In the meantime WG 13 started its work and has met two times.

MINIATURE FUSES

Available IEC-Publications

For miniature fuses there are two main IEC documents:
Publication 127 for the fuse-links and Publication 257 for the fuse-holders:

127 (1974) : Cartridge fuse-links for miniature fuses.
This publication relates to miniature fuse-links for the protection of electric appliances, electronic equipment and components thereof.
It establishes requirements and defines performances and tests.
The Publication contains four Standard Sheets:

No. 1 covers fuses	5	x 20 mm,	characteristics	F, HBC
No. 2 " "	5	x 20 mm,	"	F, LBC
No. 3 " "	5	x 20 mm,	"	T, LBC
No. 4 " "	6.3	x 32 mm,	"	F, LBC

F stands for fast-acting, T for time-delay, HBC and LBC for high-breaking and low-breaking capacity respectively.

127A (1980): First Supplement: Colour Coding.
Gives requirements for colour coding as an additional identification for current ratings and the time-current characteristics.

127-3 (1984): Sub-miniature fuse-links.
This Publication also specifies four Standard Sheets:
Nos 1 and 2 for fuses with radial and axial leads respectively, having fast acting characteristics, mainly in accordance with UL.
Nos 3 and 4 for fuses with radial leads, characteristics F and T respectively, mainly in accordance with the IEC gates 1.5-2.1.

127-B (1985): Second supplement.
This supplement contains (among other matters) tables in the Standard Sheets which are provided with an extra column giving requirements for safe dissipation values.

257 (1968): Fuse holders for miniature cartridge fuse-links.
Applies to fuse-holders with a maximum rated current of 16 A and a maximum rated voltage of 1000 V a.c. and d.c.
In 1980 was added amendment no. 1, applying to a definition and requirements for accepted power of a fuse-holder.

It is envisaged to publish in the near future all documents related to miniature fuse-links and fuse-holders in one standard: IEC Publication 127, which will be subdivided in 7 parts, covering different parts and subjects of miniature fuses.

Documents in final Stage

Survey of recent Central Office documents, related to the main topics.

32C (CO) 39 (Mar. 1984): Maximum sustained dissipation values.
32C (CO) 42 (Dec. 1985): Standard Sheet 5, fuse-links 5 x 20 mm, Char. T, HBC.
32C (CO) 43 (Dec. 1985): Warning note regarding the use of miniature fuses.
32C (CO) 44 (Feb. 1986): Part 5: Quality assessment of miniature fuses.
32C (CO) 45 (Feb. 1986): Fuse-holders for miniature fuses.
32C (CO) 46 (Apr. 1986): Part 1: General requirements.
32C (CO) 47 (Apr. 1986): Part 2: Cartridge fuse-links for miniature fuses.
32C (CO) 49 (May 1986): Part 3: Sub-miniature fuses.

Work under consideration

Within sub-committee 32C five Working Groups are active:

WG 1 drafts a new scope for Publication 257, inclusive of test holders. In WG 4 the policy and philosophy for miniature fuse specifications are developed. WG 5 studies possibilities of introducing homogeneous series into Publication 127, in order to simplify the test procedures.
WG 6 has to prepare a document on Universal Modular Fuses (UMF), based on 32C (secretariat)57 from July 1983 and the comments received since. The scope of WG 7 is the quality assessment of miniature fuse-links. It has to prepare a proposal for a standard on acceptance-tests and (a second step) to prepare a document on reliability tests.

Future work in Sub-Committee 32C and its Working Groups will probably concentrate on the following items:

- Marking the breaking capacity on miniature fuses.
- Preparing a final solution for the gates for the UMF series based either on the values 1.25-1.7 or 1.5-2.1
- Total revision of Publication 127 with respect to the gates for all 5 x 20 mm and 6.3 x 32 mm fuses gate 1.5-2.1.
- Study of possible model protection for the UMF version in connection with gates $1_2$25-1.7.
- I^2t gates especially for time delay fuses.
- Solution of the controversy between IEC SC-32C and UL 198. This controversy has been caused by equipment manufacturers who, when exporting their products to both USA oriented countries and Europe, were forced to use miniature fuses with size 6.3 x 32 mm in order to comply with the USA requirements. However, in Europe smaller (5 x 20 mm) fuses with IEC characteristics were available for many years.
  Wishing to provide 5 x 20 mm fuses acceptable for listing by UL, fuse makers manufactured such fuses and the UL organisation granted listing (approval) of such fuses. However, when equipment, provided with UL 5 x 20 mm fuses, needs replacement of fuses in Europa (where only such fuses with IEC characteristics are available), the consequences can be very serious due to the totally different characteristics.
  Such a substitution involves a serious risk of damage or even fire due to overheating and/or electric failure.
  The above pictured case of trespassing international standardization philosophy might even result in law suits questioning whom should be held responsible for the damages.

CONCLUSION

Standardization is a continuous process to keep up with new technical developments and improved understanding of physical phenomena. In this respect it is likely that existing standards will regularly be subject to amendments. In IEC, experts of many countries are member of the Technical Committee 32 and its Sub-Committees and Working Groups in order to draft standards for all kinds of electrical fuses.
For both low-voltage fuses and miniature fuses there is a trend to specify world-wide acceptable fuse systems, although this will not be an easy task.
Anyway, the IEC TC 32 activities are directed towards improvement of certification of electric fuses, for safer and more reliable electrical equipment and installations.

o-o-o-o-o-o

Closing Address

TRENDS AND POSSIBILITIES

By L. Vermij

During the 1950's, Prof. Lerstrup from Copenhagen made the statement :"fuse designing is an art, not a science". It seems to me that ever since it is becoming more and more a science. However, this science has not, up until now, produced any major break-through. At best, what has been achieved, is an explanation of certain aspects of the art.

Since the invention of the fusible link by Edison around 1880, only two major steps in the development of fuses have been made, viz :

- the current-limiting HBC-fuse.
- the M-effect.

All the rest are refinements and improvements. The major steps have been made during the "art-period" and did, roughly speaking, not result from science.

The last 10 - 20 years we entered the "science-period". What can be expected from putting more science in our designs? What are we going to do in our laboratories and institutes and what should be done in future? Perhaps this question can be put in another way :Why are we doing what we are doing and why are we not doing something else? Really the question is : how to realise a reliable protection at the lowest cost.

Let us realise that the best fuse is no fuse. That means that the ideal situation is a system which is so reliable that no overcurrent protection or short-circuit protection is needed. Probably such a situation can never be achieved. However it means that a protection device like a fuse is the best of all evils or, if you like, the most acceptable evil. Having said that, it may be concluded that a fuse must be :

- very cheap.
- not creating additional unreliability to the system.
- small in dimensions.
- easy to mount or to install.

We must realise that from a technical point of view a fuse still has some disadvantages, viz :

- it operates only once.
- it is a heat source.
- it is sensitive to environmental conditions, especially temperature.
- many types and ratings are required.
- obviously it is difficult to standardize.
- ageing still occurs with some designs.

Furthermore, there still are some difficulties in designing a reliable protection scheme, using fuses, viz :

- There is still a lot of misunderstanding regarding the functioning of fuses by users, system engineers, etc.
- Do we know exactly and in all detail what are the "ideal" or required characteristics of fuses from an application point of view? Sometimes it appears to me that we are making solutions and afterwards we are looking for the problems which belong to those solutions.

It is at least interesting to compare the above problem areas with the overview of recent advances Dr. Turner presented in her introductory lecture and with the topics presented during this conference. As an example, what has been done during the last years to overcome the problem of the "operating-only-once" of a fuse?

A couple of years ago, especially the Japanese did a lot of work on the so-called Permanent Power Fuse (PPF), using a liquid metal as a fuse element. Up till now it still not resulted in a completely reliable and economic solution of a "re-usable" fuse. At the Liverpool Fuse Conference in 1976 two papers have been presented on the PPF-fuse. The last three years only one (Russian) paper has been devoted to this subject. Why is that? Is it no longer promising to work on this? Or are the Japanese now quietly concentrating on making their PPF more reliable and economical?

Another example. We have seen recently the introduction in the market of the so-called self-restoring polymer fuse (also called current-sensitive resistor, or PTC current protector), for lower current ratings and for use in low-voltage circuits. The present devices have switching times of several seconds and depending rather strongly on ambient temperature. Furthermore, to keep such a device in the high-resistance-mode requires a minimum power dissipation which, in low voltage circuit as e.g. used in electronic circuitry, cannot be supplied by the energy source. So the device may start to oscillate under faulty conditions. As a conclusion at this point in time such a device cannot replace a fuse. However, can it be the start of a new generation of protection devices? That brings me to the question : what do we, fuse engineers, know about developments in adjacent areas of technology? In how far should the development of other current-limiting devices be of influence for future developments of fuses?

Another point I like to raise is the following :
From an application point of view mainly 4 areas in fuses exist, viz :

- high-voltage fuses.
- low-voltage industrial fuses.
- fuses for the protection of semi-conductor devices.
- miniature fuses.

The number of papers devoted to these main areas on the last Fuse Conferences and on the present Conference are shown in the following table :

	HV-fuses	LV-fuses	Semi-conductor fuses	Miniature fuses
Liverpool 1976	6	2	6	1
Trondheim 1984	10	5	2	0
Eindhoven 1987	9	4	1	7

I have the impression that the market volume in money is more or less in reverse proportionality with the figures for 1984 and 1987. It is certainly the case that at least two manufacturers of miniature fuses have each individually a turn-over in miniature fuses greater than the total market-volume in HV-fuses. It is also well-known that the market for semi-conductor fuses is huge in comparison with the HV-fuse market.

An economist, aware of market volumes but, knowing nothing of fuses, should possibly draw the following conclusions from the above table.

- There is no or only limited need for further R & D work on semi-conductor fuses. The big markets are there, also for the near future, and all problems have been solved adequately.
- A lot of R & D work has to be done on HV-fuses to develop this market further.

Or does the above table suggests that the HV-fuse is the most challenging to us (scientists and technicians), regardless what the market value is or will be? Do we create solutions without regard to the problems to be solved?

In the preliminary I raised a number of questions, no more than that. It is my believe, however, that putting the right questions may at least be helpful in finding the right direction for future work.

Although some people obviously still believe that fuse designing is an art, I think it is not exaggerated to state that fuse designing was an art, by now it can be a science. This science will bring us more optimized designs of fuses, will also create a better insight in requirements to be fulfilled and, possibly, will bring about new designs and concepts. It is my believe that some areas need more attention, as there are :

- Thin-film technology. Only one paper presented to this Conference touches on this area. However, without doubt this technology opens new and unexpected possibilities. We look forward to a number of papers on this subject on the next Fuse Conference.
- The use of ablative materials. During this Conference we had two papers on this subject, but both restricted to miniature fuses. It seems to me that this subject needs also attention in other fuse areas.
- New possibilities stemming from material sciences and solid-state physics, including manufacturing technologies used in these fields of activity, need our attention.
- More attention should be paid to adjacent areas of technologies which are influencing or might influence the application of fuses.

At the next Fuse Conference a great deal of the subjects will of course be discussed again. Not all problems have been solved yet. I do hope, however, that new subjects will be added to the existing ones. Let us try to answer real questions, not finding answers on questions which never have been raised.